The Response of

Non-Sway Steel Framed Structures

with Semi-Rigid Connections

Volume II

by

Sui Ming LAU

A thesis submitted in part fulfilment of the requirement
for the degree of Doctor of Philosophy

Department of Civil and Structural Engineering
University of Sheffield

December, 1993

The Response of Non-Sway Steel Framed Structures with Semi-Rigid Connections

Volume II

This thesis deposited in the University Library has been divided into two volumes due to the restriction of the new procedures for the mircrofilming of thesis for the British Library. Volume I contains chapters 1 to 7 and Volume II contains chapters 8 to 11. Apologies for any inconveniences caused to the readers arising from this.

Sui Ming LAU

Chapter 8

Comparisons of Experimental Results with Analytical Predictions

8.1 Declaration

In this chapter the behaviour of all five frame tests are compared with the response predicted by two finite element programs, SERFA and SERVAR [8.1,8.2] written by others and available for in house use. Some previous work [8.3,8.4] has included a detailed study of the behaviour and ultimate capacity of the columns for the two Sheffield frames. The study described herein extends the scope of the investigation to include all five frames. The sensitivity of frame behaviour to differences in moment-rotation response has also been examined using these programs.

8.2 Introduction

One principal objective of this research project was to provide results to verify programs which are capable of incorporating the effect of geometric non-linearity, plasticity and the influence of semi-rigid connections on column and frame response. The experimental data has been used to assess the ability of the two computer programs to model the behaviour of real frames. If such programs can be shown to accurately predict the behaviour of experimental tests, then extended investigations to study the influence of many parameters may be conducted more conveniently analytically rather than by expensive experimental studies. Finally, the restrictions and the limitations of the two computer programs are outlined and

further improvements are suggested.

8.3 Computer Programs Selected for Study

8.3.1 SERFA

SERFA was developed by Ahmed [8.4] modifying the subassemblage program of Rifai [8.5]. The program uses an incremental iteration algorithm for handling the elastic and inelastic analysis of planar steel frames with semi-rigid connections and was designed to trace the full load-deflection response up to the ultimate load for a structure. At the present time, the program is limited to in-plane response.

8.3.2 SERVAR

SERVAR was developed by Poggi of the Politecnico di Milano [8.6]. Non-linear behaviour is considered and elastic or elastic-plastic analysis may be chosen. Local plasticity is taken into account in the analysis by dividing the cross section into a number of layers. This program had been used to analyse a number of steel frames and was found to be satisfactory [8.6,8.3].

8.4 Comparison of Experimental and Predicted Behaviour

In this section, all the properties of the material (the elastic modulus, the yield stress) and the section properties, are to be taken as measured in the tests and have been recorded in Table 4.1. The loading histories used in the tests are modelled for each analytical prediction.

Figure 8.1 shows a model used in the analysis of SERFA and two design models used in this study of SERVAR are illustrated in Figure 8.2. At the time of usage, SERFA could not model the true initial geometric imperfection in each column. To compare the two programs, no initial deflections of columns (see Figure 4.1) were incorporated into each analytical model at this stage (the initial deflection of columns measured in the tests are taken account in the later study of SERVAR). It is evident from the references [8.3,8.7] that the measured residual stress in the member sections were highly irregular and did not conform with the idealised residual stress pattern for hot rolled sections [8.8]. This was attributed to the effect of roller straightening and the relatively light sections used (frames

3 and 4). From these measured stresses, it was impossible to apply a single residual stress pattern which would be valid along the section of beams and columns. Thus, all the models for two programs were modelled assuming zero residual stress in the member sections.

The moment-rotation characteristics are collected from the modified Sheffield database - a detailed discussion of which was presented in Chapter 3. Both moment rotation curves from the frame (i.e. using twelve different moment rotation curves in frames 1, 2, 4 and 5 and ten M-ϕ curves for frame 3) and joint tests are used in the analyses in order to study the sensitivity of the behaviour of the frame to the different moment rotation responses. The analysis was conducted using an approximate multi-linear relationship closely fitted to the M-ϕ curves obtained from the joint and frame test as shown in Figure 8.3. For the joint test, a trilinear representation was selected which closely follows the observed response. For the frame test the M-ϕ curve was assumed being the linear section from the frame test measurements and continued up to the final linear characteristic from the joint test.

Table 8.1 presents a summary of the comparison between experimental and analytically predicted ultimate capacities under beam loads only. Column (1) shows the test results. The two sets of predicted total load on beam, recorded in columns (2) to (5), are determined using the two programs in which (F) represents the M-ϕ model using the moment rotation curve extracted from the frame tests and (J) a model utilising M-ϕ data from isolated joint tests. The capacities predicted by the two programs are compared with the test results and the ratios are in columns (6) to (9). In frame 1 premature failure of a weld occurred in the joints below the predicted failure load. For frames 2 and 3 good correspondence was obtained using SERFA; slightly better than was obtained with SERVAR.

Table 8.2 shows a summary of experimental and analytically predicted ultimate capacities of the column members. Column (1) records the column head load at failure and column (2) shows the total axial loads in the lowest lift at failure. The predicted ultimate capacity of columns are also recorded in Table 8.2 and columns (3) to (6) are the total axial loads in the lowest lift of the column at failure. Columns (7) to (10) make comparisons for the column results as in Table 8.1 for beam capacities.

Comparing the predictions and test results shown in Tables 8.1 and 8.2, the average discrepancy between the actual and the predicted ultimate capacities of members from the two programs is only 4 % for beams and 9 % for columns. It is of interest to note that there is no significant difference in results predicted by using the different moment rotation curves (frame and joint tests). This indicates that the ultimate capacity of members are not

unduly sensitive to variations in M-ϕ response (ranging from modest to quite large) arising from differences in measured behaviour in the frame and joint tests. It is also noted that the predictions using SERFA are slightly higher than the ultimate capacities determined from SERVAR and are generally slightly closer to the experimental values.

The following section presents graphical comparisons of the frame moment distributions and the load deflection behaviour for the tests. Salient features of the one-to-one comparison between the test results and the two finite element programs are highlighted. Possible explanations are proposed for the discrepancies which have been observed.

8.4.1 Frames 1 and 2

The bending moment distributions at the level of design load applied to all six beams in frame 1 are shown in Figures 8.4 and 8.6 for SERFA and Figures 8.5 and 8.7 for the SERVAR. The magnitude of the moments and their distribution around the frame using different sets of the M-ϕ curves all show a good agreement with the experimental results.

In frame 1, failure of beams 5 and 6 was due to weld fracture in the connections at joints I, J, K and L. It is of interest to determine the actual ultimate capacity of these two beams assuming that the joints were adequately designed and to compare the results of two computer programs. All six beams were loaded to their design load and additional loads with 10 kN increments were then applied to beams 5 and 6 separately up to failure. The failure load was determined as 333 kN and 344 kN in the two beams using frame and joint moment rotation curves from SERFA. Failure loads of 326 kN (M-ϕ from frame test) and 330 kN (M-ϕ from joint test) were predicted in the two beams by SERVAR. Figures 8.8 and 8.9 show the load deflection response of beams 5 and 6 and a good agreement of the predictions with the test results up to the weld fracture is obtained.

In frame 2, actual failure was achieved in beams 5 and 6 due to the formation of plastic hinges at applied loads of 350 kN in beam 5 and 335 kN in beam 6. Both programs give very good predictions of response as can be seen from Figures 8.10 and 8.11 which show the load deflection plots for the predictions together with experimental results for the two beams. Again, quite similar load deflection curves are predicted when the different M-ϕ responses in the frame and joint tests are adopted in the models. This implies that the deflection of beams are not sensitive to the variation of the M-ϕ curves in different test conditions. SERFA gives the ultimate capacity of 338 kN for both beams and SERVAR

predicts a failure load of 340 kN for beam 5 and 324 kN for beam 6 when using the joint moment rotation response from the frame tests. When the M-ϕ from the joint tests are considered, the failure load increases only 6 kN to 344 kN in both beams for SERFA whilst there is no change in the ultimate capacity using SERVAR. It is noted in Table 8.2 that the error in failure loads predicted by two programs is up to only 3 %. The predictions appeared to closely simulate all aspects of the observed experimental behaviour.

8.4.2 Frame 3

A comparison of the test performance of the major axis frame with the predicted results was made. Figures 8.12 (a) and 8.13 (a) show bending moment distributions under full beam loading. It is noted that the predicted frame moments compare quite well with the experimental results. The eccentricity of the applied load produced at the head of the column due to the rotation of the column head during the beam load phase was not considered for the model. Referring to the loading arrangement recorded in Table 6.7, all beams were loaded to their dead load (about 53 kN per beam) in five equal increments. Beams 2, 3, 4 and 6 were then loaded up to their design load (about 117 kN per beam) in five equal increments with beam 5 held at its dead load value. All three columns were loaded to just above 250 kN before the central column in position 2 (CP2) was brought up to failure. The two programs indicated that the further axial load to fail the central column was 518 and 499 kN (total axial load of 781 and 762 kN in the lowest lift of column). The ultimate capacities of the central column are predicted quite well with a maximum error of 7 %. The frame moments at failure of the central column are shown in Figures 8.12 (b) and 8.13 (b) and the correspondence with the test results is again good. Figures 8.14 and 8.15 show the predicted results for beam 3 and column C4 from SERFA and SERVAR together with the experiment results and the numerical results developed by Sibai and Frey using the M-ϕ response of frame test [8.9] in a single plot. It may be observed from Figure 8.15 that SERVAR underestimates the deflection of columns which may be due to the omission of initial deflections in the model. However, the absolute difference is low being only 2 mm. Although the initial deflections have also not included in the model of SERFA, the predictions appear to closely simulate all aspects of the observed experimental response.

For the external column in position 3, as for failure of the central column, all the beams were loaded up to their design load with an exception of beam 5 which was at its dead load and all three columns were then loaded just above 250 kN. Referring to the loading arrangement recorded in Table 6.7, the central column was then loaded up to about 400 kN and

held constant. Additional load was applied to the external column in position 3 (CP3) up to failure.

The results determined for the external column in position 3 show that the programs predict total column axial loads in C9 of 760 and 768 kN from SERFA and 719 kN (the same values are determined using the frame and joint M-ϕ curves) from SERVAR. These values compare with the total axial load in the test of 766 kN. The errors for this column, recorded in Table 8.2, were only 1% and 6%. Figures 8.12 (c) and 8.13 (c) show comparisons of the frame moment for column C7 at failure of this edge column. The predictions appear to closely simulate all aspects of the observed experimental behaviour. The load deformation plot is shown in Figure 8.16 which exhibits a double value of deflection in mid-height under its maximum applied beam load when compared of the test result. It may be due to ignoring the initial curvature in the model and it would make deflection larger in prediction.

Considering the failure of beams B3 to B5, it can be seen from Table 8.1 that both programs predict a good result with an average error of only 5%. In Figures 8.12 (d) to (f) and 8.13 (d) to (f), the moments at failure of beams 4, 5 and 6 are predicted well when they are compared with the test results. The mid-spans of three beams are observed to achieve their plastic capacity. Examination of the results shows that for these three beams the predictions from the two programs predict collapse mechanisms that actually formed. A good agreement of the load deflection response for beams 3 and 5 is shown in Figures 8.17 and 8.19. However, there is a significant difference between the predictions and the test result for beams 4 as shown in Figure 8.18. It is noted in these figures that the test shows a quite similar value of the mid-span deflection of about 20 mm in beams 3, 4 and 5 at their design load (117 kN). The programs predict a lower ultimate capacity and larger deflections in beam 4 compared to beams 3 and 5 due to lack of the restraint from the column above that level. It is not surprising that both programs predicted a lower ultimate capacity and larger deflections in beam 4 than the experimental results.

The analysis described above ignored the initial deformation of the columns in both programs. To investigate the effect on the column behaviour a single curvature initial geometric imperfection of 0.001L in the column was assumed. A further run of each of the two programs to fail the central and edge columns CP2 and CP3 was conducted. No significant difference for the column capacity was found using SERFA.

The prediction from the model of SERVAR with a single curvature initial geometric imperfection in the column of 0.001L showed a modest reduction of the total axial load in

the column to cause failure and was determined as 735 kN for CP2 and 706 kN for CP3 compared with 762 kN and 719 kN respectively.

A repeated study for SERVAR was conducted to investigate how the actual initial deformation of the column affected the ultimate capacity of columns. The initial frame geometry, as shown in Figure 4.1, is used in for each analytical model to re-run the program of SERVAR. Cases 3 and 4 recorded in Table 8.3 show a set of results with the M-ϕ of the frame and joint tests used in the study. As expected, a slight drop of 5 kN was determined in the central column CP2 whilst there is no change in the ultimate capacity in the edge columns CP3.

As discussed in chapter 6, as beam loads were applied, deformation at the head of the column was produced and some eccentricity appears to have been unavoidable. Further runs of SERVAR were conducted to investigate the sensitivity of the column to the eccentricity 'e' of the applied load. With the axial load applied at eccentricities of 10 and 30 mm (cases 5 and 6 in Table 8.3), the total axial load required to cause failure of the central column in position 2 (CP2) reduced from 762 to 725 kN (no significant change occurring with an eccentricity of 10 mm) and that for the external column (CP3) reducing to 705 and 603 kN from 719 kN.

These results indicate that the collapse load of the column was relative insensitive to the initial deformation of the column but quite sensitive to the degree of eccentricity of the applied axial load. Unfortunately the exact value of the eccentricity in the test cannot be determined and Davison [8.3] identified this as a shortcoming of the experimental tests. However, eccentricities of 14 mm and 4 mm in the central and edge columns are determined from computations using the out of balance moments computed from test measurements. These values were used to re-run the program. The ultimate capacity of the central column CP2 reduces to 748 kN compared with 757 kN ignoring this effect whilst there is no significant change for the edge columns. As a result, it may be concluded that the eccentricity of the column head applied load significantly reduced the ultimate capacity of the internal column.

8.4.3 Frame 4

A study by Davison [8.3] showed that accurate prediction of the failure loads of the columns in the minor axis frame could not been undertaken using SERVAR program be-

cause it could only handle minor axis sections by assuming that they are represented by equivalent rectangular sections. This is likely to be a significant limitation for inelastic buckling because a rectangular section can have either a correct area or second moment of area corresponding to the I section to be represented; it cannot correctly represent the values of both. (The SERVAR manual had recommended that [8.2] when the rectangular cross section is adopted to replace the minor axis framed columns, the flange thickness should be assumed to zero and the web thickness should be equal to the cross section width of the 'I' section.) When a rectangular section of column was adopted to replace the minor axis column, the ultimate capacity in the lowest lift was determined as 806 kN in the edge column (CP1) and 855 kN in the central column (CP2). Thus only SERFA was used to predict the behaviour of this minor axis frame.

Figures 8.20 (a) and (b) show the bending moment distribution at failure of each of each of two columns. It is noted in these figures that the moments in the columns for test are higher than the predictions from SERVAR. This is due to failure in programs occurs when stiffness is very small but in test extra column load can be added giving much greater moment (due to distortions) i.e. moments are very sensitive to small changes in load at this condition.

The connection to the external column was observed to be more flexible than the internal one due to the absence of a similar connection on the other side of the column web as explained in chapter 6 (see Figures 6.36 to 6.38). Note that there is a significant difference in connection response between external and internal joints due to column web flexibility. Figures 8.21 and 8.22 show the comparison of the predicted and experimental deformation at the mid-height of column C1 and C5. Remembering that the actual deflections are very small (up to about 10 mm). The correspondence is initially once again quite good for both columns but deformations are underestimated at higher loads. The central deflection produced by the beam load was recorded as 1.5 mm in two columns and predicted by SERFA as about 1.4 and 1.7 mm. It is noted that the column deformation is affected by the use of different M-ϕ curves taken from the frame and joint tests; however the difference is low being only 1 mm at the end of beam load.

8.4.4 Frame 5

Frame 5 was the last frame to be studied using the two computer programs SERFA and SERVAR. Figures 8.23 and 8.24 give the experimental frame moments at the end of

the beam load phase and failure of the central column in position 2 respectively together with the predicted values from two programs. Observations show that both SERFA and SERVAR provide quite good predictions of the moment distribution around the frame. The predicted frame moments from the two programs are compared with the values determined from a new program developed by El-Rimawi [8.10] together with the test results as shown in Figure 8.25. All predicted values closely simulate the experimental results and thus the ability of the programs to mimic non-sway behaviour is further validated. At this time, El-Rimawi's program is limited to determine the behaviour of the frame at a single load level and cannot be used to determine the capacity of the column in a convenient manner.

Figure 8.26 shows the mid-height deformation of one lift of the central column under increasing load. The predicted results again appear to simulate the general response of the experimental results; the test responses lying between the deformations predicted using joint and frame M-ϕ behaviour for each of the programs.

The failure of this frame is in column lift 6, the lower length of the central column. From the frame test result, a total failure load of 1100 kN was observed. The total axial load to fail the column was predicted to be between 1252 kN and 1262 kN by SERFA and 1240 kN by SERVAR when using both sets of M-ϕ curves (frame and joint tests). It was found that no significant difference existed when the model of SERVAR was used with an initial deformation of the column and when eccentricities of 10 and 30 mm at the column head were adopted. When an eccentricity of 80 mm was considered in the model with the M-ϕ curves in frame test to re-run the program, the total axial load to failure the column dropped to 1219 kN. A re-run of SERFA with the residual stress pattern shown in Figure 8.27 indicated that the axial load to cause failure of this column drops to 1244 and 1248 kN (a reduction of only about 11 kN). Residual stress were at least present in the off cut from the column and their presence is likely to slightly reduce the strength of frame. The comparison of the results suggests that the test behaviour was influenced by yielding of the cross section at an earlier stage than the predicted result.

However, the discrepancies between the predicted and experimental ultimate capacity are probably at least partly due the eccentricity of the applied axial load at the tops of columns with residual stress having little influence.

8.5 Conclusions and Suggestions for Further Study

8.5.1 Conclusions

Two programs of SERFA and SERVAR have been used to predict the ultimate capacity of members from all five frame tests. Based on the study, some conclusions are drawn.

1. Examining the results showed that both programs can provide a good prediction for the behaviour and ultimate capacity of beams and columns.
2. Perhaps the most significant findings in this study was that the behaviour of the frame is not significantly affected by minor differences in the moment rotation characteristics used and that ultimate capacities of members and the deflection of beams were little changed by significant changes which indicates that a precise knowledge of these characteristics is not essential.
3. The study has shown that for the comparison of the test results with the predicted values from two programs, the initial deformation of the columns were found to have very little effect on the ultimate capacities of columns but eccentricity of the column head applied load significantly reduced the ultimate capacity of the columns whilst the presence of residual stresses in the members had a modest influence.

8.5.2 Suggestions for further study

SERFA uses an incremental iteration algorithm for handling the inelastic analysis in this study. The program terminates when a plastic hinge has formed in any location (joint or member). Thus it is not suitable for use to investigate the behaviour and ultimate capacity of beams. However, this problem was overcome by using a small stiffness when defining the maximum capacity of the M-ϕ curve with a large value of rotation capacity (usually the maximum capacity of joint M-ϕ curves with zero stiffness). Thus the joints cannot achieve their true plastic strength at the point where a hinge would form and the moment will increase continually.

A number of improvements are suggested as listed below :

1. In the analysis to determine of the ultimate capacity of the beams, the connections achieve their plastic capacity first and possess sufficient rotation capacity

to re-distribute moment to the beam span to form a plastic hinge at mid-span. To improve the ability of SERFA to model this response, it should be modified to include elastic-plastic analysis enabling plastic hinges to be developed at the connections and in the span of beam to form the collapse mechanism.

2. Although the standard forms of the initial deformation of column can be input, i.e. a single curvature initial geometric imperfection in the column of 0.001 L, the program cannot accept the actual initial deformation of columns. Modification should include this feature.

3. The program only handles the bare steel beam and column sections. Thus its applicability is restricted as nowadays composite structures have become a common feature in buildings. It is suggested that the program is modified to include composite sections.

4. At the time, the rotation stiffness of column bases could be input either zero (truly pin) or infinite (fully rigid). However, the columns base are in reality semi-rigid joints which provide some rotational restraint to columns. Modification of this program to take account of such behaviour is also suggested.

5. Due to the difficulty and inconvenience of using the output data in a tabular form, the author strongly recommends that some graphics facilities are developed to directly output figures e.g. load deflection curves and moment distribution around the frame.

6. This program is limited to in-plane actions, an improvement to include full three-dimensional action is suggested.

7. The predicted results from SERVAR provide good agreement with the experimental results whenever failure of beams or column was investigated. However, this program was limited to the response of frames with the columns having their major axes in the plane of the frame as described in section 8.4.3. A suggestion to include the minor axis framed column is proposed.

References

[8.1] Ahmed, I., 'A User Guide for the Finite Element Program for Semi-Rigid Frame Analysis (SERFA)', Department of Civil & Structural Engineering, University of Sheffield, August, 1992.

[8.2] Nadjai, A., 'Computer Programs Available in the Department of Civil & Structural Engineering', University of Sheffield, May, 1992.

[8.3] Davison, J. B., 'Strength of Beam-to-Column in Flexibly Connected Steel Frames', Ph.D. Thesis, University of Sheffield, England, June, 1987.

[8.4] Ahmed, I., 'Semi-Rigid Action of Steel Frames', Ph.D. Thesis, University of Sheffield, England, September, 1992.

[8.5] Rifai, A. M., 'Behaviour of Column Subassemblages with Semi-Rigid Connections', Ph.D. Thesis, University of Sheffield, England, 1987.

[8.6] Poggi, C., 'A Finite Element Model for the Analysis of Flexibly Connected Plane Steel Frames', International Journal for Numerical Methods in Engineering, Vol. 26, 1988, pp. 2239-2254

[8.7] Buller, P. S. J., 'Full Scale Steel Frame Tests : Residual Strain Evaluation', BRE report N62/87, 1987.

[8.8] Lay, M. G. and Ward, R., 'Residual Stresses in Steel Sections', Aust. Institution Steel Construction, Vol. 3(3), 1969, pp. 2-20.

[8.9] Sibai, W. A. and Frey, F., 'New Semi-rigid Joint Elements for Non-Linear Analysis of Flexibly Connected Frames', Journal of Constructional Steel Research, Vol. 25, No. 3, 1993, pp. 185-199.

[8.10] El-Rimawi, J. A., 'A Program for the Structural Analysis of 2-D Frames at Elevated Temperatures', Research Report, University of Sheffield, January, 1993.

Frame	Test	Failure Member	Total Applied Beam Load (kN)					Capacity Comparisons			
			(1)	(2)	(3)	(4)	(5)	(6)	(7)	(8)	(9)
			Test Result	Analysis				Analysis / Test			
				SERFA		SERVAR					
				F	J	F	J	(2)/(1)	(3)/(1)	(4)/(1)	(5)/(1)
1	29	B5 [a]	260	333	344	326	330	-	-	-	-
		B6 [b]	297	333	344	326	330	-	-	-	-
2	42	B5	350	338	344	340	340	0.97	0.98	0.97	0.97
		B6	335	338	344	324	326	1.01	1.03	0.97	0.97
3	4	B3	145	147	147	136	136	1.01	1.01	0.93	0.93
		B4	147	137	137	131	131	0.93	0.93	0.90	0.90
		B5	138	147	147	134	134	1.07	1.07	0.97	0.97

[a] failure due to weld fracture of connections
[b] failure due to weld fracture of connections

Remark : In table (1) - (5) for B3 - B6 loads are total loads on beam
F for M-ϕ of frame tests
J for M-ϕ of joint tests

Table 8.1 : Comparison of Experimental and Predicted Results of Ultimate Capacity of Beams using SERFA and SERVAR

Frame	Test	Failure Member	Load in Column at Failure (kN)						Capacity Comparisons			
			(1)	(2)	(3)	(4)	(5)	(6)	(7)	(8)	(9)	(10)
			Test Result		Analysis				Analysis / Test			
					SERFA		SERVAR					
					F	J	F	J	(3)/(2)	(4)/(2)	(5)/(2)	(6)/(2)
3	2	CP2	464	727	781	781	762	762	1.07	1.07	1.05	1.05
		CP3	620	766	760	768	719	719	0.99	1.00	0.94	0.94
4	3	CP1	468	646	706	706	(806)	(806)	1.09	1.09	-	-
		CP2	404	728	823	823	(855)	(855)	1.13	1.13	-	-
5	17	CP2	490	1100	1252	1262	1240	1240	1.13	1.13	1.13	1.13

Remark : In table (1) for column head load at failure
Columns (2) - (6) loads in CP1 - CP3 are total axial loads in the lowest lift which is determined from the Applied Column Load plus Half of the Loads Applied to Each Connected Beam above the Section
F for M-ϕ of frame tests
J for M-ϕ of joint tests
( ) elastic buckling due to use rectangular section to replace the minor axis framed column

Table 8.2 : Comparison of Experimental Results to Predicted Results of Column Failure Loads from SERFA and SERVAR

Frame	Test	Failure Member	Test Result	Load in Column at Failure (kN)					
				SERVAR (Study Cases)					
				1 (F)	2 (J)	3 (F1)	4 (J1)	5 (J2)	6 (J3)
3	2	CP2	727	762	762	757	757	757	725
		CP3	766	719	719	719	719	705	603
5	17	CP2	1100	1240	1240	1240	1240	1240	1238

Remark : F : no initial deflection, M-ϕ of frame tests e=0
J : no initial deflection, M-ϕ of joint tests e=0
F1 : with initial deflection, M-ϕ of frame test e=0
J1 : with initial deflection, M-ϕ of joint tests e= 0
J2 : with initial deflection, M-ϕ of joint test, e=10mm
J3 : with initial deflection, M-ϕ of joint test, e=30mm

Table 8.3 : Predicted Results based on Different Factors considered in the Model of SERVAR

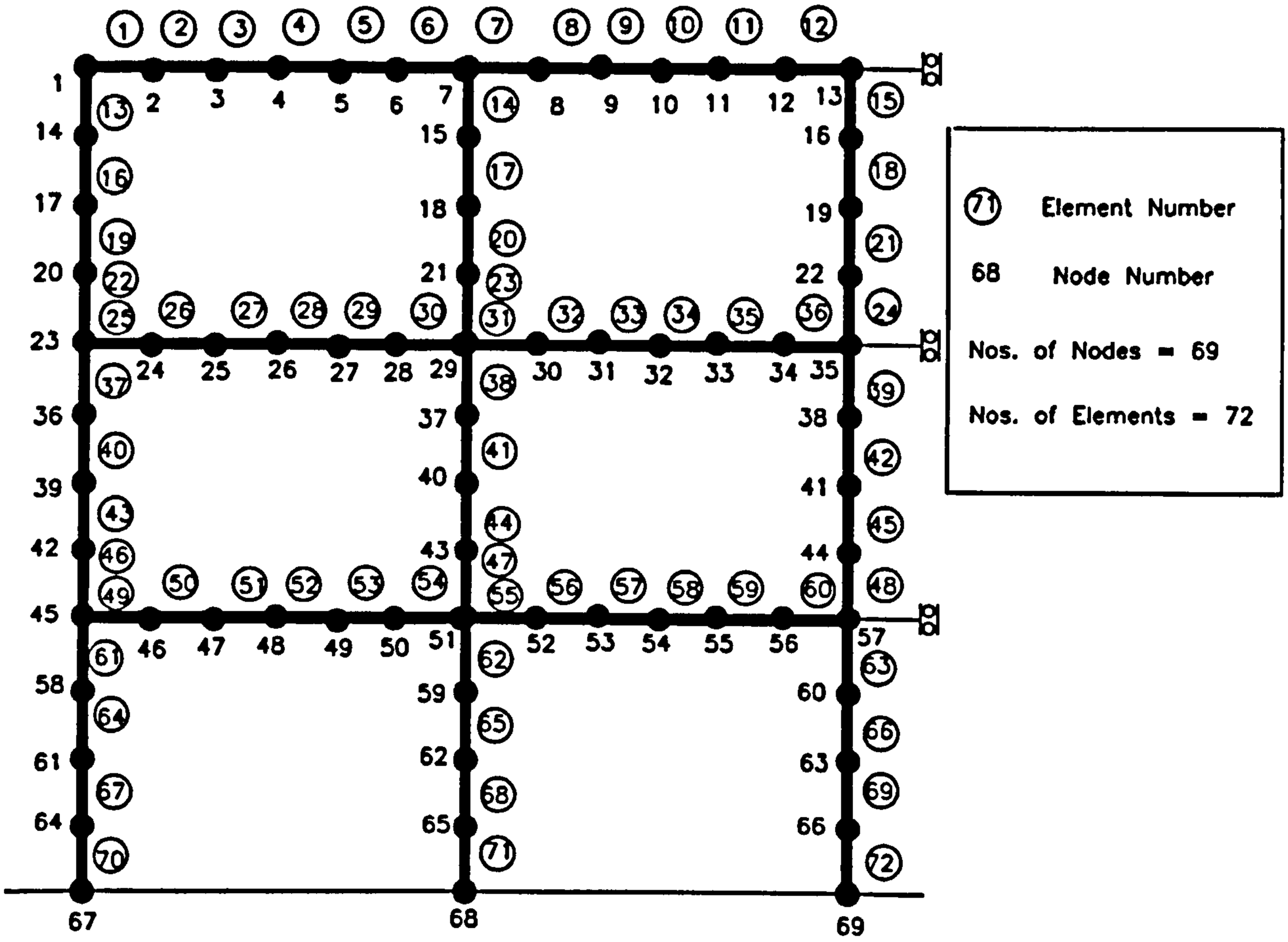

Figure 8.1 : Model designed for SERFA

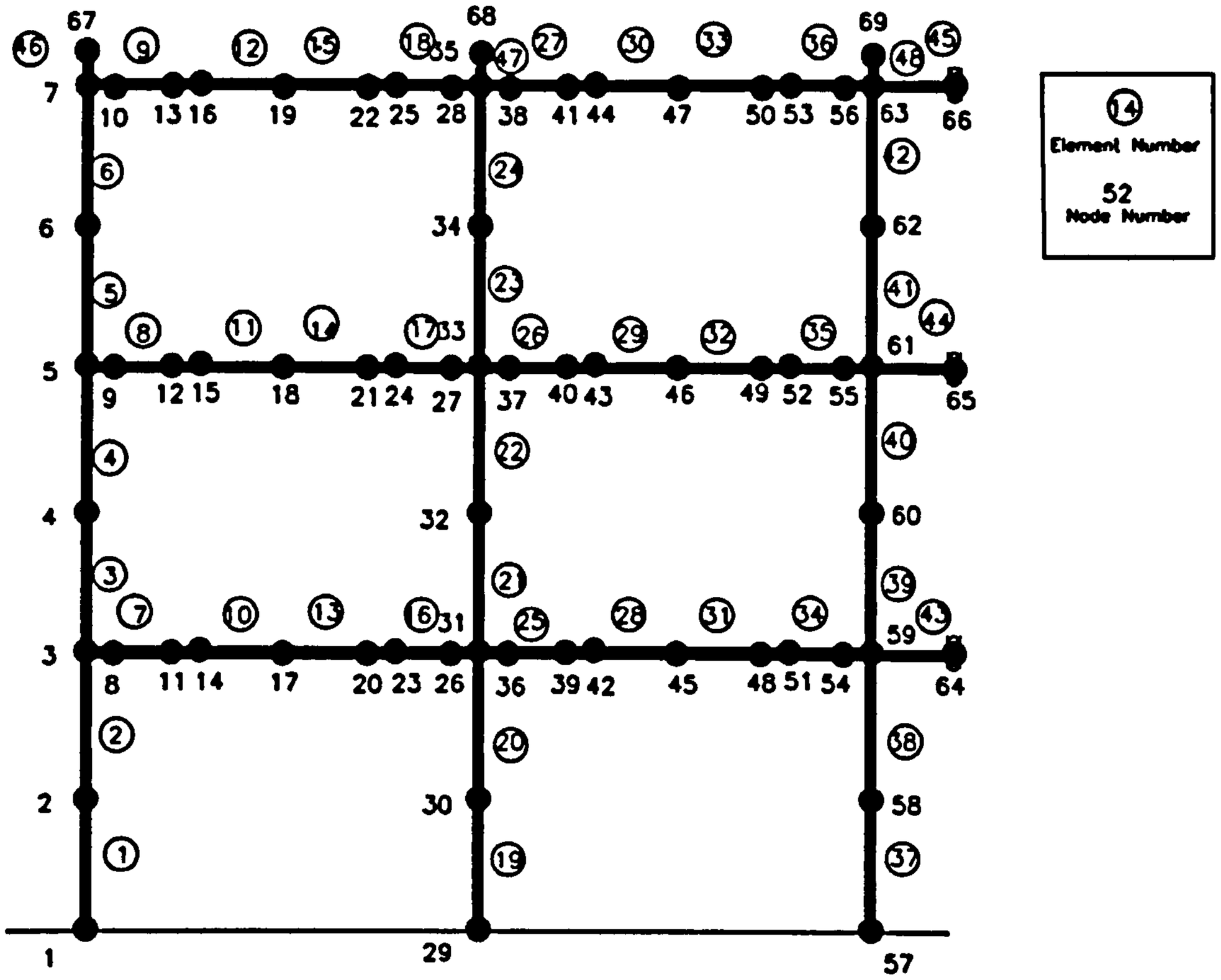

Model Designed to Frames 1, 2, 4 & 5 for SERVAR

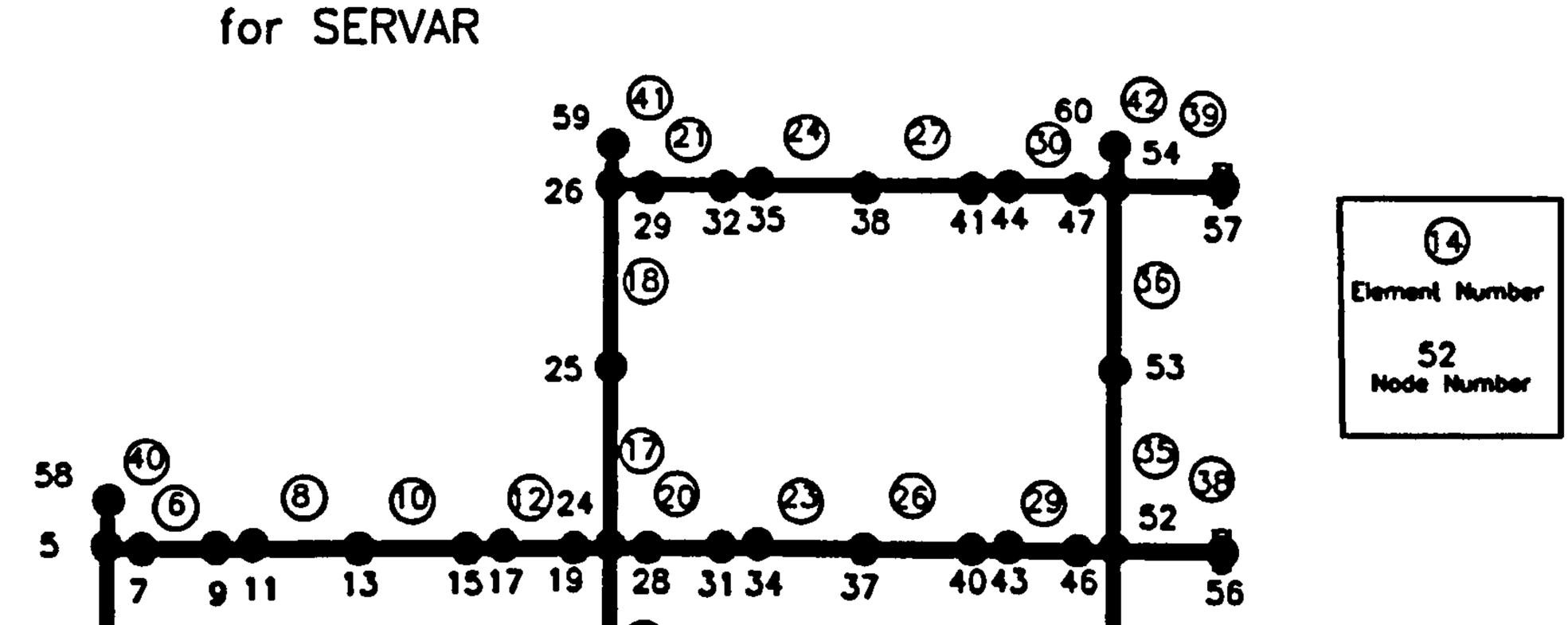

Model Designed to Frame 3 for SERVAR

Figure 8.2 : Models designed for SERVAR

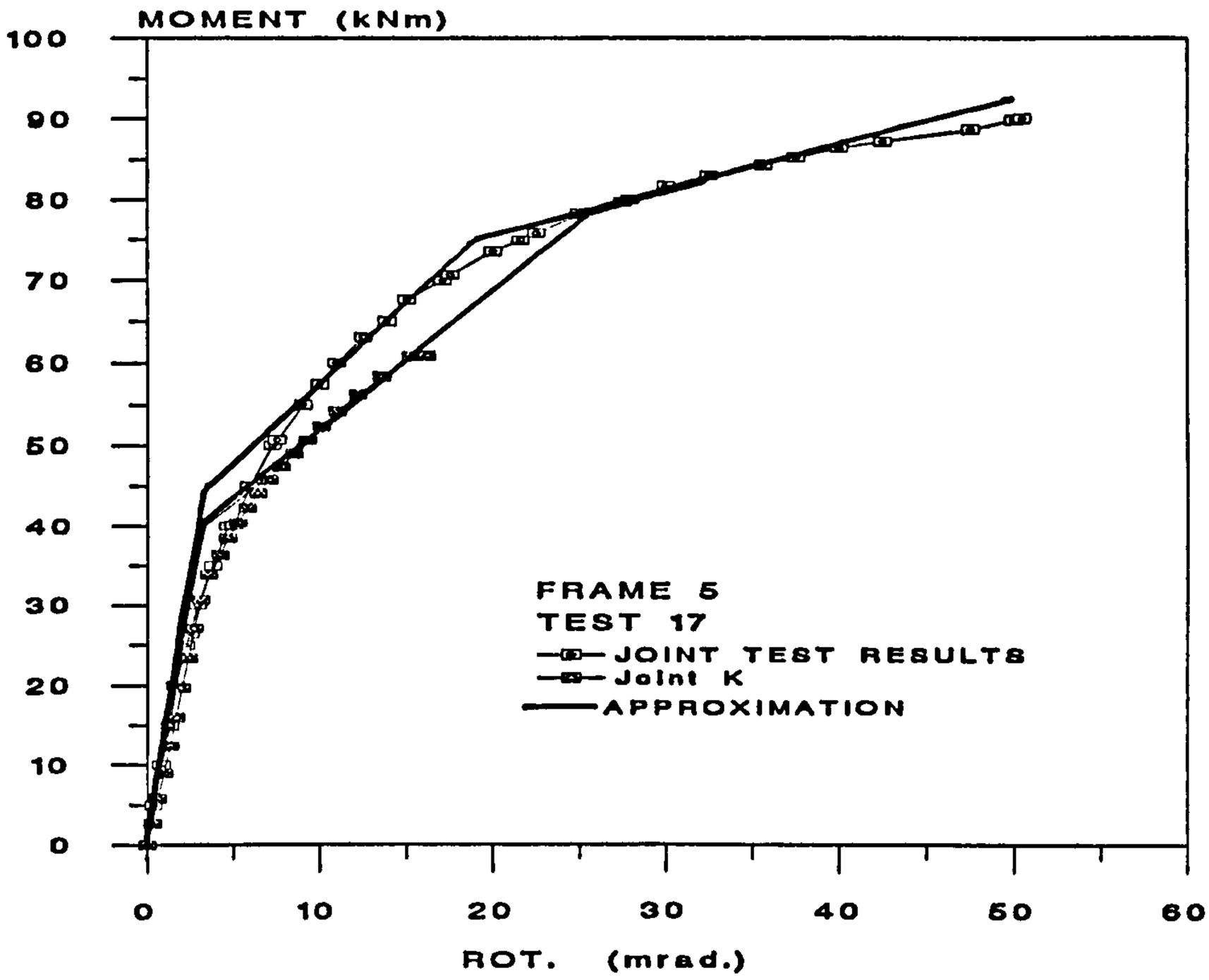

Figure 8.3 : Linearised Moment Rotation Characteristics used in the Computer Programs

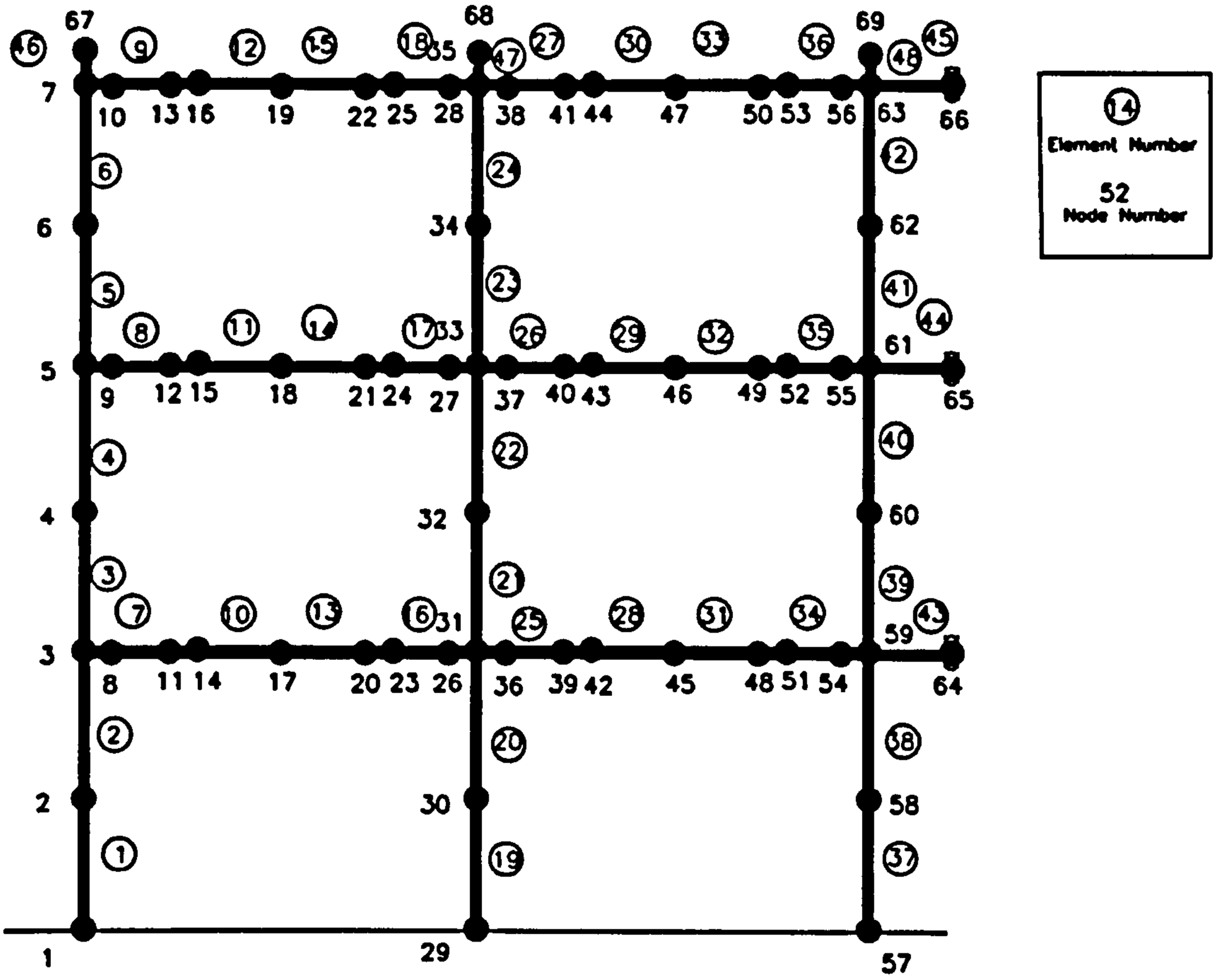

Model Designed to Frames 1, 2, 4 & 5 for SERVAR

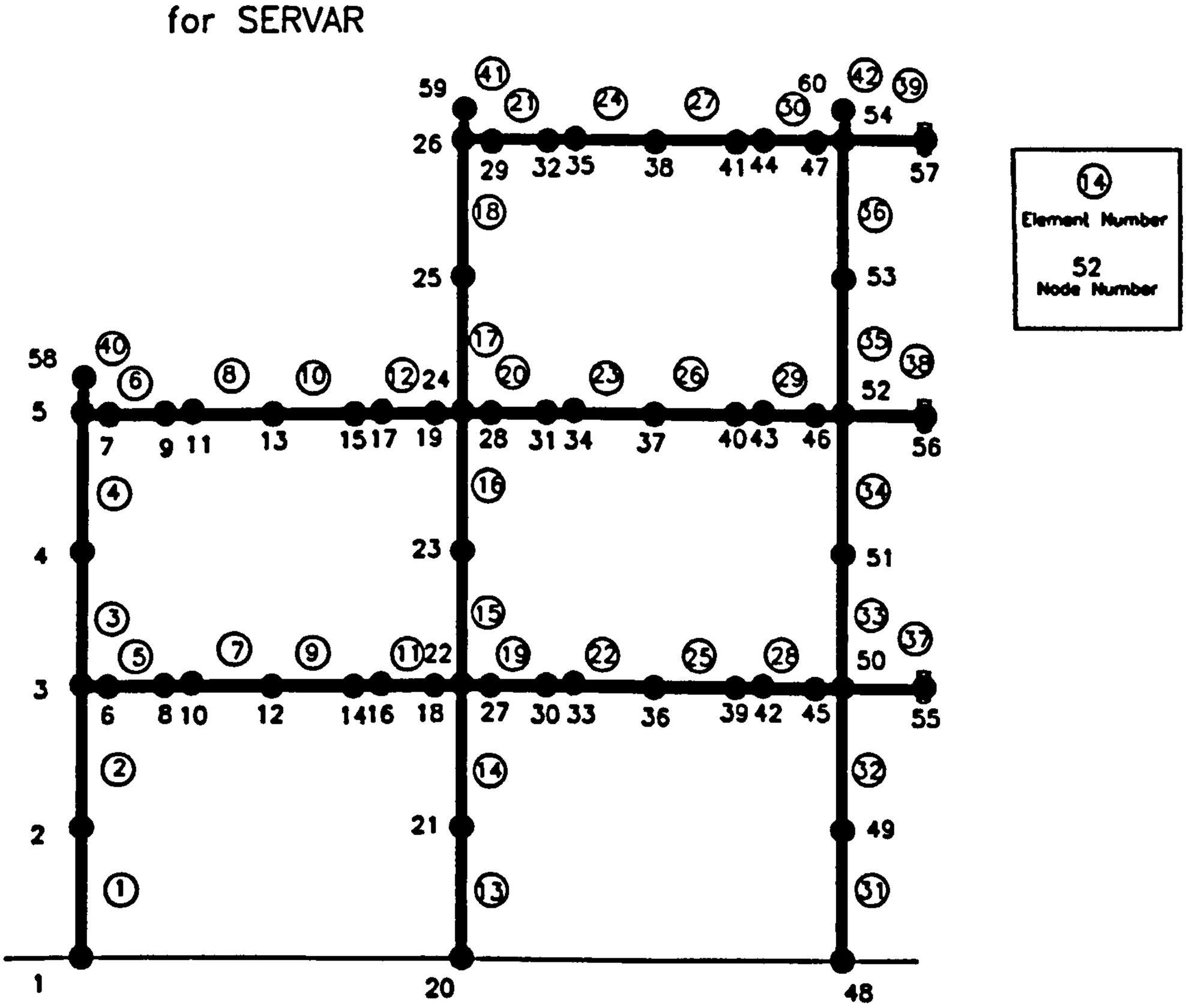

Model Designed to Frame 3 for SERVAR

Figure 8.2 : Models designed for SERVAR

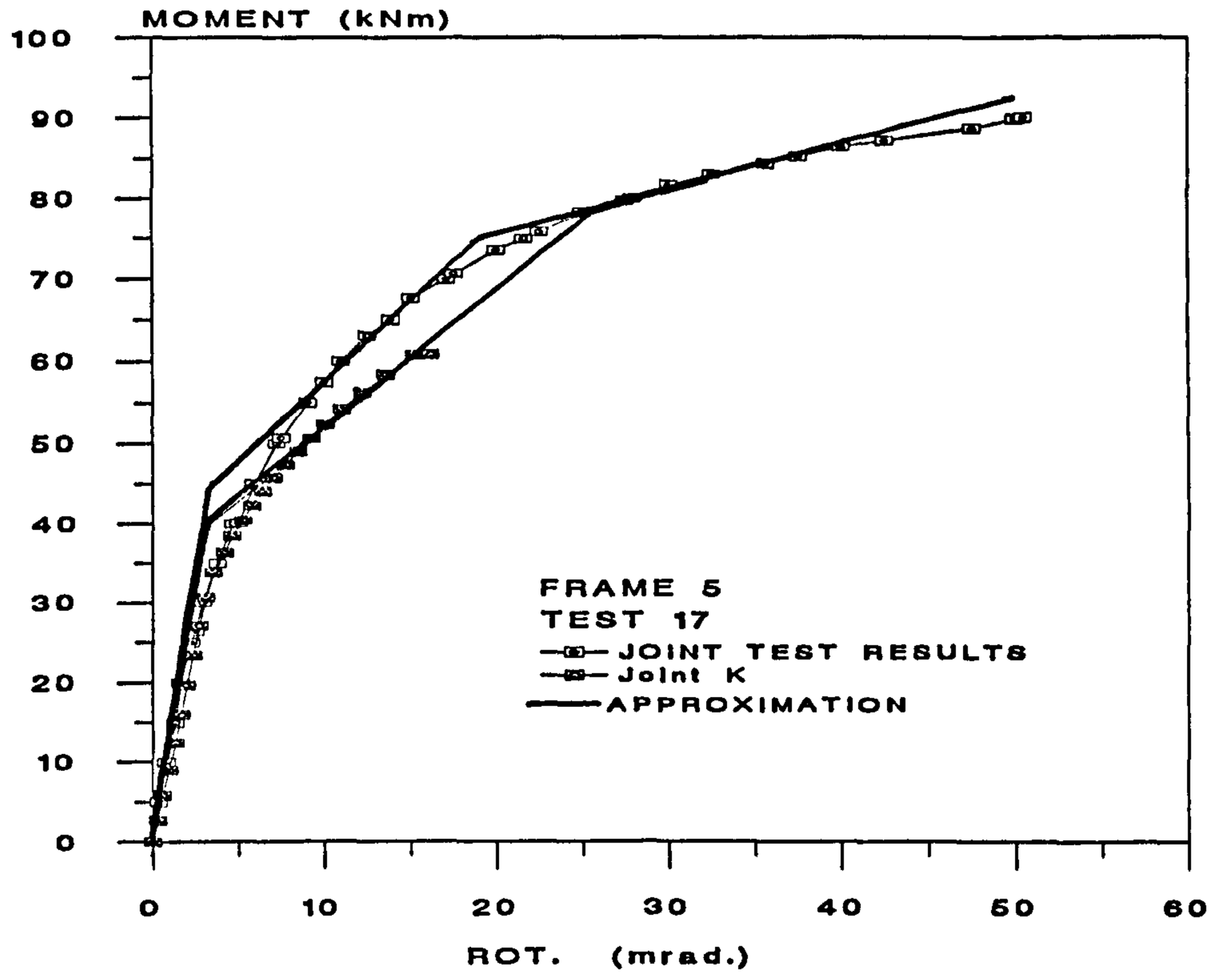

Figure 8.3 : Linearised Moment Rotation Characteristics used in the Computer Programs

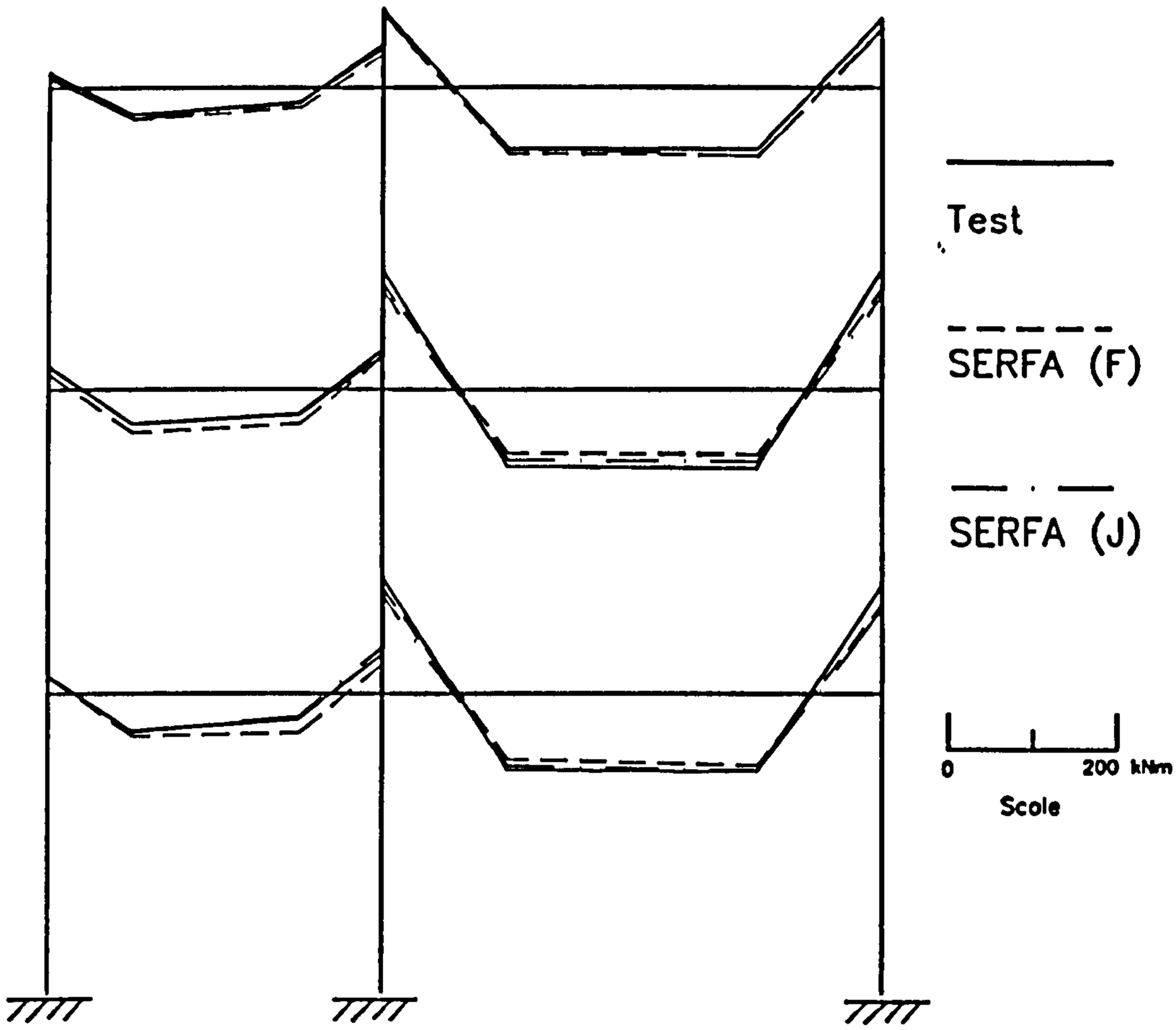

Figure 8.4 : Comparison of Test Moments to Prediction at End of Beam Load Phase in Test 28 of Frame 1 (SERFA)

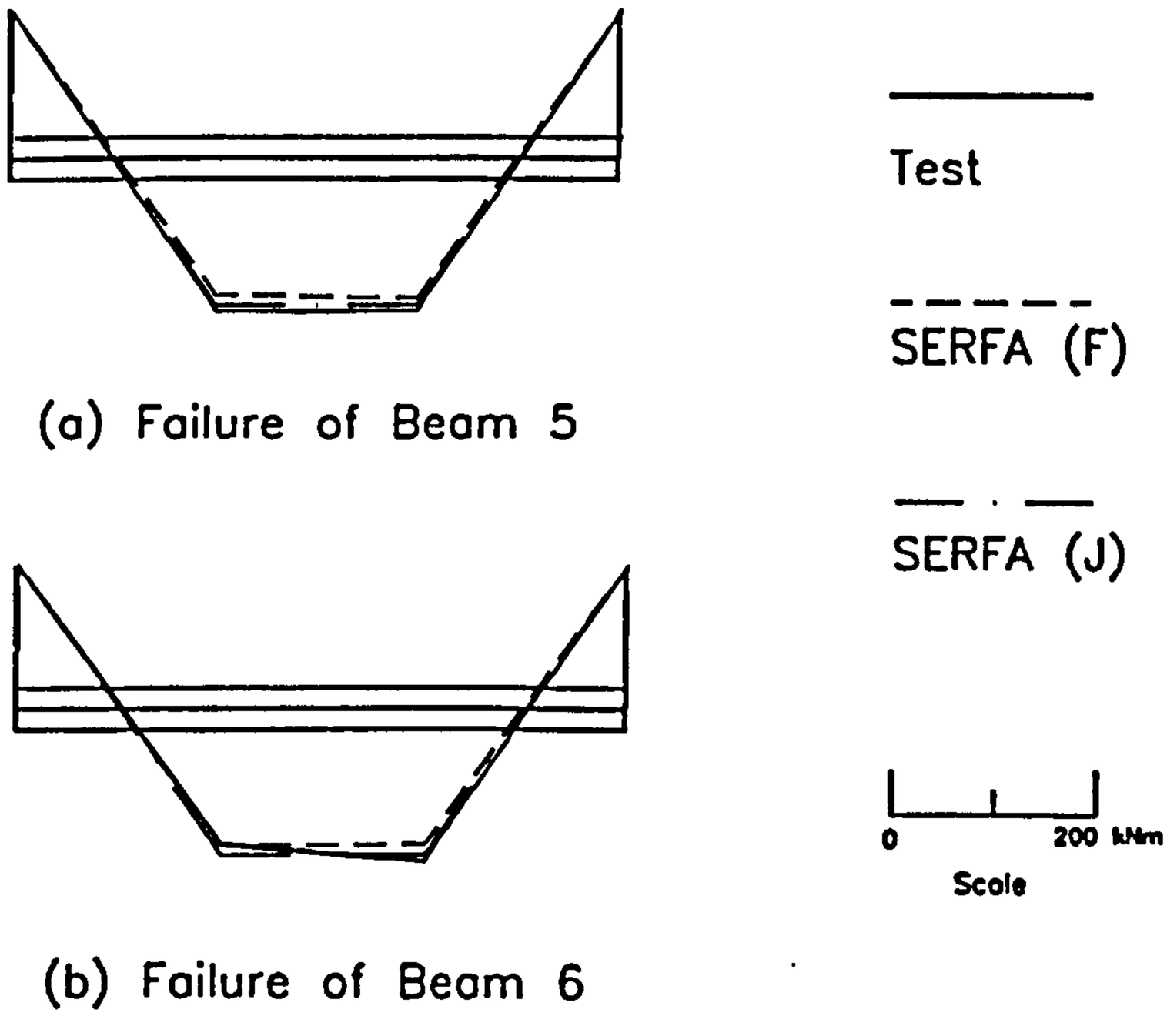

(a) Failure of Beam 5

(b) Failure of Beam 6

Figure 8.5 : Comparison of Test Moments to Prediction at Failure of Beam 5 and 6 in Test 42 of Frame 2 (SERFA)

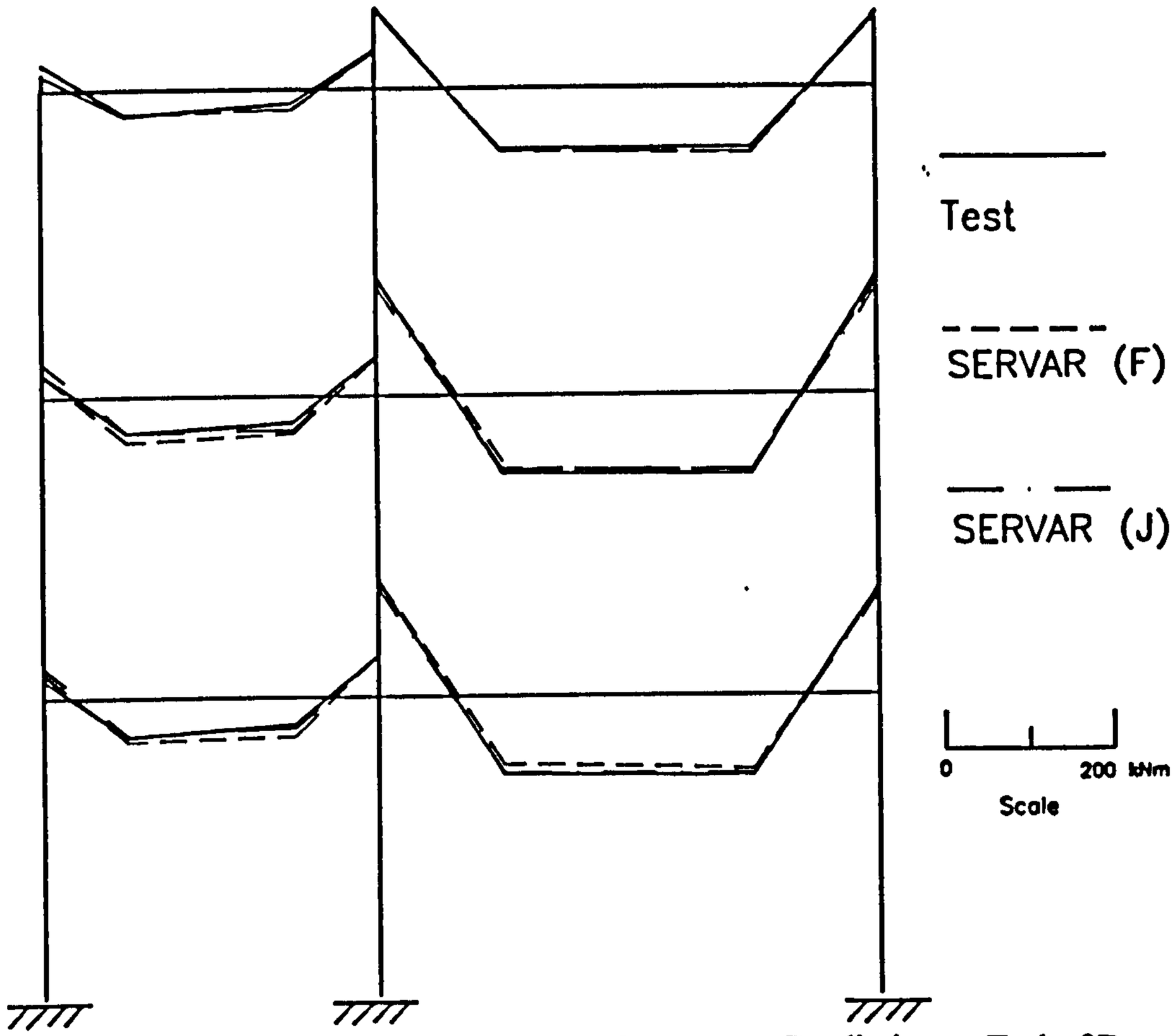

Figure 8.6 : Comparison of Test Moments to Prediction at End of Beam Load Phase in Test 28 of Frame 1 (SERVAR)

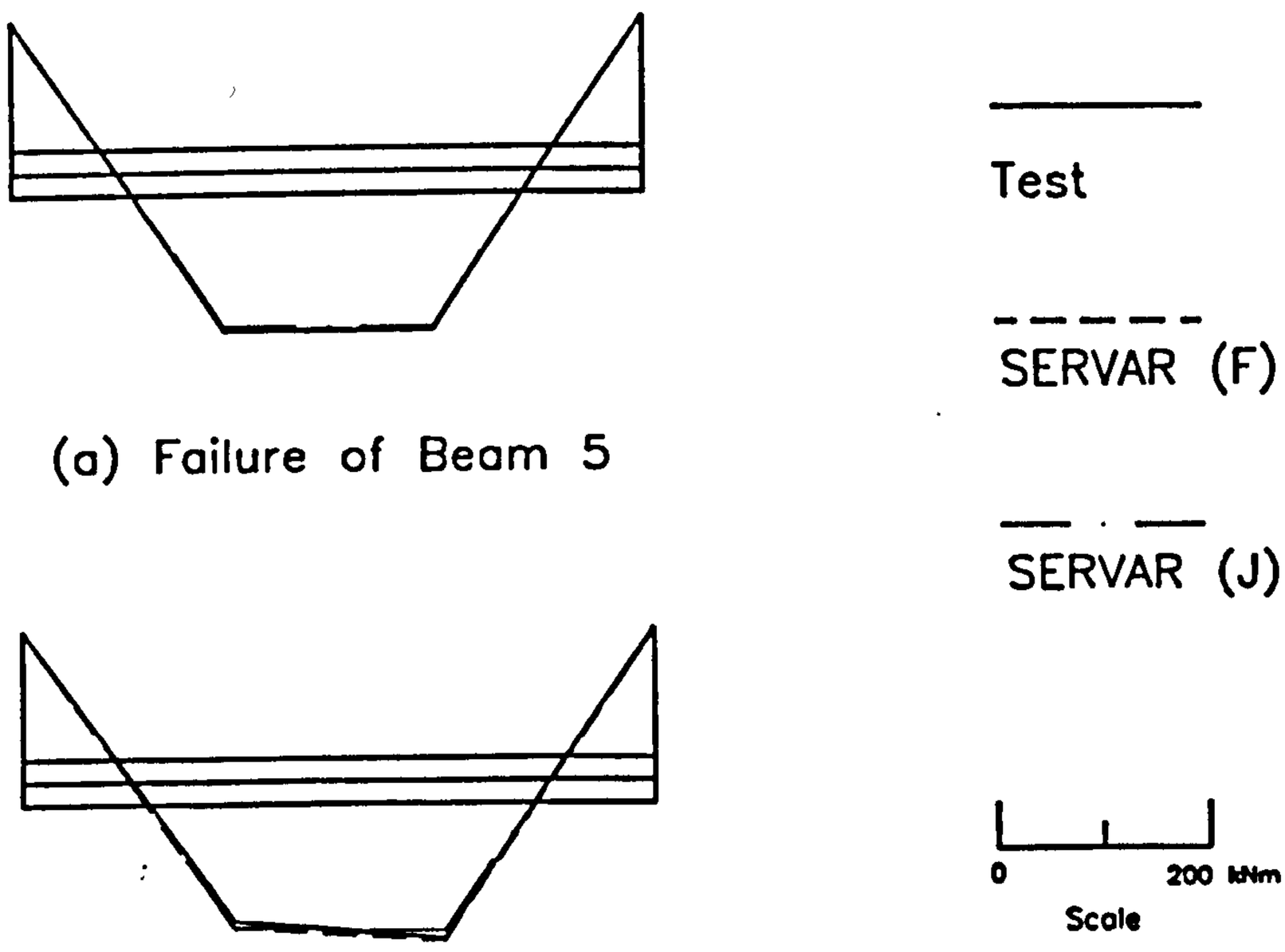

(a) Failure of Beam 5

(b) Failure of Beam 6

Figure 8.7 : Comparison of Test Moments to Prediction at Failure of Beam 5 and 6 in Test 42 of Frame 2 (SERVAR)

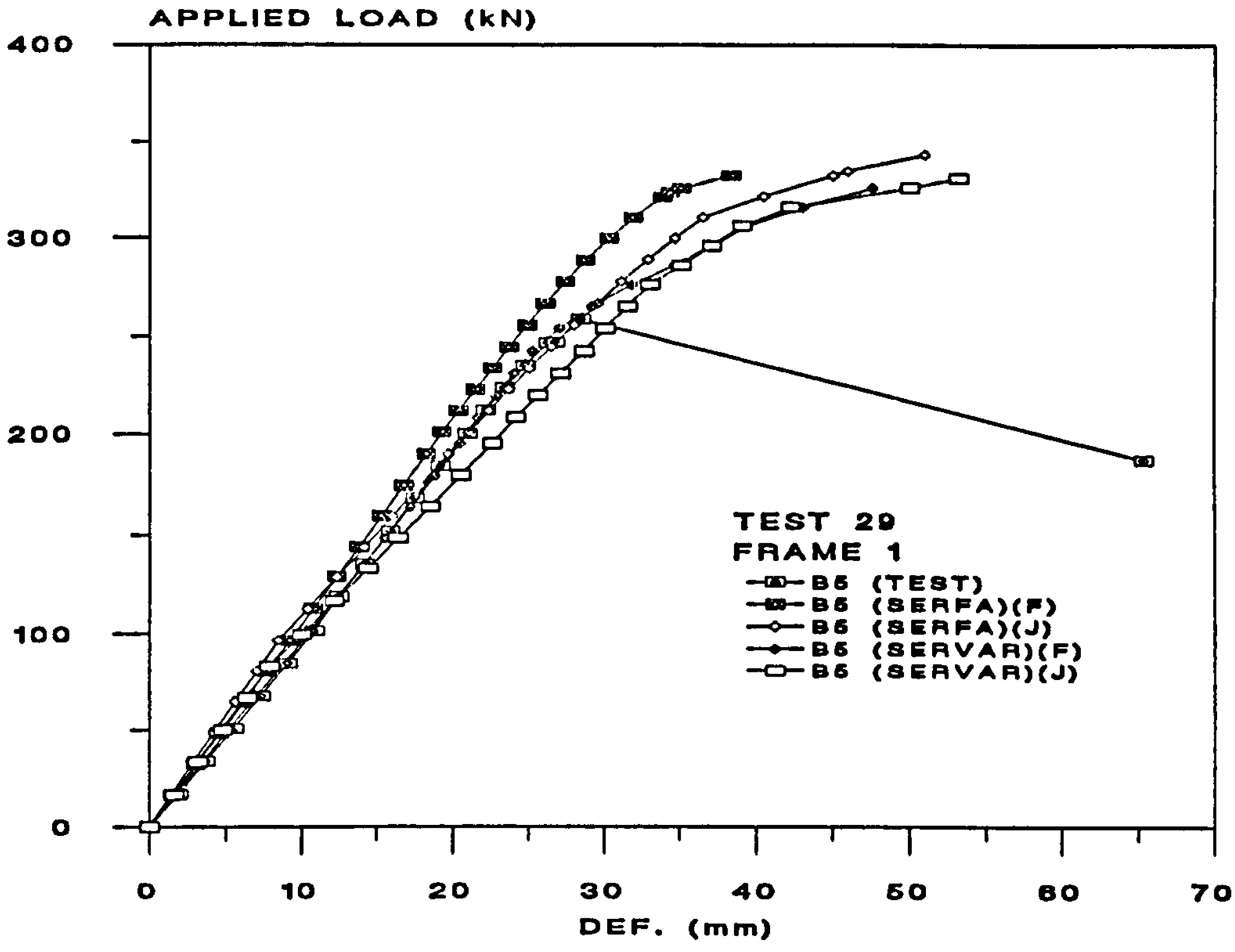

Figure 8.8 : Comparison of Predicted and Test Total Applied Load against the Mid-Span Deflection of Beam 5 in Test 29 of Frame 1

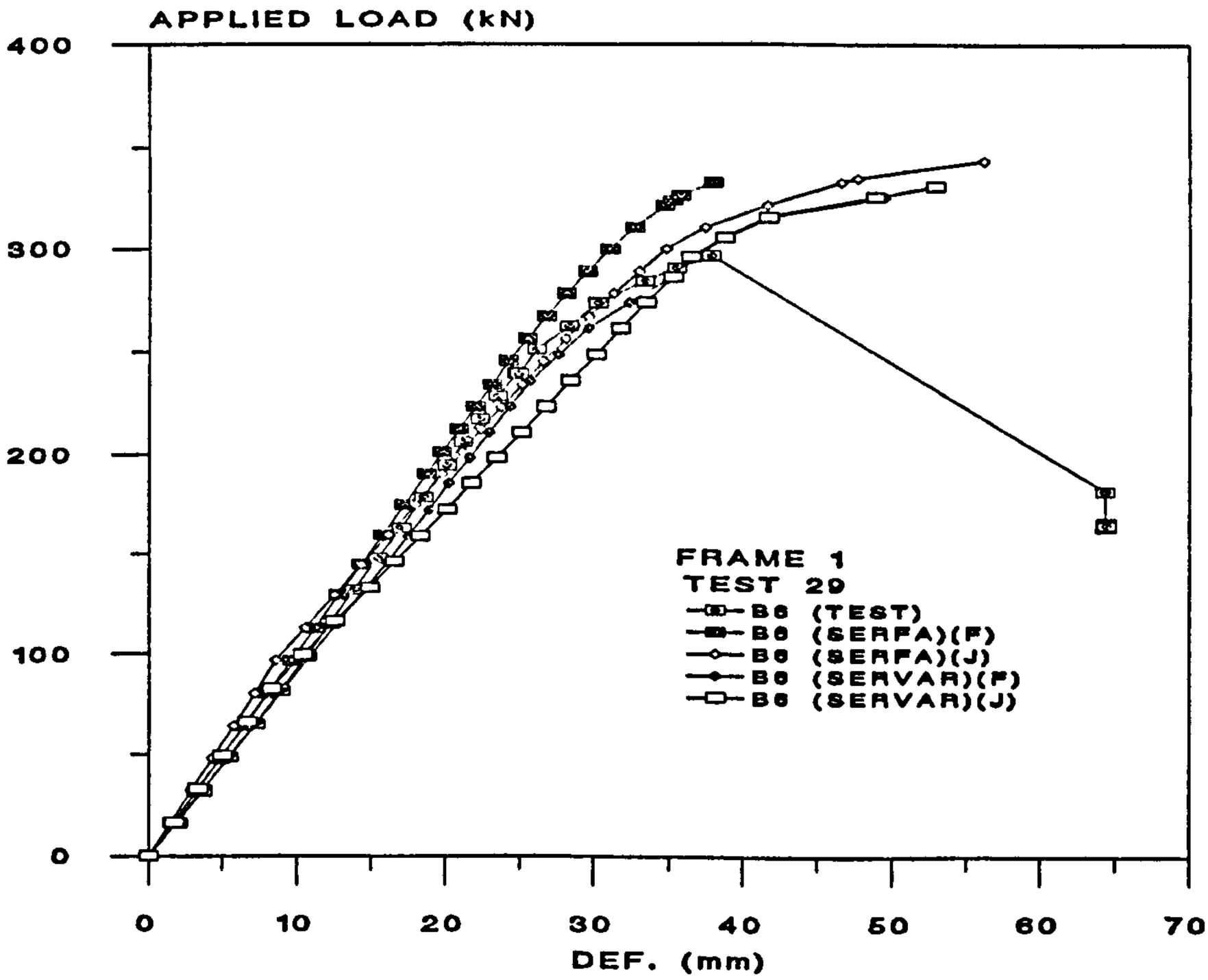

Figure 8.9 : Comparison of Predicted and Test Total Applied Load against the Mid-Span Deflection of Beam 6 in Test 29 of Frame 1

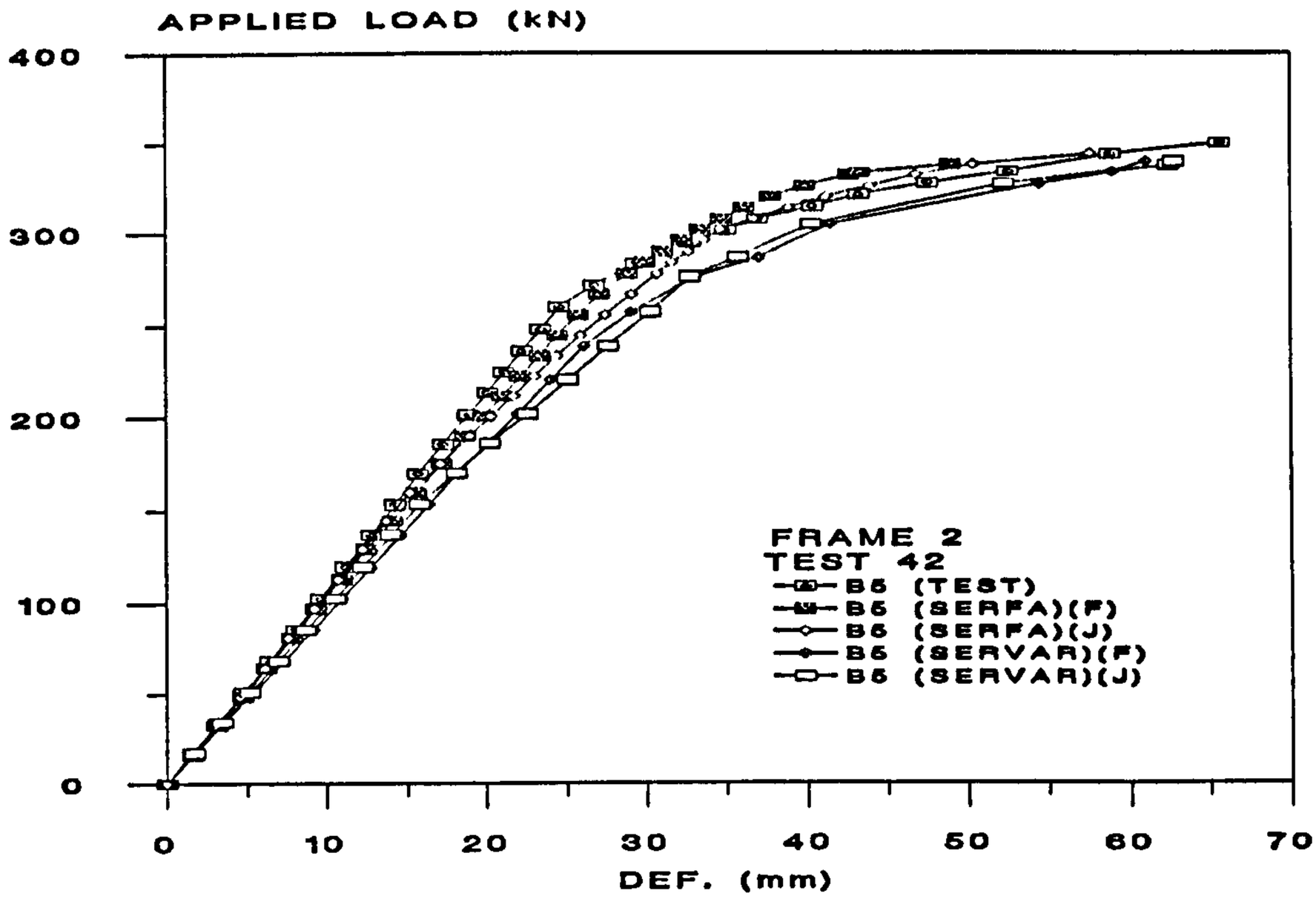

Figure 8.10 : Comparison of Predicted and Test Total Applied Load against the Mid-Span Deflection of Beam 5 in Test 42 of Frame 2

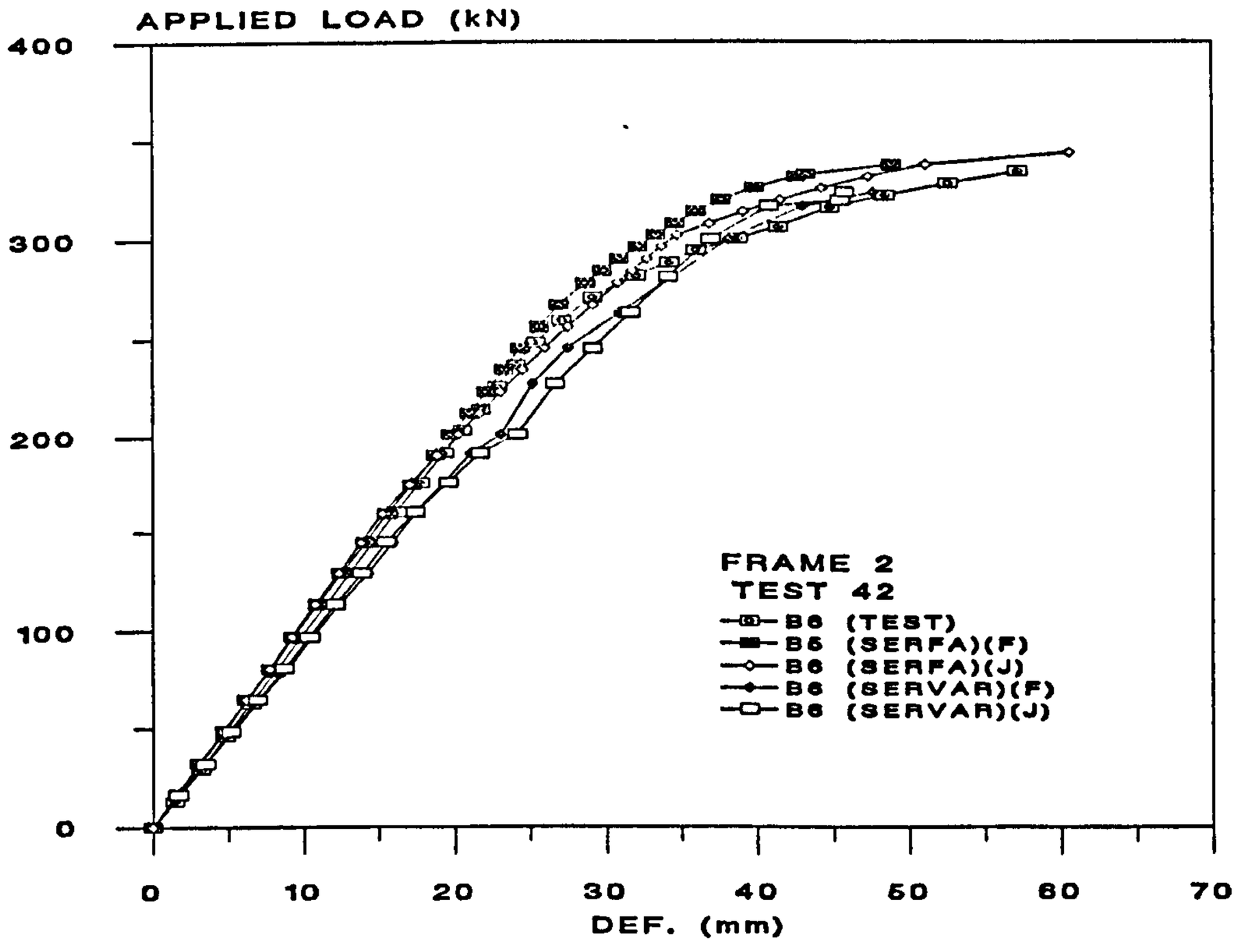

Figure 8.11 : Comparison of Predicted and Test Total Applied Load against the Mid-Span Deflection of Beam 6 in Test 42 of Frame 2

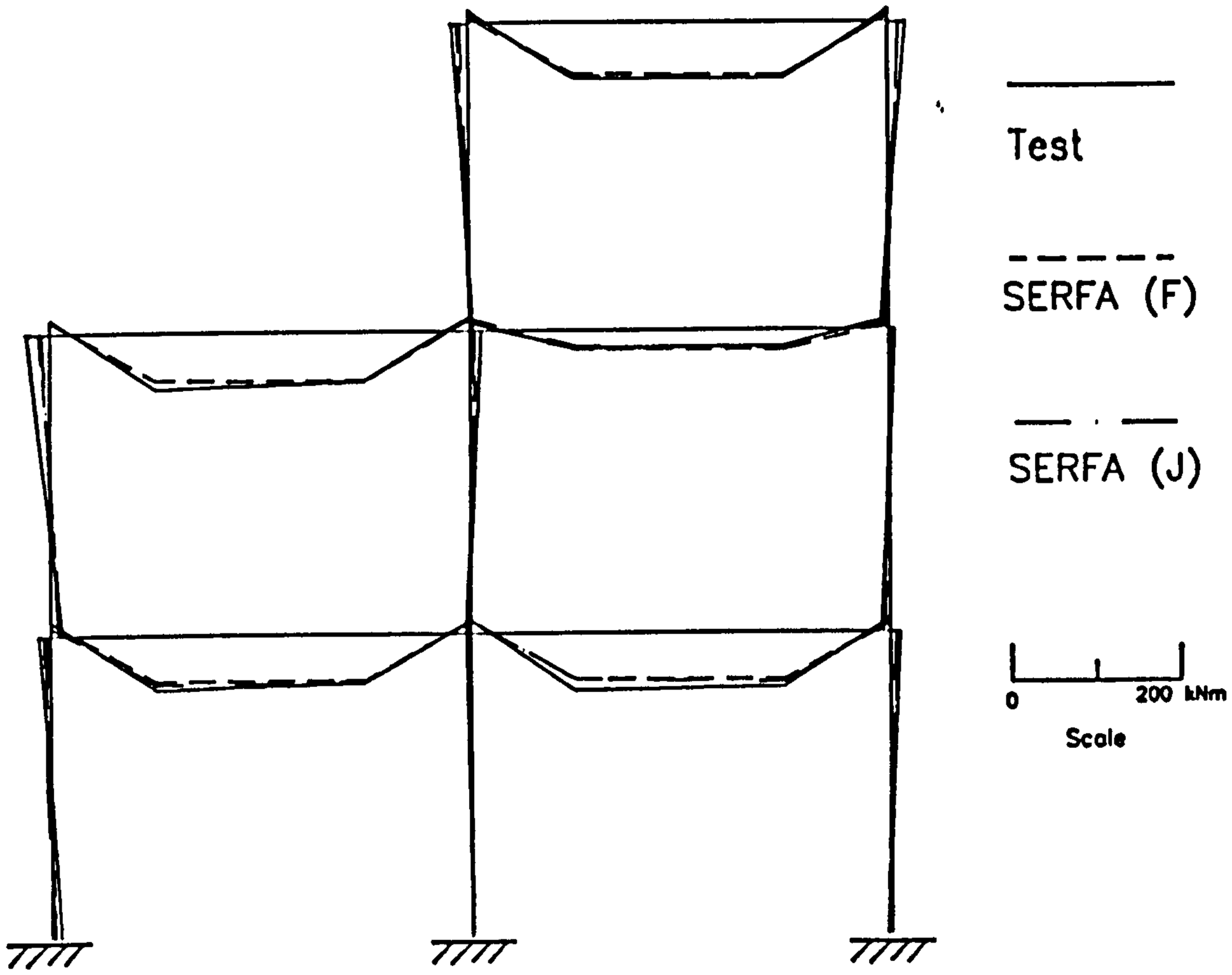

(a) End of Beam Load Phase

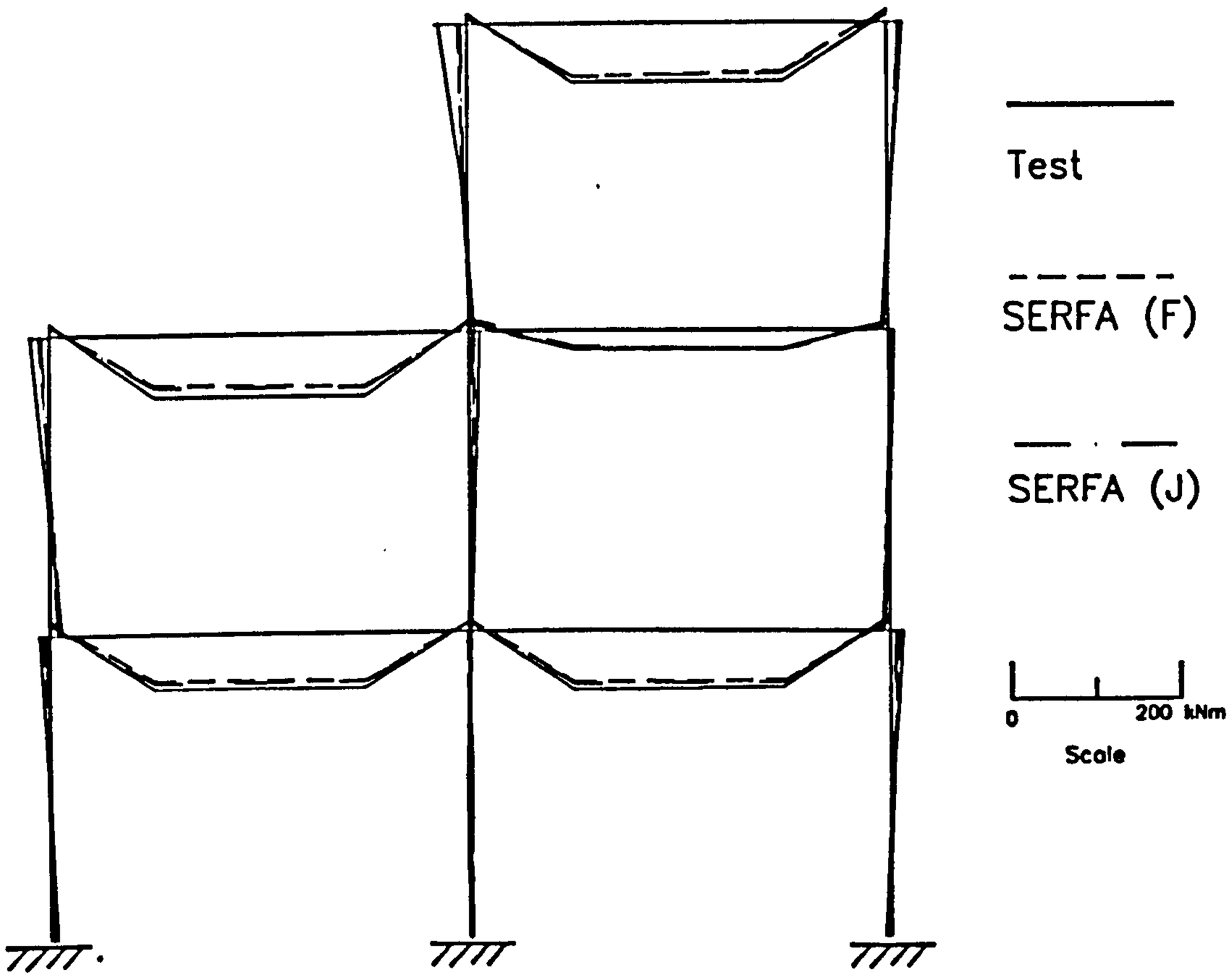

(b) Failure of Central Column in Position 2

Figure 8.12 : Comparison of Test Moments to Predictions of Frame 3 from SERFA

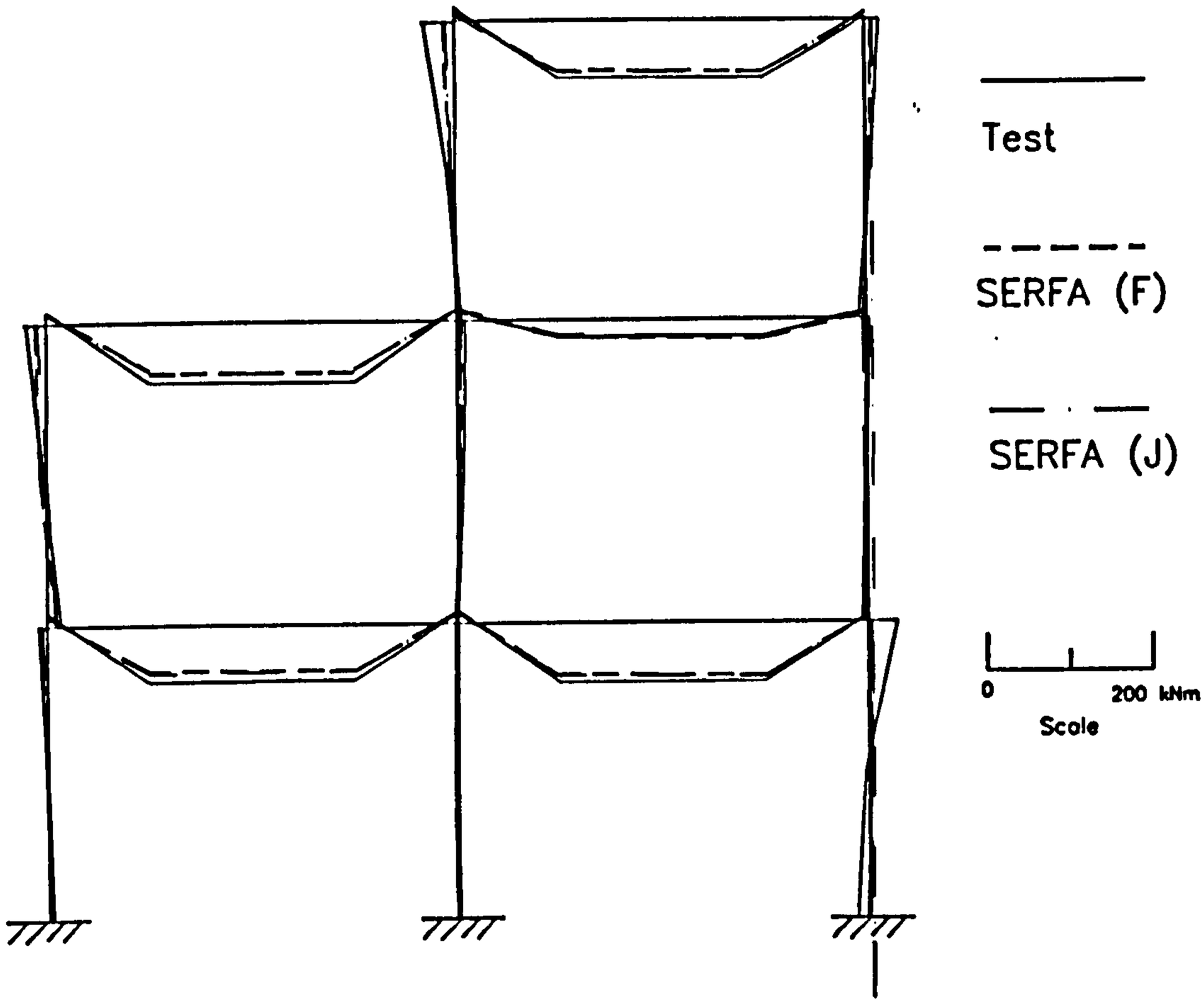

(c) Failure of the Edge Column in Position 3

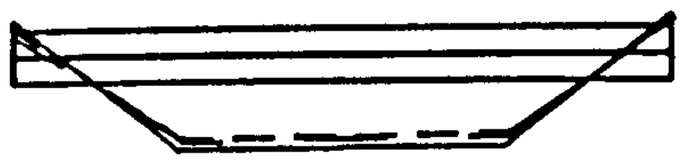

(d) Failure of Beam 3

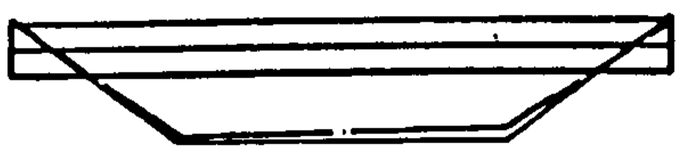

(e) Failure of Beam 4

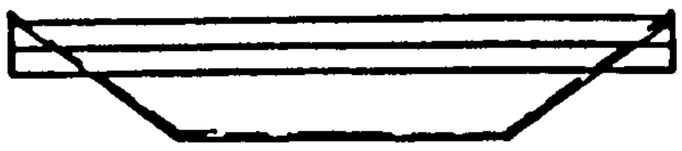

(f) Failure of Beam 5

Figure 8.12 : Comparison of Test Moments to Predictions of Frame 3 from SERFA (cont'd)

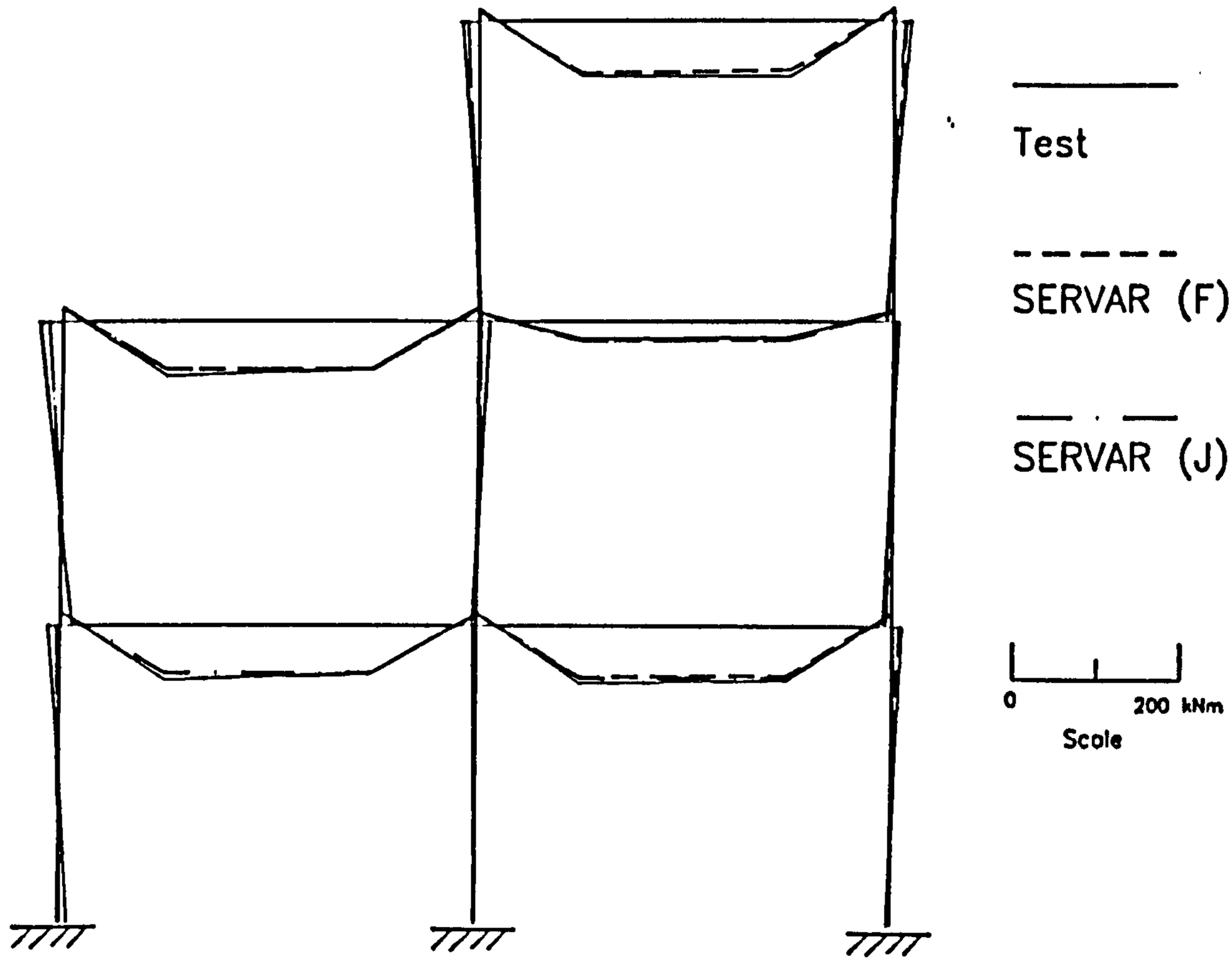

(a) End of Beam Load Phase

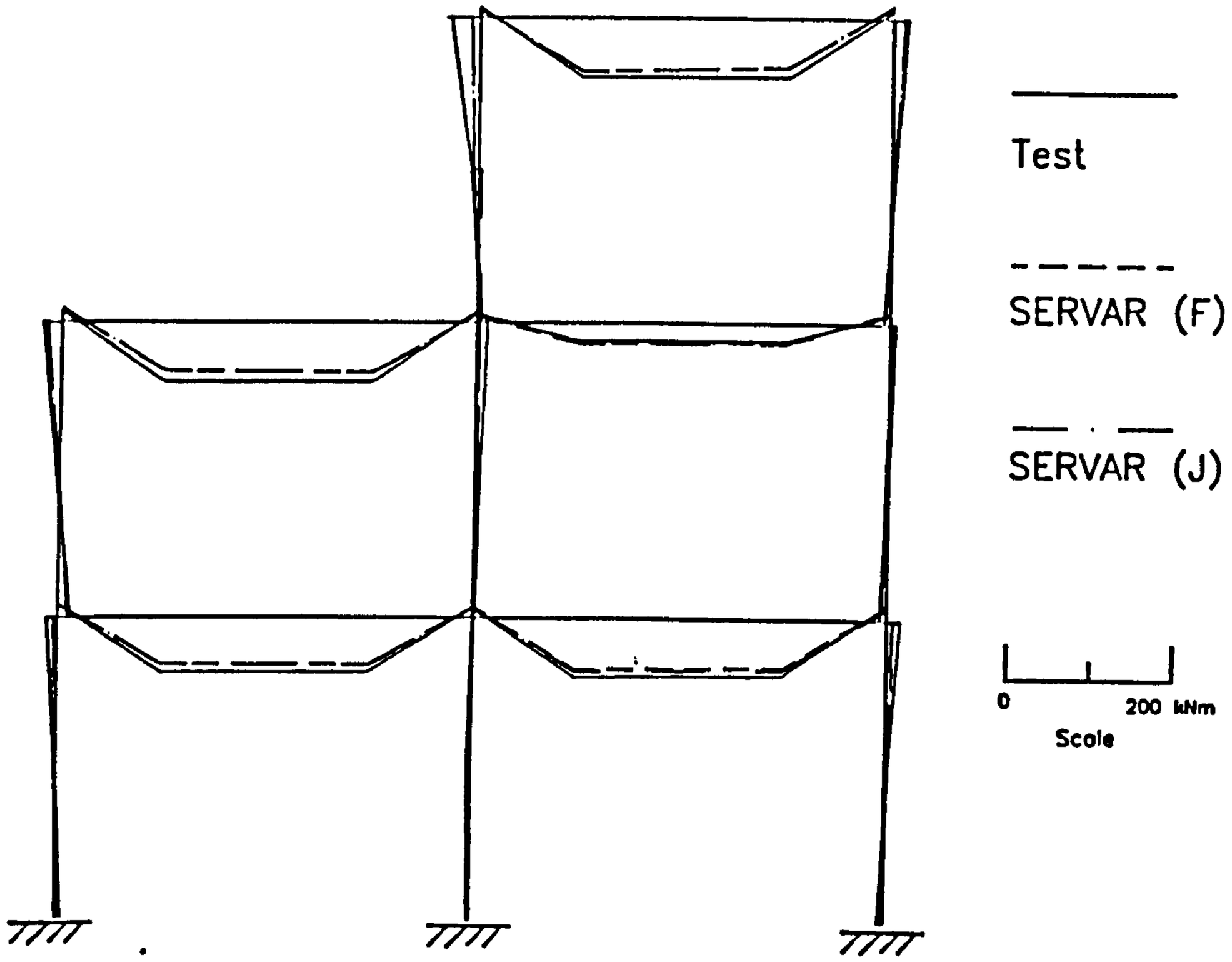

(b) Failure of Central Column in Position 2

Figure 8.13 : Comparison of Test Moments to Predictions of Frame 3 from SERVAR

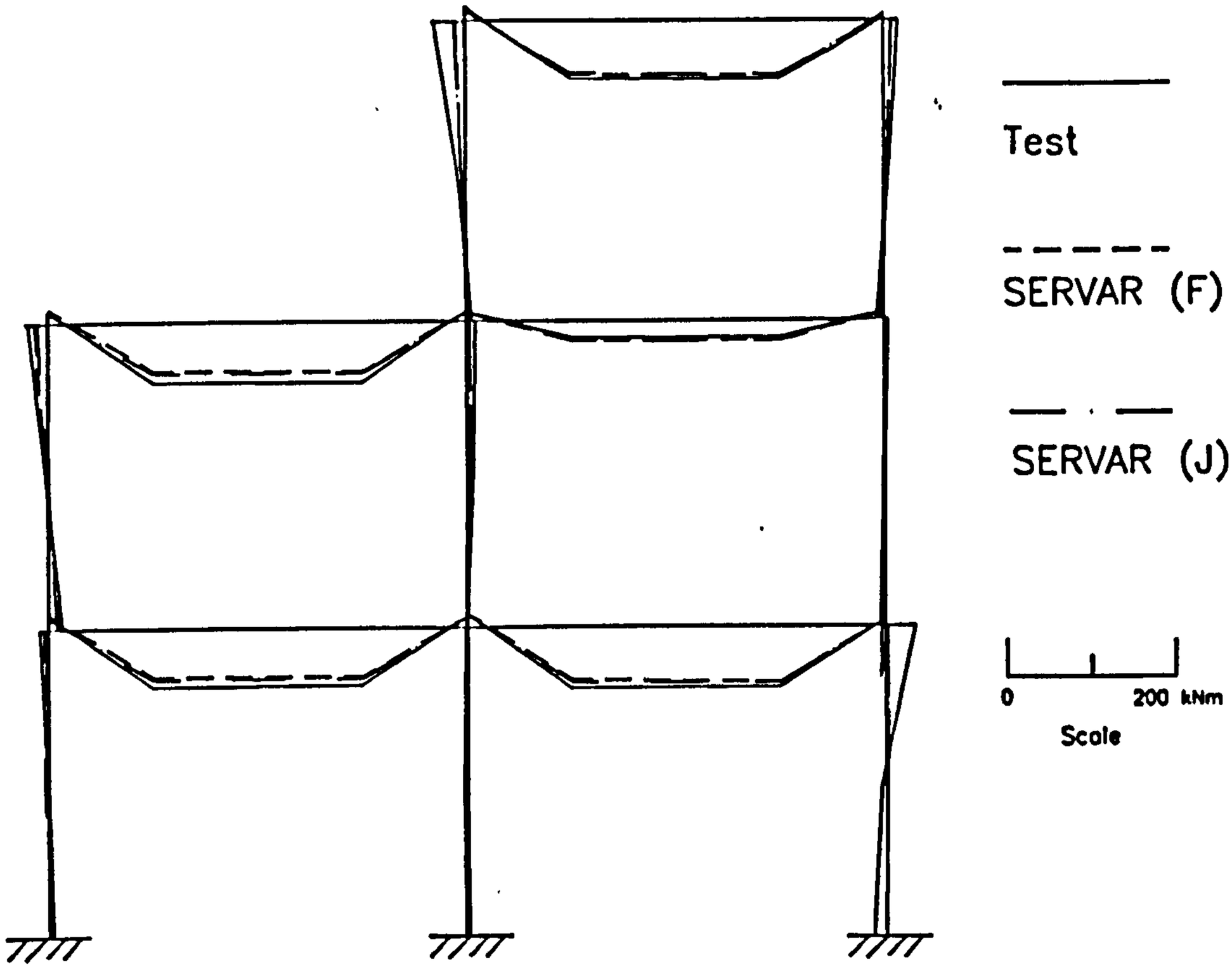

(c) Failure of the Edge Column in Position 3

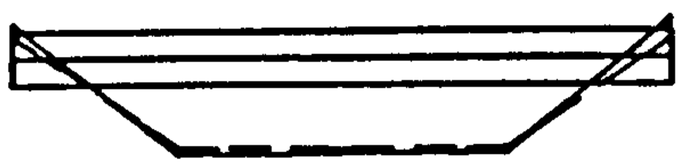

(d) Failure of Beam 3

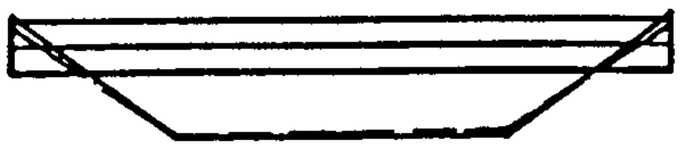

(e) Failure of Beam 4

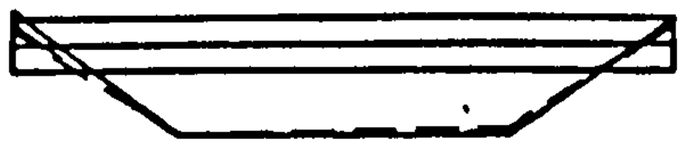

(f) Failure of Beam 5

Figure 8.13 : Comparison of Test Moments to Predictions of Frame 3 from SERVAR (cont'd)

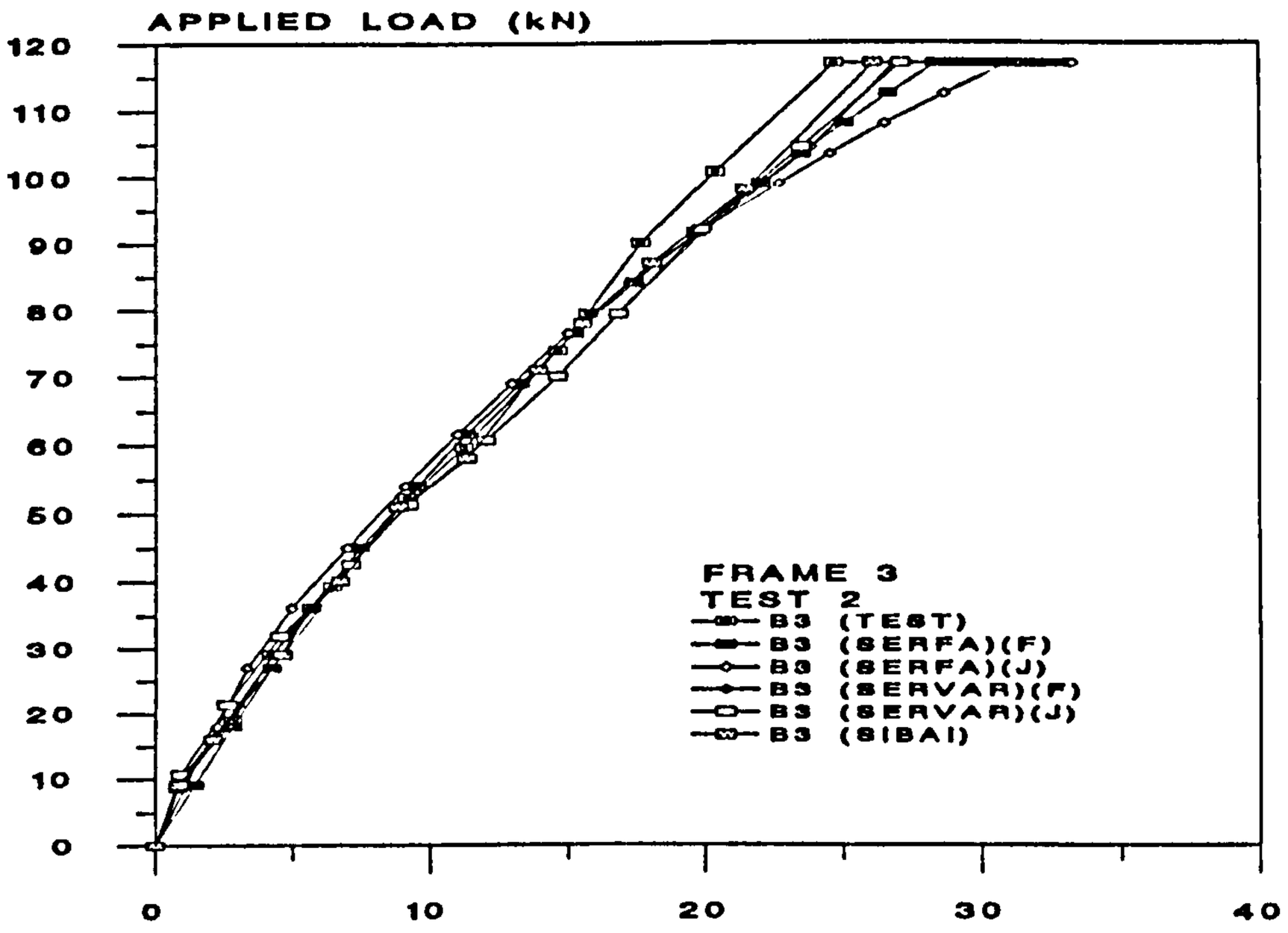

Figure 8.14 : Comparison of Predicted and Test Total Load against Mid-Span Deflection of Beam B3 in Test 2 of Frame 3

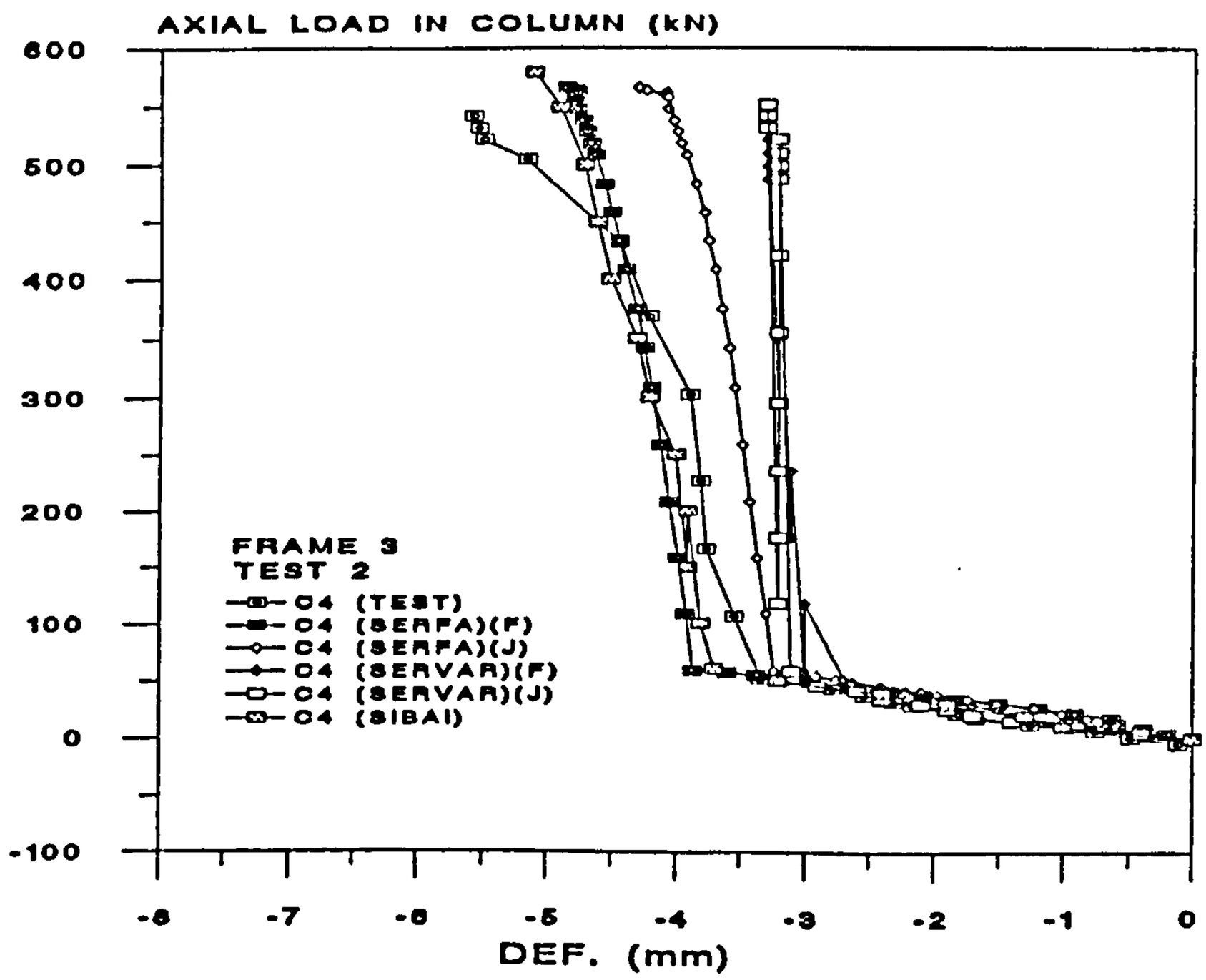

Figure 8.15 : Comparison of Predicted and Test Axial Load against Mid-Height Deflection of Column C4 in Test 2 of Frame 3

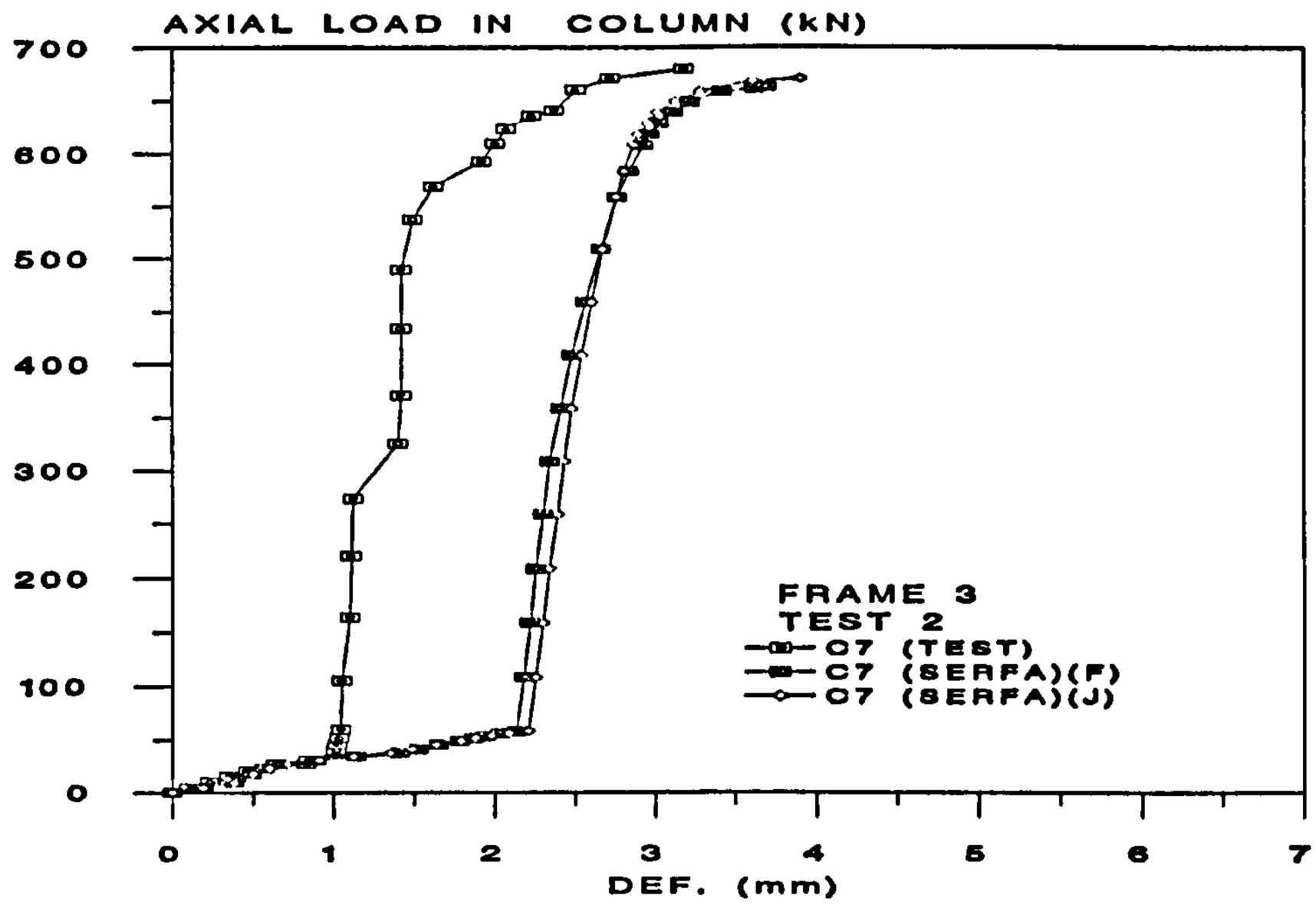

Figure 8.16 : Comparison of Predicted and Test Axial Load against Mid-Height Deflection of Column C7 in Test 2 of Frame 3

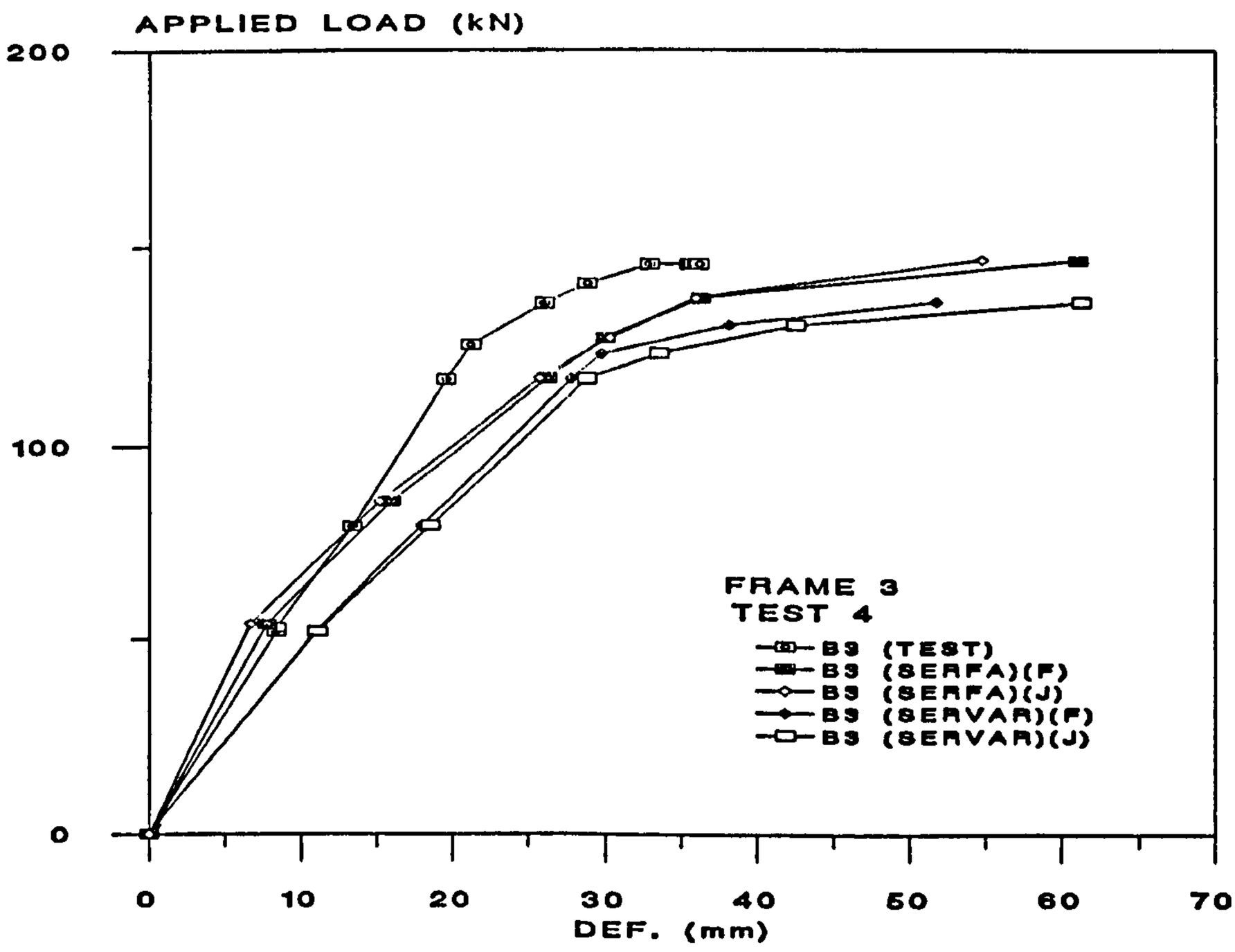

Figure 8.17 : Comparison of Predicted and Test Total Load against Mid-Span Deflection of Beam B3 in Test 4 of Frame 3

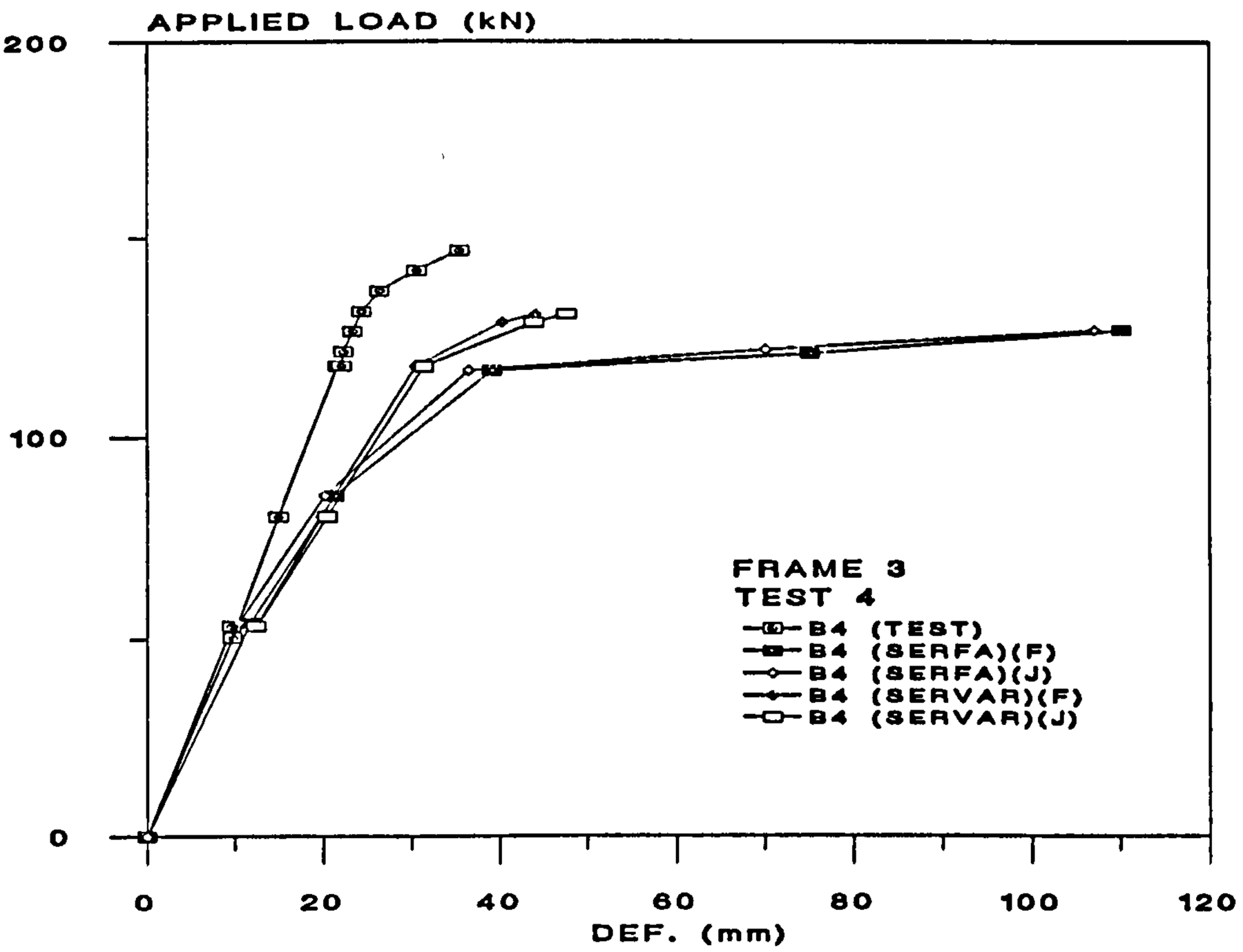

Figure 8.18 : Comparison of Predicted and Test Total Load against Mid-Span Deflection at Beam B4 in Test 4 of Frame 3

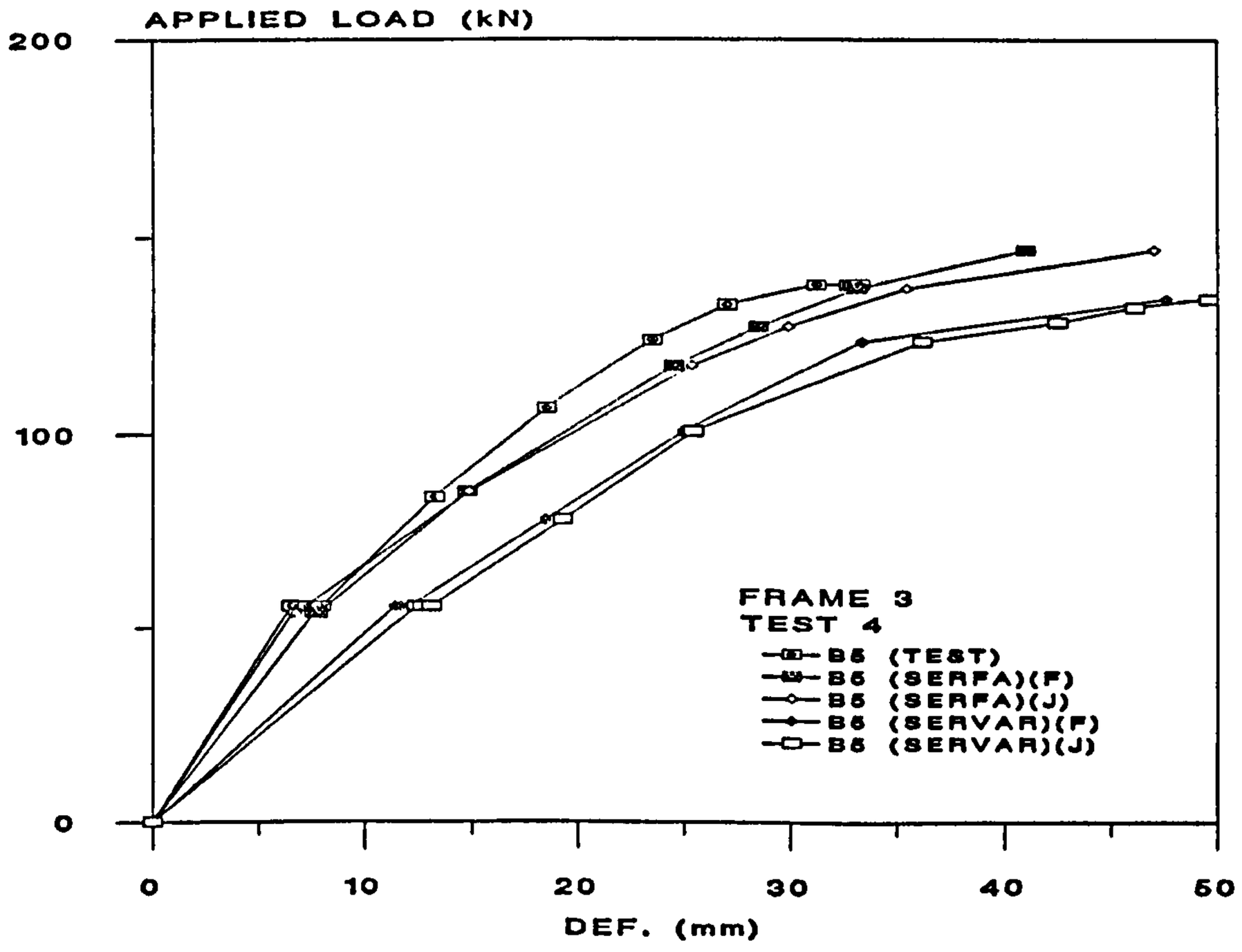

Figure 8.19 : Comparison of Predicted and Test Total Load against Mid-Span Deflection of Beam B5 in Test 4 of Frame 3

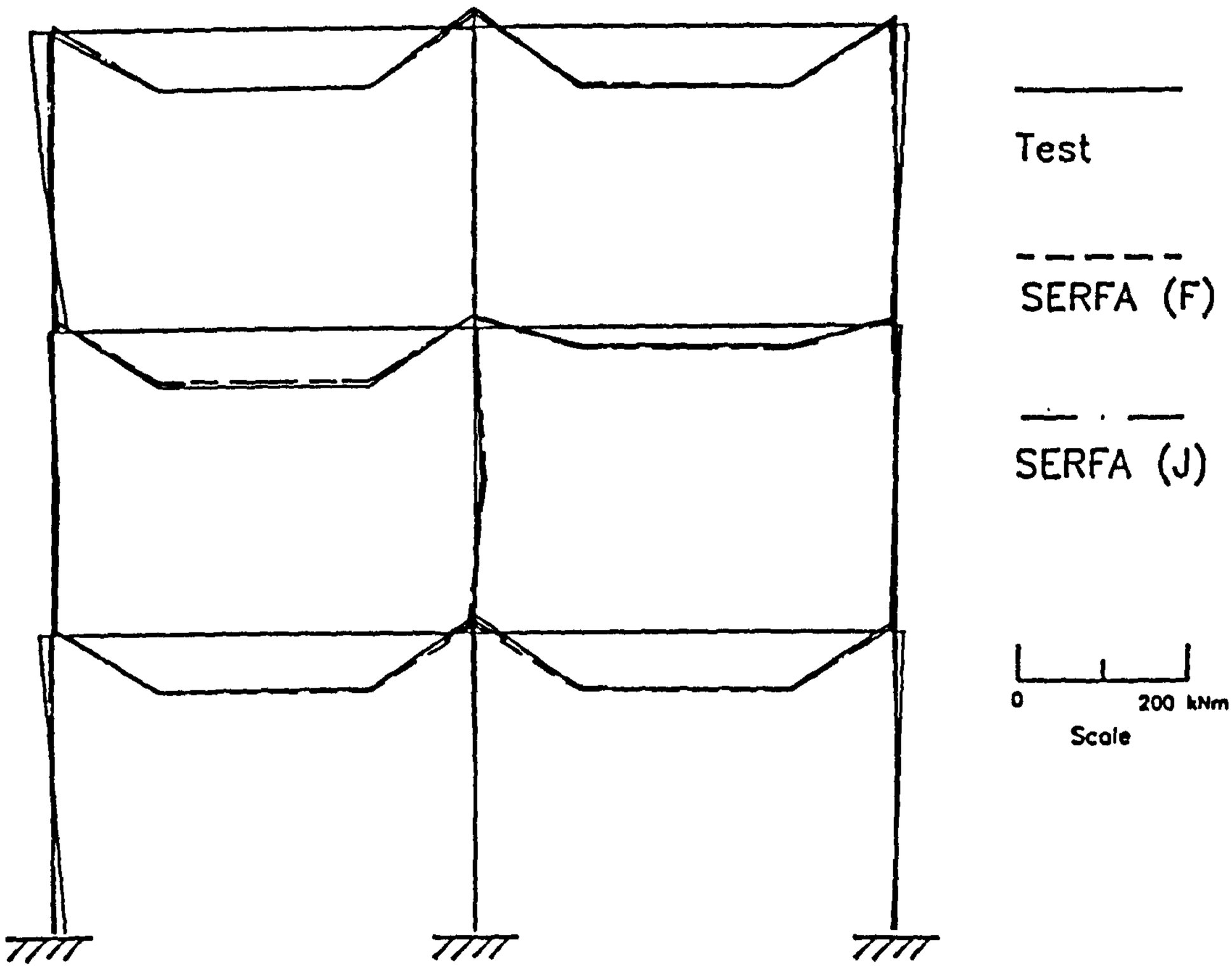

(a) Failure of Edge Column in Position 1

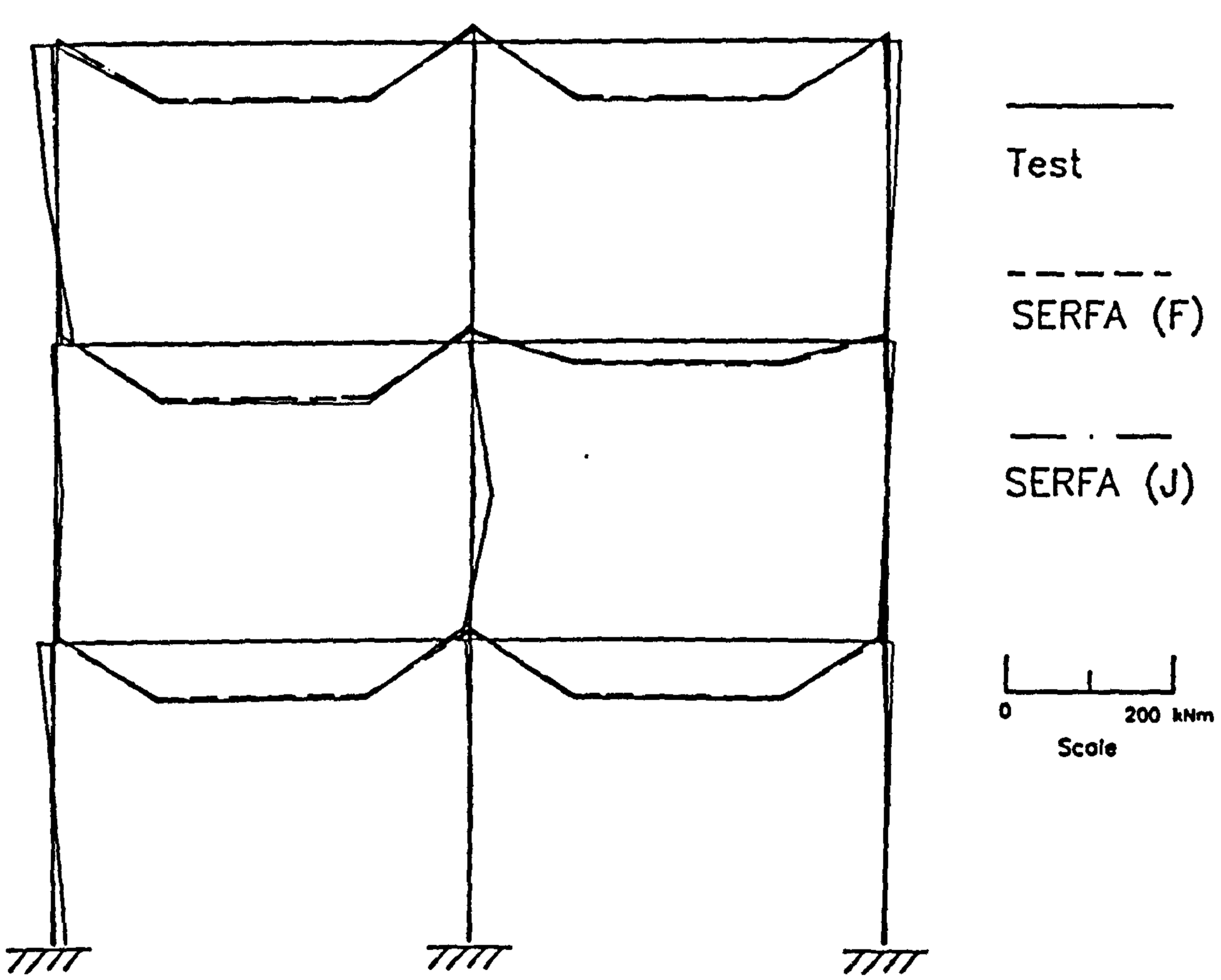

(b) Failure of Central Column in Position 2

Figure 8.20 : Comparison of Test Moments to Predictions of Frame 4 from SERFA

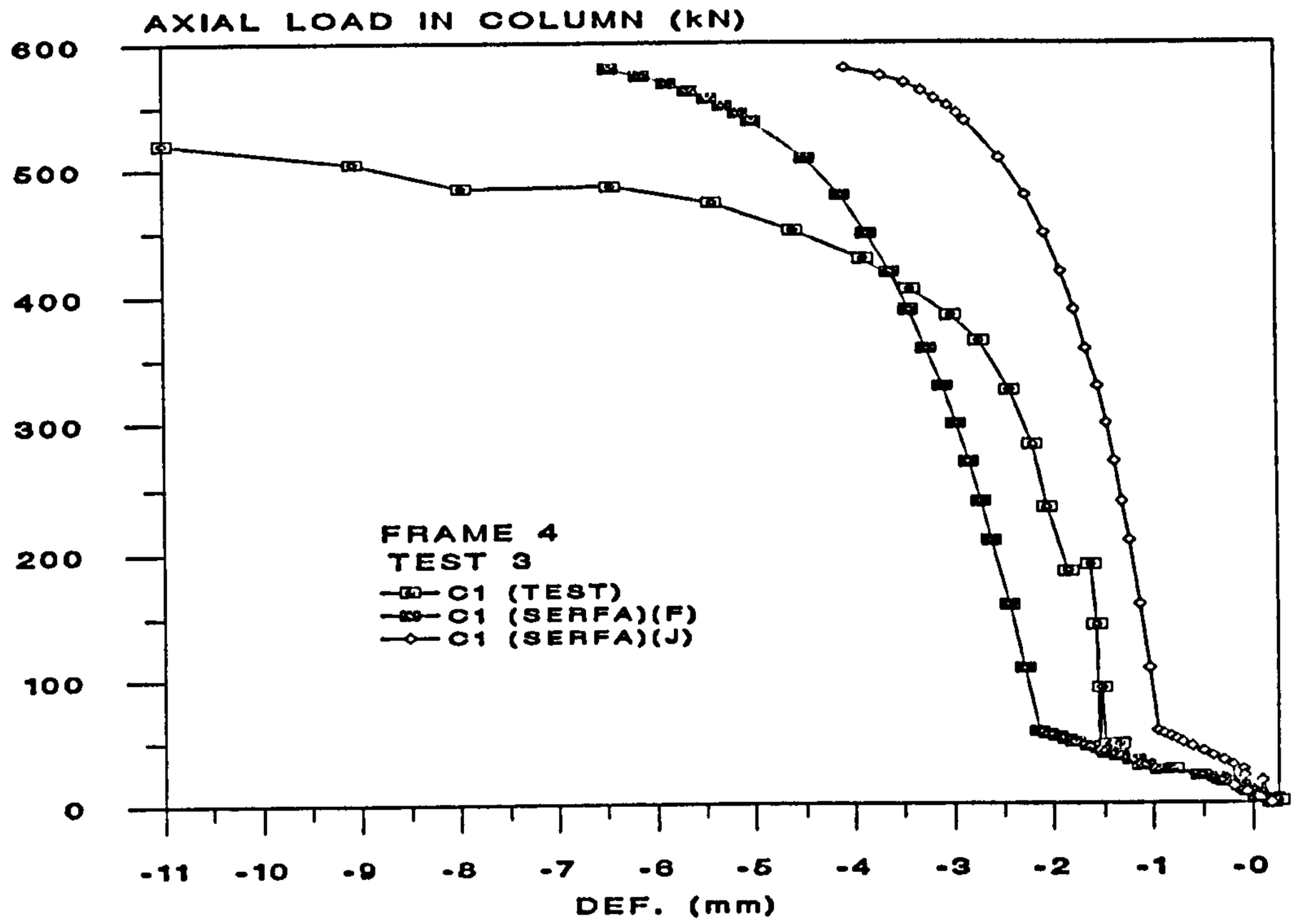

Figure 8.21 : Comparison of Predicted and Test Axial Load against Mid-Height Deflection of Column C1 in Test 3 of Frame 1

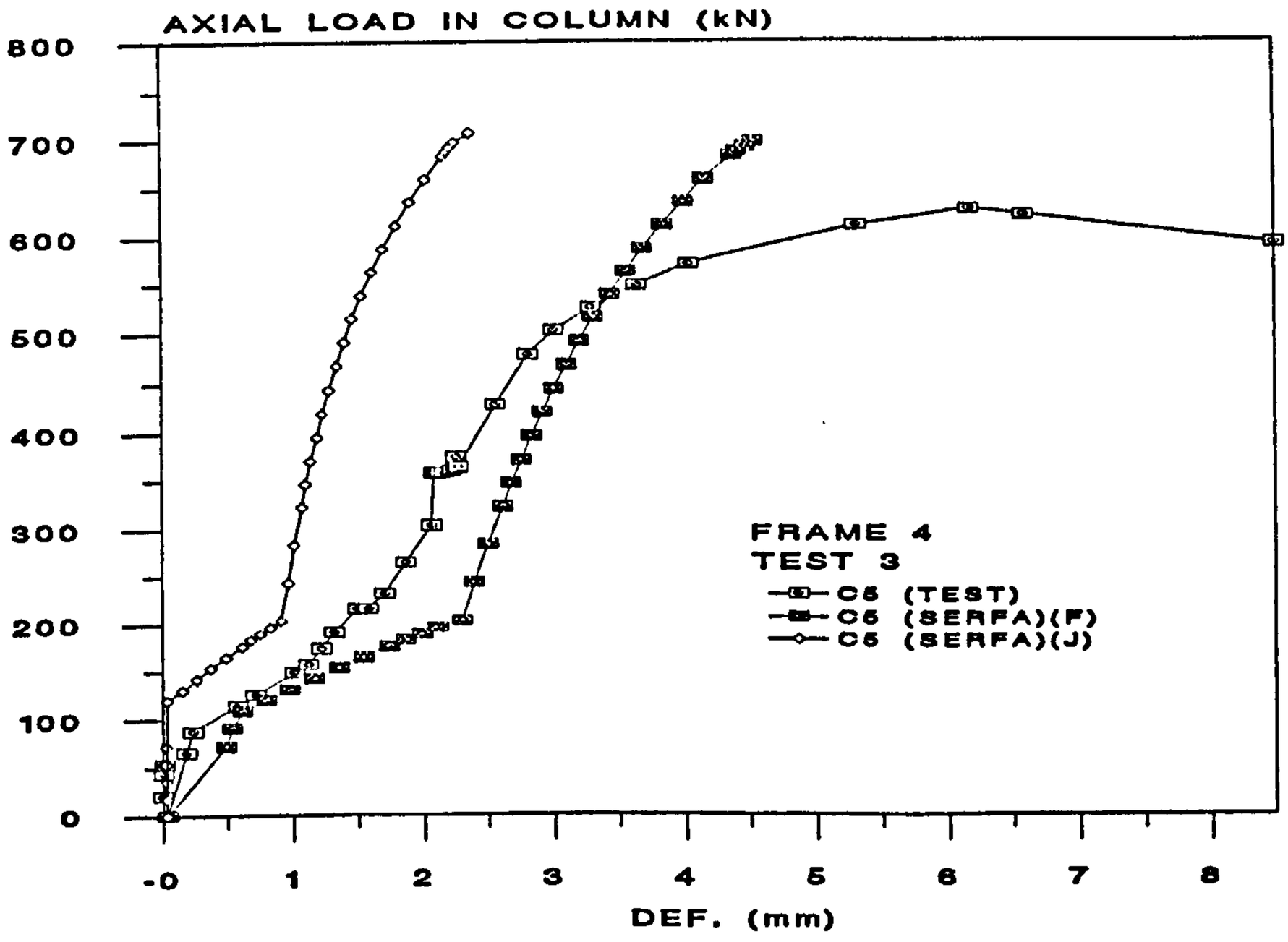

Figure 8.22 : Comparison of Predicted and Test Axial Load against Mid-Height Deflection of Column C5 in Test 3 of Frame 4

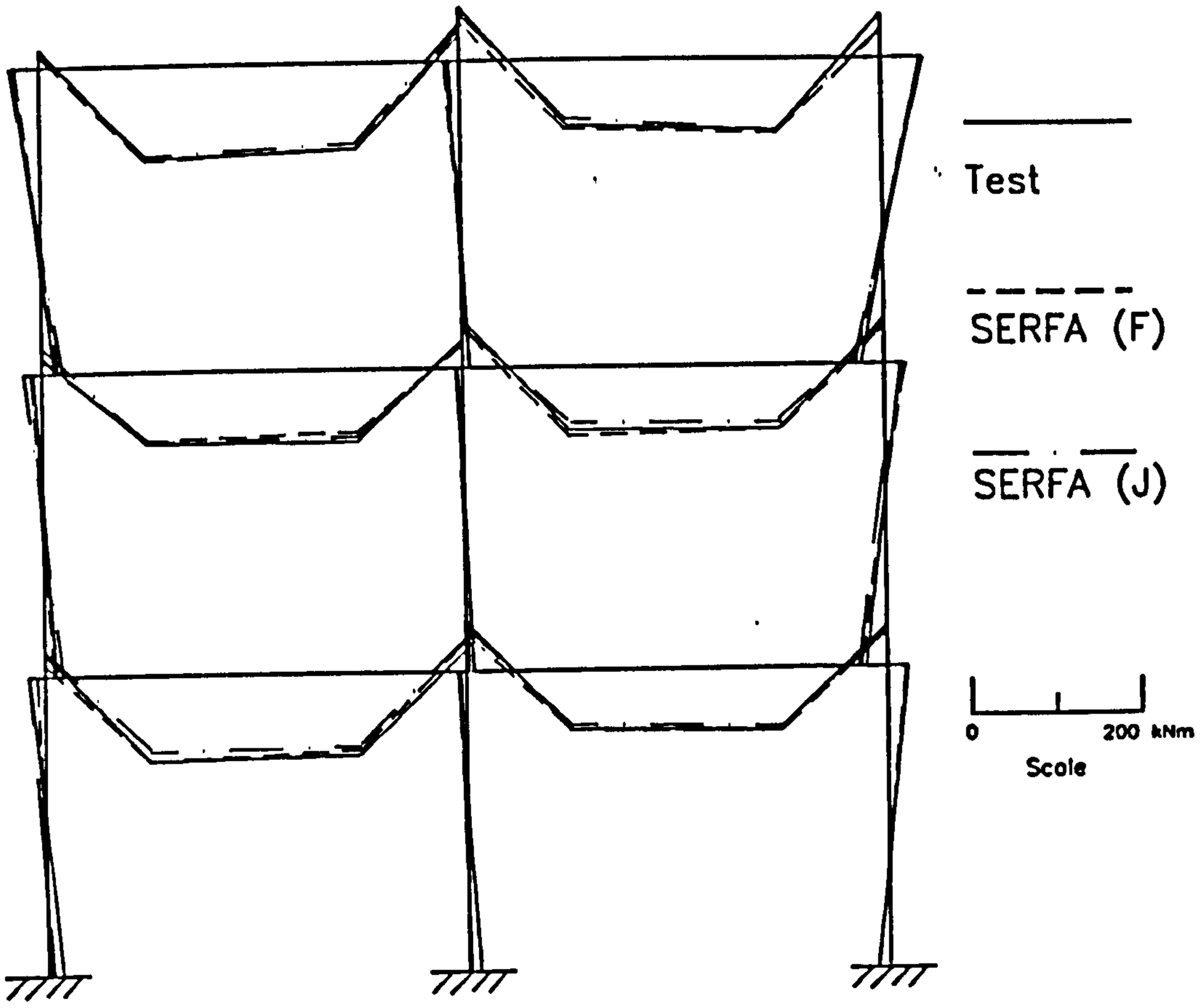

(a) End of Beam Load Phase

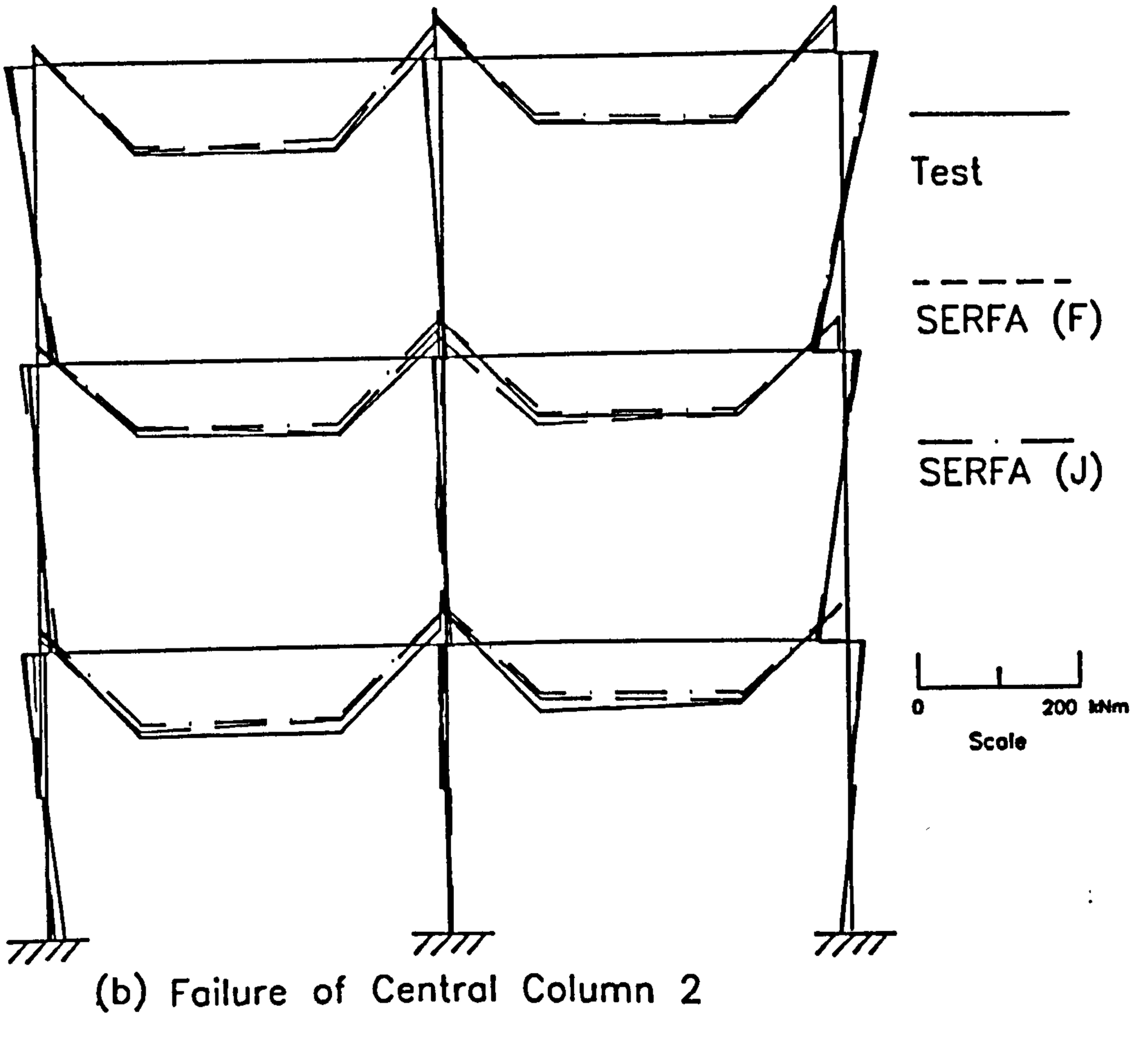

(b) Failure of Central Column 2

Figure 8.23 : Comparison of Test Moments to Predictions of Frame 5 from SERFA

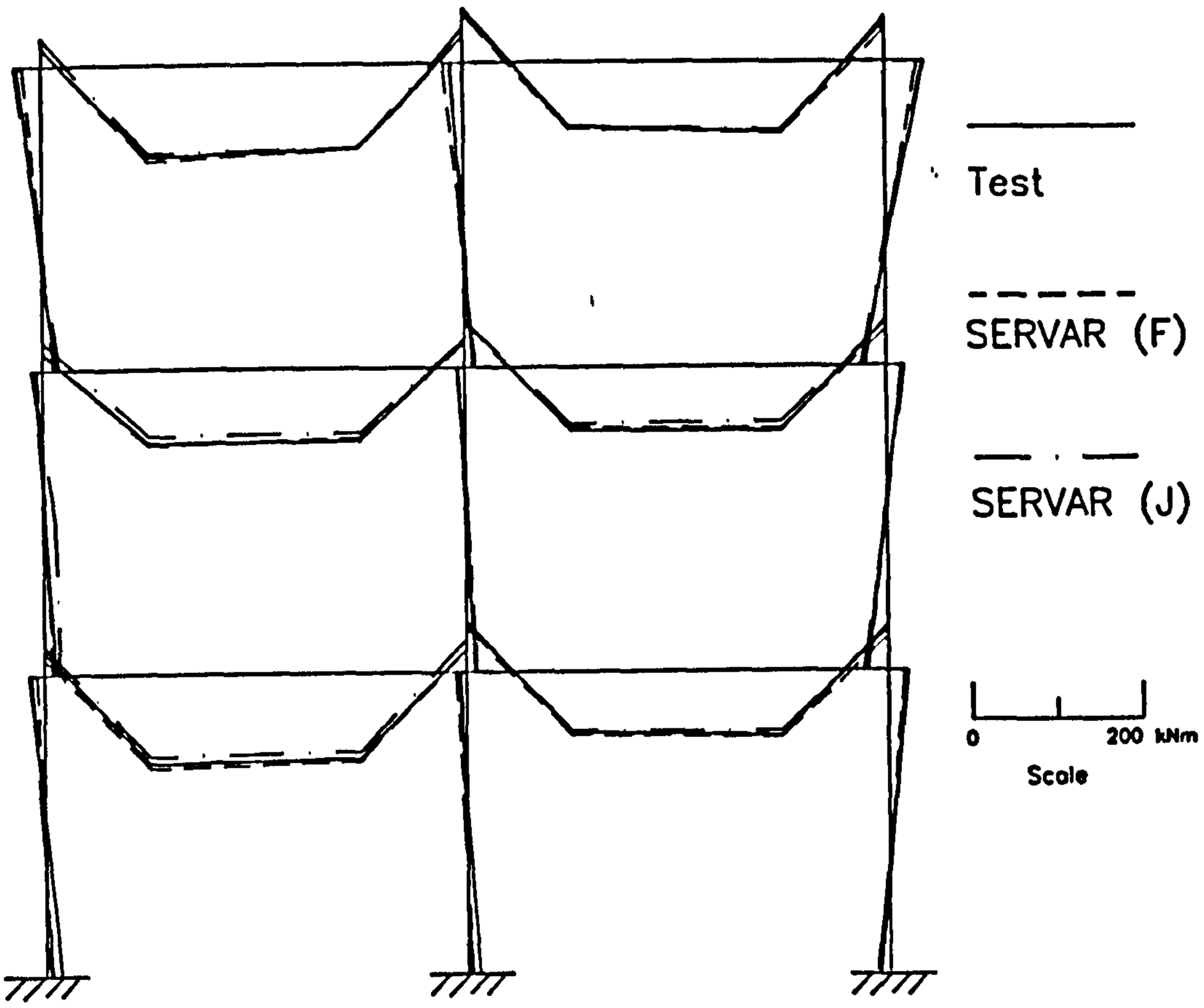

(a) End of Beam Load Phase

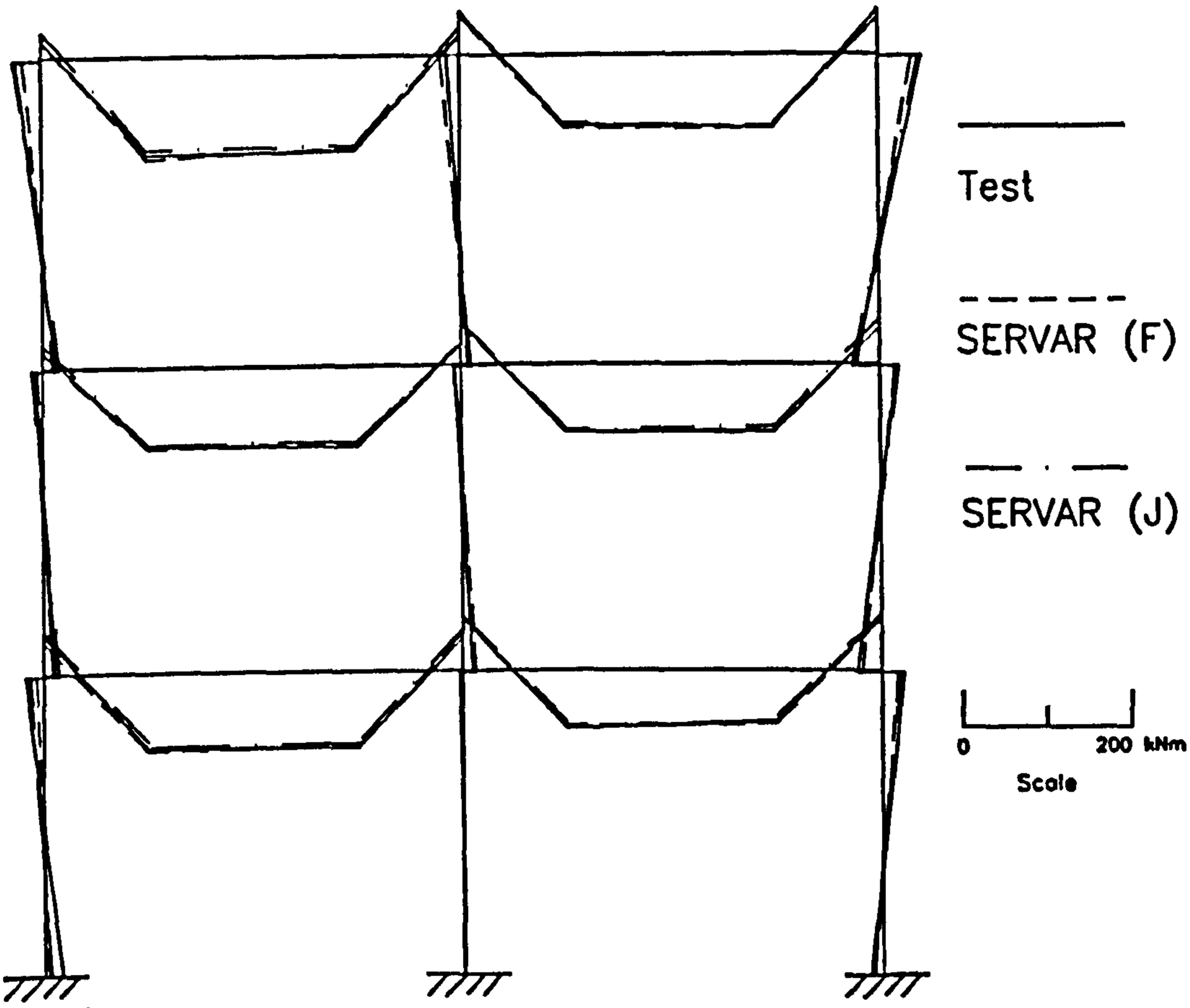

(b) Failure of Central Column 2

Figure 8.24 : Comparison of Test Moments to Predictions of Frame 5 from SERVAR

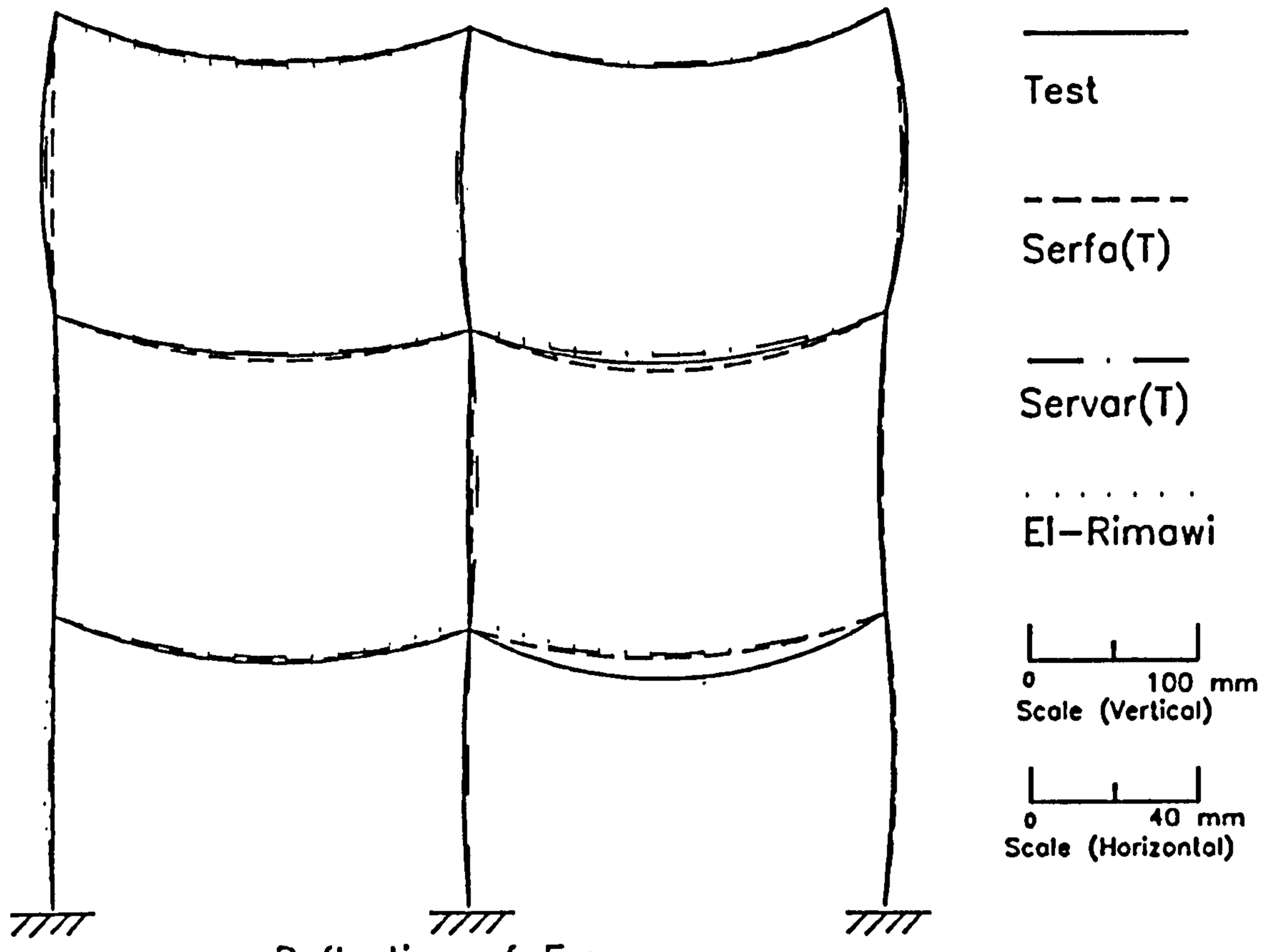

Deflection of Frame

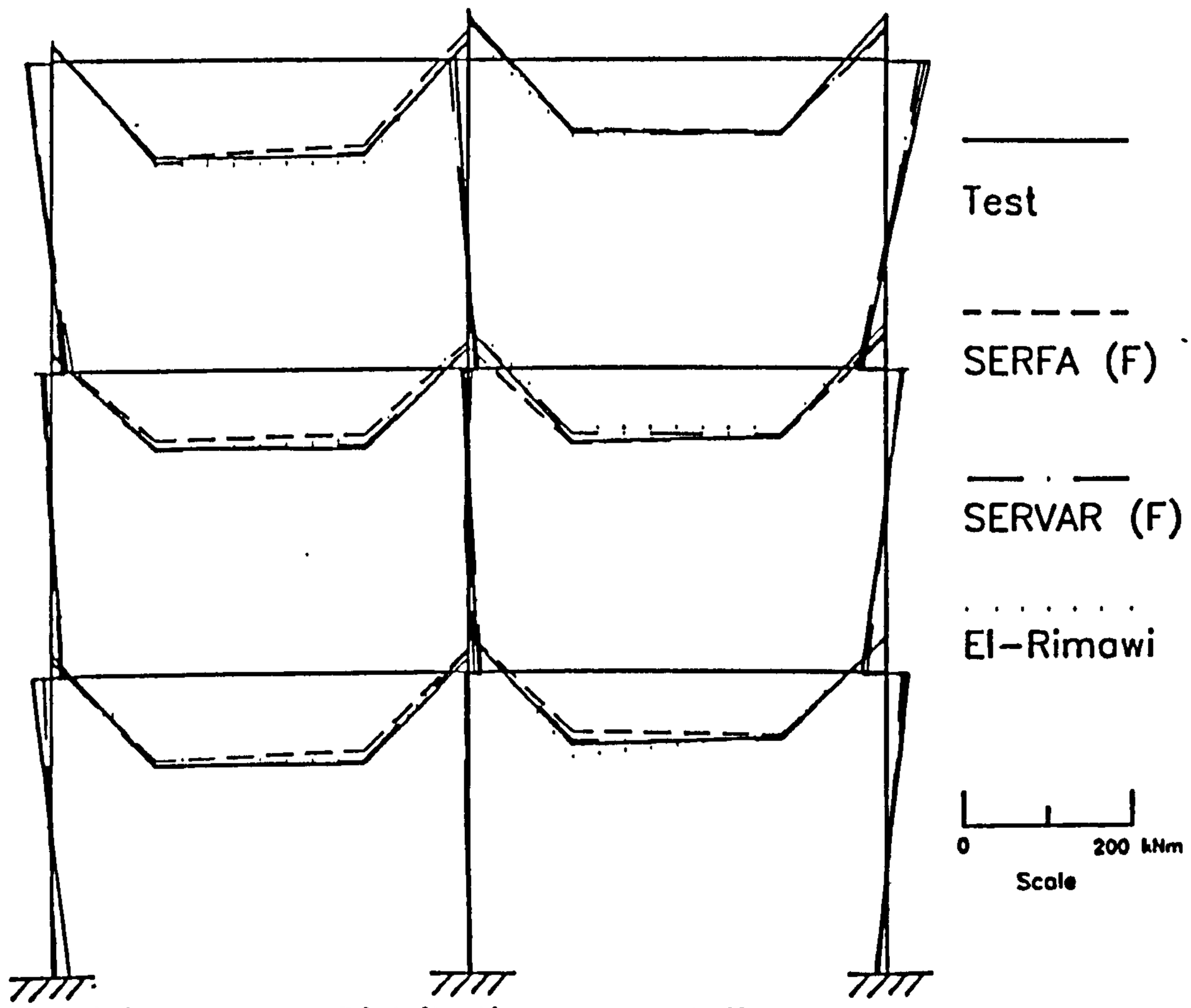

(b) Moment Distribution around Frame

Figure 8.25 : Deformation and Bending Moment Distribution around Frame 5 with Different Predicted and Test Results at Failure of the Central Column

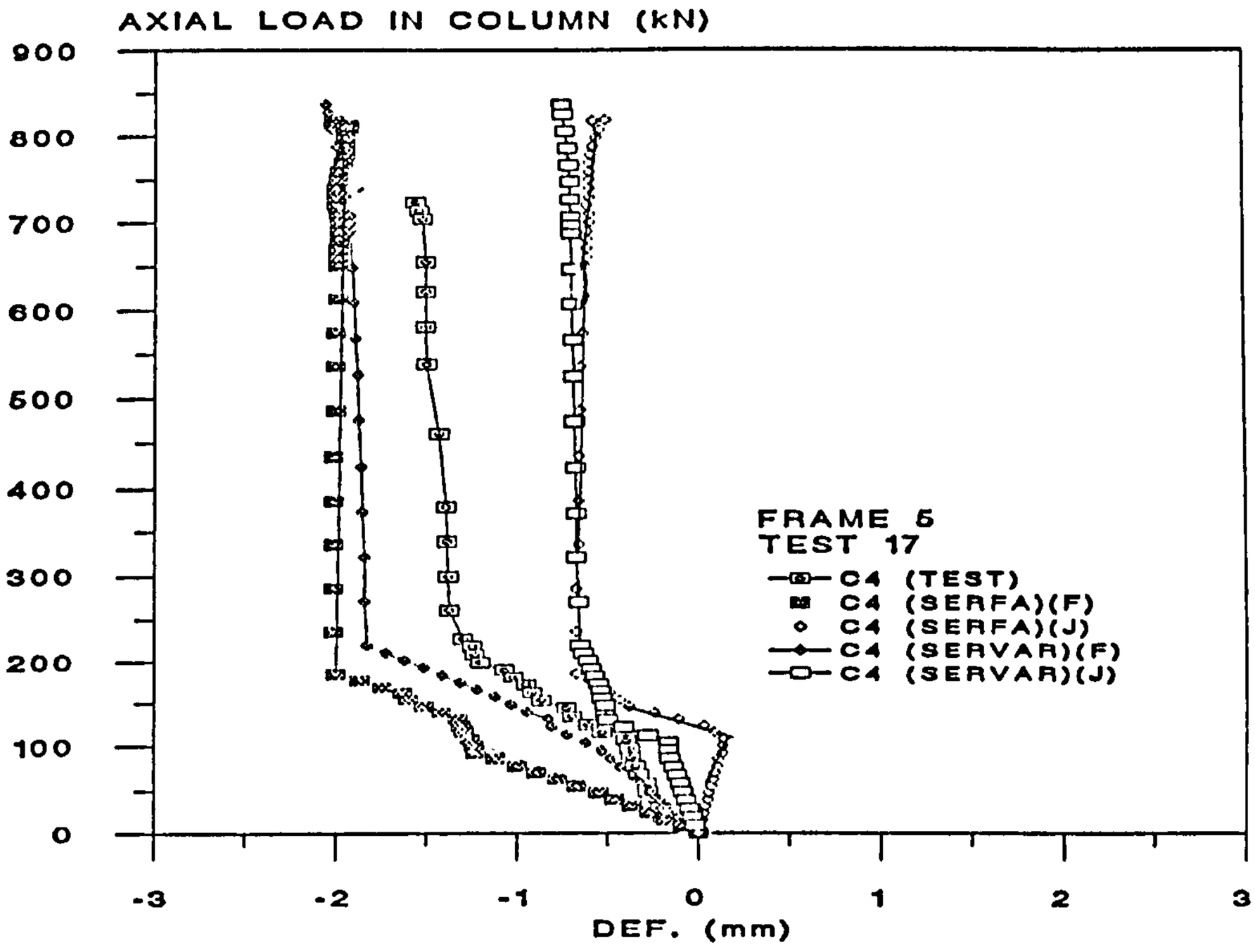

Figure 8.26 : Comparison of Predicted and Test Axial Load against Mid-Height Deflection of Column C4 in Test 17 of Frame 5

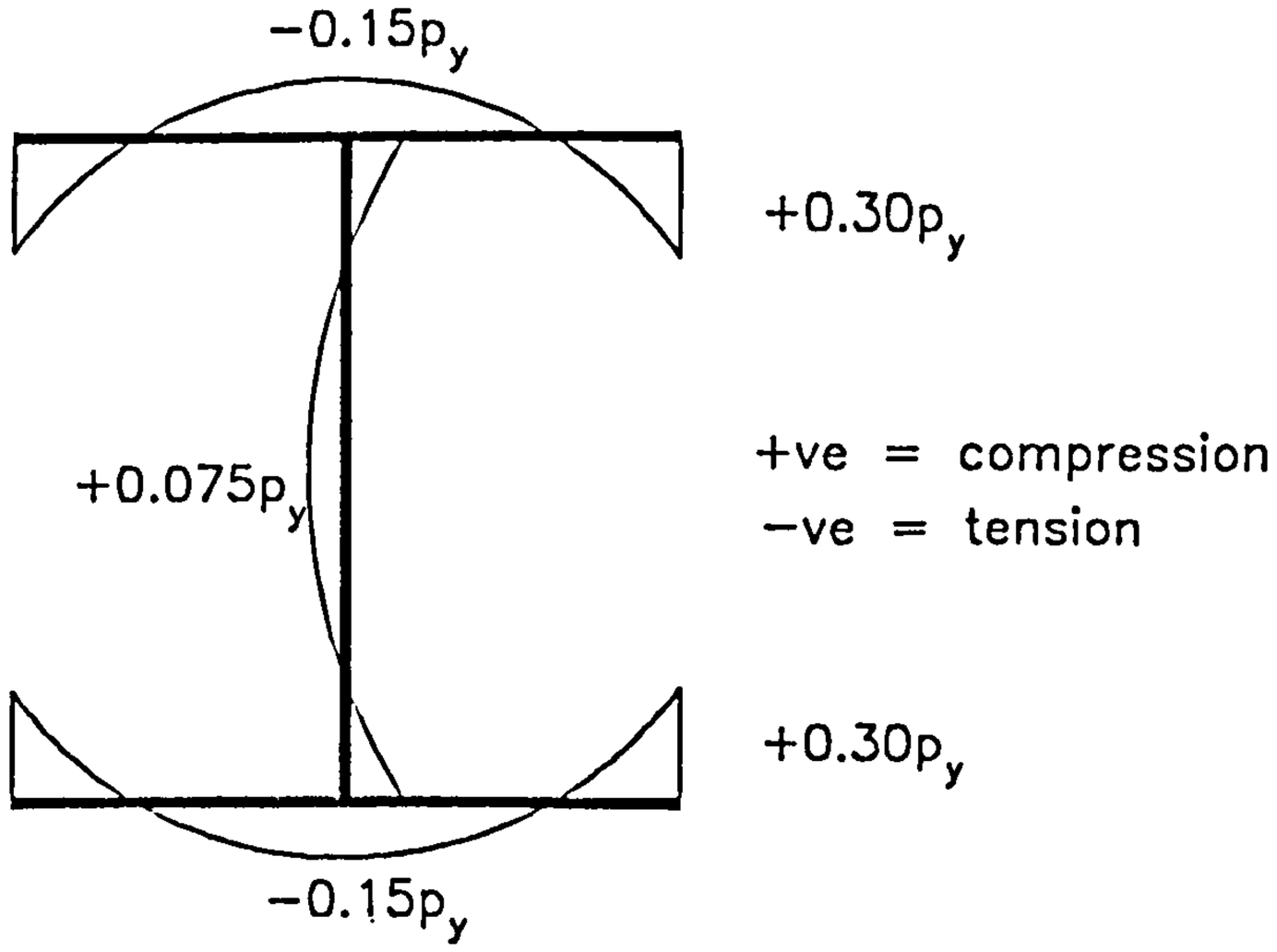

Figure 8.27 : Pattern of Residual Stress assumed in Column used in the Models of SERFA

Chapter 9

Parametric Study for Subassemblage Structures

9.1 Introduction

The subassemblage structure is a limited isolated frame from a full steel structure and is a convenient way of representing the complex analysis of complete structures. Two series of subassemblage tests have been completed in the University of Sheffield [9.1,9.2,9.3] to provide experimental data on the behaviour of columns restrained by different beam to column connections in both two and three dimensional modes. The advantage of a subassemblage test is that it permits the effects to be investigated without the expense and space requirements associated with full frame tests. Two and three dimensional subassemblage computer programs have been developed in the University of Sheffield [9.4,9.5] and the three dimensional version is used here to perform a parametric study.

The validity of the three dimensional subassemblage computer program is established by comparison of the predicted results with actual test records for a set of selected subassemblage tests as is discussed in next section. The moment rotation characteristics are collected from the databank as described in chapter 3.

A limited parametric study of the behaviour of subassemblages with semi-rigid connections is presented together with a discussion of the results obtained from the study. Some of the more important parameters considered in this study are :

1. presence of pinned and rigid beam-to-column connections and base connections
2. presence of semi-rigid beam-to-column connections
3. effect of the type of applied loads

4. effect of the different M-ϕ response obtained from different test conditions
5. the α_{pin} concept is examined for a range of parameters

9.2 Development of the Computer Program

The starting point of this computer program was developed by Jones [9.6] to investigate the behaviour of an isolated two dimensional beam-column subject to non-linear end restraint. The original program was then modified by Rifai [9.4] to include the effect of beams framing into the column which permitted the analysis of a two dimensional beam column 'I' shaped subassemblages incorporating the characteristics of semi-rigid connections. The subassemblage program of Rifai was then modified by Ahmed [9.7] to develop the computer program SERFA, a planar frame analysis which has been validated in chapter 8. At the same time, Jones' original program was also reformatted by El-Khenfas [9.8] to permit the analysis of an isolated three dimensional beam-column with non-linear end restraints. The latest version was subsequently developed by Wang [9.5] which combined the techniques of Rifai and El-Khenfas to develop a useful three dimension subassemblage computer program. Figure 9.1 illustrates the computer programs which developed in the University of Sheffield. The Wang version was used to predict the behaviour of small scale tests conducted by Gent and Milner [9.9]. Gibbons [9.3] used this program to compare the predicted results with the actual subassemblage tests responses. A further extension of the program has been made by Bitar [9.10] who added additional column lengths above and below the column under consideration but which requires a transputer for running. Thus Wang's program is considered in this study.

El-Khenfas [9.8] described most of the subroutines in the original program, therefore, these are not repeated here. Wang [9.5] has provided a detailed description of his program, the technique adopted and analytical method used. A manual of this latest version the computer program, its operation and the basic technique used has been written by the author [9.11].

9.3 Validity of the Computer Program

9.3.1 General

To confirm the validity of the program, the three dimensional subassemblage tests which were conducted by Gibbons [9.3] have been selected and the predicted values compared with the test results.

9.3.2 Comparison with Predicted Results to Actual Test Values for Subassemblages

A series of ten column subassemblage tests has been carried out and a full description of the test arrangements, procedures and results is presented in reference [9.3]. The columns were 6m long with up to three 1.5m long beams framed in at one end. A column subassemblage with three beams at one end represents edge column in a more extensive structure whilst when only two beams occur this represents a corner column. Figure 9.2 shows the arrangement of this series of subassemblage tests. In some cases the primary beams framed into the column flanges and in other cases into the column web. A variety of connections was employed ranging from web cleats to flush end-plates as listed in Table 9.1 which also shows the symbols adopted and other test conditions used.

Beam loads were first applied up to the levels as described in Table 9.2 and then held constant. Then column load was applied up to failure. Typically the beam loads were applied in a minimum of ten equal increments up to their prescribed limiting value, with instrumentation being scanned at every increment.

The sections used in Gibbons tests [9.3] showed clear evidence of roller straightening and thus such residual stresses as occurred were impossible to predict and moreover would vary rapidly change along the member length, thus no residual stress were incorporated into the analysis. The yield stress and Young's modulus used for the beam sections were derived from tests on tensile coupons. The actual measured dimensional and geometric properties of the subassemblage members were used in the analytical model. The moment-rotation characteristic for each joint was taken from the databank which was a record of the tests conducted by Gibbons [9.3] as described in chapter 3. The out-of-plane flexibility of the connection was not considered in this study as the out-of-plane beam rotation was almost nil. Furthermore it has been found that changes to the out-of-plane connection characteristic in the analytical model had negligible effect on the predicted subassemblage

behaviour. The subassemblage was modelled assuming that the connection had infinite torsional stiffness, an assumption supported by tests conducted by Celikag [9.2] which showed that connection flexibility is negligible compared to member flexibility. Negligible rotation existed in both major and minor axes at the column base.

The failure loads determined from the subassemblage tests are presented in Table 9.2 together with the failure loads predicted by the finite element computer program. For all subassemblage analyses, the maximum error between the experimental and predicted results is only 6 % with the exception of test S5. The predicted failure of all subassemblage columns was a result of excessive minor axis deformation which was confirmed from observation in the actual tests. Apart from the failure loads indicated by asterisks the correspondence is good and, in test S5, it is thought that the analysis may have been terminated prematurely due to numerical divergence.

Figure 9.3 shows a comparison of the predicted and observed deflection in the mid-height of the column for test S4 and Figure 9.4 shows a comparison of the bending moment in the centre of column for the same test together with the moments computed by Gibbons from strain gauges located at the cross section [9.3]. It is evident that the analytical model closely simulates all aspects of the observed experimental behaviour. The reliability of the program is thus established.

9.4 Parametric Studies

9.4.1 General

The purpose of this study was to use this validated software to examine subassemblage configurations and loading arrangements which are of a more direct practical significance. The aims of the study were as follows:-

1. To investigate the effect of two extreme types of connection, pinned and fully rigid, using different test conditions and loading arrangements.
2. To investigate the influence of semi-rigid connections on the performance of subassemblages representative of frames encountered in practice.
3. To quantify the adverse effect, if any, of the transferred moment from a semi-rigid connection to subassemblages.
4. To investigate the effect of different loading arrangements and column orientations.

5. To investigate the difference in the predicted failure load of columns resulting from the use of moment rotation characteristics obtained from different test conditions and arrangements.
6. To investigate how the parameters of beam section, column section and connection stiffness affect the column capacity.
7. The examination of the full body of information on the behaviour of subassemblages with a range of semi-rigid connections from which comparison could be made with present methods of design.

9.4.2 Formation of Study

The study was conducted in three stages. The initial stage examined one model with eight cases based on different column orientation, base conditions and connections (pinned or rigid). Three different beam loading cases of no load, load applied on one side only and loads applied on both sides of the column on the primary beams were then studied. The second stage considered the effect on the column capacity of the three different semi-rigid connections used in the subassemblages and different moment rotation characteristics obtained from two different sets of test arrangements collected from the databank. Finally, the effect of variation in the M-ϕ response on column capacity is included.

9.4.3 Subassemblage Configurations

Subassemblages incorporating four beams, two primary and two secondary beams, were considered to represent an interior column of a steel frame structure. Figure 9.5 shows the arrangement of the subassemblage and the analytical model used in the study.

The effect of column continuity through the floor level was not investigated in this study. It is clear that the continuity of a column would tend to distribute the applied connection moment, thereby reducing the maximum disturbing moment on the column. A study by Bitar [9.12] has shown that no unexpected results occur when column continuity is considered. As a result, the more onerous case was considered in order to investigate the extent of the adverse effects of moment transfer associated with semi-rigid design.

The basic reference model is taken from the two Sheffield frames conducted by Gibbons [9.3]. A column height of 3.8m was adopted to represent the actual height of a storey in a typical office building. The typical span of the primary beam and secondary beams of 5m and 4m, although suitable for the beam section used, are somewhat smaller than that

would be found in a practical building. The subassemblage examined in the parametric study comprised a 152 x 152 x 23 UC column and 254 x 102 x 22 UB beam sections. All the steel used was nominally grade 43A with the yield stress being assumed to be 275 N/mm^2. To determine the response range for a particular subassemblage, frames with connections from each end of the range of the connection stiffness was considered in the initial phase of the study. Three further types of semi-rigid connections taken from the flexible to mid stiffness range, i.e. web cleat, web and seat cleats and flush end-plate connections, were considered in the second phase of study. All the subassemblage models included an initial sinusoidal geometric deformation with a maximum amplitude of L/1000 (3.8mm) about both major and minor axes. The assumed pattern of column residual stress is shown in Figure 8.27.

In all cases, beam loads were applied proportionally in equal increments up to their design values which were based on the steel design code BS 5950 assuming simple construction [9.13]. After the application of beam loading, concentric load was applied to the head of the column in small increments until the maximum supported load, corresponding to column failure, was achieved. The loading sequence was therefore similar to that adopted in the experimental study conducted by Davison [9.1] and Gibbons [9.3].

9.5 First Phase of Study

The initial phase of the study investigated the effect on the capacity of column resulting from two extreme types of connection i.e. pinned and fully rigid. Two types of the column orientation and base condition are also included. Table 9.3 shows the symbols used in the different test conditions and the arrangements in the first phase of study. In orientation 'A', the primary beams framed into the column web whilst for orientation 'B' the primary beams framed into the column flange. Pinned (PB) and rigid bases (RB) were used. Different loading arrangements, in which type (0) represents no load applied to the primary and secondary beams, type (1) represents point loads applied to the mid-span of two primary beams and type (2) represents point load applied to one primary beam only are considered and the results compared. Tables 9.4 presents the total failure load of the column, for the three loading cases, 2 forms of connection, 2 column orientations and 2 base conditions - a total of 24 different analytical models.

9.5.1 Discussion of Result

Table 9.4 demonstrates the effect on the column failure load of different test conditions and arrangements. The failure axial loads are computed by the finite element computer program. The failure loads are also presented in a non-dimensional form by dividing the ultimate loads computed by the program, by the capacity determined using the program but assuming the column to be pinned at its ends and subject to axial load only. The ratio is designated the α_{pin} factor [9.12]. The α_{pin} factor gives an indication of the benefit of the restraint from the beam to column connection after incorporating the potentially disadvantageous influence of moment through the connection. The value of the failure load of a pin ended column in the column orientation 'A' was determined as 412 kN using the same computer program. The α_{pin} factor is determined by the ratio of the ultimate load of column to the ultimate load of column pin connected at each end, i.e. 702/412 = 1.70 for case (1), loading case (0) and column orientation 'A'. The results of all computations are listed in Table 9.4.

Considering the effect of the restraint to the ends of columns, the results in Table 9.4 clearly show that the highest value of the failure load was computed in the subassemblages with rigid beam-to-column connections and base conditions (RB:RC) due to largest rotational restraint to the column leading to a reduction of the effective length of the column. Conversely, the lowest value was calculated without any rotational restraint provided in the both ends of columns (PB:PC). Turning to examine the influence of the variation of applied beam load pattern it can be seen that, a similar failure load was determined for the loading cases (0) when it is compared to the value for the corresponding loading case (1). In theory, no moment is transferred to the column in the loading case (1) due to the balanced nature of the moment arising from the two adjacent primary beams. However when load is applied to only one of the two primary beams (case 2), significantly lower column failure loads occur for the rigid connected subassemblage when compared to loading cases (0) and (1). This is due to the additional moment introduced to the column head.

As expected, a similar total axial load in case (4) of Table 9.4, for the truly pinned connection with pinned base condition, for different loading cases and column orientations, was recorded in Column 4. Such differences as do arise are due to unbalanced beam loading introduced at an eccentricity.

It is important to note that, for cases (1) to (3) i.e. 18 different study cases the α_{pin} values shown in Table 9.4 are all greater by at least 20 %. This is in line with previous stud-

ies and adds further confirmation to the premise that the benefits of column end restraint outweigh the detrimental effects of moment transfer and as a result, the failure loads are greater than those of the equivalent pinned-ended column (case (4)). The column capacity considered by this study is increased by a minimum of 21 % over the corresponding pin-ended column due to the rotational restraint offered to the column by the connections.

Column orientation is of potential economic significance. The highest α_{pin} value is 1.71 for case (1), column orientation 'B' and loading cases (0) and (1) with full restraint at both ends of the column. The lowest value of 1.21 is determined in the case 3, column orientation 'A' and loading case (2). It is interesting to note that a subassemblage in the column 'B' orientation with primary beam connected to the flange of column can significantly increase the α_{pin} values. Thus, adopting the most appropriate column orientation will increase the capacity of column without the need provide any rotational restraint to one or both end of columns. The results in Table 9.4 indicate that the α_{pin} values increase from 1.59 to 1.61 for case 1 and loading case (2), from 1.44 to 1.46 for case 2 and load in case (0), from 1.21 to 1.32 for case (3) and loading case (2).

Based on the first phase of study, the following conclusions are drawn,

1. The subassemblage with fully rotational restraint to both ends of columns increases the capacity of column by the largest amount due to the rotational restraint of the column.
2. Similar column capacity was determined between the loading cases (0) and (1) due to the balance moment introduced to both primary beams. A lower value was obtained in load case (2) in which load was applied to one primary beam only leading to a disturbing moment being introduced to the column head.
3. Increasing the applied beam load (loading case (1)) reduces the axial carrying capacity of the column.
4. The results show that the failure load of a subassemblage was never lower than the failure load of an axially loaded pin-ended column.
5. All the subassemblages in this study failed as a result of excessive minor axis bending.
6. It is evident from this study that the capacity of column could be maximised by choice of an appropriate column orientation.

9.6 Second Phase of Study

The beneficial effect of continuity in beam-column joints was shown in the above section. In practice the high cost of fabrication of a rigid joint may offset savings resulting from a reduction in the weight of steel and it is more usual to use joints designed as simple connections. However, from the experimental studies [9.1,9.3], it is evident that most simple beam to column connections are in fact capable of developing some degree of moment transfer and column restraint. The advantage of incorporating the semi-rigid characteristic into steel frame designs are a better distribution of bending moment in beams, compared to simple design and in restraint provided to the columns, whilst the advantage over the rigid design is the reduction in fabrication and hence in the cost of connections.

The results obtained from the first phase of the study show that stiffer connections and base supports provide larger restraint to the column (giving a reduction of the effective length) and thus increase the ultimate load capacity. The results also show that for the subassemblage with different restraint and loading arrangements, α_{pin} was always greater than unity. This implies that the benefit of beam-to-column connection is greater than the detrimental effect of the transferred disturbing moment. However, the results are based only on comparison of the rigid and pinned beam-to-column and column base subassemblages. The second phase of the study therefore concentrates an investigation of the effect of the real, semi-rigid, connection stiffness on the ultimate capacity of subassemblages.

The basic same arrangement of subassemblage used in the first phase of study is used but the characteristics of common connections are included. The following have been selected for study;

1. flush end plate (FE);
2. web and seat cleats (WAS) and ;
3. double web cleats. (WC)

The results of the two extreme types of connection (pinned and fully rigid) obtained from the first phase of study are also used in conjunction with the results obtained from a range of semi-rigid connections. Initially, only the case of the primary beams framing to the column flange is examined in the study. Table 9.5 shows the symbols for the different test conditions and arrangements used in the second phase of study. The same loading arrangement as was used in the first phase of study is also considered here.

The generally accepted M-ϕ response of a semi-rigid connection is shown in Figure 5.23 [9.14]. The plot comprises a non-linear loading phase followed by a linear unloading phase of slope equivalent to the initial tangent stiffness. The usefulness of the correlation between the loading and unloading phases of the connection behaviour has been realised by many researchers and has formed the basis of a number of semi-rigid design techniques [9.15]. A close examination of the behaviour of all joints in frames 3, 4 and 5 as the columns were brought up to failure (chapters 6 and 7) showed that the unloading stiffness of the joints was of more benefit to the column than the loading stiffness of an adjacent joint. For example, Figure 6.52 shows the behaviour of joint A, C and E as the external column in position 1 was brought up to failure. The much larger unloading stiffness is readily apparent. It would therefore seem that the investigation of the unloading stiffness of a joint is at least as important as the determination of the initial stiffness. Davison [9.16] pointed out that the studies of joint behaviour should pay particular attention to their action in the initial part of the M-ϕ curves and also to their unloading behaviour.

To understand the effect of different types of applied load in the loading and unloading stages, the deflection modes of three cases for the subassemblage with semi-rigid beam-to-column connection are described as follows,

1. Type (0)

   Figure 9.6 shows the deflected shape of the subassemblage which is under the action of column load only. Without applied column load (P_c is zero), the chain dotted line shows the geometry of the subassemblage with the column bowed to the right of its chord line. When load is applied to the column head, the angle between the column and right hand side beam continues to close as P_c is increased. The angle between the column and the underside of the beam to the left of the column head starts to open and continues to open.

2. Type (1)

   Loads are applied to both sides of beam in the first load stage, then, while the beam loads are held constant, column load is applied. During the beam load phase, the deflected shape of the subassemblage and the moments at the intersection of the joint are as shown in Figure 9.7(a). The directions of the moments applied to the connections are shown in Figure 9.7(a). When the beam loads are applied, a clockwise moment is produced in the right hand side beam (closing) whilst an opposite direction of moment occurs in the left hand beam (closing). After the column load is applied, an anti-clockwise disturbing moment

is produced in the column head leading to further closure of the right hand joint as shown in Figure 9.7(b). Thus the joint between the left hand beam and the column initially moves in one sense and then reverses in direction which means that during this second action it is on an unloading path on its M-ϕ characteristic.

3. Type (2)

In this case, a beam load is applied to the subassemblage in the first load stage and axial load is then applied to the head of column with the beam load remaining at the same level of load. At the end of the beam load phase, the deflected shape is shown by the continuous lines in Figure 9.8(a). As the column load is applied, the deflected shape is changed to that shown by the continuous lines in Figure 9.8(b). Although the column and beam deflections are still increasing, this increase is not as it was when the beam load was increasing. The column head shares the resistance of the moment transmitted through connection and that produced by the beam reaction through the joint offset distance, half depth of column section (D/2). Both beams assist the column to resist the applied load. After applied column load, the right connection opens whilst the left one closes as shown in the same plot. Thus both connections follow an unloading path on their M-ϕ plots.

One of the important characteristics of the semi-rigid connection is that the connection may show alternate loading and unloading response even under a set of monotonic load increments. Thus the loading and unloading characteristics of a connection should be incorporated in any proper analysis routine [9.7]. Available moment-rotation curves of connection tests under cyclic and alternating loads [9.17,9.18,9.19,9.20] show a distinct linear range during unloading, with the stiffness being equal to the initial loading stiffness C_i. Nonlinear behaviour sets in again after moment reversal loading leading to a stiffness under reversed loading equal to the under monotonic loading (see Figure 9.9). Based on the cyclic loading tests conducted by Celikag [9.2], a single M-ϕ can be constructed from a maximum positive and negative points of each cycle comparable to those from test subjected to monotonic as illustrated in Figure 9.10. In the analysis [9.2], the M-ϕ curve in the upper right quadrant is assumed to have an equivalent part in the lower left quadrant. Because of the absence of sufficient M-ϕ characteristics for unloading and reloading conditions, one possible simplification for frame analysis under monotonic loads [9.7] could be to use a linear unloading part.

Two sources of moment rotation characteristics have been provided by the experimen-

tal results from Davison (D) and Celikag (C) which have been extracted from the database as discussed in chapter 3. Generally, the tests conducted by Davison were on cruciform arrangements with single monotonic applied load whilst the tests carried out by Celikag used cantilever arrangement with slow cyclically applied loads. Details of the test arrangements and the discussions of the results are presented in references [9.1,9.2].

The subassemblage with the cruciform test arrangement for balanced loads will, in general, provide a higher initial stiffness and ultimate capacity for the connection relative to the cantilever arrangement due to differences in the load paths. This matches the experimental M-ϕ response in the internal joints for balanced loads in frames 3, 4 and 5 as discussed in chapters 6 and 7. This phenomenon can be explained by the distribution of the forces due to the applied beam load in a major axis framed column as shown in Figure 9.11. In Figure 9.11(a), the force distribution and joint rotation in an external joint is illustrated. It is clear that rotation of the beam occurs due to the applied beam load. The tension force in the top of the beam flange $F_{t.sd}$ will transfer to the web panel of column in the tension zone V_{sd} ($F_{t.sd}$ should be equal to V_{sd}). An equal but opposite compression force $F_{c.sd}$ act in the bottom flange of beam will transfer to the compression zone of the column web. Thus the shear force due to the applied moment M_{sd} due to the applied beam load will be resisted by the shear zone of the column web panel. The strength of the column web may limit the moment resistance of the connection. The deformation of the beam-to-column is shown in Figure 9.11(a).

A different phenomenon is observed in the internal joint as shown in Figure 9.11(b). As symmetrical load is applied to the both sides of beam, same value of the tension $F_{t.sd}$ and compression forces $F_{c.sd}$ occur in the top and the bottom flanges of the beam. These forces V_c are self equilibriating in the column web due to the balanced actions from both of beams. Thus the shear zone of the column web panel is not active. The shear force V_b due to the applied beam load will be transferred to the column flanges. Figure 9.11(b) also illustrates the deformation of an internal joint which is likely to have a higher moment resistance than a similar external one.

Consider the M-ϕ results for the minor axis frame 4, it can be seen that the M-ϕ curves for the internal joints resemble the cruciform joint test results. However, the external joints are far more flexible. This is due to the effects of column web flexibility which are included in a 'cantilever' connection test but which are nullified in a 'cruciform' test due to the symmetrical arrangement of beam loads. The differences between the 'cantilever' and the 'cruciform' connection tests for the minor axis frame highlighted the importance of web

flexibility to effect on the performance of connection have been reported by Gibbons [9.3]. Figures 9.12 to 9.17 compare the moment rotation behaviour of two different test arrangements used in analysis. All the curves show that the curve obtained from the cruciform arrangement conducted by Davison provides a larger initial stiffness and higher sustained moment for nominally the same of connection.

The results recorded in Table 9.6 present the total load in the column at failure, for each of the three loading cases, 5 forms of connections (one set of results obtained for the rigid and pinned beam-to-column connections and two sets of results obtained for the other semi-rigid connections), 1 column orientation 'B' and 2 base conditions - a total of 36 different analytical models for the semi-rigid connections and 12 different analytical models for the two extreme cases from the first phases of study are included.

9.6.1 Discussion of Results

Comparison of the effect of the behaviour of subassemblages using the M-ϕ characteristics with different test arrangements, it is important to note that the two sets of moment rotation data from Davison and Celikag predict similar column failure loads for each of the three different types of semi-rigid beam-to-column connections the maximum difference observed being less than 2 %. This implies that for column response it is not necessary to know the M-ϕ relationship with any high degree of precision.

Table 9.6 demonstrates the effect of two different base conditions in column orientation 'B' (primary beams connected to the column flange) on the column capacity and the α_{pin} values. For the rigid base condition as shown in Table 9.4, similar column capacity is determined from loading cases (0) and (1). This is at variance with explanation from Figures 9.6 and 9.7 - the first of which is monotonic loading only and the second has one reversal of joint rotation. It implies that the joint rotations under beam loads only may be still on the linear portion of the M-ϕ relationship or that there is a balanced effect between the change of stiffness in the connections and differences in the moment applied to the column resulting from these changes of stiffness, so that different unloading stiffness effects do not occur. The failure load reduces as the stiffness of the connections reduce (left to right in the table).

As expected, the α_{pin} values for the semi-rigid connections are all greater than unity. Thus the column subassemblage with semi-rigid connections in this study are shown to benefit from column end restraint and furthermore the benefits outweigh the detrimental

effects of moment transfer. It is of interest to note that the α_{pin} value is determined as 1.42 for the flush end-plate FE {D} in the loading case (1) with a pinned base - showing the potential benefit of including the true behaviour of a relatively flexible connection and even a very flexible web cleats joint, WC {D}, gives an α_{pin} value of 1.31. This implies that the restraint provided by the connection can give a very significant improvement in load carrying capacity.

The highest α_{pin} value is 1.71 for FE {D} (which is the same value as for the rigid connection) in loading case (0) with a rigid column base. The lowest value of 1.28 is determined in the WC {D} in loading case (2) with pinned column base whilst it is noted that the subassemblage with a rigid base and flush end-plate beam-to-column connection significantly increase the α_{pin} values, the cost of constructing a rigid column base may offset the saving in the weight of steel.

At the top of column, flush end-plate gives essentially same result as rigid connection. The results of this study show that using the flush end-plate beam-to-column connection with a suitable column orientation (major axis in this study cases) can provide a economic design for a steel frame. This will increase the capacity of the column leading to a reduction in the weight of steel. However, the conclusion drawn here is only based on a limited study. Further works are thus suggested in future to compare of the construction costs employing different connections and column bases for the structures.

As with the results from the first phase of the study, there is no significant difference in the failure loads determined from the pinned beam-to-column connection for the three loading cases as no beam moment was transferred to the column head. As explained in section 9.5.1, the slightly lower column failure load determined for loading case (2) is due to the additional moment introduced to the column head by the pattern beam loading. Consider the results of the subassemblage with pinned base condition as shown in Table 9.6, again there is no significant difference between the results obtained from loading cases (0) and (1); and once more the failure load reduces as the stiffness of the connections reduces.

Figures 9.18 and 9.19 show the applied beam load again mid-height minor axis deflection for subassemblages using the different types of connections from the tests conducted by Davison and Celikag with the two extreme case, fully rigid and pinned being used to determine upper and lowest boundaries of the load deflection curves. Figure 9.18 shows the plot using the M-ϕ data obtained from the test of Davison. The curves determined from the flush end-plate and web and seat cleats connection are shown to give behaviour similar re-

sponse to that of the rigid connection whilst only a slightly lower axial load was determined for the subassemblage with double web cleat connection as the column approached failure. The stiffness of the semi-rigid connected subassemblages was seen to reduce deflections in the mid-height of column significantly. Figure 9.19 shows the corresponding plot using the M-ϕ data obtained from the test of Celikag from which identical conclusions may be drawn.

9.6.2 Conclusions of Second Phase

From the study, some conclusions are drawn,

1. For column load carrying capacity, it is not essential to know the M-ϕ response to a high degree of precision
2. Economy can be achieved by use of semi-rigid action.
3. All the failures were due to excessive minor axis bending even when primary moments were applied about the major axis.

9.7 Third Phase of Study

In theory, nominally identical joints do not respond in identical ways. The third phase of study concentrates on further investigating the 'sensitivity' of column capacity due to variation in the M-ϕ response in a great detail. The first and second studies have provided evidence that the restraint of the beam-to-column connections and column base increases the capacity of the column. This suggests that a lower cost, in steelwork terms, may be possible if frames are designed by a semi-rigid method. The results of the second phase of study show that the behaviour of the frame using the identical beam-to-column connection with different test conditions and arrangements is largely unaffected by the variation of the M-ϕ response. Designers may initially be concerned about the accuracy to which the M-ϕ response may be required. This is the subject of this phase of the study.

9.7.1 Using M-ϕ Curves from Nominally Connections

The first and second phases of the study were limited to the use of M-ϕ characteristics obtained from two joint test arrangements. To extend the study, a set of five M-ϕ curves with the flange cleat connection conducted at the University of Sheffield was selected for study. The five M-ϕ data are;

1. Joint test from Celikag FC {CJ}

2. Joint test from Davison FC {DJ}
3. Subassemblage from Davison FC {DS}
4. Frame test from Davison FC {DF}
5. Subassemblage from Gibbons FC {GS}

Comparison of the response of subassemblages using the five beam-to-column connection characteristics for a pinned base column, orientation 'B' and loading arrangement (1) only are considered here in order to keep the volume of computation manageable.

The moment rotation behaviour for these five tests are compared in single plots as illustrated in Figures 9.20 (major axis) and 9.21 (minor axis). These clearly show significant variation. Table 9.7 lists the results in terms of the column capacity; together with the limiting values for rigid and pinned connections. The α_{pin} values are also given for completeness. It is noted from Table 9.7 that the failure load is approximately 575 kN in all semi-rigid cases. The α_{pin} factor is calculated as about 1.40. The results are similar to those determined from the web and seat cleats connection as recorded in the Table 9.6. This has implications for design as it confirms that designers need not know precisely the M-ϕ behaviour. Figure 9.22 shows five load deflection curves in a single plot to represent the results determined from the different M-ϕ characteristics from the five sets of moment rotation data with the same subassemblage arrangement, whilst Figures 9.23 to 9.24 show comparisons of the bending at the top and mid-height of the column. As expected, all curves are similar despite the variations in the M-ϕ response.

9.7.2 Further Study of Variation of M-ϕ Response

In this study, three nominally identical semi-rigid connections used in the second phase of study, namely flush end-plate, web and seat cleats and web cleat, are selected. Only the column orientation 'B', pinned column base and loading arrangement (1) are considered. For each type of connection, variations of the moment rotation curves of 10 % and 20 % were considered to investigate the effect on the load carrying of the column and the behaviour of the subassemblage. The method adopted to change the M-ϕ for the flush end-plate connection is illustrated in Figure 9.25 where at a particular value of rotation and moment is changed. It is noted from this figure that the curve from Davison's test shows a larger initial stiffness and sustained moment. Thus the moment for the Davison's curve is increased to 10 and 20 % with the same rotation whilst a reduction of 10 and 20 % is applied to the curve from Celikag.

Table 9.8 illustrates the results determined from all different study cases. FE {D} and FE {C} are the curves determined from the original M-ϕ curve of Davison and Celikag , the curves noted FE {D1} and FE {C1} are the variation of 10 % and FE {D2} and FE {C2} are 20 % for the moment with constant rotation. It can be seen that there is no significant effect in terms of column carrying capacity with a maximum discrepancy of only 1 %. The load deflection response for each type of connection due to the variation of the moment rotation response is compared in Figures 9.26 to 9.28. All three plots show a good correlation with that without change in M-ϕ response. As expected, it is evident from the plot that all different variation of the M-ϕ response has given a very close prediction of the ultimate column capacity. Furthermore, all curves with the variation of the M-ϕ response appeared to closely simulate all aspects of the curve determined from the original M-ϕ data.

9.7.3 Conclusions of Third Phase

From the final phase of study two conclusions are drawn,

1. Similar responses of the subassemblage are determined using nominally identical semi-rigid connections with different test conditions and arrangements.
2. Significant variations of the M-ϕ response have a negligible effect on the load carrying of the column and the behaviour of the subassemblage.

9.8 Concluding Remarks on the Parametric Study

From the results obtained in the previous section, the author has made a number of observations on subassemblage behaviour. The ability of the finite element program has been further confirmed by its ability to replicate test results. The presence of the beam-to-column connections with realistic stiffness and the column base condition will both have a dominant effect on the capacity of column. The beneficial influence of the restraint to the column from the semi-rigid beam-to-column connections exceeds the detrimental effect of the moment transferred.

Several studies conducted at the University of Sheffield [9.1,9.3,9.5,9.6] have also indicated that use of semi-rigid action can decrease the cost of a structure when it is compared with one using the simple design method. Perhaps the most significant finding was that for the cases considered, the semi-rigid characteristics obtained from different test arrangements and conditions predict similar failure loads of the column in a subassemblage. The

differences in behaviour of frames using moment rotation curves of a nominally identical beam-to-column connections with different test criteria are negligible. Furthermore, it is evident that, in this instance, the different types of the stiffer beam-to-column connections (WAS, FEP) predict similar behaviour of the subassemblages and similar to rigid connections (see Figures 9.18 and 9.19). This study also showed that the column capacities are not significantly affected by quite large changes in the moment-rotation response. This implies that the precise form of the M-ϕ curves is not important.

It is appreciated that although a large number of analytical models have been examined to represent the different arrangement and loading case for subassemblages, the conclusions obtained are based on a limited study and the cases considered may be not sufficient to represent the full range of real structures. Thus further research is highly recommended. Due to the limitation of time, only the two extreme column base conditions, pinned and rigid, are considered in this study. In real frames, the rotational stiffness of the column base is neither infinite nor zero. The stiffness and strength of the column base conditions influence the ultimate strength and the behaviour of the column response. Selecting and achieving a level of stiffness of stiffeners which approximates to rigid at the column base will significant influence the construction cost. Thus subassemblages with a more representative semi-rigid effect for typical column bases should be considered in a further study. Further work to compare the construction cost which employs different connections and base conditions for the steel frames is also suggested. Finally, typical studies could concentrate on longer beams and columns, different types of the semi-rigid connection, different strengths and sizes of beams and columns and various loading arrangements.

References

[9.1] Davison, J. B., 'Strength of Beam-Columns in Flexibly Connected Steel Frames', Ph.D. Thesis, Department of Civil and Structural Engineering, University of Sheffield, U.K., June, 1987.

[9.2] Celikag, M., 'Moment-Rotation Behaviour of Steel Beam-to-Column Connections', Ph.D. Thesis, Department of Civil and Structural Engineering, University of Sheffield, U.K., February, 1990.

[9.3] Gibbons, C., 'The Strength of Biaxially Loaded Beam-Columns in Flexibly Connected Steel Frames', Ph.D. Thesis, Department of Civil and Structural Engineering, University of Sheffield, U.K., December, 1990.

[9.4] Rifai, A. M., 'Behaviour of Columns Subassemblage with Semi-Rigid Connections', Ph.D. Thesis, Department of Civil and Structural Engineering, University of Sheffield, U.K., June, 1987.

[9.5] Wang, Y.C., 'Ultimate Strength Analysis of Three-Dimensional Structures with Flexible Restraints', Ph.D. Thesis, Department of Civil and Structural Engineering, University of Sheffield, U.K., June, 1988.

[9.6] Jones, S. W., 'Semi-Rigid Connections and their Influence on Steel Column Behaviour', Ph.D. Thesis, Department of Civil and Structural Engineering, University of Sheffield, U.K., 1980.

[9.7] Ahmed, I., 'Semi-Rigid Action of Steel Frames', Ph.D. Thesis, Department of Civil and Structural Engineering, University of Sheffield, U.K., September, 1992.

[9.8] El-Khenfas, M. A., 'Analysis of Biaxial Bending and Torsion of Open Section Beam Columns', Ph.D. Thesis, Department of Civil and Structural Engineering, University of Sheffield, U.K., 1987.

[9.9] Gent, A. R. and Milner, M. R., 'Ultimate Load Capacity of Elastically Restrained H-Columns under Biaxial Bending', Proceeding of the Institution of Civil Engineers, Vol. 43, December, 1968, pp. 1685-1704.

[9.10] Bitar. S, Ph.D. Thesis, in preparation.

[9.11] Lau, S. M., ' Ultimate Strength Analysis of Three Dimensional Structures with Flexible Restraints - Computer Program, Department of Civil and Structural Engineering, University of Sheffield, U.K., January, 1991.

[9.12] Kirby, P. A., Bitar. S and Gibbons, 'C., 'The Design of Columns in Non-Sway Semi-rigid Connected Frames', First World Conference on Structural Steel Design, Dec, 1992, pp. 54-63.

[9.13] British Standards Institution BS 5950: Part 1: Structural Use of Steelwork in Building. BSI, London, British Standards Institution, 1990.

[9.14] Davison, J. B., Kirby, P. A. and Nethercot, D. A., 'Rotational Stiffness Characteristics of Steel Beam-to-Column Connections', Journal of Constructional Steel Research, No.8, 1987, pp. 17-54.

[9.15] Bjorhovde, R., 'Effect of End Restraint on Column Strength - Practical Application.' AISE Engineering Journal, Vol.20, No.1, 1st Quarter, 1984, pp. 1-13.

[9.16] Davison, J. B., Kirby, P. A. and Nethercot, D. A., 'Semi-Rigid Connections in Isolation and in Frames', State-of-the-Art Workshop on Connections, Strength and Design of Steel Structures, Cachan, France, May, 1987.

[9.17] Prov, E. P., and Pinkney, iR. B., 'Cyclic Yield Reversal in Steel Building Connections', Journal of Structural Divison, ASCE, Vol.95, No. ST3, March, 1969, pp. 327-353

[9.18] Moncarz, P. D., and Gerstle, K. H., 'Steel Frames with Nonlinear Connections', Journal of Structural Divison, ASCE, Vol.107, No. ST8, March, 1981, pp. 1427-1441

[9.19] Marley, M. J., 'Analysis and Test of Flexibly Connected Steel Frames', Report to AISI, University of Colorado, Boulder, USA, March, 1982.

[9.20] Bernuzzi, C., 'Cyclic Response of Semi-Rigid Steel Joints', First World Conference on Structural Steel Design, Dec, 1992, pp. 196-209.

Type	Symbol	Description
Connection Type	1	Web Cleat
	2	Flange Cleat
	3	Web and Seat Cleats
	4	Flush End Plate
	3 & 4	Web & Seat Cleats in Beams 1 and 3 Flush End Plate in Beam 2
Edge/Corner	E	Edge
	C	Corner
Column Orientation	A	Beams 1 and 3 connected to Column Web
	B	Beams 1 and 3 connected to Column Flange

Table 9.1 : Symbols used in the Comparison with Predicted Results to the Subassemblage Test

Test	Connection Type	Edge/ Corner	Column Orientation	Applied Load of Beam (kN)			Failure Load of Column (kN)		$\frac{Analysis}{Experiment}$
				1	2	3	Exp.	Analysis	
S1	1	E	A	5	50	50	468	442	0.94
S2	2	E	A	50	50	50	503	512	1.02
S3	3	E	A	50	50	50	543	547	1.01
S4	4	C	A	-	50	50	495	474	0.96
S5	1	E	B	30	30	60	479	413	0.86 *
S6	2	E	B	30	30	60	614	615	1.00
S7	3	E	B	45	45	90	490	497	1.01
S8	1	E	A	10	85	85	482	491	1.02
S9	2	E	A	95	95	95	526	510	0.97
S10	3 & 4	E	A	88	132	88	520	518	1.00

Remark : asterisk means numerical divergence

Table 9.2 : Comparison with the Failure Load predicted by Program

Type	Symbol	Description
Column Orientation	A	Primary Beams connected to Column Web
	B	Primary Beams connected to Column Flange
Base Condition	RB	Rigid
	PB	Pinned
Type of Connection	RC	Rigid
	PC	Pinned
Loading Case	0	No Load applied to Beam
	1	Point Load applied to Two Primary Beams
	2	Point Load applied to One Primary Beam

Table 9.3 : Symbols used in the First Phase of Study

Case	Column Orientation	Total Axial Load at Failure (kN)			
		1	2	3	4
Base Condition		RB	RB	PB	PB
Type of Connection		RC	PC	RC	PC
Loading Case 0	A	702 (1.70)	600 (1.46)	579 (1.41)	421 (1.02)
Loading Case 1	A	702 (1.70)	600 (1.46)	579 (1.41)	421 (1.02)
Loading Case 2	A	655 (1.59)	600 (1.46)	500 (1.21)	421 (1.02)
Loading Case 0	B	703 (1.71)	595 (1.44)	584 (1.42)	412 (1.00)
Loading Case 1	B	703 (1.71)	597 (1.45)	584 (1.42)	416 (1.01)
Loading Case 2	B	665 (1.61)	596 (1.45)	543 (1.32)	414 (1.00)

Remark : ( ) indicates the α_{pin} factor

Table 9.4 : Predicted Column Failure Load from the First Phase of Study

Type no.	Type	Symbol	Description
1	Column Orientation	A	Primary Beams connected to Column Web
		B	Primary Beams connected to Column Flange
2	Base Condition	RB	Rigid
		PB	Pinned
3	Type of Connection	RC	Rigid
		FE	Flush End Plate
		WAS	Web and Seat Cleats
		WC	Web Cleat
		PC	Pinned
4	Source of M-ϕ Data	D	Davison, J. B.
		C	Celikag, M.
5	Loading Case	0	No Load applied to Beam
		1	Point Load applied to Both Primary Beams
		2	Point Load applied to One Primary Beam

Table 9.5 : Symbols used in the Second Phase of Study

Type of Connection	Base Condition	Total Column Axial Load at Failure (kN)							
		RC	FE		WAS		WC		PC
Source of M-ϕ		-	D	C	D	C	D	C	-
Loading Case 0	RB	703 (1.71)	703 (1.71)	700 (1.70)	702 (1.70)	697 (1.69)	686 (1.67)	693 (1.68)	595 (1.44)
Loading Case 1	RB	703 (1.71)	702 (1.70)	700 (1.70)	701 (1.70)	697 (1.69)	686 (1.67)	694 (1.68)	597 (1.45)
Loading Case 2	RB	665 (1.61)	674 (1.64)	673 (1.63)	678 (1.65)	675 (1.64)	674 (1.64)	684 (1.66)	596 (1.45)
Loading Case 0	PB	584 (1.42)	583 (1.42)	576 (1.40)	577 (1.40)	567 (1.38)	537 (1.30)	557 (1.35)	412 (1.00)
Loading Case 1	PB	584 (1.42)	583 (1.42)	578 (1.40)	579 (1.41)	568 (1.38)	538 (1.31)	558 (1.35)	416 (1.01)
Loading Case 2	PB	543 (1.32)	550 (1.33)	545 (1.32)	555 (1.35)	543 (1.32)	527 (1.28)	546 (1.33)	414 (1.00)

Remark: ( ) indicates the α_{pin} factor

Table 9.6 Predicted Column Failure Load with Different Connections for Column Orientation 'B' in the Second Phase of Study

Type	Column Failure Load (kN)						
	RC	FC{CJ}	FC{DJ}	FC{DS}	FC{DF}	FC{GS}	PC
Axial Load	584	570	574	576	578	576	416
α_{pin} factor	1.42	1.38	1.39	1.40	1.40	1.40	1.01

Remark :

Study Conditions Base Condition (PB)
Loading Case (1)
Column Orienatation (B)
(see Table 9.5 for the Symbols used in Study)

Table 9.7 Predicted Results from the M-ϕ Curves using different Tests for Flange Cleat Connections

Variation of M-ϕ	Base Condition	Total Column Axial Load at Failure (kN)							
		RC	FE		WAS		WC		PC
Source of M-ϕ		-	D	C	D	C	D	C	-
NIL	RB	584 (1.42)	583 (1.42)	578 (1.40)	579 (1.41)	568 (1.38)	538 (1.31)	558 (1.35)	416 (1.01)
±10%	RB	- -	583 (1.42)	576 (1.40)	579 (1.41)	567 (1.38)	541 (1.31)	557 (1.35)	- -
±20%	RB	- -	583 (1.42)	576 (1.40)	579 (1.41)	564 (1.37)	542 (1.32)	555 (1.35)	- -

Remark : ( ) indicates the α_{pin} factor

Table 9.8 Change of Ultimate Capacity of Columns due to the variation of M-ϕ Response

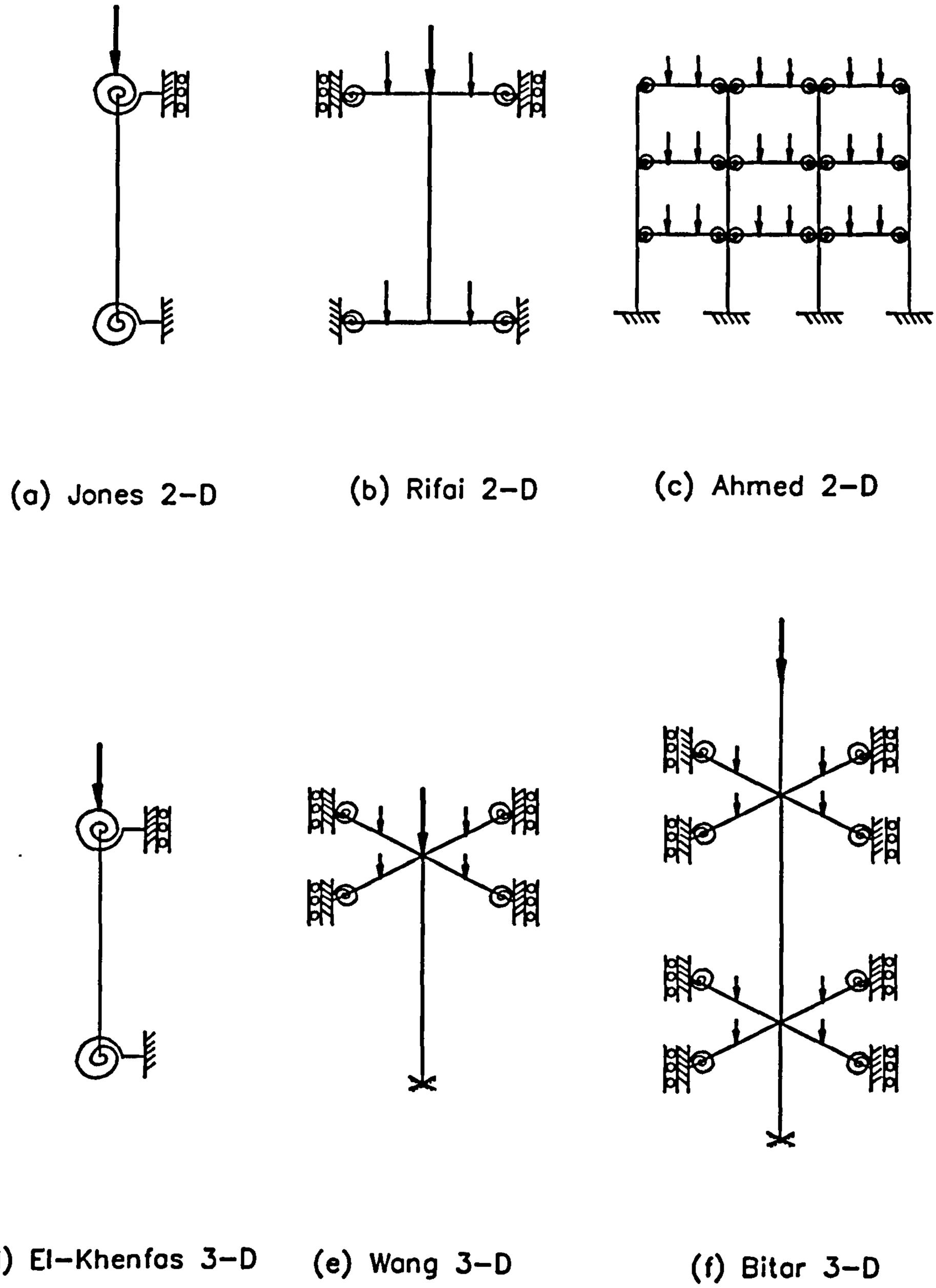

(a) Jones 2-D (b) Rifai 2-D (c) Ahmed 2-D

(d) El-Khenfas 3-D (e) Wang 3-D (f) Bitar 3-D

Figure 9.1 : Computer Programs developed at the University of Sheffield

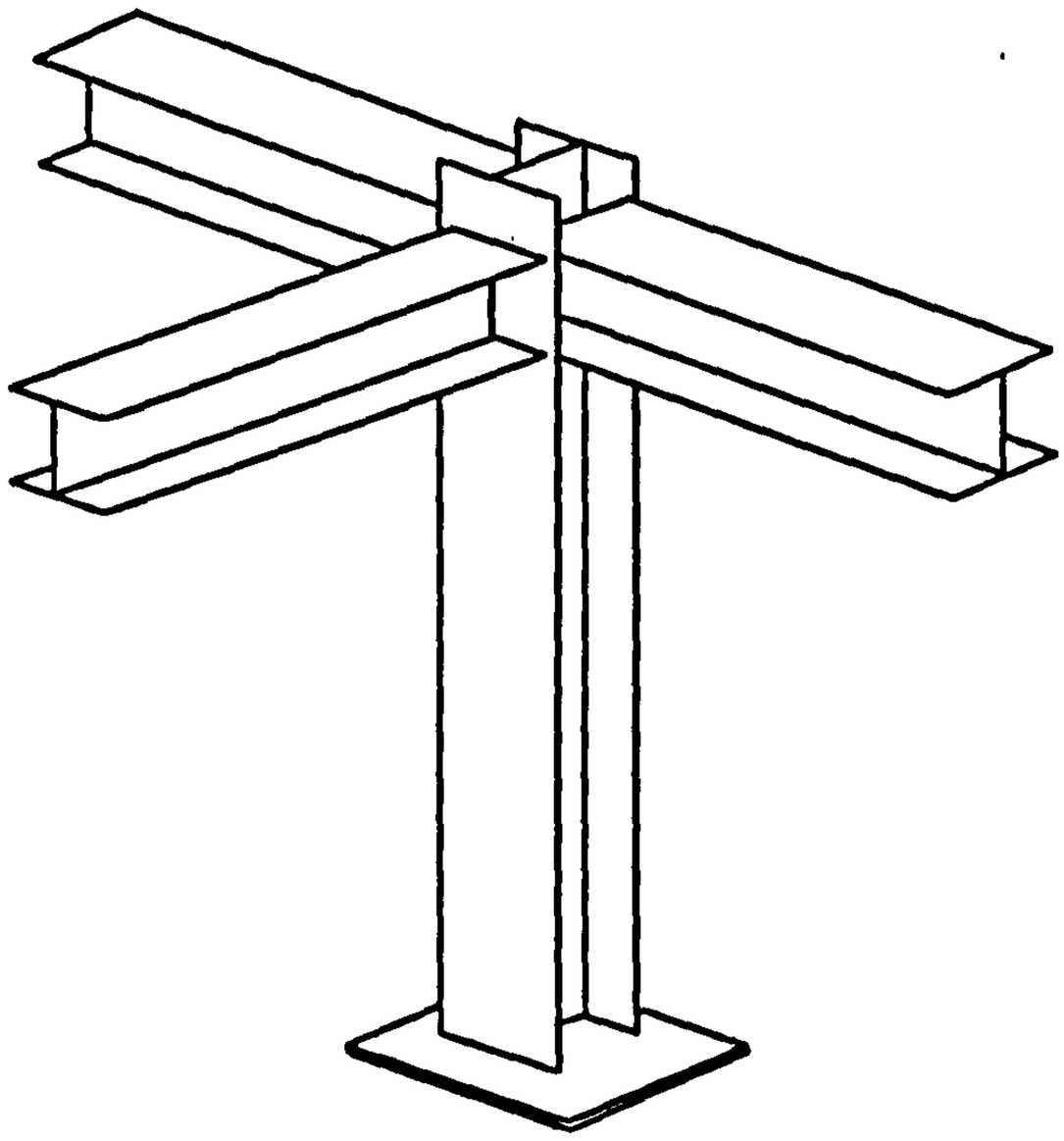

Subassemblage representing a Edge Column

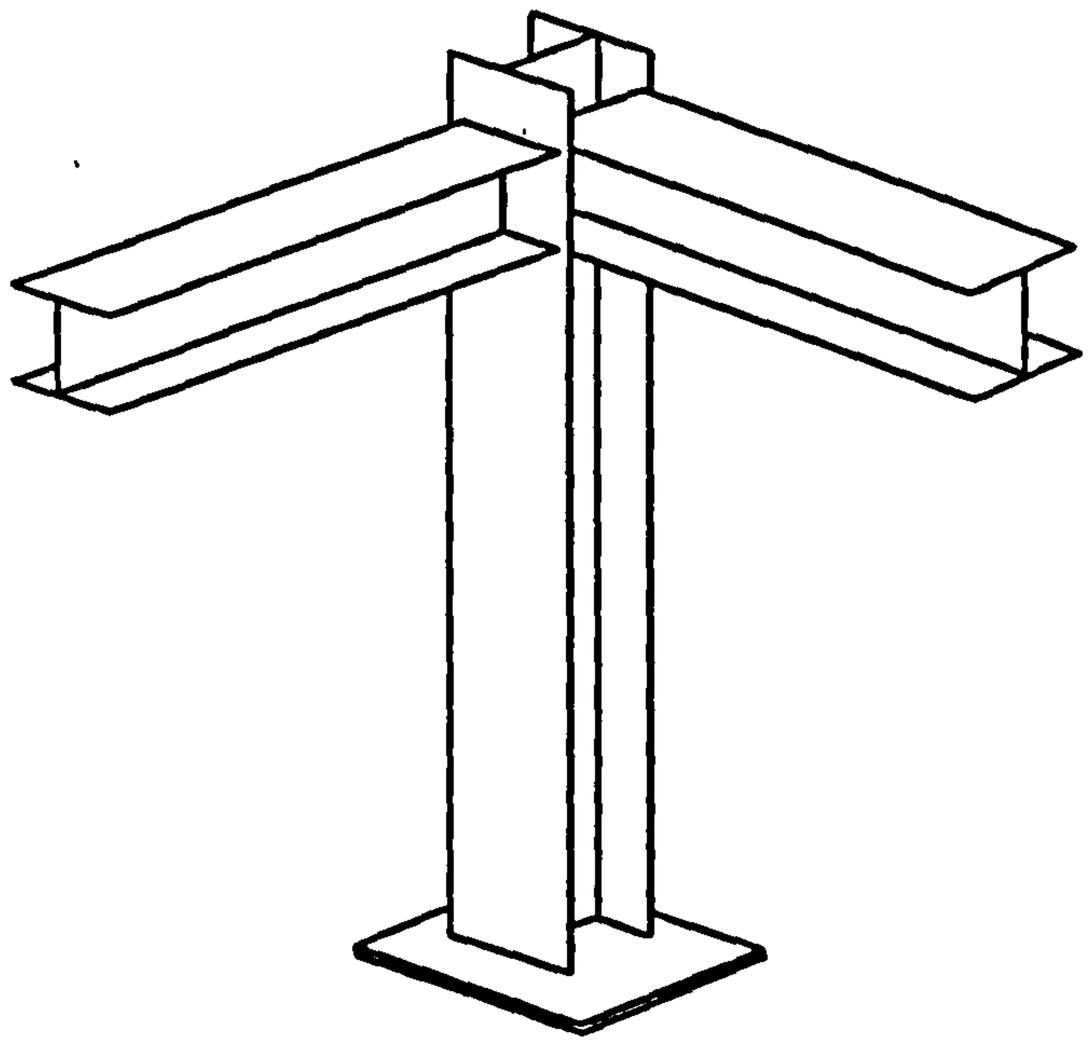

Subassemblage representing a Corner Column

Figure 9.2 : Subassemblage Tests conducted by Gibbons

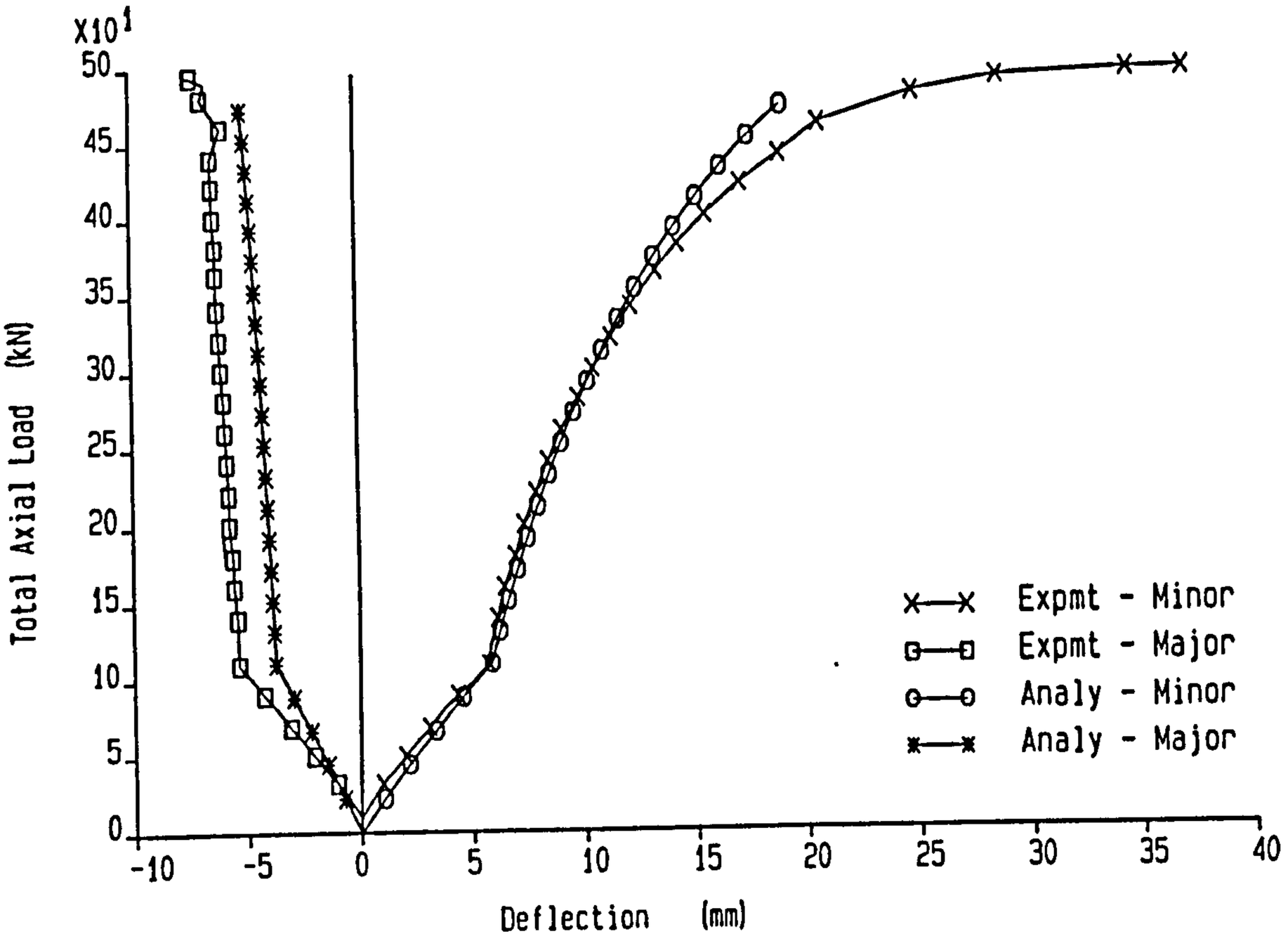

Figure 9.3 : Comparison of the Predictied and Experimental Deflections at the Column Centre of Test S4

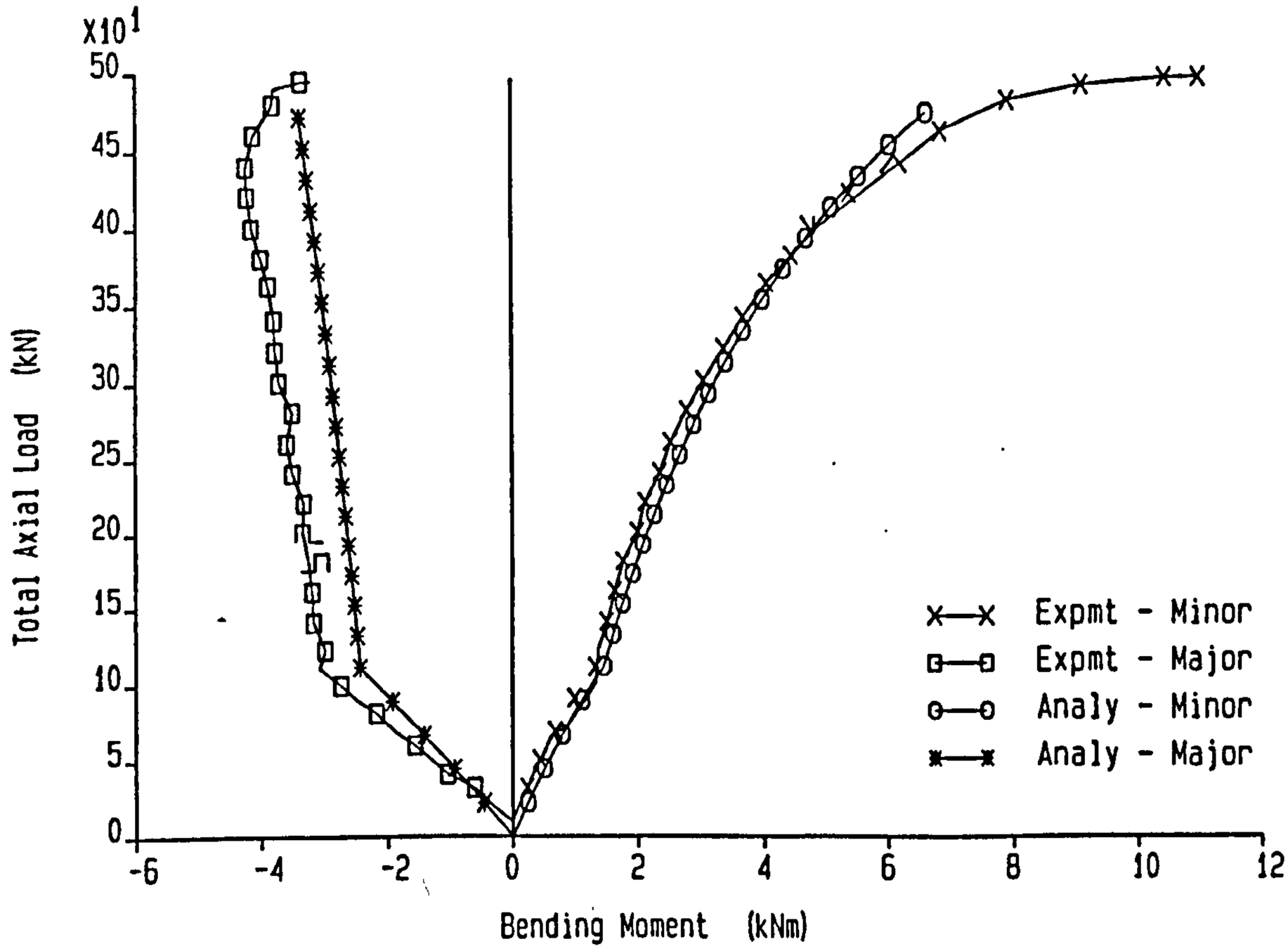

Figure 9.4 : Comparison of the Predicted and Experimental Moments at the Column Centre of Test S4

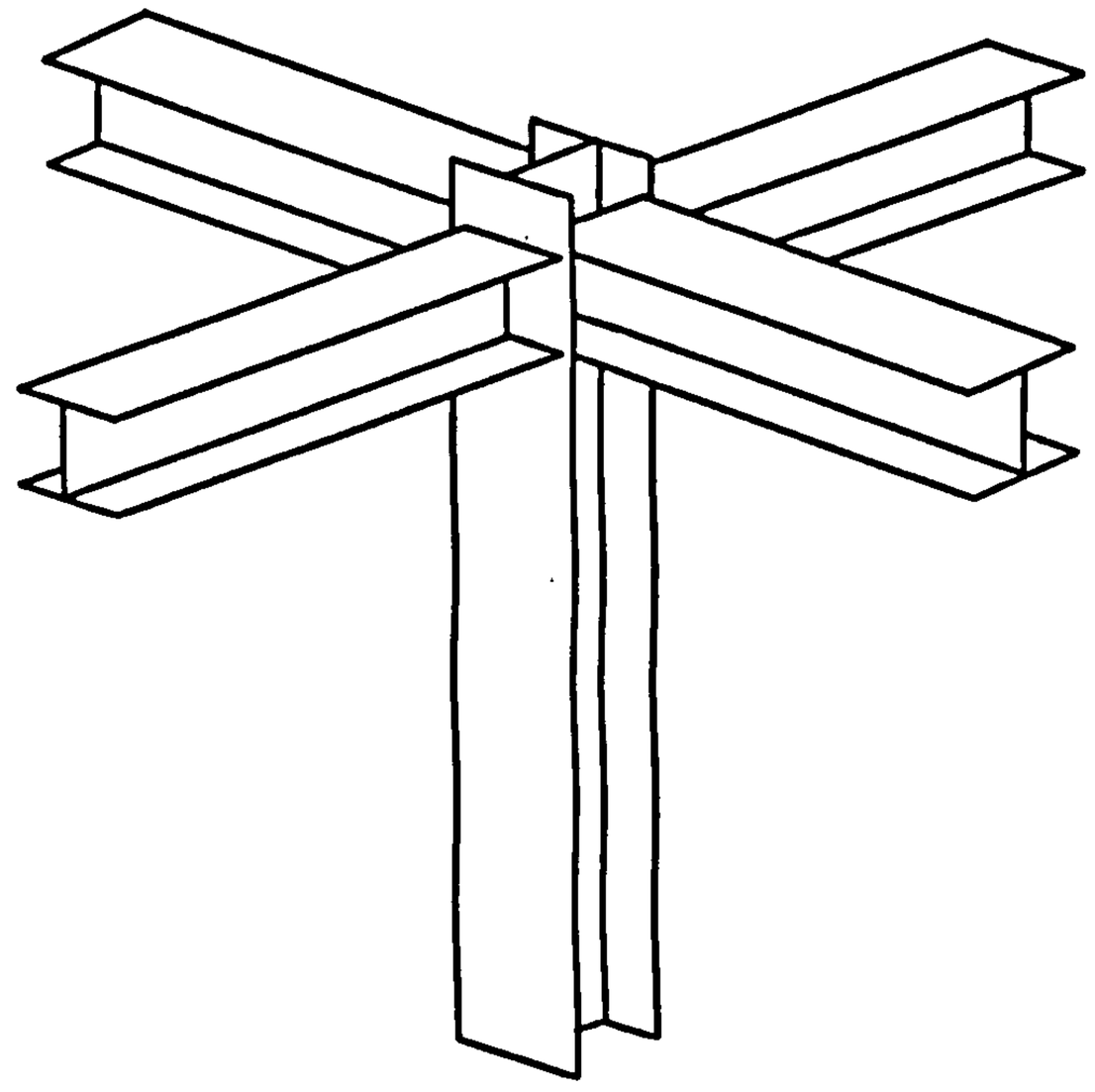

Design Model for Study

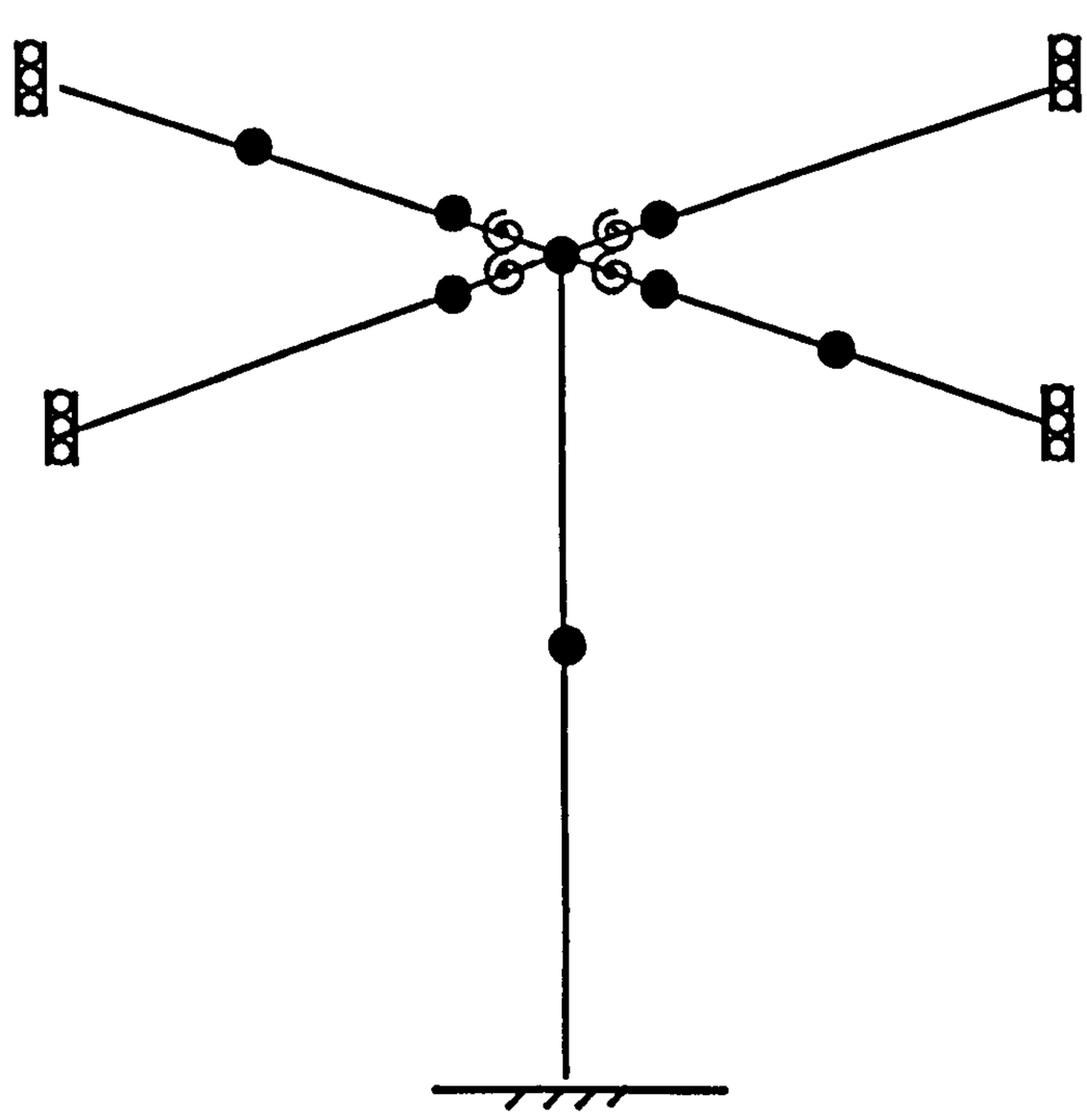

Analytical Model

Figure 9.5 : The Design Model Arrangement and its Analytical Model

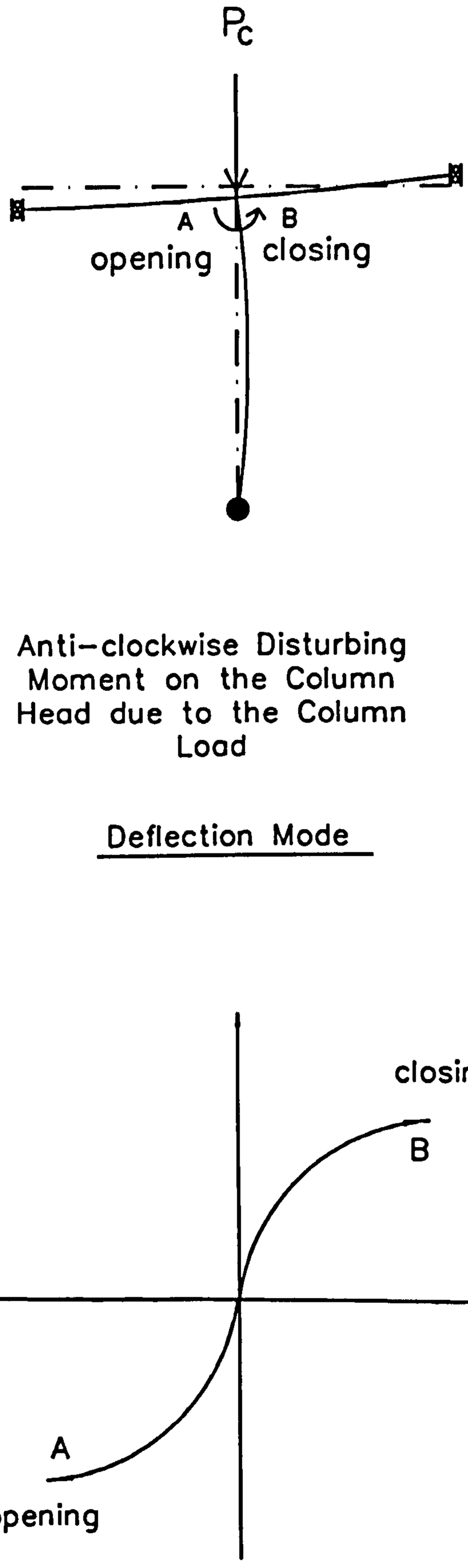

Figure 9.6 : Deflection Mode of Subassemblage in Loading Case (0)

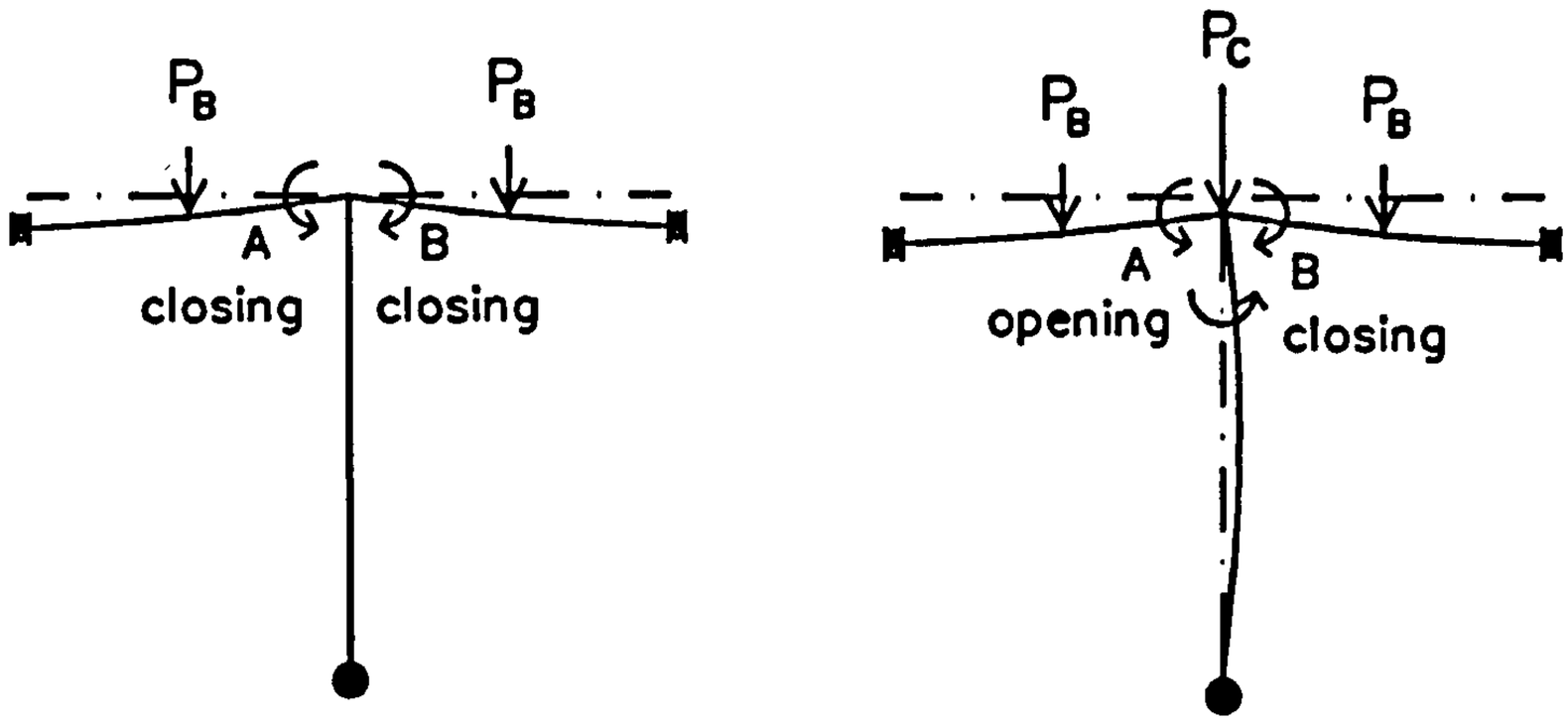

No Moment on the Column Head due to Balanced applied Beam Moments

After Load applied to the Column Head, an Anti-clockwise Moment produces on the Column Head.

(a) Beam Load Phase

(b) After Applied Column Load

Deflection Modes

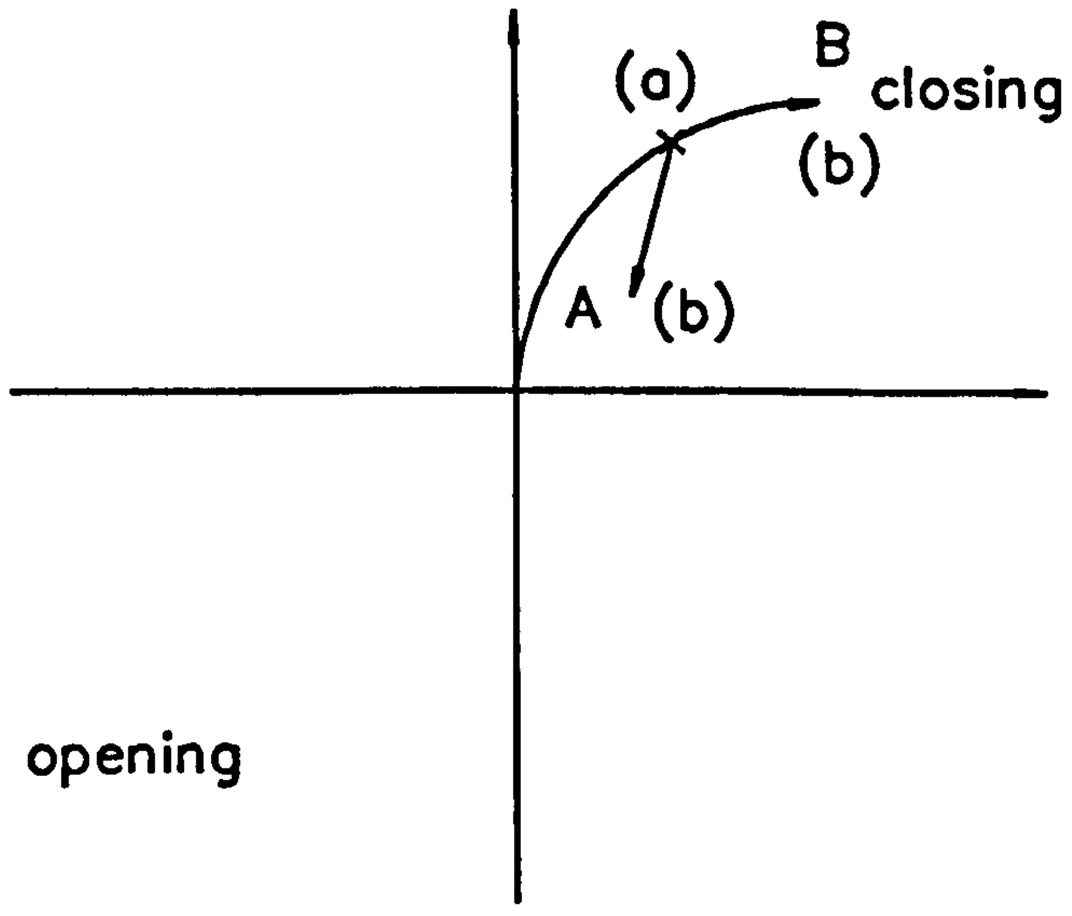

Moment Rotation Response

Figure 9.7 : Deflection Mode of Subassemblage in Loading Case (1)

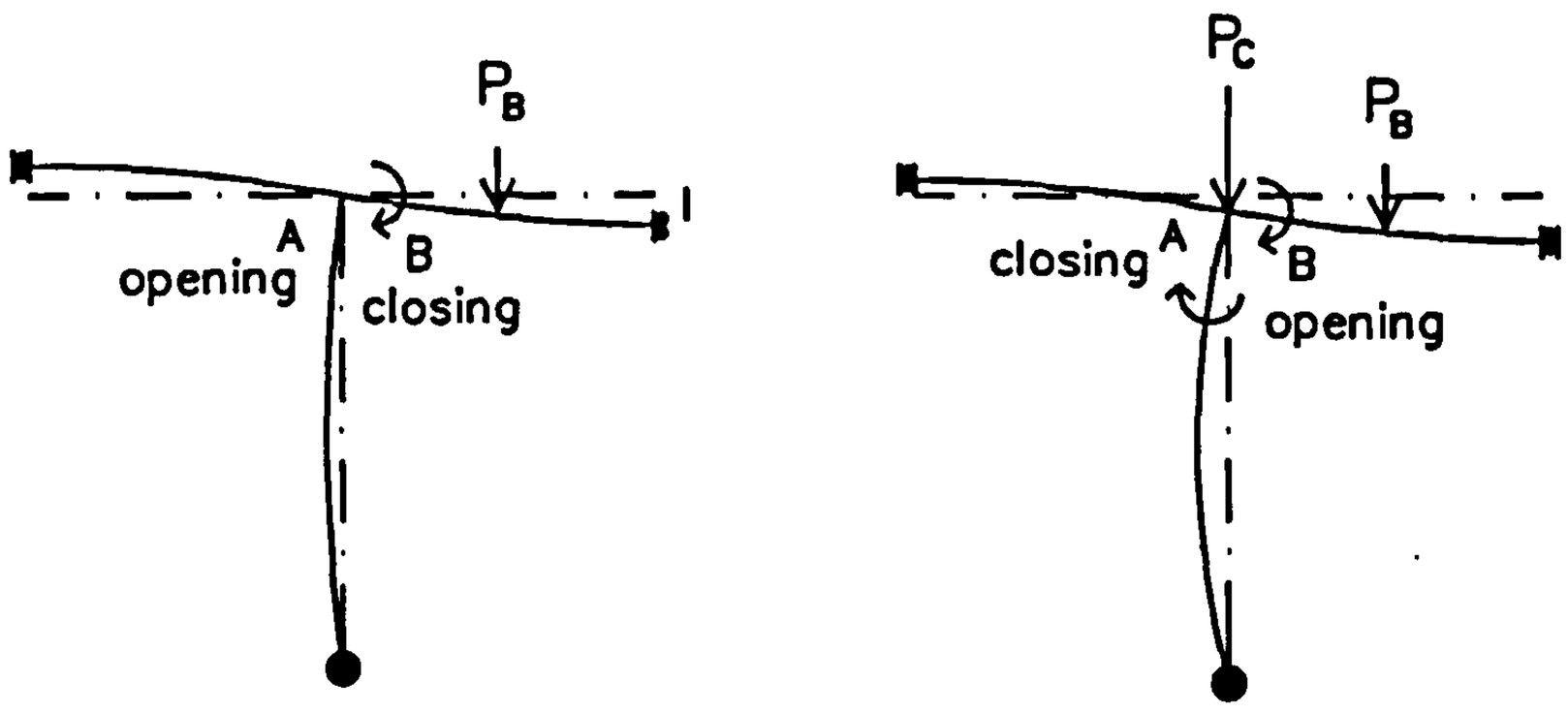

Clockwise Disturbing Moment on the Column Head due to the effect of applied Beam Load

After Load applied to the Column Head, Moment continues to increase (Clockwise)

(a) Beam Load Phase

(b) After Applied Column Load

Deflection Mode

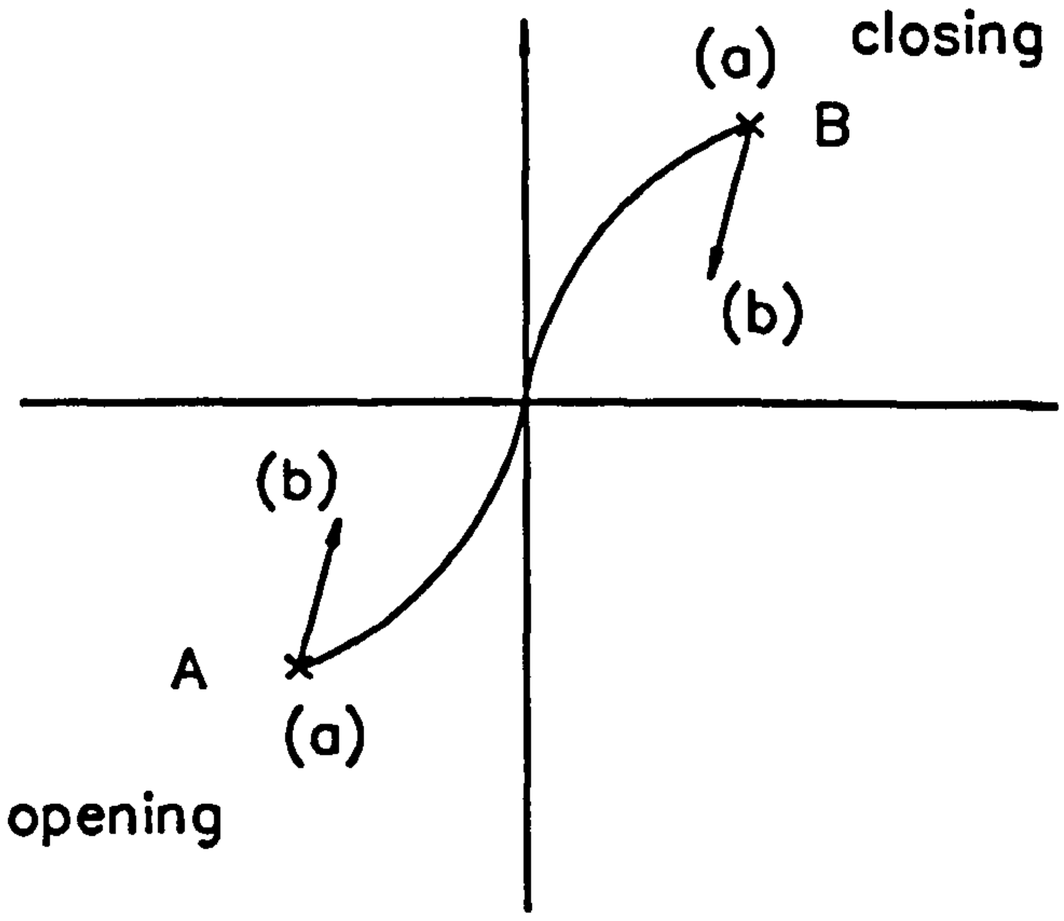

Moment Rotation Response

Figure 9.8 : Deflection Mode of Subassemblage in Loading Case (2)

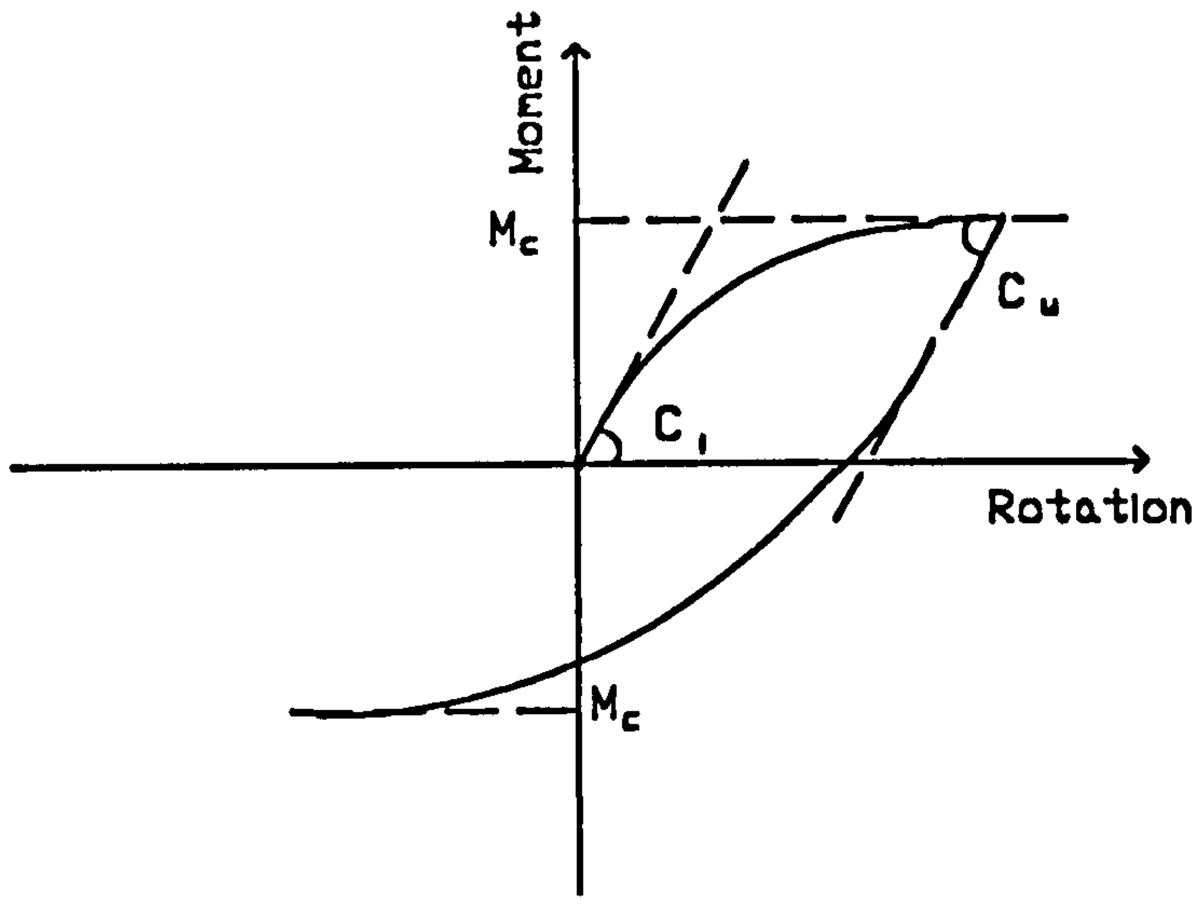

Where $C_i = C_u$

Figure 9.9 : Loading-Unloading Characteristics of Flexible Connections

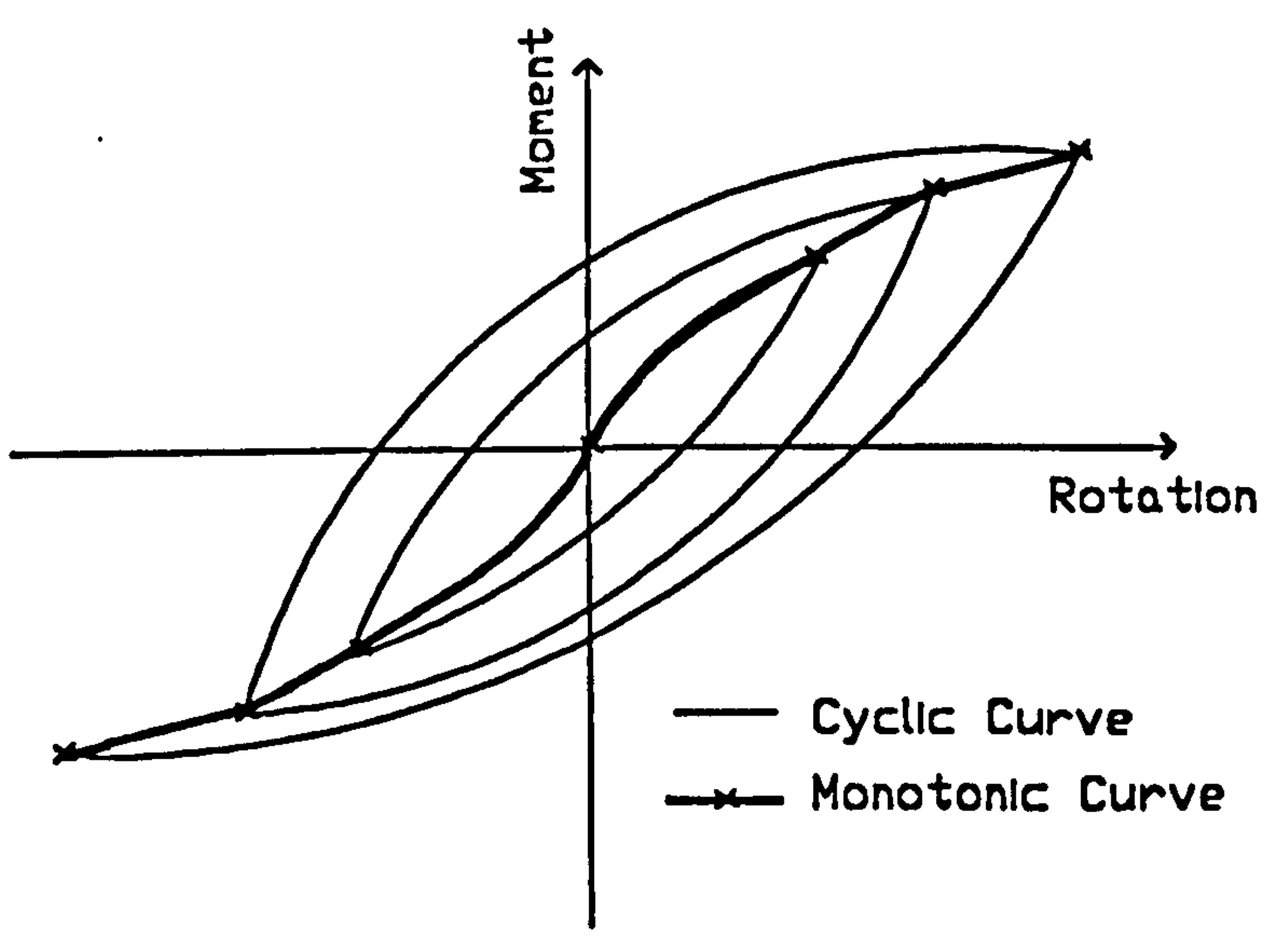

Figure 9.10 : Moment Rotation Response for Cylic and Monotonic Loading

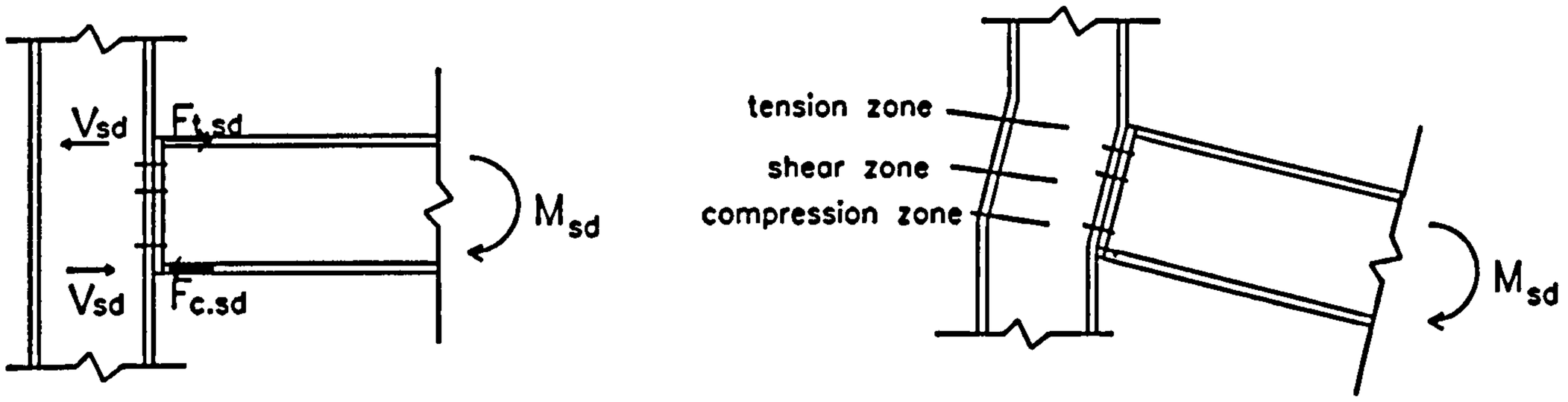

Force Distribution

Rotation of Joint

(a) Loading of an External Joint

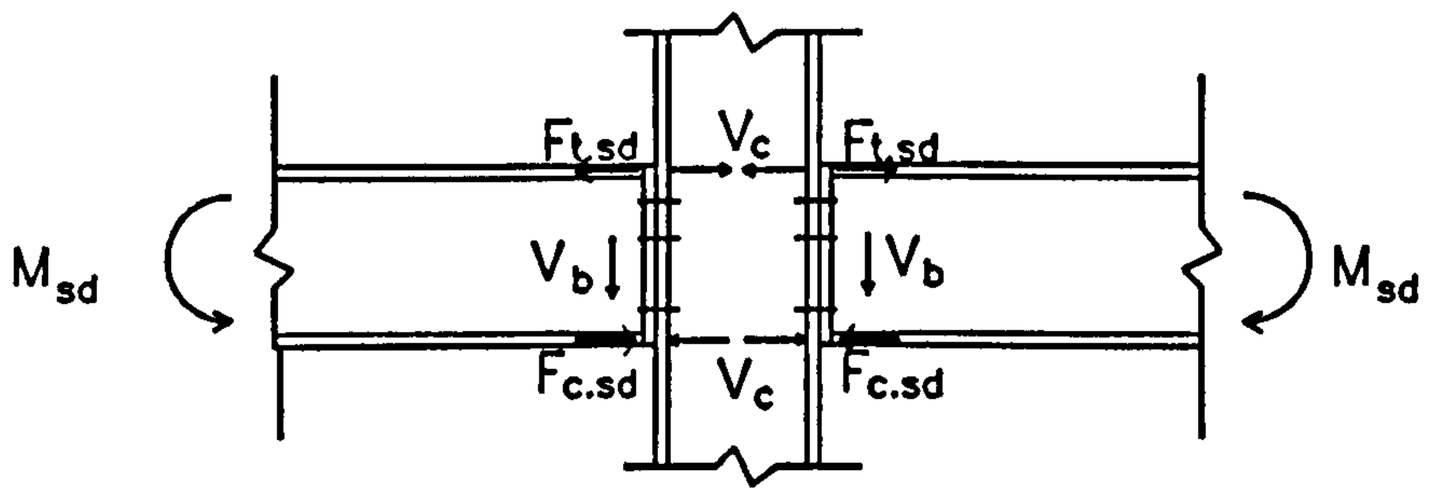

Force Distribution

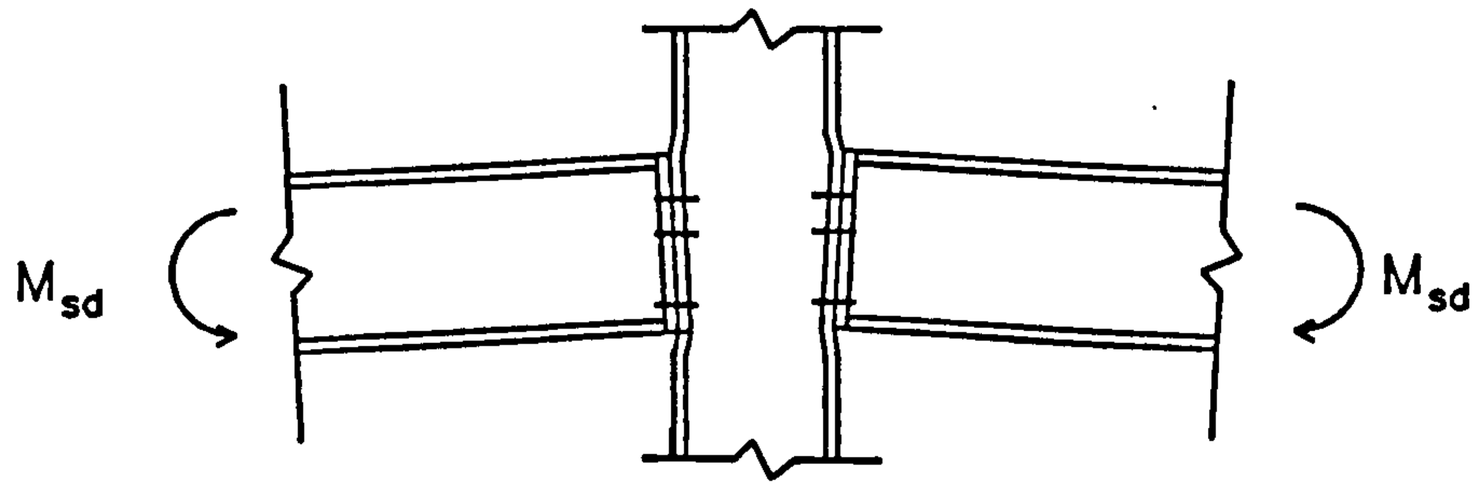

Rotation of Joint

(b) Loading of an Internal Joint

Figure 9.11 : Force Distribution and Rotation of Joint for Flexible Connections

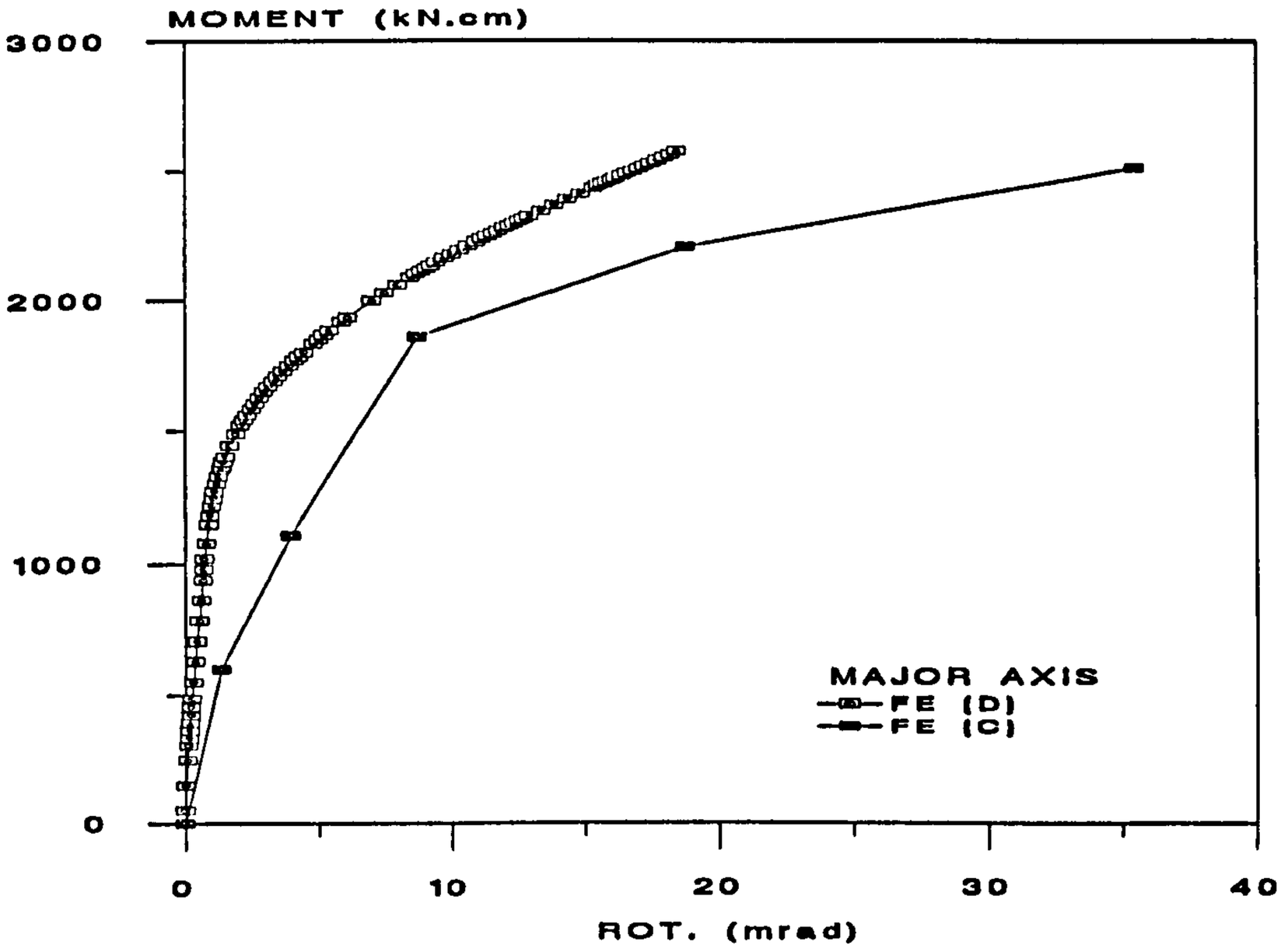

Figure 9.12 : Comparison of Moment Rotation Curves of Flush End-Plate Connections (Major Axis) from Davison and Celikag

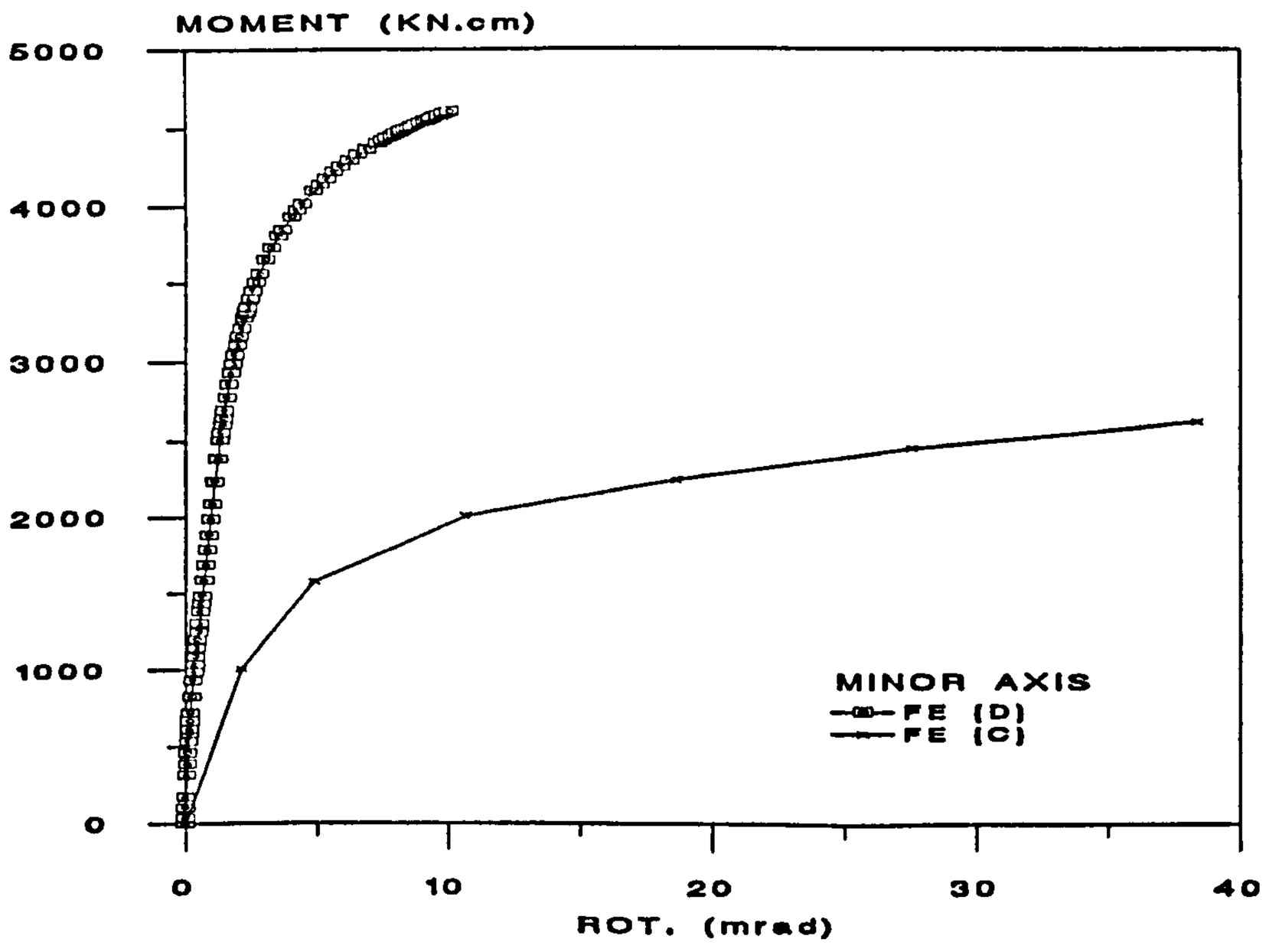

Figure 9.13 : Comparison of Moment Rotation Curves of Flush End-Plate Connections (Minor Axis) from Davison and Celikag

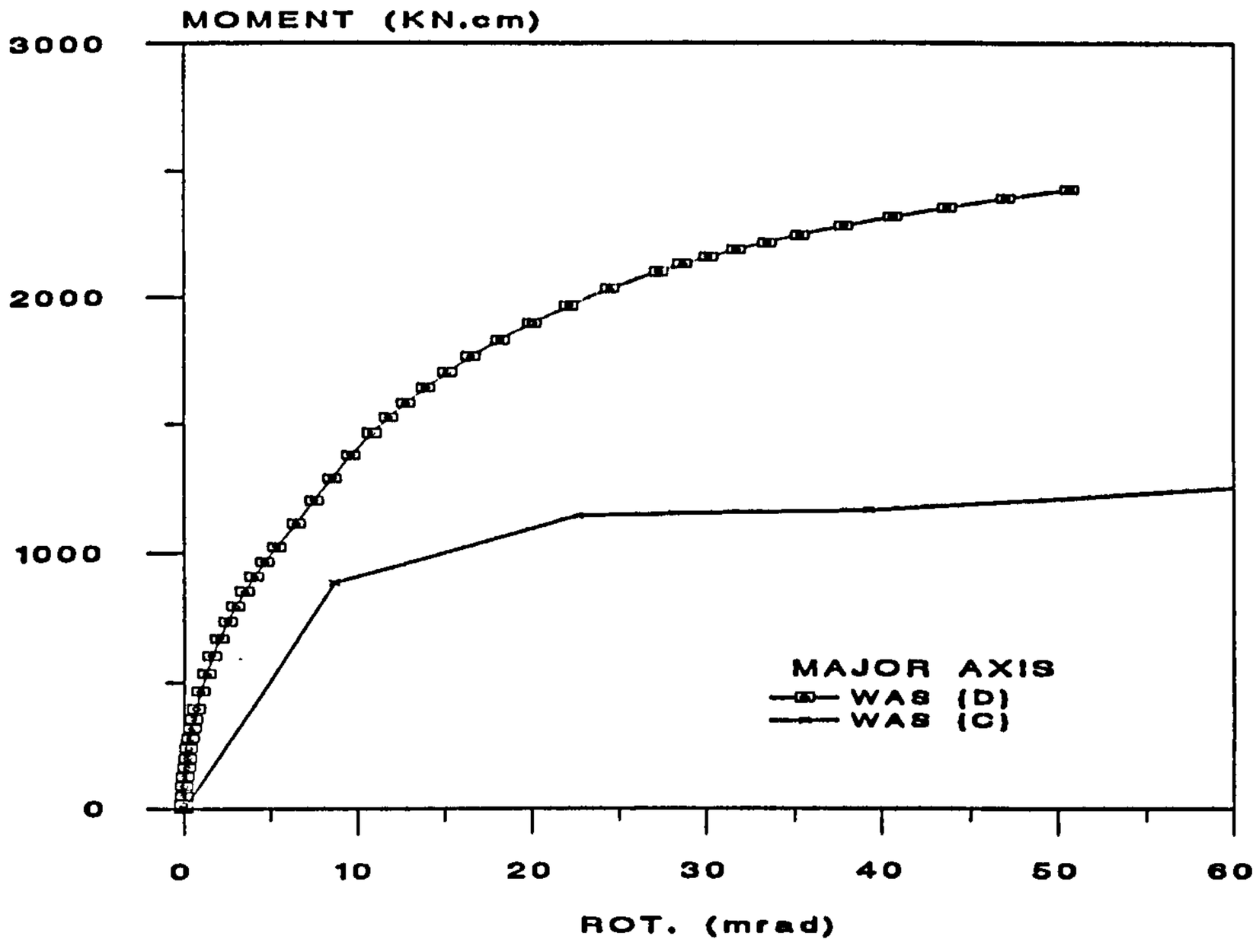

Figure 9.14 : Comparison of Moment Rotation Curves of Web and Seat Cleats Connections (Major Axis) from Davison and Celikag

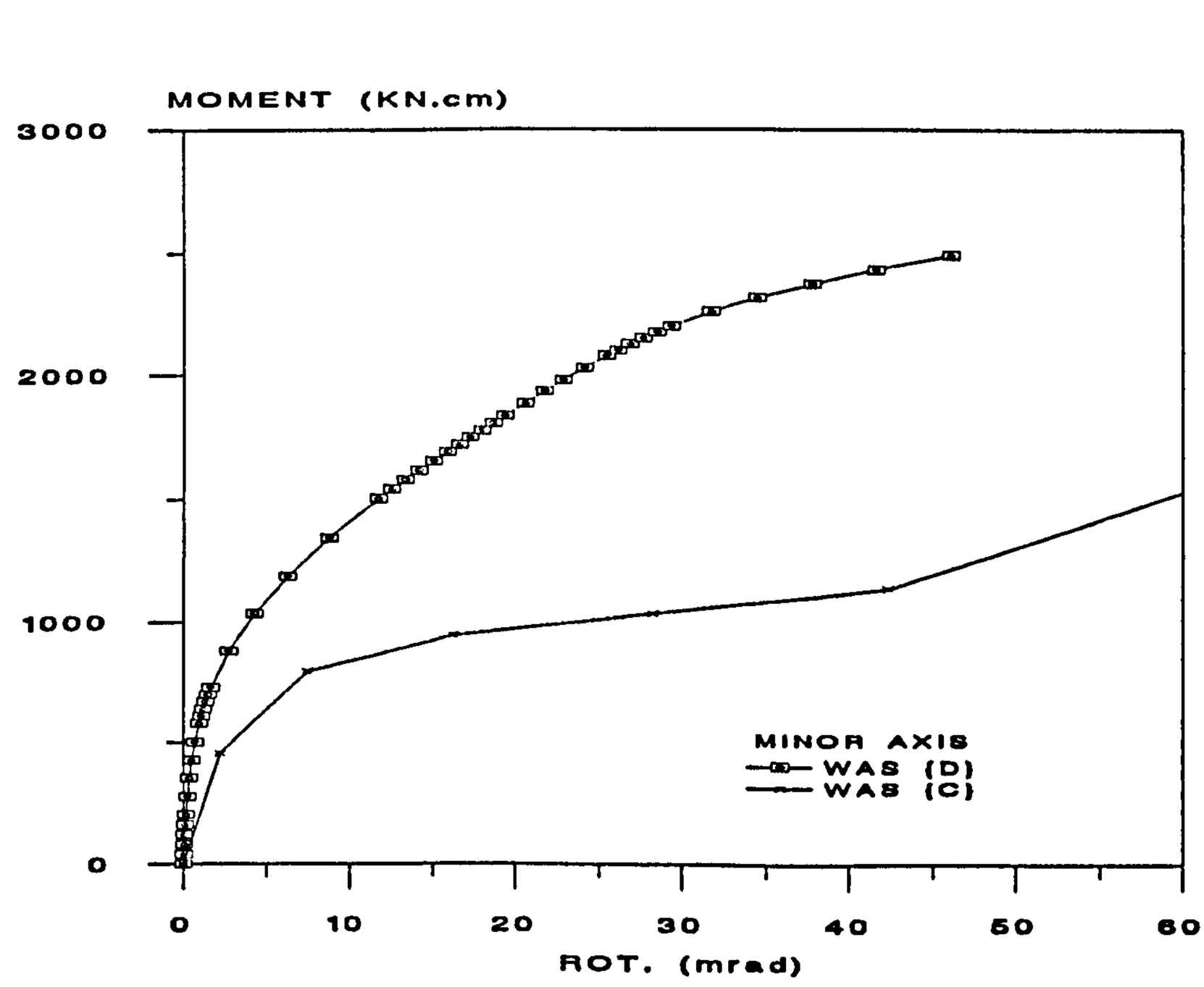

Figure 9.15 : Comparison of Moment Rotation Curves of Web and Seat Cleats Connections (Minor Axis) from Davison and Celikag

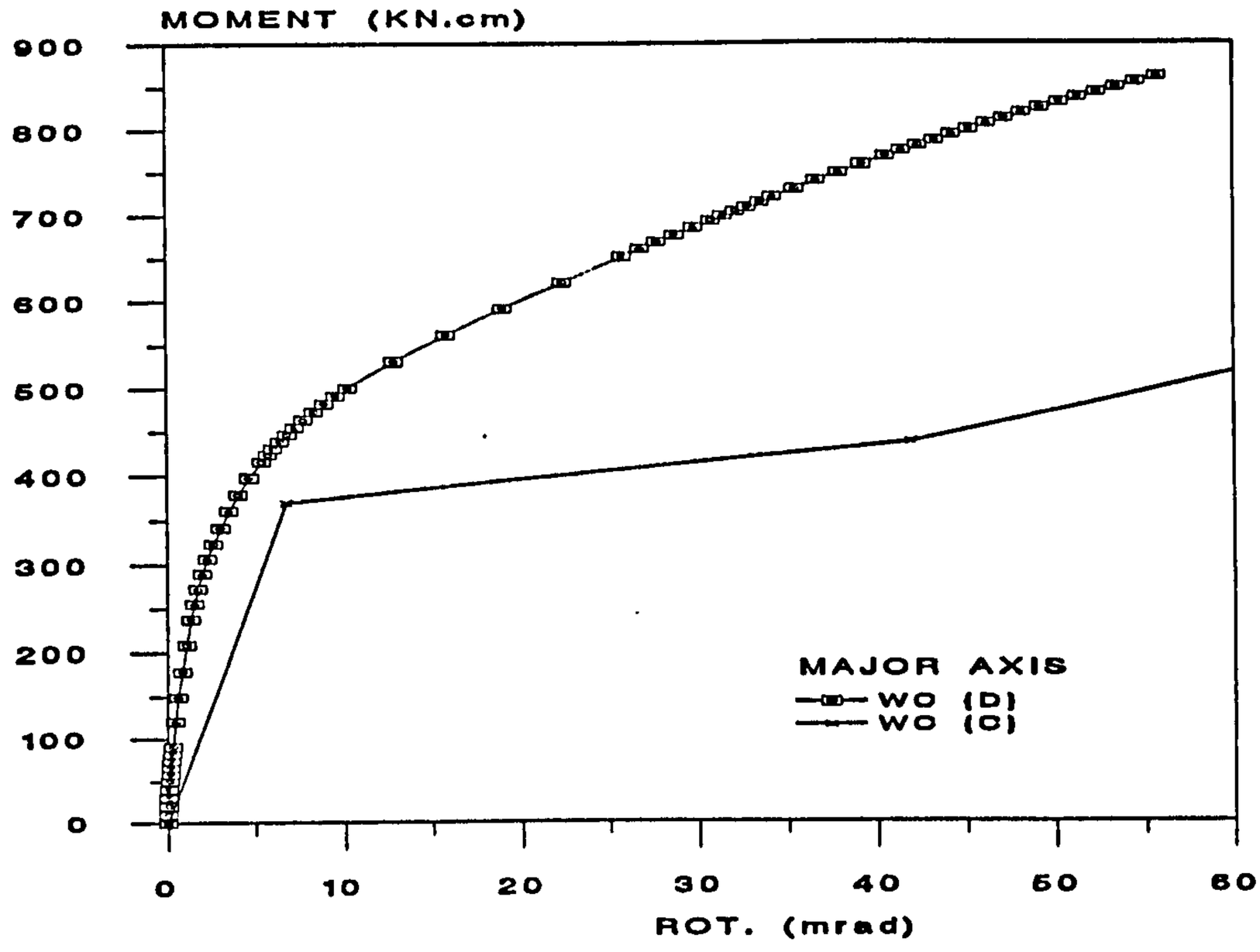

Figure 9.16 : Comparison of Moment Rotation Curves of Double Web Cleats Connections (Major Axis) from Davison and Celikag

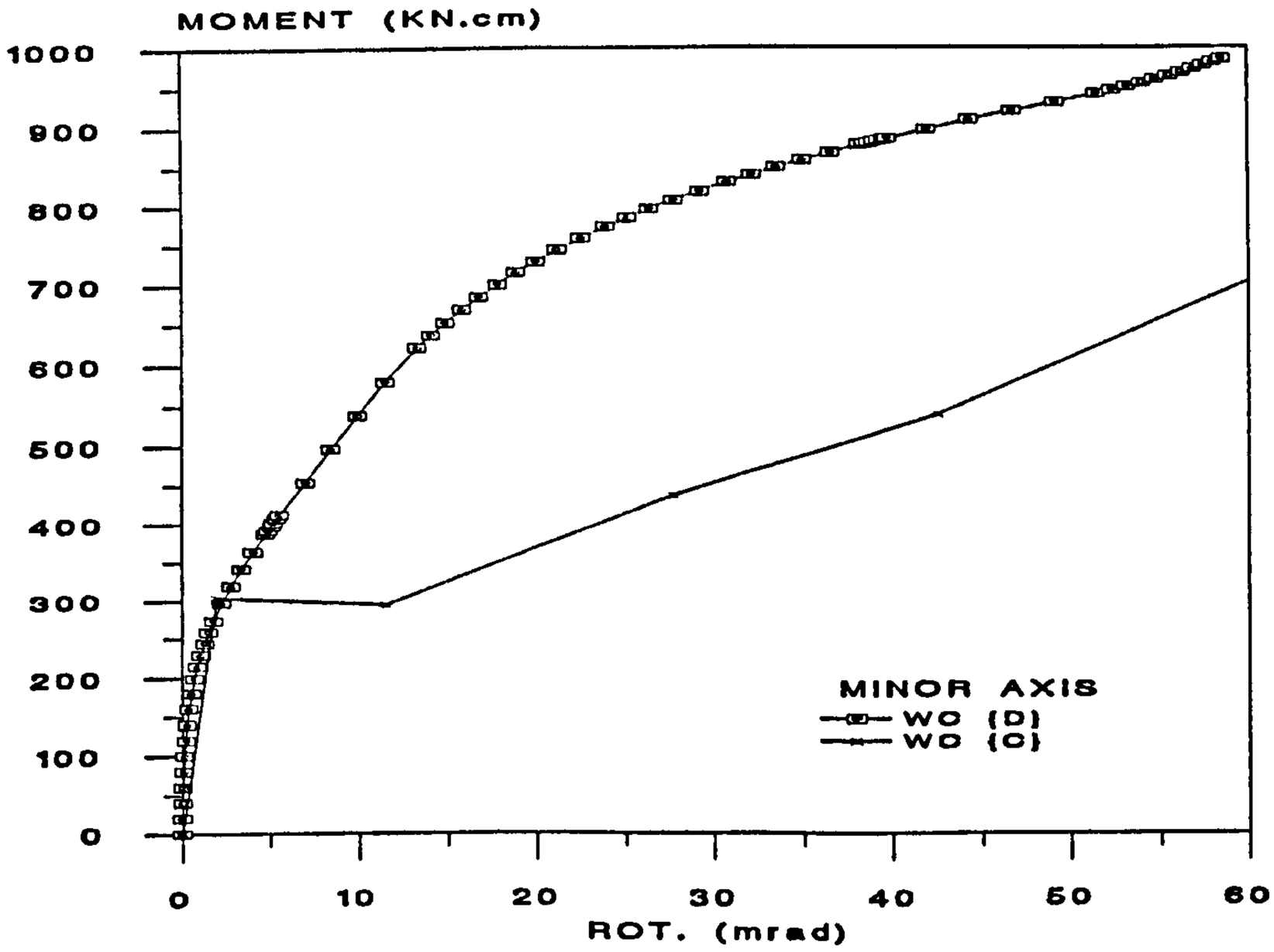

Figure 9.17 : Comparison of Moment Rotation Curves of Double Web Cleats Connections (Minor Axis) from Davison and Celikag

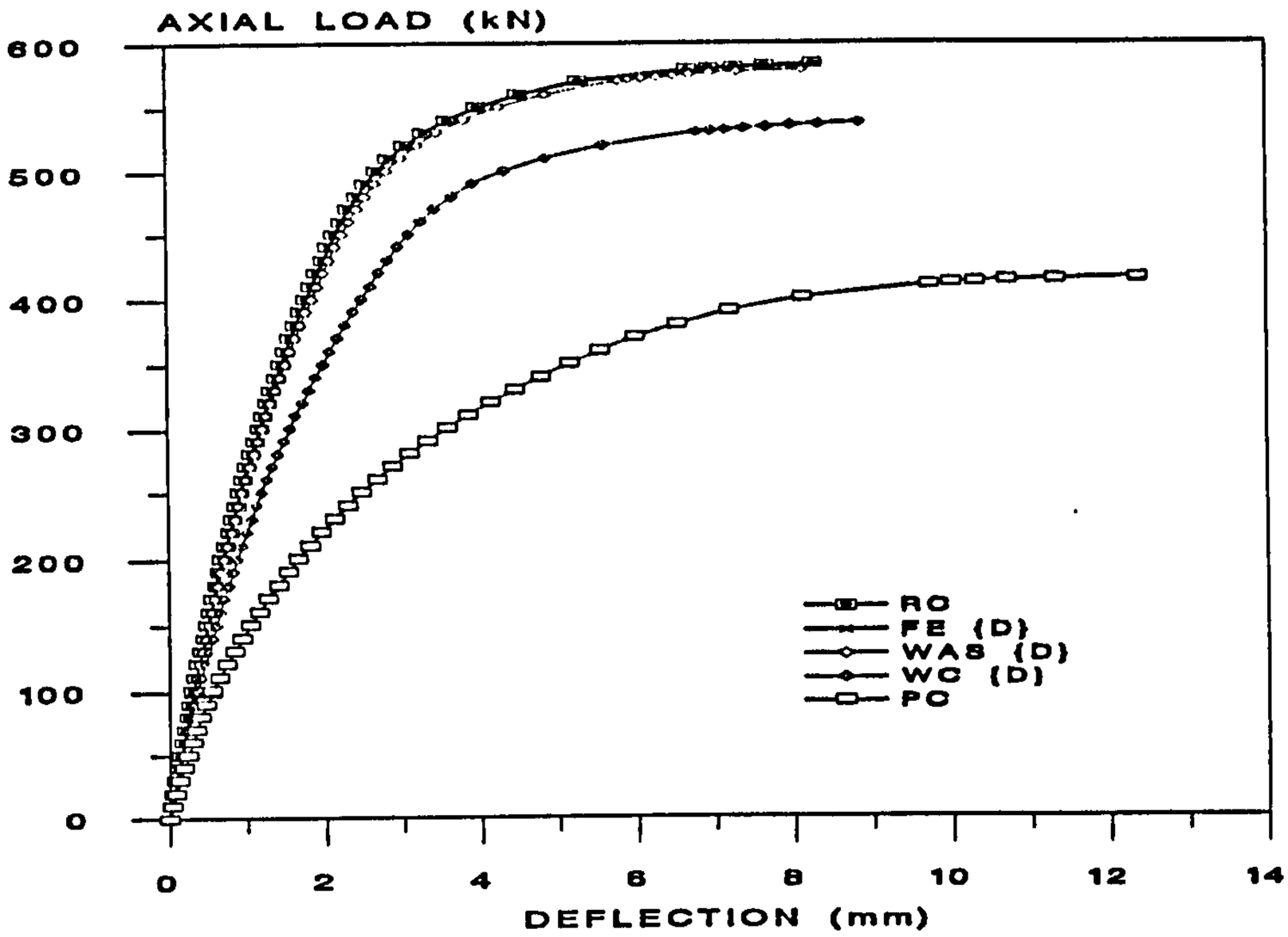

Figure 9.18 : Total Axial Load against Mid-Height Deflection of Column (Minor Axis) used different Moment Rotation Curves from Davison

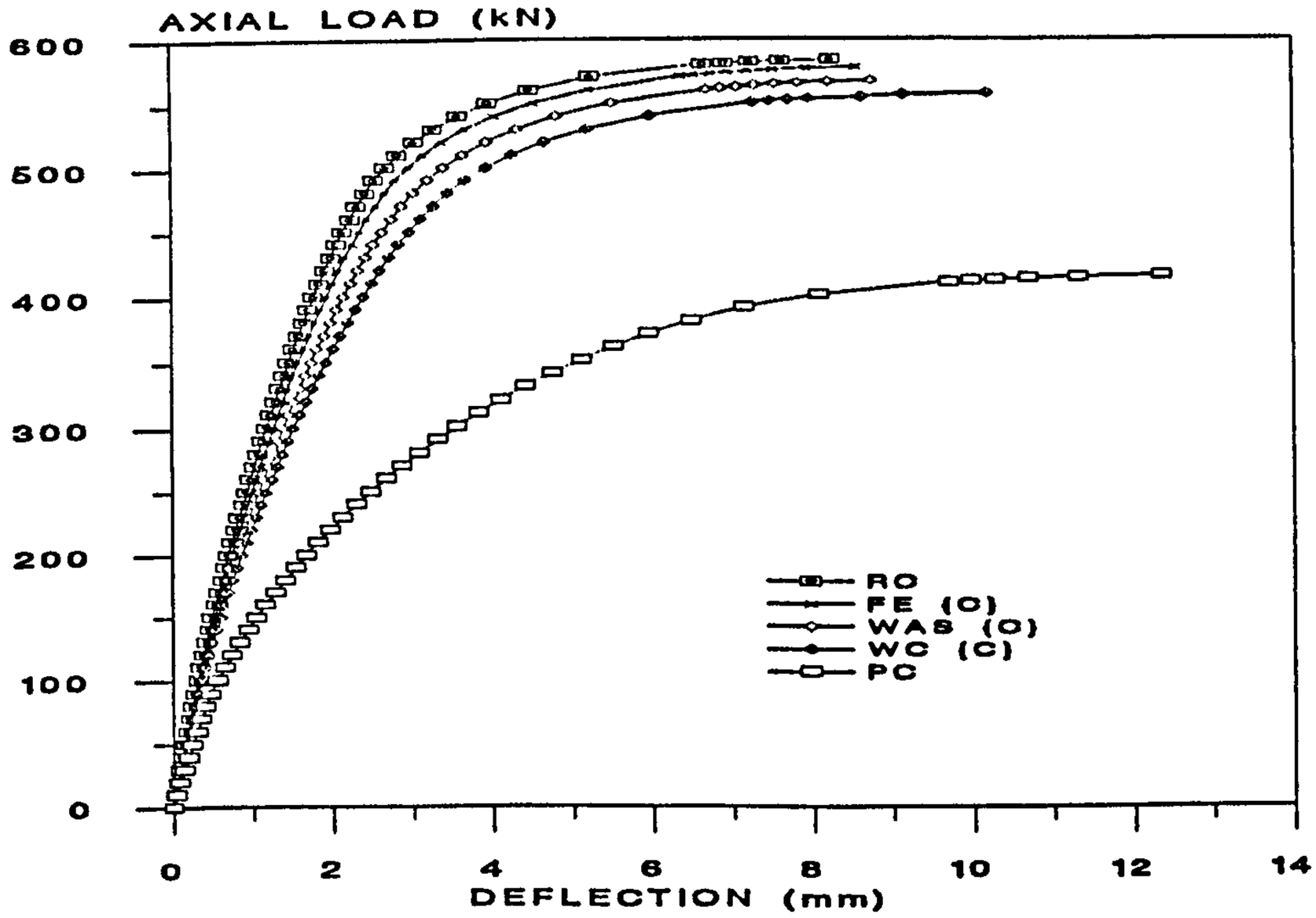

Figure 9.19 : Total Axial Load against Mid-Height Deflection of Column (Minor Axis) used different Moment Rotation Curves from Celikag

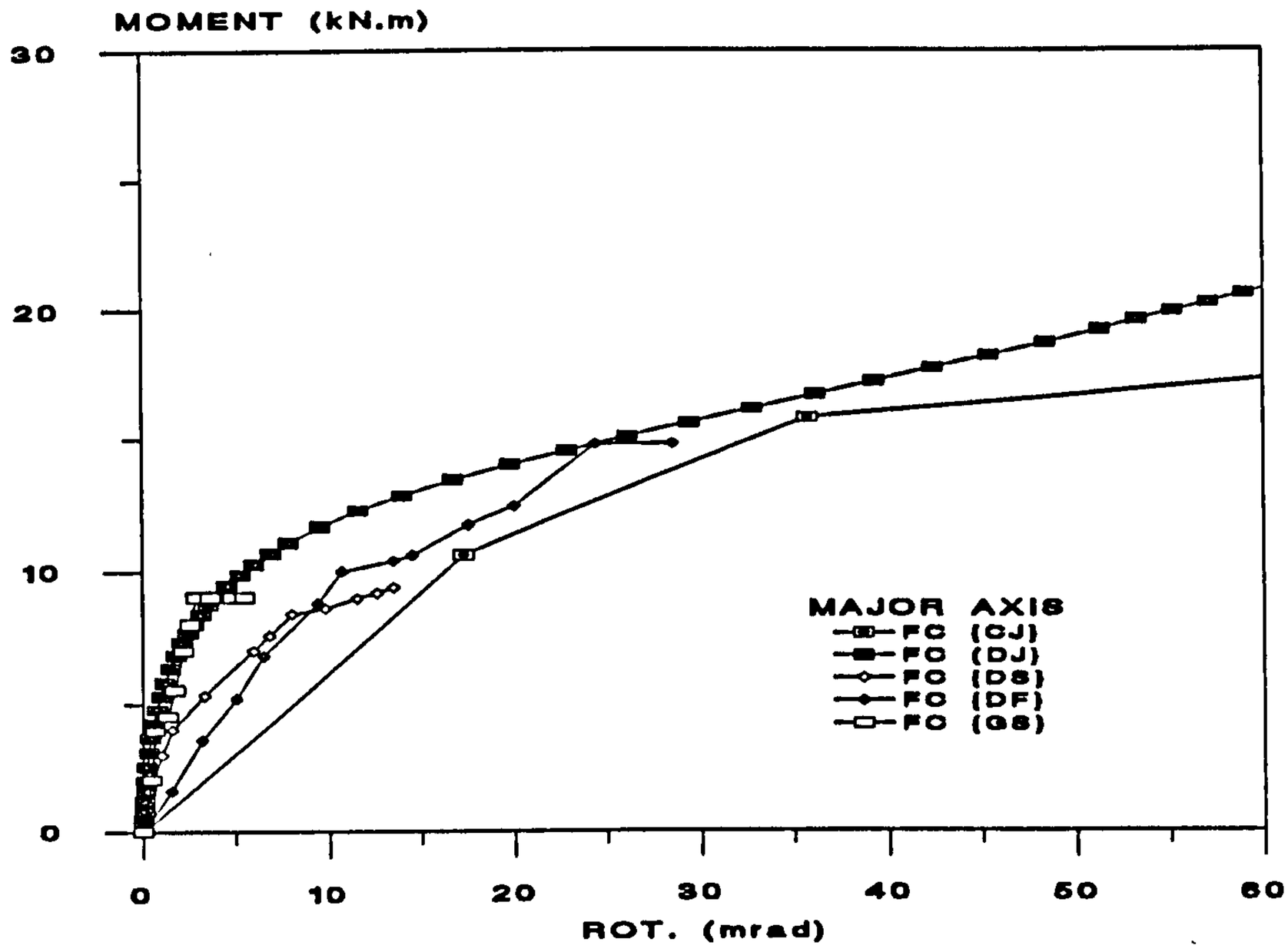

Figure 9.20 : Moment Rotation Curves of Flange Cleat Connection (Major Axis) in different Test Conditions

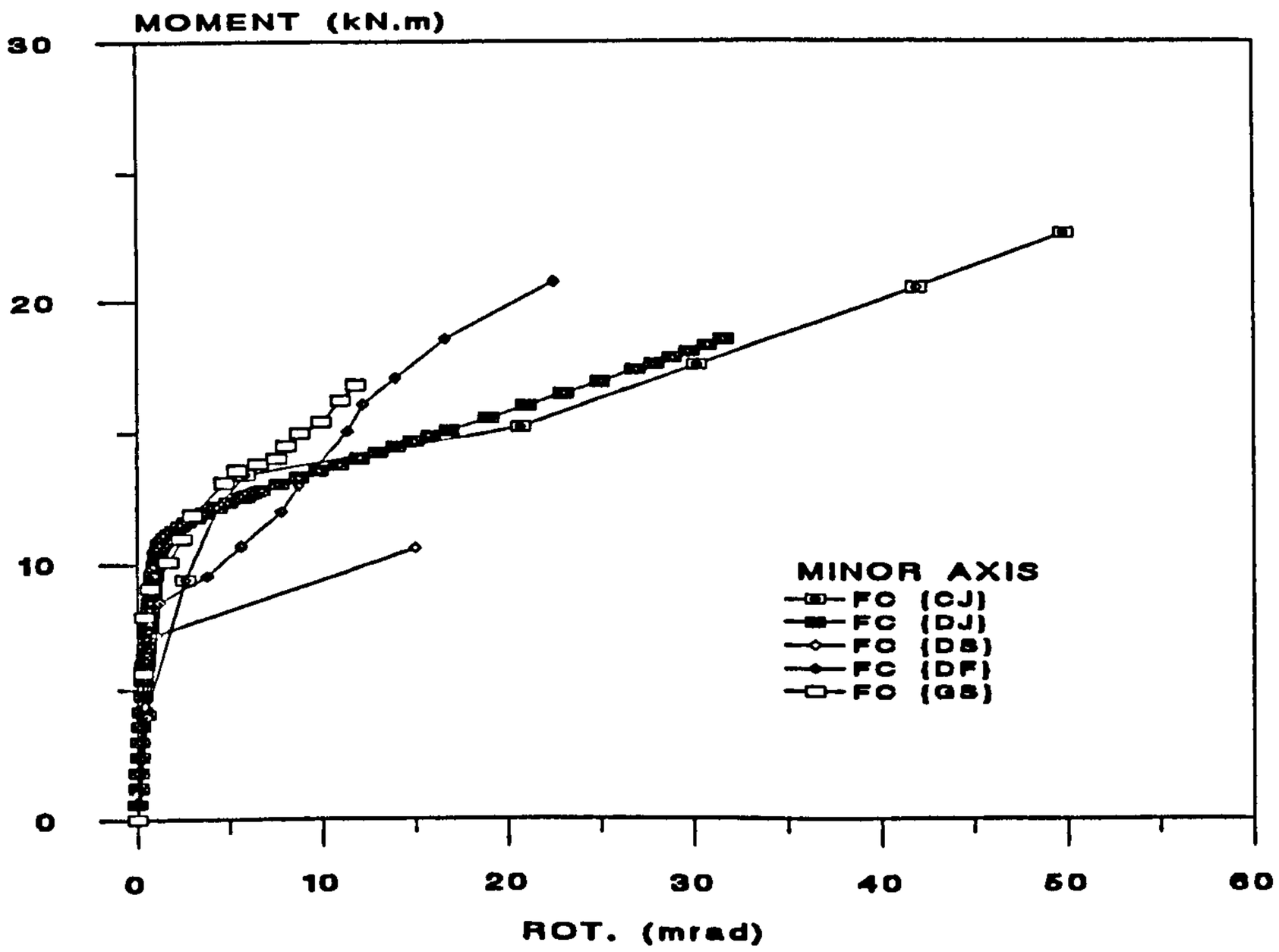

Figure 9.21 : Moment Rotation Curves of Flange Cleat Connection (Minor Axis) in different Test Conditions

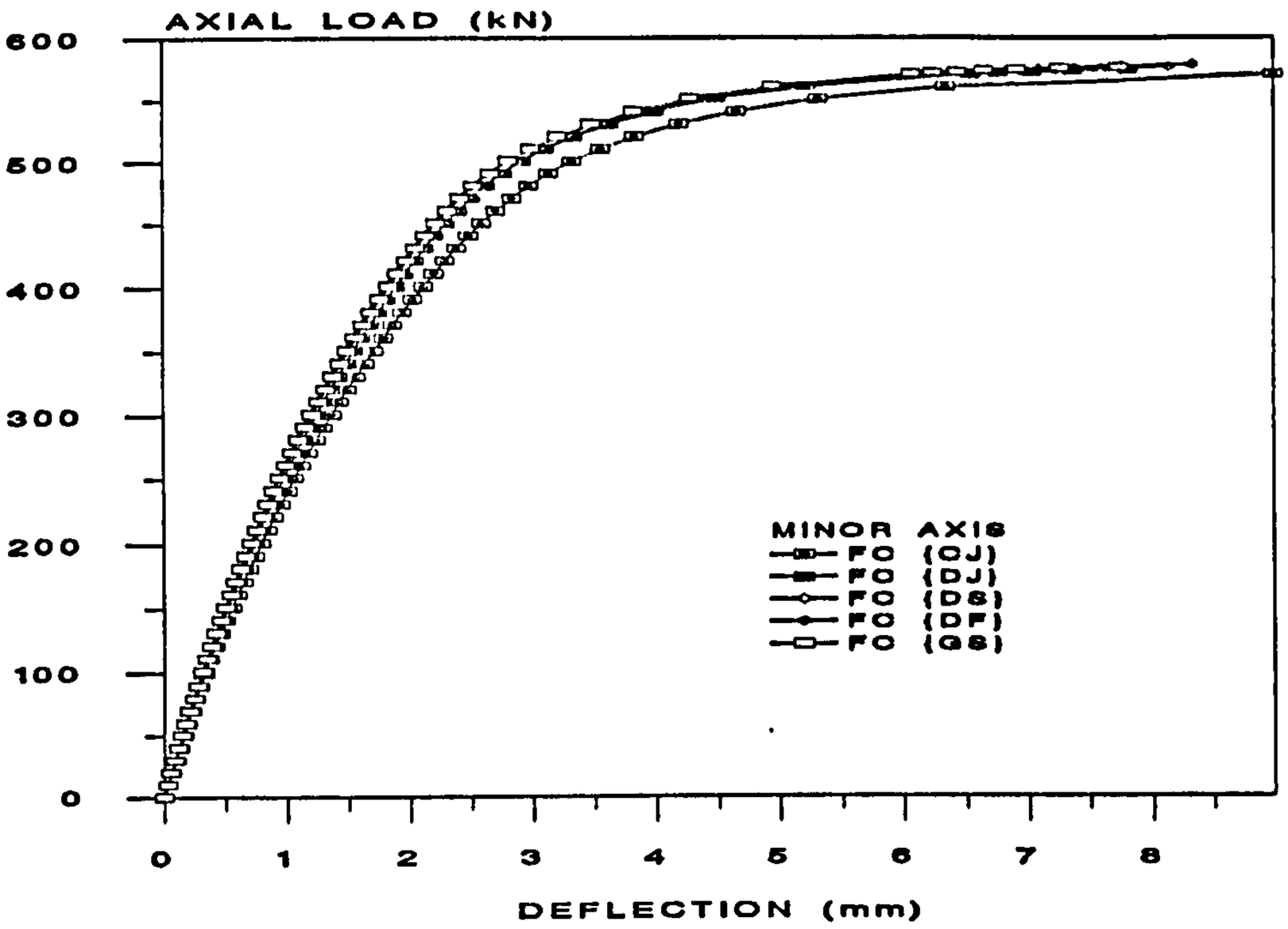

Figure 9.22 : Total Axial Load against Mid-Height Deflection of Column using different Moment Rotation Curves (Flange Cleat)

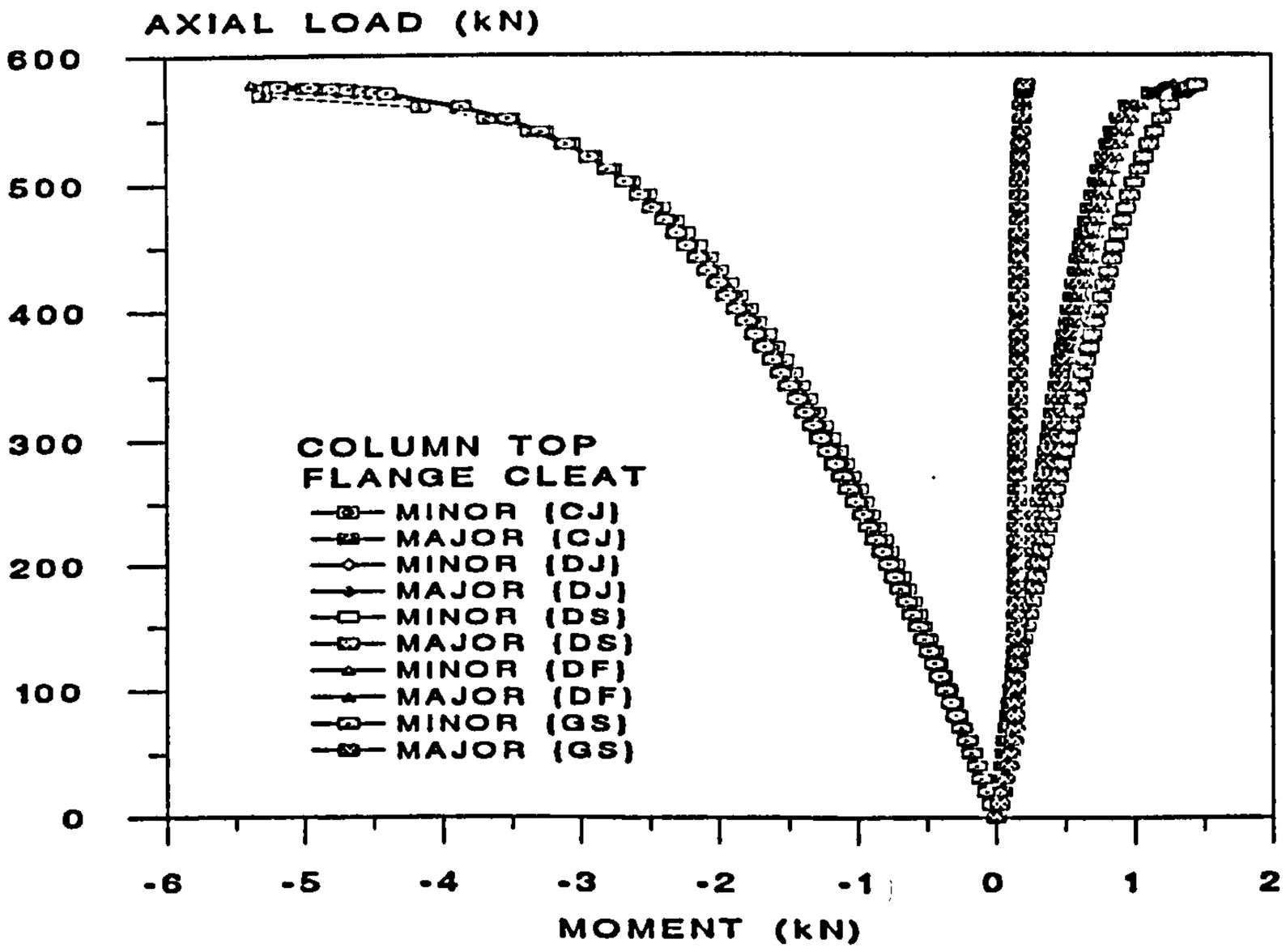

Figure 9.23 : Total Axial Load against Moment at Column Top using different Moment Rotation Curves (Flange Cleat)

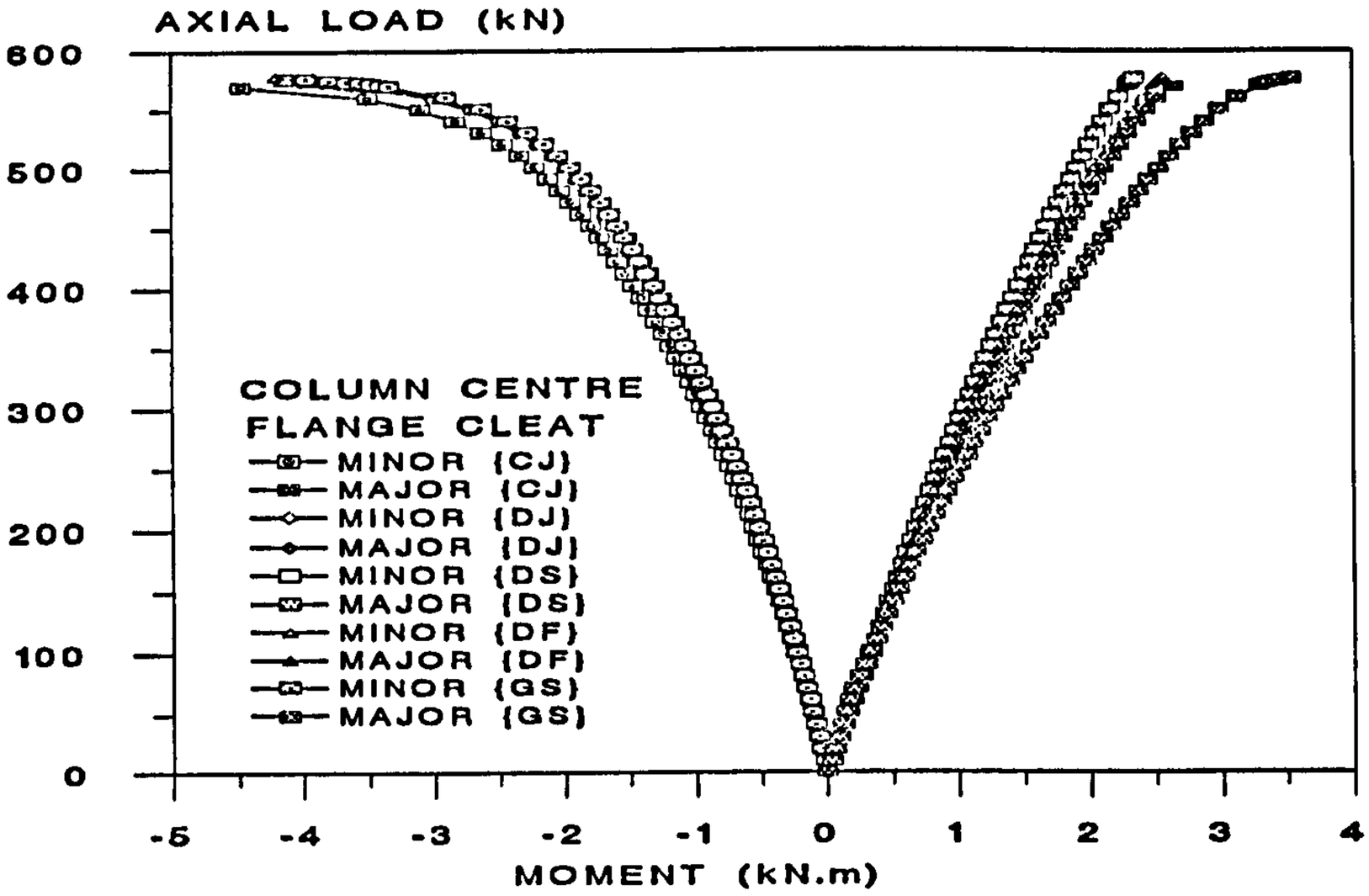

Figure 9.24 : Total Axial Load against Moment at Column Centre using different Moment Rotation Curves (Flange Cleat)

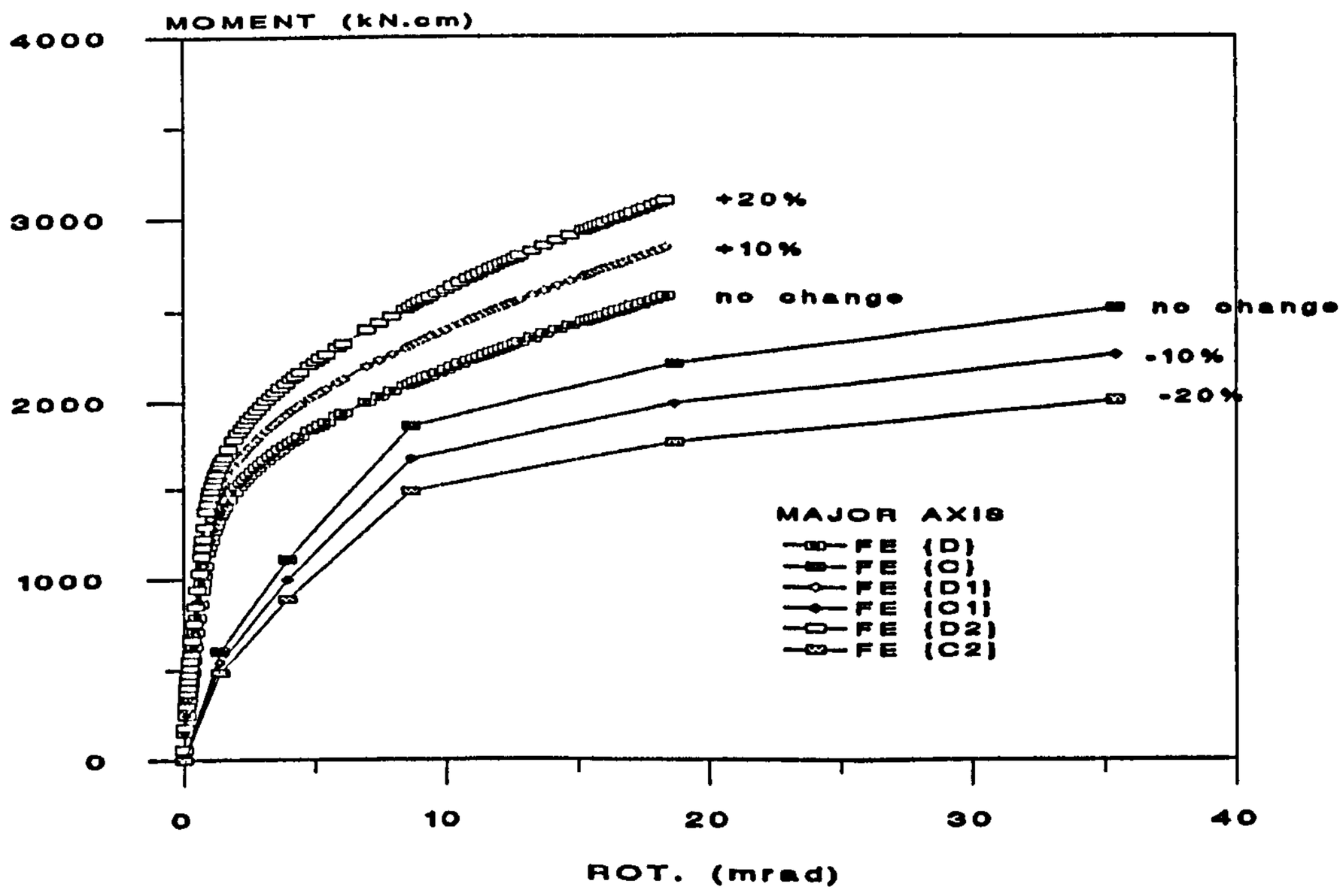

Figure 9.25 : Variation of the Moment Rotation Responses for Flush End-Plate Connections from Davison and Celikag

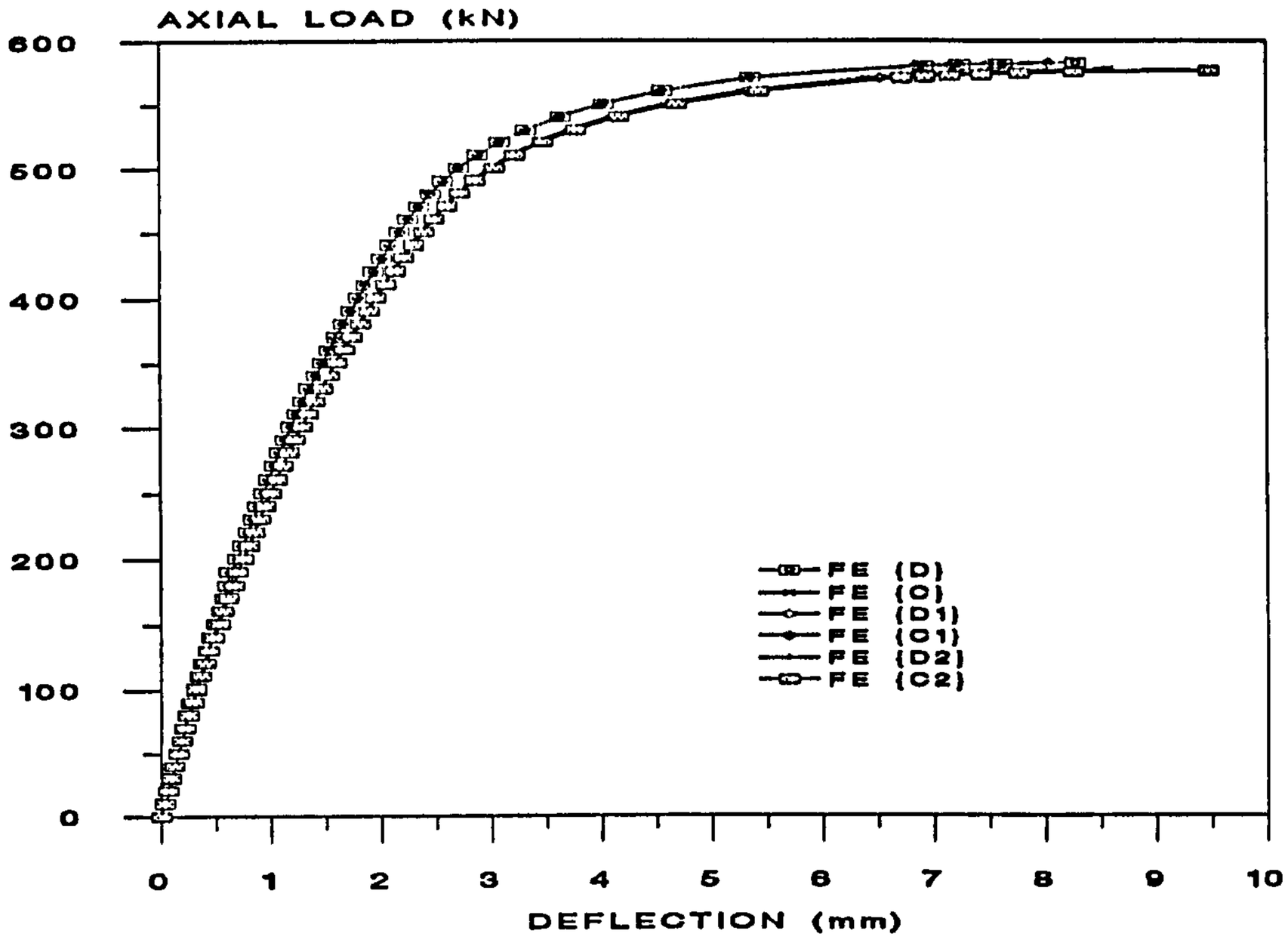

Figure 9.26 : Total Axial Load agaist Mid-Height Deflection with the Variation of Moment Rotation Curves (Flush End-Plate)

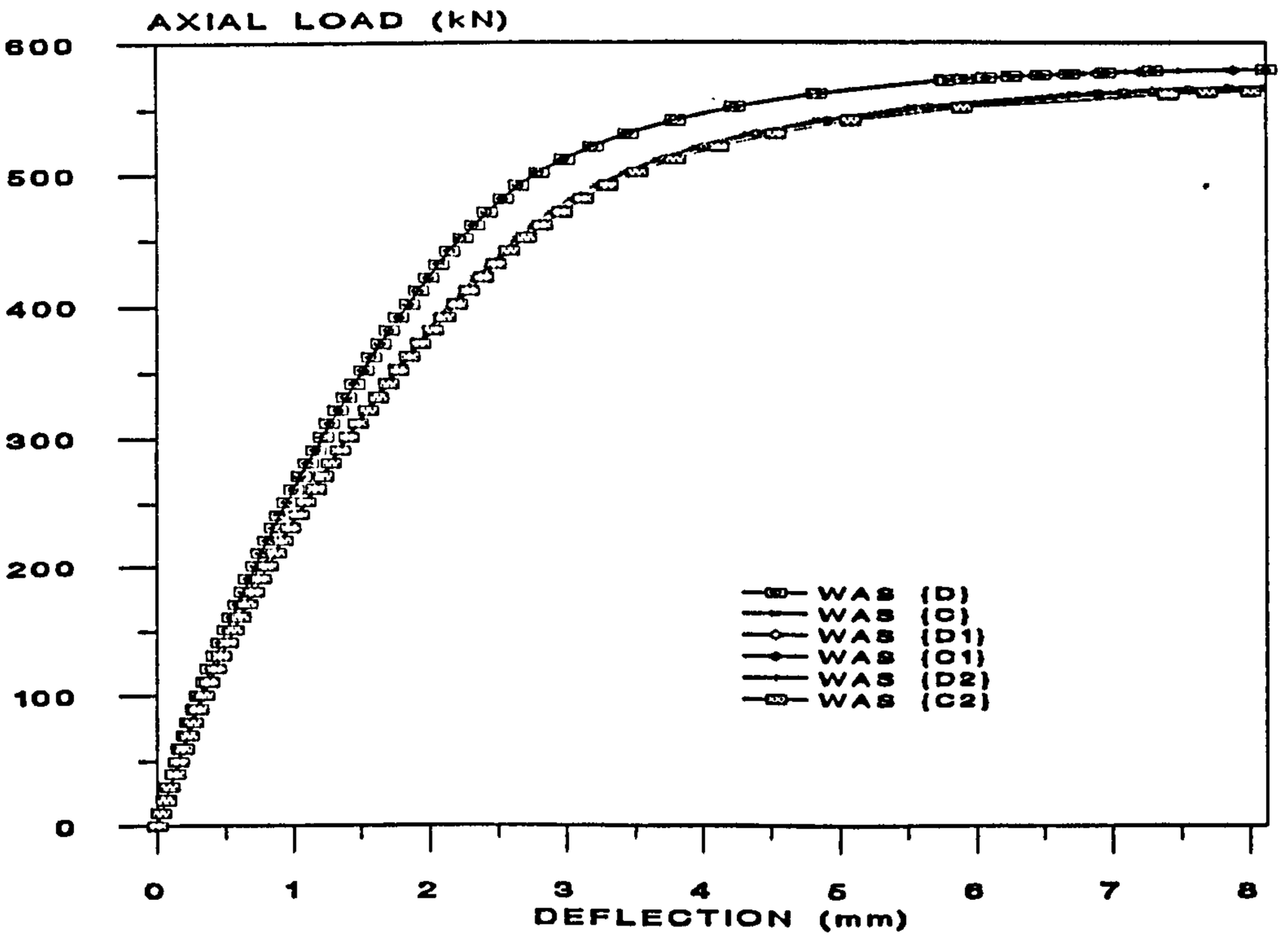

Figure 9.27 : Total Axial Load agaist Mid-Height Deflection with the Variation of Moment Rotation Curves (Web and Seat Cleats)

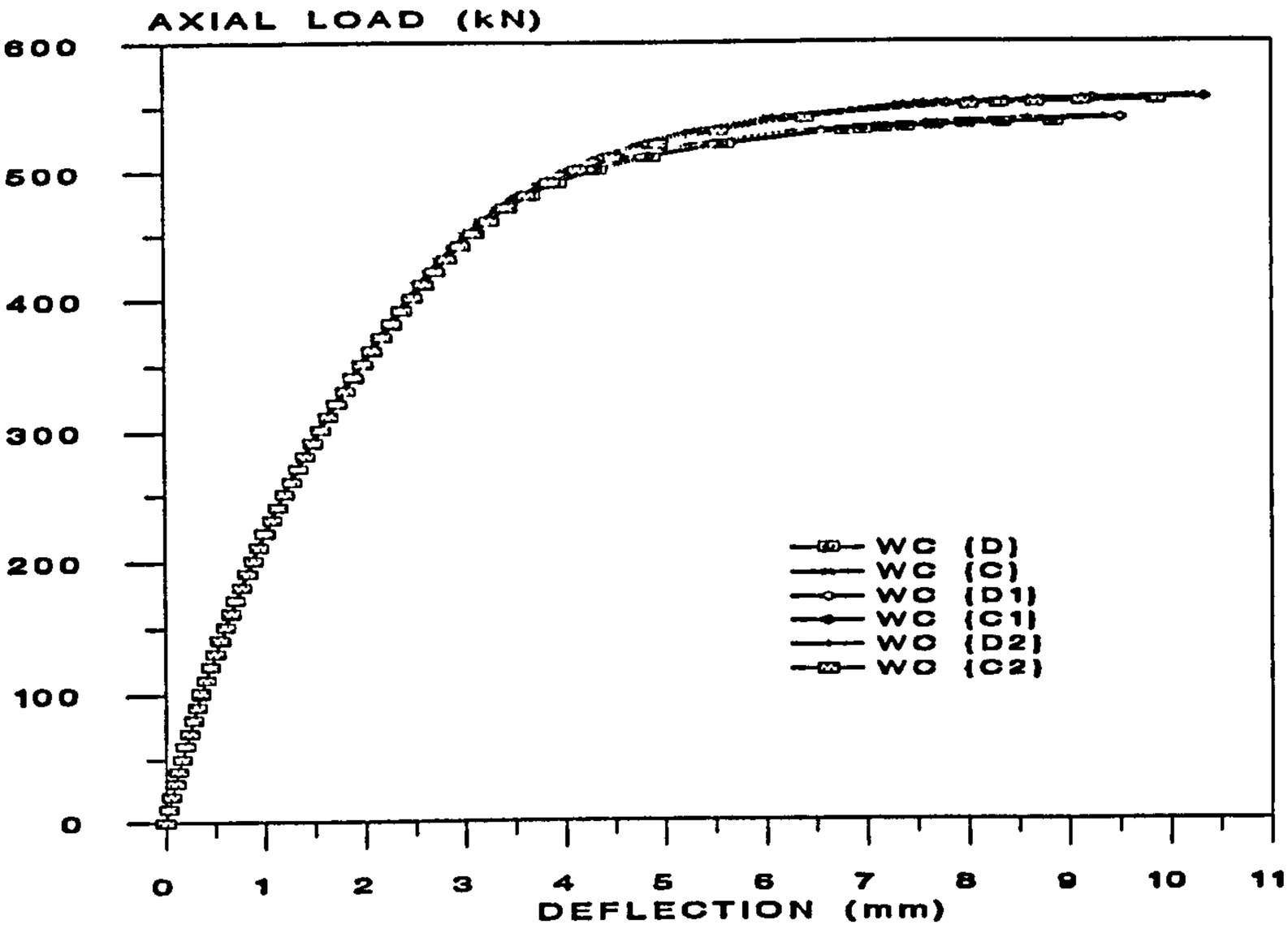

Figure 9.28 : Total Axial Load agaist Mid-Height Deflection with the Variation of Moment Rotation Curves (Double Web Cleats)

Chapter 10

Development of Semi-Rigid Design Methods

10.1 Introduction

Examination of the five frames in chapters 4 to 7 showed that each type of joint exhibited some degree of moment resistance and rotational stiffness leading to frame responses involving significant interaction between beams and columns. This affects beam and column deflection, the pattern of frame moment, the ultimate capacity of members and the collapse modes. Thus the results indicate that the behaviour of a frame is influenced by the response of the connections and it is postulated that exploitation of semi-rigid joint action will lead to better economic design.

In this chapter, existing semi-rigid design methods are examined and the limitations of each method are outlined. Modified methods and new proposals are presented and all the predicted values are compared with the actual frame test results. The new methods require only slightly more calculation than the current method and are easy to use. A complete method is outlined here, the use of which is illustrated by an example demonstrating the potential for weight saving in a non-sway steel frame.

10.2 Current Design Methods

For the design of steel frames, three methods are outlined in BS5950 part 1 [10.1] - simple, rigid and semi-rigid. For the simple design method, the rules for columns essentially repeat the procedure of BS449 [10.2] whereby columns should be designed to withstand

moments produced by assuming that beam reactions act at 100mm eccentricities from the faces of the column. In passing it is of interest to note that the U.K. code is the only one to the use these 'notional eccentricities', other design codes in Europe and elsewhere assume the point of transfer of beam reactions to be the column face.

Rigid design assumes that the connections maintain the initial angle between members, and that they must be capable of transferring whatever moment results from rigid analysis. However, since the actual behaviour of connections lies between these two extreme cases an approximate method of semi-rigid design is permitted in BS5950 [10.1]. The procedure of 'semi-rigid' design was first included in BS449 [10.2] by reference to an additional document PD3343 [10.3]. Guide-lines for semi-rigid design are also presented in section 6 of BS5950 [10.1], but its use is thought to be extremely rare.

EC 3 [10.4] is one of 'harmonised' codes to come from the European Community covering the design of steel structures and will stand alongside a number of European Community codes covering design in other materials. In Part 1.1 'General rules and rules for buildings', EC 3 presents a method to predict the M-ϕ response for end-plate connections. This section of the code is as yet incomplete and is currently under review.

10.3 M-ϕ Characteristics for Beam-to-Column Connections

From the structural detailing point of view the application of simple-to-produce semi-rigid connections, can lead to economical frames compared with complicated stiffened connections [10.5,10.6]. The M-ϕ response is of fundamental importance and the success (or failure) of a semi-rigid design method hinges upon. Taking it into account i.e. incorporating actual joint flexibility in routine design practice. This section presents a survey of joint modelling approaches which have been recently proposed by researchers.

Some models require the use of microcomputers and appropriate software packages for frame analysis [10.5]. In such cases, the connection parameters enlarge the input and output data of a structural analysis program. Other methods use simplified analytical models (eg. EC 3 [10.4]) and are intended to be suitable for hand calculation; the formulae frequently result from the curve fitting of actual experimental results. The joint and frame test moment rotation responses have been used to examine the predictions of some simplified analytical models and the results are presented in sections 10.3.2 and 10.3.3. The study in this section formed the basis of a paper [10.7].

10.3.1 Current Practice

A number of connection models have been proposed by researchers [10.4,10.8,10.9, 10.10,10.11] and Table 10.1 illustrates the applicability of the models. Most of the well-known mathematical models available in this table have been reported by Nethercot and Zandonini [10.12] or by Bursi [10.13]. Four main categories are classified as follows:

1. Curve Fitting
   The models attempt to fit a mathematical representation to characteristic M-ϕ curves obtained by either experimental test in the laboratory or numerical simulation. It is also possible to attempt to link the coefficients of the mathematical representation with physical parameters of the connection.
2. Simplified Analytical Models
   These models are used to predict the main characteristic values of the M-ϕ responses, i.e. the initial stiffness and the moment of resistance. They require knowledge of the mechanical and geometrical properties of the joint. Most models have been verified by comparison with actual experiments or numerical simulations. Generally, they also describe the M-ϕ characteristics by curve fitting using the calculated initial stiffness and the design ultimate moment capacity.
3. Mechanical Models
   These are a set of rigid and deformable elements representing the behaviour of specific parts of a joint. Non-linearity of the joint response is accounted for by inelastic constitutive laws adopted for the deformable elements. These constitutive laws are determined from test data, analytical models or numerical simulations.
4. Finite Element Analysis
   The M-ϕ curves are predicted by finite element analysis of a complete joint.

The simplified analytical models and the mechanical models are characterized by a wider field of application than curve fitting. The former are the only models currently suitable for hand calculation. The most up to date models of this kind, i.e. EC 3 [10.4] for the end-plane connections (frames 1, 2 and 5) and Liew and Chen model [10.11] for the flange cleat connections (frame 3) are selected to study. All the predictions will be discussed in

detail and compared with the frame and joint test results.

10.3.2 EC 3 Design Method for End-Plate Connections

10.3.2.1 Design Philosophy

The use of semi-rigid partial strength connections in structural steel frames implies the formation of a 'plastic hinge' within the connection at a level of load lower than the design loads. The philosophy adopted in this connection design method is to allow each bolt row to attain its design strength in turn, thus resulting in progressive yielding of the connection. This approach is best explained as an extension of the existing design methods for end-plate connections. Figure 10.1 shows two approaches for the design of a flush end-plate connection. For the first approach shown in Figure 10.1 (a), it is assumed that the centre of rotation is in line with the compression flange of the beam with the end plate rotating as a rigid link about this fulcrum. With this assumption it is possible to compute the relative bolt extensions at each bolt row. The connection is assumed to attain its maximum capacity when the force in the top row of bolts reaches the bolt design strength. The disadvantage of this method is that to achieve the assumed bolt force distribution, the designer often has to stiffen the column flange, with the result that bolt fracture may occur before the column flange or end-plate deform.

The second approach illustrated in Figure 10.1 (b) has been adopted by EC 3 [10.4]. This approach makes no assumption about the distribution of bolt forces. Instead, each bolt row is allowed to attain its full design strength and the design moment capacity of the connection is computed by adding together the products of the design strengths and corresponding lever arms. This design method relies on adequate ductility of the connecting parts in the top row of bolts to develop the design strength in the lower bolt rows. The limitation of this method found by Moore [10.14] is that not all connections possess sufficient ductility to allow each bolt row to attain its design strength. Moreover, this may also be prevented by other modes of failure i.e. buckling of the column web. These problems have been recognised by the EC 3 drafting committee and are currently being addressed. The developments presently under way are discussed below.

10.3.2.2 Development of the EC 3 Design Method

The method presented in EC 3 annex J [10.4] for the design of semi-rigid beam-to-column connections is based on research work carried out at Delft University in Holland.

The treatment is noticeably more detailed than the design procedure given in BS 5950 [10.1], including information on the moment-rotation responses for connections. The rules have been determined largely from Dutch research.

In EC 3 the rules governing the type of structure appear in the section dealing with connections (section 6) rather than in the frame design part (sections 1 to 5). Rules are also given to cover the selection of connections in plastic design and to give guidance on both strength and rotation capacity.

The distribution of forces between parts in a connection may be determined by elastic or plastic methods [10.15], provided that equilibrium is maintained. Rules have been given for the design strength using bolts in clearance holes, high strength friction grip bolts and rivets - some countries still use them on a reasonable scale for other than repair work. There is a specific requirement for the inclusion of prying forces in the design of connections when tension is present in the joint. The bolts in the tension zone of an extended end-plate connection are assumed to act in direct tension, whereas the vertical shear force is assumed to be carried by the lower bolt rows and, when bolts are used to carry an applied tension force, they should be proportioned to resist the additional force due to prying. Figure J.3.2 of EC 3 [10.4] illustrates the failure modes of a T-stub flange.

10.3.2.3 Connection Design Method of EC 3

A designer needs to know how the connection respond to moment. The behaviour of a connection can be characterised by a number of parameters [10.16]. In EC 3, these properties are moment resistance, rotation capacity and stiffness. The moment capacity of the beam-to-column joint is governed by the lowest resistance of the three critical zones, i.e. tension, compression and shear. Rotation capacity of the joint need only be checked if the governing connection component fails in a brittle manner and the moment of resistance of the connected member is higher than the moment of resistance of the connection. Rotational stiffness is dependent on the flexibility of the components. A secant stiffness is derived for the joint, based on the deformability of six parts; the column web in shear, tension and compression, the column flange in tension, bolts in tension and the beam end plate in tension. The flexibility of other components in the connection is neglected.

EC 3 presents a method to determine the mechanical properties of beam-to-column joints for 'I' and 'H' shaped beams and columns. The beam is assumed to be connected to the flange of the column. The model covers welded connections and bolted end plate

connections including both extended and flush end-plates. The column may have a stiffener in line with the top and/or bottom flange of the beam. According to EC 3 [10.4], parts of the methods can also be applied to the relevant parts of other types of connections. The EC 3 method to predict the M-ϕ characteristics for some published results had been performed by some researchers [10.17,10.18,10.19].

10.3.2.4 Comparison the EC 3 predictions to the Experimental Results

The experimental results discussed in chapters 4 to 7 together with the joint M-ϕ curves obtained from the database (chapter 3) have been used to validate the EC 3 predictions for bolted end plate connections. Frames 1, 2 and 5 incorporating end plate connections are thus selected for study. Figures 5.2 and 7.2 show the general arrangement and Figure 4.13 shows the nomenclature adopted for these three frames.

The beams were framed into the column flange and all the frames were tested in-plane and in a non-sway condition in the tests to failure. The first two frames employed high stiffness end-plates to provide moment capacities approaching the plastic moment capacities of the beams. Figure 5.3 illustrates the detail of the connections. Heavy columns were used in order to permit the development of large beam end moments and to assess the effect of connection response on the performance of the beams. Frame 5 used much lighter end-plates, commonly regarded as being capable of transmitting shear only, than frames 1 and 2 - Figure 7.3 shows these connections. Frame 2 used pre-loaded bolts in the connections whilst the other two frames employed hand tightened bolts. Since there is no particular method provided in EC 3 for the prediction of the bolt pre-loading in the end plate connection, the values computed for frames 1 and 2 will be identical. In fact, the experimental results in frames 1, 2 and reference [10.20] show that using pre-loaded bolts increased the initial stiffness but did not significantly affect the ultimate capacity of connections.

In this section, the characteristics of the M-ϕ curves predicted by EC 3 are compared with the experimental results for the flush end-plate and extended end-plate connections in frames 1, 2 and 5. The accuracy of the method in predicting the moment rotation response is discussed. The restrictions and the limitations of this design method are outlined.

(1) Discussion

Table 10.2 illustrates the ultimate capacity of the connections predicted by EC 3 [10.4]. The results for the different thickness of the beam ended plate are reported separately in order to compare the M-ϕ behaviour due to the effect of different parameters. The moment rotation characteristics have been determined according to the step by step procedure J.3.1 of Annex J in EC 3 assuming a plastic bolt force distribution. The rotation capacity of the connection was calculated following the procedure J.3.8.

First consider the resistance of the column flange in the tension zone - the tension resistance is given in terms of equivalent T stubs with a given length depending on the yield line pattern of the failure mode. The predicted length both for individual bolt rows and for groups of bolt rows is dependent on the distance to any stiffening element. Stiffening elements were located in the connections of frames 1 and 2 whilst no stiffeners were present in frame 5. The effective length for each particular bolt row differs depending on whether the bolts are classified as inner or end bolts. It is noted in Figures 5.3 and 7.3 that only three bolt rows were used for the flush end-plate and extended end-plate connections in the three test frames. The top row clearly contributes to the tension resistance but in EC 3 the tension zone is not clearly defined making it difficult to decide to which group the second row belongs and this directly affects the results. For the extended end-plate connections used in frame 5, it is assumed that both rows are calculated for the case of end bolts (J.3.4.1.(2)). The resistance of the end plate is determined separately for each bolt row concerned, separated by the tension flange of the beam. The total resistance of all bolt rows in the tension zone is determined from the lowest resistance of the two values obtained. It is clear in Table 10.2 that the resistance of all the bolt rows in the tension zone increase with the thickness of the plate whilst no significant difference is determined for the joint locations (i.e. internal or external).

The resistance of the column web in the tension and compression zones are determined following the procedures J.3.1.(6)-(8). It is noted that there was no virtual difference for each type of connection due to the same column section being used in each frame. The resistance of the column web in the compression zone is affected by the maximum normal compression stress in the web of the column due to the combined normal force and bending moment in the column. For this reason, M-ϕ curves should be determined for different column stresses when the stress level exceeds the column stress of 180 N/mm^2 (see J.3.4.1.(3)). For the test frames, there is no adverse effect on the strength of the column web when the maximum sustained load and moment are adopted. This is because larger column sections

were employed in test frames 1 and 2. However, for frame 5, a smaller section of column was adopted and a larger effect was expected. In order to investigate the predicted moment rotation curves within the elastic range of joint, the stress level should be low enough such that the M-ϕ response of the connection is not affected. Thus, a sufficiently low value of stress was selected when calculating the column web strength in the compression zone.

According to J.3.5.1.(3), the resistance of the column web to buckling, as indicated in figure J.2.4., should be verified using cl.5.7.5. There is no significant effect in frames 1 and 2 due to the presence of stiffeners in line with the top and bottom beam flanges. The results of Table 10.2 show that the column web strength is reduced to 248 kN in the extended end-plate connection in frame 5 due to the resistance of the column web buckling in a column mode governing the design and the resistance is thus lower than the flush end-plate connections.

Turning to discuss the resistance of the column web in the shear zone, it is only affected by the shear area of the column (J.3.6.1.(1)). Because same column section is used throughout each frame, there is no virtually difference between the connections in each frame (362 kN in frames 1 and 2, 210 kN in frame 5).

For the internal joints, the shear panel of the column web is not activated and thus the controlling component becomes the lowest one ignoring the value from column (4). Thus a comparable larger design moment capacity was determined for the internal joints B, D and F than the identical external joint C although the same resistances are determined for components (1) to (4) as shown in Table 10.2. A similar phenomenon is observed in other joints.

The rotation capacity for all joints in frames 1 and 2 are also recorded in Table 10.2. It is stated in J.3.8 of EC 3 [10.4] that, when the moment resistance of a beam-to-column connection is governed by the resistance of the shear zone or the tension zone (either in the column flange or in the beam end plate) and provided that it is governed by mode 1 failure, rotational capacity is assumed to be sufficient for plastic analysis. Thus connections E, C, H, J and L in frames 1 and 2 (moment resistance governed by failure of column web in shear zone) are deemed to have sufficient rotational capacity for plastic analysis and calculation of a value is not required. In frame 5, sufficient rotation capacity is obtained for all the external joints. For internal joints it was necessary to calculate a value for rotation capacity using equation J.56 and the rotations of the joints are determined as 34.3 mrad in joints B, D, F and 32 mrad in joints G, I, K of frame 5. As expected, Table 10.2 and Figures 10.2 and 10.3 show that high moment and initial stiffness in end-plate connections is gained at

the expense of ductility.

Table 10.3 gives predicted values for the joint stiffness, moment and rotation of the connections in the three frames. Values are determined at working load stage based on the value taken at $\frac{2}{3}$ of the design moment i.e. C_i, $\frac{M_{Rd}}{1.5}$, and $\frac{\phi_{Rd}}{1.5}$, and at the ultimate design load stage C_{Rd}, M_{Rd} and ϕ_{Rd}. As discussed in chapters 5 and 7, the maximum stiffnesses were not observed in the initial stage for some joints due to the lack-of-fit in the end-plate connections of frames 1, 2 and 5. Thus the maximum stiffness in the loading stage was then used for comparison of initial stiffness obtained using EC 3 [10.4] (see figure 6.9.4. in EC 3).

Figures 10.2 and 10.3 show the predicted M-ϕ responses for frames 1, 2 and 5. Figures 10.4 to 10.15 illustrate the comparison of the predictions to the experimental joint and frame M-ϕ curves. The elastic initial stiffness is calculated as the stiffness at $\frac{2}{3}$ of the design moment capacity. The predictions for all flush end-plate connections and the external joint of the extended end-plate connections in frames 1 and 2 show a lower initial stiffness and ultimate moment than the test results; the internal joint of the extended end-plate connection shows a similar stiffness but lower ultimate moment than the tests. For the unstiffened end-plate connections in frame 5, a good agreement of the initial stiffness is obtained along with predicted moment capacity lower than the experimental value. From these results it is concluded in this instance that the design method in EC 3 gives conservative values of ultimate design moment for all flush end-plate and extended end-plate connections with three bolt rows. The rotation capacity for all joints is within the design rotation capacity predicted by EC 3. As EC 3 either predicted a similar or lower initial stiffness, the predicted moment rotation curves could be safely used in frame and column stability checks and also conservatively in deflection checks.

(2) Conclusions and Comments

The method of designing bolted end-plate connections in the draft for development of EC 3 DD ENV 1993-1-1:1992 is presented and the general method on which it is based is identified and discussed. The predictions are compared with the experimental results for frames 1, 2 & 5 and the following conclusions and comments are drawn:

1. EC 3 underestimates the initial stiffness and ultimate capacity of flush end-plate connections and the external joints of the extended end-plate connections in frames 1 and 2. A good prediction of initial stiffness in the internal joints of the extended end-plate connection in frames 1 and 2 and all connections in frame 5

is observed.

2. The method used in EC 3 is limited to bolted and welded end-plate connections framed to the column flange. Although, it is stated that part of the methods can also be applied to the relevant parts of other types of connections, the methods are not mentioned. Furthermore, these application rules only apply to 'I' or 'H' section members. The effect of bolt pre-loading is not taken account in EC 3. In fact, the experimental results in frames 1, 2 and reference [10.20] show that using pre-loaded bolts increases the initial stiffness but does not significantly affect the ultimate capacity of connections. It is suggested that EC 3 should be extended to include these factors and more types of connections.

3. The design procedure in EC 3 is considered to be too complex and time consuming for designers. Furthermore, some of the steps are not clearly explained and could easily be mistakenly applied. The procedures are amenable to computer programming and this would appear to be the most likely method to solve the problems unless wholesale redrafting of the method is to be undertaken.

10.3.3 Design Method for Flange Cleat Connections

The connections in frames 3 and 4 were of the flange cleat type and the method provided by EC 3 cannot therefore be applied. In the absence of a modified method to predict the M-ϕ curves for the flange cleat connection, a simplified analytical model proposed by Liew and Chen [10.11] has been considered to predict the M-ϕ characteristics in frame 3 (major axis frame). This model uses a three-parameter power model proposed by Kishi and Chen [10.10] to predict the M-ϕ curves of the beam-to-column connection. The general equation used is,

$$m = \frac{\phi}{(1+\phi^n)^{1/n}} \tag{10.1}$$

for $\phi > 0$ and $m > 0$

where $m = \frac{M}{M_u}$

M = connection moment

M_u = ultimate moment of connection

n = shape parameter

$\phi = \frac{\phi_j}{\phi_p'}$

ϕ_j = rotation of joint

ϕ_p' = reference plastic rotation $\frac{M_u}{C_i}$

C_i = initial stiffness

The shape parameter n varies with the type of angle connections (e.g. web cleat, flange

cleat and web and flange cleats) and for the flange cleat connection is based on the statistical analysis of 15 test curves by Kishi *et. al* [10.21]. The connection initial stiffness and the ultimate moment capacity are computed based on the steel properties and the main geometrical variables. The method to determine the ultimate moment capacity of the connection is that proposed by Drucker [10.22]. This study of the initial connection stiffness is based on the experimental observations of a number researchers [10.23,10.24,10.25,10.26].

The calculation of initial elastic stiffness of the flange cleat connection is based on the following assumptions about the behaviour of the components:

1. The centre of rotation for the connection is at the edge of the angle attached to the compression flange of the beam, and located at the end of the beam.
2. The top angle acts as a cantilever beam in which a fixed support is assumed to be at the fastener-hole edge closest to the beam flange, and in the leg attached to the column face.
3. The bending rigidity of the angle leg at the centre of rotation is so small that it can be neglected.

The above is a brief description of this method, the equations adopted to calculate the moment resistance, initial stiffness and the shape parameter for the flange cleat connection are recorded in Appendix A and a more detailed account is reported in reference [10.11].

Figure 10.16 is a plot for a bi-linear curve represented the predicted initial stiffness and ultimate moment together with the M-ϕ curve in joint and frame tests. Table 10.5 records numerical values of the initial stiffness and the ultimate moment capacity predicted by the Liew and Chen model together with the experimental results. It is noted in this table that a massive overestimate (about 10 times) of initial stiffness was observed from this model which may be attributed to the level of bolt tightening in the connections. As mentioned in chapter 6, all bolts were symmetrically tightened from 80 Nm to 160 Nm in 40 Nm increments. Thus slipping of joints was expected to occur at some stage of loading which would significantly reduce the initial stiffness of the connections. Using this predicted initial stiffness of the M-ϕ curve to calculate the beam deflection in service would result in a very significant underestimate. The predicted ultimate moment, recorded in Table 10.5, was also observed to result in an over-estimation; about twice the experimental results. The shape parameter n is determined as 0.1 which is smaller than the range suggested in equation A.6 ($n \geq 0.3$) since the test data are not available. Liew [10.11] advised that the method be restricted to connection designs for which the behaviour has been well established. However,

in this instance, it is suggested that equation 10.1 is not applicable.

The results in this particular case show that this model does not reliably predict the initial stiffness and ultimate capacity; it is not conservative and thus is unsuitable for design. However, these results are only based on M-ϕ curves for one frame. The model does not consider the effect of the different joint locations (external or internal) or pattern loading (symmetrical or asymmetrical load) on M-ϕ behaviour. Thus this model needs further development considering these factors.

10.3.4 Joint Classification Systems

Frame design methods are classified in terms of the assumed behaviour of the connections i.e. pinned, semi-rigid and rigid. It is thus helpful to classify connection types so that appropriate connections can be selected consistent with the frame design assumptions.

Pinned and rigid connections are the common assumptions used in numerical analysis and design provisions; nonlinear connection response is rarely considered in the overall analysis of the structure. However, the idealization of the M-ϕ response as perfectly pinned or fully rigid should more correctly be reserved for a small range of typical connection types. All connections sustain some moment and have some rotation capacity, thus all could be classified as semi-rigid. In this section, two classification systems, one proposed by EC 3 [10.4] and the other by Bjorhovde *et. al* [10.26] are examined. These classification systems are intended for use in the analysis of steel structures, including those designed using semi-rigid connections.

(1) EC 3

In cl.6.9.6 of EC 3 [10.4], the beam-to-column connections may be classified by rotational stiffness and moment resistance. Based on the rotation capacity, three types of connections are identified - nominally pinned, rigid and semi-rigid. This system uses the length of the beam in the steel frame to define the beam stiffness and compares this with that of the joint. Due to the greater influence of joint stiffness in sway frames, a different classification system is used for such frames. However, in this study, consideration is limited to non-sway frames. Figure 10.17 shows the recommended classification boundaries for beam-to-column connections. Two non-dimensional parameters are used in the

classification;

$$\overline{m} = \frac{M}{M_p} \tag{10.2}$$

$$\overline{\phi} = \frac{\phi_j}{\phi_p} \tag{10.3}$$

where M_p = the fully plastic moment of the beam

$\phi_p = \frac{M_p}{\frac{EI_b}{L_b}}$

I_b = second moment of area of the beam

L_b = length of the beam

E = modulus of elasticity

For a braced frame, the regions for classification of beam-to-column connections as semi-rigid are written as:

If $\overline{m} < \frac{2}{3}$ then $\overline{m} < 8\overline{\phi}$

If $\frac{2}{3} < \overline{m} < 1.0$ then $\overline{m} < \frac{20\overline{\phi}+3}{7}$

EC 3 also uses these parameter to classify the M-ϕ as pinned,

- In terms of stiffness; a joint is defined as pinned if

$$C_i \leq \frac{EI_b}{2L_b} \tag{10.4}$$

- In terms of strength; a joint is defined as pinned if

$$M \leq \frac{M_p}{4} \tag{10.5}$$

It is implicitly assumed that, if the moment capacity of the beam-to-column connection is larger that 1.2 M_p, the connection rotation capacity need not be checked. This is because the plastic hinge will always form in the member. However, in cases where plastic hinges may be developed in the connection, the connection rotation capacity needs to be checked if redistribution of moments is considered in the global analysis of the structure. The method to determine the rotation capacity is given in procedure J.3.8 and it has been used to determine the rotation capacity of frames 1, 2 and 5 in section 10.3.2.

However, some anomalies may arise in actual design using this classification system. For example, a connection may be very stiff but have low capacity (i.e. M < 0.25M_p) and would be classified as pinned using the EC 3 classification system. As discussed in early sections, the initial stiffness is very important for the beam deformation in the serviceability condition and also for column stability. Ignoring this beneficial effect leads to an over-design

and thus increased cost. Moreover, some types of connection may be classified as pinned, semi-rigid or rigid depending on the length of beam to which it is attached. This may be a source of confusion for designers who will therefore have difficulty in applying semi-rigid design procedures. However, whilst the classification system will add to the complexity of the design methods, it will allow the designer more freedom in his method of design.

(2) Bjorhovde

Bjorhovde *et. al* [10.26] proposed a similar classification system but they based the stiffness on a standard reference length beam (rather than actual length) equal to 5 times the depth of beam (5D). The non-dimensional parameters used in their classification of the connections are the same as those used in EC 3 and Figure 10.18 shows this classification system. ϕ_p of a joint is defined as,

$$\phi_p = \frac{M_p}{\frac{EI_b}{5D}} \tag{10.6}$$

where M_p, E and I_b are as defined in equations 10.2 and 10.3
The regions are defined by two criteria, strength and stiffness as,

- In terms of Strength
  $\overline{m} \geq 0.7$ (full strength)
  $0.7 > \overline{m} > 0.2$ (partial strength)
  $\overline{m} < 0.2$ (flexible)

- In terms of Stiffness
  $\overline{m} \geq 2.5\,\overline{\phi}$ (rigid)
  $2.5\overline{\phi} > \overline{m} > 0.5\overline{\phi}$ (semi-rigid)
  $\overline{m} \leq 0.5\overline{\phi}$ (flexible)

where $\overline{m}$ and $\overline{\phi}$ defined as equations 10.2 and 10.3

Bjorhovde *et. al* [10.26] have also proposed an expression for calculating the required normalized rotation capacity of the connection. This simplified form is;

$$\overline{m} = \frac{5.4 - 2\overline{\phi}}{3} \tag{10.7}$$

From the formula, it is noted that the required rotation capacity of beam is dependent on the ratio of the ultimate moment capacity of the connection to the plastic moment of the beam. It is also inversely proportional to the reference stiffness of the beam - a larger rotation capacity is necessary for connections with low stiffness.

(3) Application of Classification Systems to Frame Tests

Figures 10.19 to 10.22 show the joint and frame test results for frames 2, 3, 4 and 5 plotted on the EC 3 system and Figures 10.23 to 10.26 illustrate the plots of frame test results for the Bjorhovde system.

Both systems classify the extended end-plate connections adopted in frame 2 as rigid. For the extended end-plate connection used in frame 5, EC 3 classifies them as semi-rigid, but the Bjorhovde system indicates the behaviour of this type of connection to be rigid. The difference is because EC 3 is based on the actual length of beam in a structure to define the beam stiffness. The analysis of the test results in frame 5 (chapter 7) showed that the behaviour of this type of connections was semi-rigid and thus supports the EC 3 system of classification.

All other beam-to-column connections in frames 2, 3, 4 and 5 can be classified as semi-rigid using both systems. Each system uses the non-dimensional form to show the moment rotation relationship for connections. As discussed earlier, EC 3 is based on the actual stiffness of the beam whilst the Bjorhovde system is based on the standard reference length of the beam. Thus to use the EC 3 system the layout of the frame and member details of the structural system must be known in advance. However, the Bjorhovde system can provide a better indication when the general steel properties and the main geometrical variables of the connections have been designed and when the member layout is not available. Both systems require knowledge of the M-ϕ curves either from database or from reliable models.

10.3.5 General Comments and Conclusions

In this section, a survey of the existing beam-to-column models is reported. Two recent simplified analytical models (EC 3, Liew and Chen) have been examined using the experimental results. The test results are also plotted in two classification systems proposed by EC 3 and Bjorhovde and the results are compared and discussed. Based on the study, the predictive M-ϕ models are found to be too complex for the designers or not reliable. Some suggestions for improvements are reported. As discussed in chapter 3, the moment rotation characteristics for some geometries can be obtained from a database where data are collected from actual tests giving a more reliable M-ϕ curves. At present, a P.C. version of the database is under development but is not yet available for designers who may find some difficulty using it in practice.

10.4 The Deformation of Steel Frames under Serviceability Loads

In the design of a frame, primary consideration is usually given the influence of joint behaviour on strength but joint behaviour also affects serviceability. Member deformation under a serviceability load condition, in which the response is usually assumed to remain wholly elastic, should be also be considered. For the elastic analysis, using the well known central deflection equation, the mid-span deflection for the pinned end supported simple beam subject to an uniform distributed load is five times greater than that assuming a total fixity at the ends. A method to predict the mid-span deformation of beams in the serviceability limit state suitable for design office use is thus required.

In the following section, such a method has been used to predict the mid-span deflection of beams in the serviceability state. Limitations are outlined and suggestions for improvements are included.

10.4.1 Development of the method to predict the Beam Deformation in Serviceability

10.4.1.1 Introduction

To provide a linear representation of connection stiffness one could choose an initial stiffness, alternatively one could use the secant stiffness from the origin to the point on the curve representing the connection moment in a working load condition. Because of the variability in connection behaviour and the inevitable scatter due to fabrication practices etc, extreme accuracy in the choice of linear stiffness appears unjustified and a fair approximation is probably sufficient. The linear-elastic method using the beam line approach outlined in this section is due to Gibbons [10.27] and appears suitable for non-sway multi-storey steel frames.

To accurately predict the behaviour of a beam, it is important that it is considered as part of a frame. Figure 10.27 illustrates a simple beam-column sub-frame of a multi-storey frame under a u.d.l. of intensity w . Assuming elastic behaviour, the slope-deflection equation gives the relationship between the end moment M_E and end rotation ϕ_b as [10.28]

$$M_E = M^F - \frac{2EI_b}{L_b}(\phi_b) \tag{10.8}$$

where M^F is the fixed end moment, E is the modulus of elasticity of steel, I_b is

the second moment of area about the major axis of beam and L_b is the length of beam.

At the serviceability limit state, restrict the analysis to the elastic range and u.d.l. of intensity w for a single beam semi-rigidly connected to fixed supports. The end rotation for the semi-rigid connection $\phi_{b_{SR}}$ is then,

$$\phi_{b_{SR}} = \frac{wL_b^3}{24EI_b} - \frac{ML_b}{2EI_b} \tag{10.9}$$

To apply this for a subframe, the upper and lower ends of columns connected to the beam are assumed to be pinned. This is the condition which will, except in extremely unusual conditions, produce a conservative estimation of beam deflection. From Figure 10.27, rotation at the node point of the column through an angle ϕ_c will produce a bending moment at that location of [10.27]:

$$M = 3\phi_c E(\frac{I_{cu}}{L_{cu}} + \frac{I_{cl}}{L_{cl}}) \tag{10.10}$$

When columns are the same section and length

$I_{cu} = I_{cl} = I_c$

$L_{cu} = L_{cl} = L_c$

$$M = 6\phi_c E\frac{I_c}{L_c} \tag{10.11}$$

Rearranging equation 10.11 gives

$$\phi_c = \frac{M}{6}\frac{L_c}{MI_c} \tag{10.12}$$

From consideration of the rotation of each of the three components, beam, column and joint, it is clear that the end rotation of the beam ϕ_c and the joint rotation ϕ_j, that

$$\phi_j = \phi_b - \phi_c \tag{10.13}$$

At the beam-to-column connection, the connection rotation should be considered in addition to the rotation of the column. From equations 10.9, 10.12 and 10.13, the joint rotation can be written as

$$\phi_j = \frac{wL_b^3}{24EI_b} - \frac{ML_b}{2EI_b} - \frac{M}{6}\frac{L_c}{EI_c} \tag{10.14}$$

In general a moment-rotation curve as shown in Figure 10.28 is approximately a straight line in its initial stage and, as the moment increases, non-linear behaviour gradually takes over. The non-linear moment-rotation behaviour of several connection types has been analysed. The M-ϕ data could be that determined from experimental tests or that derived from numerical techniques [10.29]. As this method aims to predict deflection response under

working loads, the approach can be simplified.

Given that linear elastic methods can be used to represent the behaviour of the semi-rigid connections [10.27], compatibility will thus be satisfied by using the beam line method [10.28] which uses the intersection of the beam line and the moment rotation curve to determine appropriate end rotation and moment of the beam to column connection (see Figure 10.28).

The semi-rigid moment may be determined by the graphical method or it may be calculated by a simple mathematical method as shown in Figure 10.29 to find the intersection point of the beam line and the secant stiffness line as [10.30],

$$M_{SR} = \frac{M_R}{1 + \frac{M_R}{R_P C_i}} \tag{10.15}$$

Define the dimensionless factor α as

$$\alpha = \frac{M_{SR}}{M_R} \tag{10.16}$$

where $\alpha = 0.0$ when $M_{SR} = 0.0$

$\alpha = 1.0$ when $M_{SR} = M_R$

As the frame is elastic under the serviceability condition, the deflection of the semi-rigid moment based on a linear connection stiffness can be predicted and thus

$$\delta_{SR} = \delta_R + (1 - \alpha)(\delta_P - \delta_R) \tag{10.17}$$

where δ_{SR} = beam mid-span deflection due to semi-rigid connection

δ_P = beam mid-span deflection due to simple support

δ_R = beam mid-span deflection due to fully rigid support

Any rigid jointed plane frame analysis computer program may be used to determine the mid-span deflection δ_R and the end moments M_R for the fully rigidly connected frame. The moment area method or the slope deflection method can be used to determine the simple end rotation R_p. Details of the analytical work will be discussed in the next section.

10.4.1.2 Development of the Methods

The linear elastic method outlined above was proposed by Gibbons [10.27] and used by the author [10.30] in an earlier study when examining the results of a three dimensional full scale frame test conducted at BRE. It was shown that the method using the

assumption of a linear initial tangent connection stiffness over-estimated the connection moment when compared with the actual moment achieved in the test. Different gradients of the stiffness line, depending on the connection moment, were then used to predict the mid-span deflection of the beam. A lower semi-rigid connection moment was predicted for a lower secant stiffness. A conservative mid-span beam deflection can be achieved by using a suitable secant stiffness in design. The validity of this approach was demonstrated by the author. Gibbons then extended this work to the experiment conducted by Bjorhovde [10.31] to show that the support rotations of simply supported beams of practical dimensions, under a u.d.l. at the maximum allowable level were less than 0.0092 rad. Gibbons then proposed a conservative lower bound connection secant for the serviceability condition of C_{10} corresponding to a rotation of 10 millirads and showed that this method can predict a more conservative result for use in design. The results of the five frame tests provide an opportunity to further validate this concept.

This method [10.27,10.33] was devised for the prediction of beam deflections when flexible connections are involved. Observations in frames 1 and 2 (connections with flush end-plates and extended end-plates) showed that the maximum moment capacity would be achieved at a rotation of less than 0.01 rad, thus precluding the determination of the stiffness C_{10}. A modified method C'_{10} is suggested by the author which draws a secant stiffness of point at horizontal line corresponding the maximum moment of the connection at the rotation of 0.01 rad (Figure 10.30), to replace the secant stiffness C_{10}. The modified method will predict a lower connection moment and thus a larger mid-span deflection will be determined than will occur in practice. Thus, this method will predict a conservative result. The preliminary examination of this method in frame 1 [10.32] by the author showed that the computed deflections were high over-estimates of the test results. However, the predictions are significantly less than the pinned calculation. Thus the investigation of a larger secant stiffness for the M-ϕ curves (a smaller joint rotation) is then considered for further study in this section.

The alternative method uses a larger stiffness derived from the tests on frames 1 and 2 of a maximum rotation of 5 mrad. The predictions using this secant stiffness are compared with the results determined from other methods. The secant stiffness C_5 is replaced by C'_5 when the rotations do not exceed 5 millirads (see Figure 10.30).

The initial tangent stiffness of C_i is a most popular technique used by researchers [10.34,10.35,10.36,10.37] which is drawn from the origin of the M-ϕ curve as shown in Figures 10.31. However, it has been shown that this method [10.30,10.27] may lead to

overestimation of the connection moment and a consequent short-fall in the mid-span deflection of the beam. The experimental results, as discussed in chapters 5 and 7, showed a lesser stiffness in the end-plate connection due to the lack-of-fit (frames 1, 2 and 5), the maximum stiffness is observed in some location at the loading stage as discussed in chapters 5 and 7. Thus a maximum stiffness is suggested to replace the uncorrected initial stiffness due to the problem of the lack-of-fit in the end-plate connections (see Figure 10.30(b)). It is noted in Table 5.11 that the value of the maximum stiffness is similar to the unloading stiffness. This is also addressed in figure 6.9.6 of EC 3 Pt. 1.1 [10.4] which states that the maximum stiffness may replace the initial stiffness for the end-plate connection due to the lack-of-fit. Thus the maximum stiffness in the loading stage was used to replace the low value of initial stiffness for end-plate connections in frames 1, 2 and 5. (The initial and secant stiffnesses of five frame tests are recorded in Tables 10.6 to 10.10).

C_c is another method proposed by Baraket and Chen [10.37] which draws a secant stiffness corresponding to the rotation of the connection at the intersection point of the initial tangent stiffness C_i with the ultimate capacity of the connection as shown in Figure 10.32. However, due to the lack-of-fit in end-plate connections, a maximum stiffness in the loading stage is again suggested to replace the existing method. The method is explained in Figure 10.32.

Finally, a technique was proposed by Moore [10.38] which uses the rigidity factor R to replace the dimensionless factor α with the actual rotation of beam and column. The rigidity factor R is defined as;

$$R = \frac{\phi_s - \phi_b}{\phi_s - \phi_c} \tag{10.18}$$

where ϕ_s = calculated end rotation of beam assuming simply supported ends

ϕ_b = measured end rotation of beam

ϕ_c = measured end rotation of column

He used the equation proposed by the Steel Structure Research Committee [10.40] with δ_R determined from a fixed end beam. However, some results showed a lower value than the experimental results and indicated that this method is not always conservative. A suggestion of the δ_R calculated from rigid frame to be taken account of the effect of the beam continually and column extended above is expected to improve the existing one.

10.4.2 Comparison predicted Beam Deflection at Serviceability to the Experimental Results

The five test frames offer the opportunity to check the accuracy of deflection calculations against test results. In frame 2, the loads were applied at third points - on the others loads were applied at quarter points. Thus the method could be examined with some variation in the applied load positions, section sizes and connection type.

Equation 10.17 assumes that the frames are elastic in working load condition. All beams were considered under the serviceability load condition of dead plus imposed load (scan 14 in test 28 of frame 1, scan 15 in test 42 of frame 2, scan 11 of test 2 in frame 3 and scan 10 in test 3 of frame 4). The serviceability condition selected for test 17 of frame 5 is based upon the maximum elastic response of the moment rotation and load deflection curves of the beams, scan 13 was the level of load selected. The level of load applied on all beams under serviceability in the tests are recorded in chapters 5 to 7.

Tables 10.6 to 10.10 contain a summary of different linear connection stiffnesses for the frame and joint tests. Due to faulty rotation measurement devices, as discussed in chapters 5 to 7, the experimental M-ϕ data for some joints are not available. It has therefore been assumed that the measured stiffness of this particular connection is equal to that joint with the same geometrical connection arrangement subject to a similar applied moment. For example, the stiffness of joint B in frame 1 was assumed equal to that of joint D. Semi-rigid frame deflections were then calculated (Table 10.12) assuming the range of different linear connection stiffness stated in section 10.4.1, namely the initial stiffness (C_i), the maximum stiffness in the loading stage (C_m), the secant stiffness at a rotation of 0.005 rad (C_5/C_5'), the secant stiffness at a rotation of 0.010 rad (C_{10}/C_{10}') and that proposed by Barakat and Chen (C_c). In each case, the stiffnesses were either determined from the M-ϕ responses of frame tests reported in chapters 5 to 7 or joint tests collected from the database as discussed in chapter 3.

An appraisal of the data recorded in Tables 10.6 to 10.10 shows, as discussed in chapter 9, a large difference in the stiffness of connection between the external and internal column joints for the minor axis frame (frame 4). This was due to the effect of beam continuity and column web flexibility. Observation of the results also shows quite large differences in the stiffness for the nominally identical joints i.e. joints G, I and K in frame 3 (see Table 10.8) demonstrating the variability of the M-ϕ responses.

A dimensionless factor α, representing the ratio of the semi-rigid moment to the rigid moment, was calculated for each beam using the various stiffness values suggested in the previous section and recorded in Table 10.11. A comparison of the different methods can be made. It is noted in Table 10.11 that a lower value of α is determined for a lower secant stiffness (methods 1 to 3) which means that the predicted semi-rigid moment are reduced as the stiffness of the joints reduce. Perhaps, the most interesting feature is that, whilst the average initial stiffness of joints I and J (beam 5) in frame 1 is 170 % larger than the secant stiffness of C_{10}, the dimensionless factor, and hence the connection moment (see Table 10.11), is only 15 % larger. This suggests that the predicted semi-rigid moment is relatively insensitive to the large variation of the connection stiffness (the most difficult parameter to determine accurately). As a result, the mid-span deformations of beams in the working load condition are not significantly affected by modest variation of the M-ϕ response - further support to a finding of chapter 9. This implies that the designers can select an M-ϕ curve to carry out their design without the consideration the effect due to the minor differences in joint behaviour between nominally identical joints.

Due to the very stiff connections used in frames 1 and 2, it was observed that the moment capacity would be achieved at a rotation of less than 0.01 rad. Using the stiffness C_{10} at a rotation of 0.01 rad was thus impossible. The modified method discussed in section 10.4.1 is adopted. The modified method of C'_{10} will predict a smaller connection moment and thus a larger mid-span deflection will be determined. Thus, this method will predict a more conservative result for the design. As a result, a lower stiffness of C_5/C'_5 is suggested based on the actual behaviour of frame. The predicted results using different methods based on the M-ϕ characteristics in the frame and joint tests will be discussed separately.

(1) Using the Frame M-ϕ Curves

The moment-rotation relationships determined from frame tests were used to predict the results as described in section 10.4.1. Different secant stiffnesses for the measured moment rotation relationships in frame tests were used to compute the mid-span deflection of the beams. All the predictions are recorded in Table 10.12 together with the values determined from the two extreme conditions i.e. rigid frame and simply supported beams and the experimental results. It is noted in this table that a slightly lower mid-span deflection at beam 1 in the tests of frames 1 and 2 was observed when compared to the rigid frame analysis. However, this is not significant as the absolute value of the deflection 1.7 mm, is low.

First consider method 3 which used the secant stiffness of C_{10}/C'_{10}. All the predictions show a larger value than the test results and indicate that using this secant stiffness is conservative. However, a quite high over-estimation between 35 to 188 % larger than the actual test result was determined in frames 1 and 2 due to the rigidity of the connections used. It is suggests that using the secant stiffness of C_{10} may be too low. When a higher stiffness of C_5/C'_5 is used (method 2), a drop of about 20 % of the predicted beam deflection was observed in frames 1 and 2 and the values observed are much closer to the test results. However, this secant stiffness is thought unsuitable for use with other flexible connections due to the predicted value being lower than the experimental results i.e. unsafe (see Table 10.12). Further increase in the connection stiffness, using the initial stiffness C_i (method 1), resulted in a further reduction of the predicted mid-span beam deflection for frames 1 and 2. Method 4 used the secant stiffness C_c and the prediction is observed within the values determined from methods 1 and 2. Examining the results showed that this method is only suitable for the stiff connections. Method 5 uses the actual rotational behaviour of joints, beam and column rotations in the test to compute the rigidity factor and predictions are expected to be closer to the test results in all frame tests. However, the results shown in Table 10.12 indicate that there is no significant improvement over other methods. Moreover, this method is unsuited to design office use as the rotation of the beam and columns are unknown at the start of a design. Only methods 1 to 3 can be used easily by designers and a further validation of these methods using the joint test results will be discussed next.

(2) Using the Joint M-ϕ Curves

In this phase of the study, the moment-rotation relationship based on the joint test was used to predict the results as described in section 10.4.1. All the joint tests in the first two frames were conducted by Prescott [10.39] under the cruciform arrangement and those for frames 3 and 4 were performed by Davison with a cruciform arrangement [10.41]. The joint tests for frame 5 was conducted by Chakrabarti at BRE [10.42]. The M-ϕ results were based on identical geometrical properties of the connections used in the frame tests. As stated above, only methods 1 to 3 are discussed and the results are recorded in Table 10.13. Examination of the results show that a similar result is determined when compared to the methods using the frame M-ϕ curves. Method 3 again predicted conservative results for all frames but it is observed that significantly over-estimate of the mid-span deflections for frames 1 and 2 occur; an average over-estimation of 50 % is determined for frame 1. When a higher secant stiffness C_5/C'_5 was considered, a significant improvement was obtained for the two frames with stiff connections. However, using the initial stiffness of method 1 an under-estimate of the deflections was achieved and was thus the method is not safe for

design.

10.4.3 General Conclusions

Based on the information presented, it can be concluded that;

1. The linear elastic method is suitable for predicting the mid-span deflection of a beam under service loads. For the frames 1 and 2 (stiff joints), a slightly higher secant stiffness of C_5/C_5' is suitable whilst for other flexible connections it is suggested that the secant stiffness of C_{10}/C_{10}' be adopted.
2. This method of analysis is shown to be appropriate to predict beam response in frames. Furthermore, it is found that a similar mid-span deflections are obtained irrespective of whether the moment rotation response is taken from joint test results or the frame test results. Thus, it is concluded that the M-ϕ curves from joint tests when used in the analysis described give adequate predictions of the mid-span beam deflection. Furthermore, the calculated deflections are not sensitive to precise M-ϕ response, thus reasonable predictions of M-ϕ characteristics are likely to be sufficiently accurate.

10.5 Ultimate Strength of Laterally Restrained Beams

10.5.1 Introduction

Many beams in a steel frame are restrained laterally by the floors which transmit the loads to them. Concrete floor slabs or roof cladding are generally able to give this lateral restraint. Alternatively lateral restraint may be provided by bracing members at specific points along the beams, as in the five test frames as discussed in chapters 4 to 7. If adequate bracing or floor slab restraint is present lateral torsional instability will be prevented.

Studies on major-axis plane frames by Anderson [10.43] have shown that when connection behaviour is taken into account using semi-rigid action, the cost of fabricating and erecting a frame designed as semi-rigid will be less than the alternative simple design. Savings priced by fabricators range up to 13 % in the most favourable circumstances, but depend on the arrangement of the frame and the available or required section size.

Based on reference [10.44], the in-plane response of an end restrained beam may be obtained by regarding the connection as non-linear springs with a characteristic equivalent

to the M-ϕ curve. This approach neglects column flexibility and is thus only appropriate for beams in frames with comparatively stiff columns. A method proposed by Nethercot and Moore to determine the ultimate strength of laterally restrained beams is examined below.

10.5.2 Modified Plastic Hinge Calculation

The method, called 'Modified Plastic Hinge Calculation' [10.38,10.44], is used to predict the ultimate capacity of the beams. Application of this form of plastic analysis requires that the beam to column joints possess sufficient rotation capacity to re-distribute moment to the beam span such that a mid-span plastic hinge is able to form. All the beams should be restrained against lateral movement. An assumption is made that [10.38] at ends of beam can develop moment resistance higher than the connection moment which is lower than the plastic moment of beam. Further assumption is that joint possess sufficient rotation capacity to develop hinges and to enable hinge at the mid-span of beam to form. Figure 10.33 shows the method. Since the joints can only sustain a fraction of the full plastic moment capacity of the beam, the usual work equation must be modified to include the available strength.

For a beam under a u.d.l. of w,

$$M_p + M_j = \frac{wL_b^2}{8} \tag{10.19}$$

where L_b is the length of beam, M_p is the plastic moment capacity of the beam and M_j is the ultimate capacity of the connection.

Assuming λ is the ratio of the connection moment to the plastic beam moment, equation 10.19 can be rearranged to determine the maximum applied load for the beam:

$$w = \frac{8(\lambda + 1)M_p}{L_b^2} \tag{10.20}$$

Based on the investigation by Moore for flexible connections i.e. top and seat cleats, flexible end plate and flush end plate [10.38], the value of λ should be within the range of 0 to 0.25. For heavier connections i.e. rigidly extended end-plates, the range of λ lies between 0.5 to 1. Thus the designer should select a reasonable value of λ for the initial design capacity of the beams.

The validity of these anticipated values can be seen by considering the results of Table 10.14 which shows the values of λ determined from the actual connection moments in the five frame tests. As expected, the highest values corresponded to the extended end-plate connections. Note too that quite similar values of λ were calculated for the flush end-plate

and flange cleat connections. The main difficulty in using this method is in selecting a reasonable value of λ to design the beam. Based on the limited experimental results, an assumed λ value with a range of 0.20 to 0.25 for the flange cleats and 0.20 to 0.30 for the flush end-plate connections, 0.54 to 0.67 for the extended end-plate without stiffeners and 0.75 to 0.85 for the extended end-plate with stiffeners would seem appropriate to determine the capacity of the trial beams in design procedure 1 as described in section 10.7. (It is noted that selecting an accurate value of λ is not critical in this stage.)

If necessary, further refinement of the design could be achieved by determined the connection moment from a reliable design model or by direct examination of M-ϕ curves from a database (chapter 3). However it should be noted that the ultimate capacity of a connection is sometimes difficult to define from an experimental M-ϕ curve under such circumstances it is suggested that value of the connection moment corresponding to a rotation of 0.005 rad is used to provide a conservative result for the design of the semi-rigid connected beams. For the rigid connections, the rotation of joint may be not achieved at 0.005 rad. It is thus suggested in this instance that the maximum connection moment achieved in the M-ϕ curves is used. Thus a more accurate but still conservative value for λ may be calculated and the ultimate capacity of the beam ascertained more precisely.

Table 10.15 shows the predicted ultimate capacity of the beams using the modified plastic hinge method of calculation and compares these values with the predictions from the simple plastic design method together with the frame test results. As expected, the new method is observed to predict quite close values to the experimental results for all the different frames. Moreover, they all show better results than the simple plastic design method.

Although the initial assumed value of λ is not critical to design the trial beam (the refinement will be obtained after the connection moment is determined from the M-ϕ curves), it is desirable that a good initial estimation of the λ is used in the early stage to minimise the calculation. The assumed values as suggested above are based on only five frame test results. In the author's opinion, more work is required in order to provide a better initial value of λ. Such work may involve testing or alternatively, a parameter study may be conducted to investigate the range of λ values for the different section and length of beams, columns and type of connections. In fact, as discussed in chapter 9, the behaviour of internal and external joints are different due to different load path mechanisms. This can significantly affect the ultimate moment capacity at the ends of the beam and thus the value of λ may be different. Further research is recommended.

10.6 Column Design at the Ultimate Limit State

10.6.1 The Current Design Methods

The limit-state design of beam-columns in structures has been the subject of research for more than 20 years [10.45]. Almost all of the current design methods are based on interaction equations which, through a combination of analytical and empirical means, fit the ultimate strength of an individual member at an effective slenderness considering the effects of geometric imperfections and residual stresses. Beam-column interaction equations can estimate quite accurately the ultimate load-carrying capacity of a simply supported beam-column with equal external loads applied at both ends. To generalize the equations such that they may be applied for members with other loading cases and boundary conditions, and for members in general frameworks, certain factors that approximate the actual behaviour of these members must be introduced. The effective length is the key factor that has been employed in many design methods to estimate the influence of the overall framework on the strength of component beam-column member equations and, since the interaction between the members in an actual frame at the strength limit state is complex, beam-column equations cannot in general provide accurate predictions of the member failure loads in an overall structural system. Gibbons [10.27] gives an overall review of the existing methods to predict the effective length and some suggestions for improvements are also included. However, the methods are very complex. A simpler method to improve the existing BS 5950 design method is suggested and examined by the author later.

In the U.K., designers use either the simple design method incorporating an eccentricity of 100 mm from the face of the column for the transfer of beam reactions or the rigid frame design method which assumes complete rotational continuity at the joints as outlined in BS 5950 [10.1]. The formulae used to assess the adequacy of the beam column are based on a good representation of the maximum strength of a member under a fixed set of end actions, their determination is normally obtained by a scaling-up of the distribution of the internal forces obtained at a lower load level. Recently, a new design method called the α_{pin} approach was developed at the University of Sheffield [10.46,10.27] and further examined by the author in chapter 9. The results indicated that the beneficial effect of restraint provided by the beams through the semi-rigid connection outweighs the disadvantageous effect of the moment transmitted through the connection. The basic α_{pin} method assumes effective length ratios equal to unity and gives conservative results - sometimes very conservative.

Taking into account the semi-rigid action of the connection, a new design approach to predict the effective length ratio is suggested. This method is examined and all the

predictions are compared with the existing design methods outlined in BS 5950 and the experimental results for frames 3, 4 and 5. The advantage of this method is outlined and the possible direction for use of this method for more rational design of steel beam-column is identified.

10.6.2 Methods incorporating Semi-Rigid Action

The study presented in the following section deals only with the behaviour and strength of columns in non-sway frames. Based on reference [10.38], Baker [10.47] investigated the slip constants of semi-rigid joints and conducted tests on full-sized frames at the Building Research Station. From his generalized slope-deflexion equations for beams, a slip factor β is defined as;

$$\beta = \frac{2EI}{L_b}\gamma \tag{10.21}$$

where I = second moment of area
L_b = length of beam
E = modulus of elasticity
γ = degree of rigidity of the connection = ϕ_j / M

β can vary between 0 and ∞, but for practical connections, β has a range from 0 to 5, in which,

$$\beta = \begin{cases} 0 & \text{(infinitely rigid joints)} \\ 1 & \text{(fairly rigid joints)} \\ 5 & \text{(very flexible light joints)} \end{cases}$$

As pointed out by Chen [10.48], columns in steel frames are connected to other structural members and so their ends are restrained. The behaviour and the strength of columns in actual building frames will be affected by the presence of these unavoidable end restraints which depended on the stiffness of the connections. It can been observed from the M-ϕ in Figures 10.4 to 10.16 that the connection stiffness reduces as rotational deformation increases and that most connections exhibit non-linear behaviour at high levels of loading. Thus a reduced level of end restraint is available to the column as it approaches failure. As column approaches failure, one side of connection will continue to load whilst the other side starts to unload as explained in section 9.6. In general γ is not linear but a joint rotation of 0.01 rad is proposed to determine the linearised degree of rigidity of a connection. This is based on the experimental results by Bjorhovde [10.31] into the secant stiffness (C_{10}, outlined in section 10.4.1) to predict the mid-span deflection at serviceability limit state. The secant stiffness at a rotation of 10 mrad is similar to the average value of the loading

C_t and unloading stiffness C_u in connections (Figure 10.34):

$$C_{10} \approx \frac{(C_t + C_u)}{2} \tag{10.22}$$

The degree of rigidity of a connection becomes;

$$\gamma_{10} = \frac{0.01}{M} = {C_{10}}^{-1} \tag{10.23}$$

The effective length of a column depends on the boundary conditions at the ends of its unbraced length which in turn depend on the stiffness of the beams framed to the column. In BS5950 [10.1], '$\frac{L_E}{L}$ factors', defining the effective length, are provided for cases where beams are rigidly framed to the column and have their far end either rigidly framed to another column, fixed, or hinged. The $\frac{L_E}{L}$ factors deduced for fixed-ended beam with a slip factor β have been modified by Wood [10.49] for a frame with semi-rigid beam-to-column connections as follows:

$$K_b^1 = K_b \left[\frac{1 + \frac{3\beta}{2}}{1 + 4\beta + 3\beta^2} \right] \tag{10.24}$$

By using this equation to modify the beam stiffness for use with the charts of Appendix E of BS 5950 [10.1], estimates of the column effective lengths accounting for the effect of semi-rigid connections can be made. The ultimate capacities of columns are then predicted and compared with the test results.

10.6.3 Discussion

Table 10.16 records the values of the degree of rigidity and slip factor for each joint in frames 3, 4 and 5 determined at the working load level and joint rotations of 0.01 rad. The slip factor for each beam is calculated as the average values of both connections at the beam ends. As explained above, the end-restraints on the column strength reduce as the column approaches failure. It is noted in Table 10.16 that higher values of β are determined when the degree of rigidity γ at the rotation of 0.01 rad are considered than γ taking at the rotation in the working load level. This method not only provides a more conservative ultimate capacity of columns but also easier to use for the designers than the degree of rigidity taking at the rotation in the working load level. As a result, it is suggested that use of the rotation of 0.01 rad to determine the degree of rigidity will be appropriate.

(1) Frame 3

Table 10.17 describes a set of nine different assumed cases, other two cases for the test results, used to predict the axial failure loads (A_x) for each computed effective length ratio

for each of the three column lifts in frame 3. Tables 10.18 and 10.19 then present the results determined from the new approach for methods 1 to 4 as described in Table 10.17. The loads applied to the column head (A_p) are calculated by the subtraction of the total applied beam loads above that column segment from the measured axial load, i.e. 763 - 59 = 704 kN in column 4 (method 1 and case 1). The results of these computations are listed on the right hand side of Table 10.18.

It will be noticed from the results obtained in Table 10.18 that the same axial load of 763 kN was determined for two columns, columns 4 and 5 (method 1 and case 1), whilst a lower axial load of 757 kN was calculated in the lowest column 6. The applied column loads corresponding to these were calculated as 704, 618 and 494 kN in columns 4, 5 and 6. The smallest applied load at the column head (obtained from table column 6) indicates that the failure will occur in the lowest storey of the column. The same methods are used to determined A_x and A_p for other methods for different cases. The low axial loads determined in case 4 were due to the use of the factor of m = 1 when predicting the failure loads. As the moments at the top and bottom of each column segment varies, reduced values of 'm' can be used according to BS 5950 in Table 18 [10.1]. Equivalent uniform moments were used to predict the failure load of columns in cases 5 and 9. The results obtained in cases 1, 2, 3, 6, 7 and 8 again show that failure is reached in the bottom storey due to the lowest value of applied axial load A_p needed to reach failure. However, different results are determined from cases 5 and 9 in which the actual column head moment in the test are used. It is not surprising that this phenomenon was due to the highest out of balance beam moment transferred to the column head as discussed in chapter 6. In fact, this phenomenon is unlikely to occur in an actual structure as it is unusual to have an extension of the column in the top lift. Thus the results obtained from cases 1, 2, 3, 6, 7 and 8 can be said to represent the failure of an actual structure whilst the results determined from cases 5 and 9 represent the failure of the central column in frame 3 due to the unusual test situation giving the large moment at the column head.

Cases 10 and 11 illustrate the axial load in column segment A_x, applied load at the column head A_p and the α_{pin} factor for the three column segments. In case 10, A_x of 542 kN is determined from the strain gauges and A_p is calculated by the subtraction of the applied beam load i.e. 542 - 59 = 483 kN in column 4. In theory, α_{pin} gives an indication of the benefit of the restraint from the beam to column connection after incorporating the potentially disadvantageous influence of moment through the connection. The value of the failure load of a pin ended and minor axis restrained column was determined as 679 kN as shown in Table 10.18 (method 4 and case 1). The α_{pin} factor is determined by the ratio

of the ultimate load of the column A_x to the ultimate load of the column pin connected at each end, i.e. 789 / 679 = 1.16 in the case 10 of column 6 (As explained before, the failure will be reached in the lowest column). The α_{pin} factor is greater than unity and indicates that the adjacent beam can provide enough restraint to the column to offset moment effects. Examination of the result showed that employing the slip factor to predict the effective length and then evaluating the column under axial load only shows a failure load of 739 kN in column 6 (case 1 and method 3). It is significantly better than the ultimate capacity of 679 kN which is computed from a pin ended column (α_{pin} approach, in method 1 and case 1) by about 8 % and the BS 5950 simplified design method (method 2 and case 4) by 4 %. Furthermore, the value is lower than the test results (783 kN). This implies that the proposed method ignoring the column head moment and using the effective length predicted from the slip factor β at the rotation of 10 mrad gives a more economic (but still conservative) design than other approaches. In the author's opinions, this could become the basis of a new design method, named the α_β approach.

A similar method is used to interpret the results in columns 7, 8 and 9 as recorded in Table 10.19. All the results show that failure occurs in the bottom column (lowest A_p determined in table column 9) and that the α_{pin} factor is greater than 1 in column 9. Again the column design used the α_β approach gives the ultimate capacity of 733 kN in column 9 (case 1 and method 3) which is higher than the predictions determined from the α_{pin} approach (679 kN) and BS 5950 simplified design method (641 kN). Perhaps the most important features is that the prediction using the α_β approach shows a lower value than the test result of 766 kN and it thus further confirms that the new approach is also conservative in design.

A new design approach, named α_β, is developed here to predict the ultimate capacity of column for the non-sway and out of plane action prevented columns. This approach essentially adopts the technique of the α_{pin} approach which indicated that the beneficial effect of restraint provided by the beams through the semi-rigid connection outweighs the disadvantage effect of the moment transmitted through the connections. The α_{pin} approach has been modified by taking into account some of the restraint due to the semi-rigid action, using the degree of rigidity at a rotation of 0.01 rad, γ_{10}, in computing the slip factor β_{10} which was then determined using equation 10.21. The '$\frac{L_E}{L}$ factor' is then obtained from the charts of Appendix E of BS 5950 with the modified beam stiffness as mentioned above. The ultimate capacity of column is then, with no applied moments, determined in accordance with BS 5950 simplified approach as noted in cl. 4.8.3.3.1. One important feature from this study of frame 3 is that a column designed using the α_β approach gives the ultimate

capacity of section which is higher than the methods using with the pin ended column under the axial load only (α_{pin} approach) and the BS 5950 method with a nominal '$\frac{L_E}{L}$ factor' and the consideration of applied moments (more economical). Moreover, the new approach is found easy for use in routine design and the predictions are observed slightly lower than the test results (conservative). To provide a further validation of this approach, the results from other columns in the frame tests will be examined.

(2) Frame 4

The prediction for the minor axis frame is now discussed. Tables 10.20 and 10.21 give the value of the predictions from the new design method and compared with other existing approaches. A slenderness ratio of approximately 100 is determined in this frame and the results indicate that additional restraint from the connections has a greater influence on the ultimate capacity of the column than for the major axis frame. This phenomenon is clearly shown in Tables 10.20 and 10.21. An α_{pin} factor much greater than unity was again determined in all column segments. Consideration of the predicted ultimate capacity adopting the α_β approach, with no applied moment, gave a value of 533 kN in column 3 (case 1 and method 3 in Table 10.20). This is significantly higher than the value of 385 kN which was determined from straight α_{pin} approach and the value 384 kN computed from BS 5950 method with the applied moment. Like column 3, the predictions for column 6 (see Table 10.21) using the new approach are observed to be higher than the values computed from other approaches but still lower than the test results.

(3) Frame 5

Finally, the ultimate capacity for frame 5, which employed the end-plate connections with two different sections of beams, was used to examine the new design method. Table 10.22 illustrates the results. Due to beam load being applied on both sides of column, the out of balance moment was small and this moment had only a slight effect on the column capacity (see cases 1 and 2). The column capacity was therefore mainly controlled by the effective length ratio of the column. The results show column failure in the bottom storey and the α_{pin} factor is just equal to an unity in column 6.

In this frame, the α_β approach was observed to predict a slightly higher ultimate capacity of 1161 kN (method 6 and case 3) than the test results of 1100 kN (method 11). However, the values of the overestimation are quite low with only 6 % and thus thought to

be acceptable but give rise for concern. Although the new proposal needs a slightly more calculation than the α_{pin} approach, it is still easy to use for the designers. However, the results obtained so far just based on only the columns in three test frames (frames 3, 4 and 5). Moreover, all the columns are only limited the in-plane action with the out-of-plane action prevented. In fact, the failure of the columns, as discussed in chapter 9, were a result of buckling in the weak axis and the excessive minor axis deformation when the column was restrained in same positions of the major and minor axis. To extend the new approach considering the three dimensional column design, more test results will need be examined.

10.6.4 Further Validation of the New Approach for the Column Design

The new design method, the α_β approach, is proposed and validated using three frame test results. To review the benefits of the new approach, the results determined in the columns of frame 3, 4 and 5 are noted and compared in Table 10.23. Table 10.23 (a) shows the predicted '$\frac{L_E}{L}$ factors' using the α_β approach. It is noted that all results are lower than those assuming an effective length ratio of 0.85 for the lowest lift of columns with a rigid base condition which indicates that the potential benefits of the new approach taking into account the semi-rigid action. Table 10.23 (b) illustrates the ultimate capacity of the columns using three different methods together with the experimental and analytical results. The 'BS 5950' results recorded in column (1) are the ultimate compressive load capacity of column taking into account the effect of applied moment, due to beam reaction applied at the column face plus 100 mm and determined in accordance with the BS 5950 simplified approach as noted in cl.4.8.3.3.1. The 'α_{pin}' results shown in column (2) are the ultimate capacities of pin ended columns, with no applied moment, determined in accordance with BS 5950. The results used the 'α_β' approach noted in column (3) are the ultimate compressive load capacities of columns with no applied moment and taking into account the restraint due to the semi-rigid action to reduce the effective length ratio of column, using the degree of rigidity γ_{10} at a rotation of 0.01 rad and the slip factor β_{10} determined using equation 10.21, to modify the stiffness of beam. The effective length ratio is then obtained from the charts of Appendix E of BS 5950 with the modified beam stiffnesses. The ultimate capacity of column is, with no applied moments, determined in accordance with BS 5950 simplified approach as noted in cl. 4.8.3.3.1. Column (4) is the record of the experimental results and Columns (5) and (6) are the analytical predictions from two computer programs SERFA and SERVAR as performed by the author and described in chapter 8. As discussed in the earlier section, the new approach predicted a higher ultimate capacity than other two methods and still lower than the experimental and analytical results in frames 3 and 4.

This new approach is now extended to consider the three dimensional action of the columns. The test data and analytical results of the columns are taken from three different sources, three dimensional frame tests conducted by Gibbons [10.27], the parametric study conducted by the author in chapter 9 and the practical frames analysis by Carr [10.50]. All the information is used to further validate the new approach taking into account the three dimensional action of columns including out-of-plane buckling.

(1) Three Dimensional Frame Tests

Two full scale test frames, F1 and F2, which are the first subjects used to validate the new design approach, were performed by Gibbons [10.27] at the Building Research Establishment. The first frame F1 had been analysed by the author [10.30]. Both frames were two and a half storeys, non-sway structures of approximate overall dimension 3.4 m x 10.0 m x 9.0 m. Figure B1 shows the general arrangement of the test frames. Each frame comprised an active and a static frame, only the active part of frames and some interconnecting beams were subjected to load and response monitoring. The static frame was used solely to provide restraint to the active frame. The frames could be considered as comprising two parallel two dimensional frames each consisting of three columns and four primary beams, with six secondary beams connecting to the frame at the panel points.

The frames were constructed used 152 x 152 UC 23 sections for columns and 254 x 102 UB 22 sections for both primary and secondary beams. All steel was nominally grade 43A throughout. The only difference between the two frames, F1 and F2, were the column orientations of the active frame and the detailing of the beam to column connections. For the first frame F1, the columns were configured such that the primary beams framed into the column web whilst in the frame test F2, the primary beams were framed to the column flange. The flush end-plate connection used in frame 1 adopted 12 mm end-plate whilst those in frame 2 were 8 mm thick. A more detailed description of two frame tests is recorded in reference [10.27].

Examination and analysis of the results by Gibbons shown that the failure occurred in the second lift of the central column C5/1-2 due to the column being subjected to high applied moment whilst the other columns i.e. C6/01, C7/01 and C8/01 failed in the bottom lift due to the high axial loads. The slopes of the load-deformation curves indicated that failure occurred due to the excessive of the minor axis deformation. To reduce the volume of calculation, all the column capacities are only checked for the minor axis buckling only.

The ultimate capacity of the central column C5 in F1 is determined using the different approaches for the second lift C5/1-2 and the lowest lift C5/0-1, for all other columns only the lowest lift is used. The M-ϕ curves for F1 are taken from the joint tests conducted by Davison [10.41] (internal joints) and Celikag [10.51] (external joints) as shown in Figure 9.13 whilst F2 are taken from Kim's test [10.52] in the databank.

Table 10.24 (a) shows the slenderness ratios and the predicted '$\frac{L_E}{L}$ factors' by α_β approach for the two test frames. In frame 1, the primary beams are connected to the column flange whilst in frame 2 they are connected to the column web. The '$\frac{L_E}{L}$ factors' are determined from the weak direction as 0.65 for frame 1 and 0.71 for frame 2. This was due to the use of a thinner end plate in frame F2, so that a lower restraint was provided by the connection giving larger effective length ratio.

Turning to compare the predicted ultimate capacity of column, Table 10.24 (b) shows the predictions adopted three different approaches, i.e. BS 5950, α_{pin} and α_β methods, which was explained in the beginning of this section, together with the test results. As expected, all the predictions used the α_β approach are higher than the values determined from other approaches (a minimum of 41 % higher than the value predicted by the α_{pin} approach and 34 % more than the BS 5950 method). Moreover, the α_β predictions are lower than the test results providing evidence that the new design approach is also conservative in this case.

(2) Parametric Study

The results from the parametric study for subassemblage structures performed by the author in chapter 9 were used to further validate the new approach for column design. Only those results from the second phase of study using the M-ϕ curves from Davison's tests are discussed. The design model used in this study is shown in Figure 9.5. The subassemblage comprised a 152 x 152 UC 23 column and 254 x 102 UB 22 UB beam sections. All the steel used was nominally grade 43A with the yield stress being assumed to be 275 N/mm^2. Three types of the connections, flush end plate (FEP), web and seat cleats (WAS) and double web cleats (WC) and two extreme base conditions, truly pinned and fully rigid, were considered in this study. The stiffness of connections and base conditions significantly affect the restraint to the column, '$\frac{L_E}{L}$ factors' reduce as the restraint increases. Therefore, the new design approach was examined with respect to the sensitivity of the stiffness of the connections and the base conditions. Different loading patterns, as described in the section 9.5, are also considered. The analytical results in the previous study are illustrated in Table 9.6.

The analysis in the second phase of study showed that all the subassemblages using different type of connections failed due to the excessive minor axis flexure even when bent about major axis. The new approach could be used to check the ultimate capacity for the major and minor axis of columns. As expected, the predictions for all study cases show a higher ultimate capacity for the major axis column than for the minor axis of column and confirming that failure occurred due to minor axis flexure.

Table 10.25 (a) illustrates the effective ratio for the subassemblage predicted using the β factor. It is noted that a slenderness ratio of 103 is determined for the minor axis column. As explained in section 10.6.3, the additional restraint from the connections in the minor axis has a greater influence on the ultimate capacity than the major axis column. The '$\frac{L_E}{L}$ factors' computed using the α_β approach are determined with the range of 0.610 to 0.675 for the rigid base condition and from 0.710 to 0.780 for the pinned base subassemblage. Obviously, the subassemblages using the flush end-plate connections with rigid base had the lowest '$\frac{L_E}{L}$ factors'. This implies that the predicted effective length of columns using the new approach are sensitive to the level of end restraint.

Table 10.25 (b) records the ultimate capacity of subassemblage computed using different methods. It is noted that the ultimate capacity of the subassemblage, is determined as 358 kN, using the α_{pin} approach for all end conditions. Although the ultimate capacity adopted the α_{pin} approach predicted significant lower values than the analytical results for all different cases, it is uneconomical for designing the column when stiff upper end connections and a rigid column base are adopted. For the α_β approach, it is of interest to note that the ultimate capacity is quite sensitive to the change of the type of connections and base conditions. All the predictions are close but still lower than the capacities predicted by the full analytical program.

(3) Trinity Court, Manchester

The first practical frame considered in this study was an eleven storey office block, Trinity Court, located in Manchester which was analysed by Carr [10.50]. The building comprised a nine storeys braced steel superstructure which sits atop a two storeys reinforced concrete substructure. All the steel used was nominally grade 50 and the frame was designed to BS 5950. Figure B2 shows the typical floor layout.

Three different types of column, C5 (four beams attached), C6 (3 beams attached) and

D/E6 (two beams attached) were considered (see Figure B3). Two types of connections were used, header plane (HP) and flush end-plate (FEP). The M-ϕ curves used by Carr are adopted in this study. The columns consisted of the same section for every three storeys, e.g. 356 x 368 UC 153 between ground to third floors in the internal column C5. The analytical results from ground to third floors and sixth to ninth floors for each types of columns are examined to compare with the ultimate capacity of columns used different approaches.

Carr's analysis shown that the critical lift was always in the lower lift of each column section i.e. ground to first floor was the critical lift between ground and third floors, as it sustained the largest axial load. The predicted failures of all study cases were a result of excessive minor axis deformation. Thus the columns C5, C6 and D/E6 between ground and first floors and sixth to seventh floors are selected in this study. As a 457 mm diameter circular hollow section was used in the edge column C6 between ground and seconds floors , the column lift between these floors was not analysed by Carr. Therefore, only the column C6 in the second to third floors are examined (to replace the ground to first floor in C6).

Two types of models are used in Carr's analysis. Subassemblage type (i) which consisted of a single column lift with beams connected to only the head of the column, the base of the column being with pinned or rigid and subassemblage (ii) which consisted of a single column with beams connected to both the head and base of the column (see Figure B3). Only model (i) with pinned base was considered for the column in the ground and first floor (the baseplate was designed by the structural engineer as a theoretically pinned joint) and models (i) and (ii) were used for other floors.

Table 10.26 (a) records the '$\frac{L_E}{L}$ factors' for each column using the α_β approach. It is noted that the slenderness ratio for this building is quite low with a range of 40 to 58 only and it indicates that additional restraint from the connections has a lesser influence on the ultimate capacity of a column than the column with a larger slenderness ratio. The '$\frac{L_E}{L}$ factors' with an average value of 0.92 are determined using the α_β approach. The ultimate capacities of the columns determined from the BS 5950 method, the α_{pin} approach and the α_β approach together with the analytical failure loads are shown in Table 10.26 (b). It is noted that the analytical failure loads give a highest failure load whilst the BS 5950 method gives a lowest. Both α_β approach and α_{pin} approach predicted a higher column capacities than the BS 5950 method (more economical) and the results are still lower than the analytical results (conservative). It is noted that the ultimate capacities predicted by the α_β approach are all higher than the results computed from α_{pin} approach due to the restraint provided from the connections at the ends of columns. As explained before, the

building was designed with quite stocky columns and the small benefits for the new column design approach were obtained. For the column at the ground to first floor level, an average slenderness ratio of 45 is determined, the column capacity computed using the α_β approach is only 3 % higher than the results computed from the α_{pin} approach. However, a larger saving of steel was possible for the column in the sixth to seventh floors (average slenderness ratio of 58) for which the ultimate capacities using the α_β approach were predicted to be an average of 6 % higher than the values computed from the α_{pin} approach. This implies that the α_β approach provides a lesser weight saving for the stocky columns (low value of the slenderness ratio) with flexible connections and pinned base than the slender column with rigid connections and base conditions when compared with the results determined from the α_{pin} approach.

(4) M.R.I. Building, Nottingham

Finally, the M.R.I. building located in Nottingham analysed by Carr [10.50] was used to examine the new design approach. The building was used to house a 'Magnetic Resonance Imager', and was a three storey, non-sway structure of the overall dimension 19.5 m x 26.0 m in plan as shown in Figure B4. The building was totally supported by 20 columns at 6.5 m centres in each direction. Two type of connections, header plate and flush end-plate, were used in this frame. The moment-rotation curves used in Carr's analysis are adopted in this study. Due to the significant imposed loads of the scanner, the building was designed with one way spanning slab over the 6.5 m between the adjacent floor beams. The suitably located crossbracing was used to provide lateral restraint to the building. For the critical case, ground to the first floor, the actual column length is 3.27 m. The column had been designed with accordance to BS 5950 'simple' design method with the effective length ratio of 1.0. All the steel used was nominally grade 50.

Three different types of column, internal (I), edge (E) and corner (C), are selected - a total of 17 columns represent the different locations. The ultimate capacity of each column is predicted using the different approaches, i.e. BS 5950 method, α_{pin} approach and α_β approach and directly compared with the analytical results conducted by Carr using the analytical model (i).

Table 10.27 (a) illustrates all the section sizes, type of connections, slenderness ratios and the predicted '$\frac{L_E}{L}$ factors' computed using the α_β approach for the selected columns in the building. It is noted that only two different sections of columns were adopted in these columns and the slenderness ratio was determined as 61.5 and 61.9. All the beam-columns

were designed with very flexible connection and pinned base condition, the additional restraint from the connection and base were low. Thus, the predicted '$\frac{L_E}{L}$ factors' were found within a very narrow range between 0.84 to 0.92. The ultimate capacity of columns using the different approaches together with the analytical results are recorded in Table 10.27 (b). As for the Trinity Court building, the ultimate capacity determined from the BS 5950 method gives a lowest value and the analytical results are the highest. The results imply that, in this instance, both the α_β approach the α_{pin} approach are conservative and are better than the BS 5950 method. All the predictions using the α_β approach give higher values than those determined from the α_{pin} approach.

It is noted in Table 10.27 (b) that all the ultimate capacities of the internal columns using the α_β approach are all lower than the analytical results whilst the new approach was observed predicted a slightly higher ultimate capacity than the analytical results for the edge column B4 and the corner column A1/A4. However, the values of the overestimation are quite low with below 3 % only and is thus though to be acceptable.

When the ultimate capacities, determined from the α_β approach, are compared with the predictions computed from the α_{pin} approach, an average of 7 % higher results is determined. An average 16 % higher ultimate capacity using the α_β approach is obtained when it is compared with the prediction adopted the BS 5950 methods. A larger saving of the weight of steel is achieved for the corner columns than the columns with low out-of-balance moment due to the applied beam loads in other locations i.e. internal or edge due to ignoring the moment effect.

10.6.5 Implication for the Design

A new column design, the α_β approach, is proposed and validated with over fifty studied results from the frame tests, parameter study and practical frames. The new design approach requires the degree of rigidly, γ_{10}, which is an inverse value of the joint secant stiffness of C_{10} taken from the M-ϕ curves. Designers may initially be concerned about the accuracy of the M-ϕ response required. Thus three columns, with the different value of slenderness ratio (97.8, 61.5 and 39.6) were selected from one of the three dimensional frames F1, M.R.I building and T.C. building. For each type of connection, variations of the moment rotation curves of $\pm$ 20 % were considered to investigate the effect on the load carrying of the column with different slenderness ratio to adopted the new approach. The method adopted in section 9.7.2 to change the M-ϕ response is used where, at a particular

value of rotation, the moment is changed. Thus changing the secant stiffness C_{10}.

Table 10.28 illustrates the experimental or analytical results and the ultimate capacity with the change of the C_{10} predicted by the new approach. It is noted that the average slip factors β_{10} reduce as the secant stiffness of connections C_{10} increase. Thus the slip factor is sensitive to the change of the secant stiffness of the connections. Perhaps, the most important feature is that, whilst the secant stiffness of the connections vary by $\pm$ 20 %, the effective length ratios are changed by less than 1 %, as are the ultimate capacities of columns (see Table 10.28). This suggests that the predicted ultimate capacity of a column using the α_β approach is relatively insensitive to a significant variation of the M-ϕ responses. All the predictions are all lower than the experimental or analytical results as recorded in Table 10.28. It is thus concluded that the significant variations of the M-ϕ response has only a very modest effect on the ultimate capacity of column computed using the new design approach. Thus the precise form of the M-ϕ relationship is not important.

10.6.6 Recommended Design Procedure

The new approach that has been developed along with the validation used different results to illustrate the practical application to the design of the non-sway columns with end restraint. The design procedure can now be summarized as follows:

1. Select connection types.
2. With frame geometry and loads defined, the trial beam is designed used the modified plastic hinge calculation with an assumed value of λ (section 10.5).
3. Using the α_{pin} approach design the trial column section.
4. The M-ϕ curve can be determined using the prediction i.e. EC 3 or experimental result i.e. database.
5. Compute the degree of rigidity γ_{10} at the rotation of 0.01 rad from the known M-ϕ curve. The slip factor β_{10} is then determined using equation 10.21.
6. Compute the beam stiffness, using equation 10.24 to determine the modified beam stiffness.
7. Repeat the procedures as mentioned above to determine the modified stiffness of other beams. Determine the stiffness of the columns.
8. Calculate k_1' and k_2'. Use the charts of Appendix E of BS 5950 to estimate the '$\frac{L_E}{L}$ factors' (effective length of columns).

9. The ultimate capacity of column is determined in accordance with the BS 5950 simplified approach as noted in cl.4.8.3.3.1. with no applied moment.
10. The followings procedures are repeated to check for other axis, if necessary. The lowest values is the design capacity of column.
11. Refine design, if necessary.

10.6.7 Comments and Conclusions

From the results obtained in the previous study, a new column design method is proposed and validated. Based on the study, some comments and conclusions are drawn:

1. All the results have shown that the new design method predicts a higher column capacity than other approaches i.e. BS 5950 and α_{pin} methods, but is still conservative for design. Moreover, the method is easy to follow and is considered suitable for design.
2. The presence of the beam-to-column connections with realistic stiffnesses (or the column base for ground floor columns) will have a dominant effect on column capacity and this is reflected in the design approach.
3. The column location, i.e. internal, edge or corner situation, is only slightly affects the predicted column failure load.
4. It is found that slenderness ratio of a column significantly affects the predicted effective length ratio. For a stocky column (i.e. low value of slenderness ratio) with flexible connections at each end or having a pinned base, the restraint provided is low and thus the '$\frac{L_E}{L}$ factors' are predicted in the range of 0.9 to 1.0. However, significantly lower values of $\frac{L_E}{L}$ are predicted for slender columns with the same type of connections and base condition.
5. The columns designed in accordance with the new approach using stiff connections and base conditions can have capacities enhanced by up to 60 % relative to the simple α_{pin} approach.
6. Significant variation of the M-ϕ response ($\pm$ 20 %) has a negligible effect of the ultimate capacity of columns using the new approach.

10.7 Recommendations for a Semi-Rigid Design Method

A number of methods to assess the performance of semi-rigid frames have been examined and discussed. In this section, all the new methods are assembled into a complete design method for semi-rigid action in steel structures. It is believed that this is the first proposal suitable for hand calculation which involves all parts of the design requirements i.e. serviceability and ultimate strength. It is important to point out that the proposal only requires slightly more calculation than the current method. The procedure of a semi-rigid design method will be presented in full in this section. The advantage of this method is then outlined and explained with a design example from a frame test result. The potential saving in weight of steel in a frame is presented.

10.7.1 Procedure for the Design of a Steel Frame using Semi-Rigid Design Methods

(1) Design Checking

In general, an analysis that incorporates semi-rigid action of a steel structure should consider the following parameters,

1. Connection Response

   Connection initial stiffness, rotation capacity, ultimate capacity can be determined from simplified analytical models i.e. EC 3. However, due to the limitation of the existing models, the moment rotation characteristic may be quite complex to calculate and the results are not yet reliable. This type of information could be also obtained from the experimental results collected from a database. The Sheffield database has been transferred to the University of Liege in Belgium and a PC version is being developed in conjunction with the University of Aachen in Germany. At this time, it is impossible for designers to use these. Moreover, these databases only cover limited test data and some practical configurations of connections are not included. To design a steel frame using semi-rigid methods, it is suggested the designer should use similar sections or those of a little lower strength and stiffness when the exact size is not available. For example for the end-plate connections, a thinner plate should be used to provide a more conservative design i.e. lower initial stiffness and ultimate moment. However, these problems are expected to be resolved in the future by the PC version of the database containing an increasing number of results or by more reliable design models perhaps using computer programs e.g. EC 3 for which a new version of

Annex J is being developed.

As was discussed in chapters 5 to 7, the M-ϕ response of the frame test results is quite similar to the joint test with same test conditions i.e. internal joints in frame tests and joint tests with a cruciform test arrangement. Furthermore, a parametric study conducted in chapters 8 and 9 showed that behaviour of frame is not significantly affected by minor differences in the moment rotation characteristics used and that the ultimate capacities of members and the deflection of beams were little changed by significant variation of the M-ϕ responses. This implies that a precise knowledge of these characteristics is not essential.

2. Beam design is based on two criteria :

   – Ultimate Limit State

     The method of modified plastic hinge calculation should be used for design.

   – Serviceability Limit State

     The prime considerations here are the deformations and other stiffness-related characteristics of the connections, and their effects on the service load deformations of the frame. The linear elastic method using the beam line approach with the secant of stiffness at 0.01 rad (flexible connections) and 0.005 rad (rigid connections) should be considered.

3. Column design based on the ultimate capacity check

   Strength and stability of the frame and its component members - the effect of partial connection restraint on the ultimate strengths of the members and frame should be considered. The structure is acceptable with respect to strength if the nominal resistance of the structure is greater than the factored load effects.

   The α_{pin} approach should be used to design a trial column section and the α_{β} approach then checked following the recommended design procedure as mentioned in section 10.6.6.

(2) Design Procedure

A design procedure for semi-rigid frames is proposed below. There are nine steps - some steps contain alternative methods, the underlined one is the recommended method.

1. Trial beams, columns and connections used ;

   – Select a suitable type of connection

- Beams designed using plastic hinge calculations with an assumed value of λ (see section 10.5) after the type of connections to be used has been selected.
- Column designed as a pinned column (α_{pin} approach) (see chapter 9)

2. Moment rotation curves from
   - Prediction (complex calculation and unreliable)(section 10.3)
   - Database (easy to use and reliable)(chapter 3)

3. Classification of M-ϕ response using EC 3
   - Rigid design
   - Simply design
   - Semi-Rigid design (economic and easy to use)

   As discussed in section 10.3.4, classification of the connection is used to classify the frame response at a early stage. After the behaviour of the connection is classified, a suitable secant stiffness is then selected to predict the mid-span beam deformation in the serviceability limit stage as outlined in procedure 5.

4. Semi-Rigid design method can be used ;
   - Computer programs (chapters 8 & 9)
   - Hand calculation

   The computer program can be used for the preliminary design or final checking.

5. Laterally restrained beam design
   - Ultimate capacity check using the plastic hinges calculation with the actual connection moments from database
   - Serviceability check at the unfactored imposed load level (outlined in BS5950)
     * use C_5 or C_5' for rigid connections
     * use C_{10} or C_{10}' for flexible connections

   The behaviour of the connections can be classified using the EC 3 classification system.

6. Column design using the α_β approach (see recommended design procedures 5 to 11 in section 10.6.6)

7. Reduce the size of beams and columns if possible and go back to procedure 2, otherwise design is completed.

Here, a procedure for a semi-rigid design method is presented and the design procedure is also presented in Figure 10.35. The design method, and a design example for frame 5 using the conventional simple design method and this proposal, will be discussed next.

10.7.2 Design Methods and Example

(1) Conventional Simple Design

Frame 5 is re-designed to the conventional simple design method. A detailed description of the basic information and the design methods for frame 5 are outlined in chapter 7. The frame layout and design loads given are used (the fundamental information for the designers). All steelwork is in Grade 43 material. Beams 1 to 3 use flush end-plate connections and are thus designed as simply supported beams with no moment attracted to the connections. The mid-span moment of 123.8 kNm was calculated under the maximum applied beam load, the beam section of 254 x 146 UB 37 is selected (same beam section is designed of the original frame). Beams 4 to 6 use extended end-plate connections and these beams are thus designed as a single fully rigid beam. Thus the maximum moment in two beam ends ($\frac{2}{3}$ of the mid-span moment for a single simply supported beam) is used to design the strength of beam. A section of beam 254 x 102 UB 28 which is also identical to the original design is selected.

The ultimate capacities of the column are designed in accordance with the BS 5950 simplified approach which takes into account the effect of applied moment, applied at column face plus the 100 mm eccentricity. The effective length ratio of 0.85 is assumed for the rigid column base. As all storey heights are identical, the lowest storey i.e. the highest axial load will control the design. Thus only the lowest storey of the internal and external columns are designed. Due to the same loads applied in both side of beam, no out-of-balance moment is calculated. With the full design load of 200 kN applied on each beam, the axial load which is calculated from half of the total loads to each connecting beam, is computed

as 600 kN in the lowest lift of the central column (column 6). For a 152 x 152 UC 23 column, the total axial load to cause the failure in the internal column is computed as 715 kN and a further axial load of 115 kN is required to give the ultimate loading. Due to same applied beam loads, two edge columns are designed with no virtual different in accordance with the BS 5950 method. The total axial load sustained in the lowest lift of columns are determined as 300 kN. The 152 x 152 UC 23 is the smallest section in the design practice, the ultimate capacity of this column under the applied moment is determined as 586 kN and a further axial load of 286 kN is required to cause the failure. In fact, the edge column in this instance could have been selected as a smaller section had a size of column been available. The sections of the new design frame used the conventional simple design are recorded in Table 10.29.

(2) Semi-Rigid Design

The proposed semi-rigid design method can now be used to redesign the frame following the procedures outlined in section 10.7.1. The type of connection is selected based on factors such as economy and experience. Afterwards, a reasonable λ value suggested in section 10.5.2 is used here to determine the section size of the beam using the modified plastic calculation (section 10.5). The trial column can be designed as pin ended under axial load only (α_{pin} approach). After the trial beams and columns are selected, the connections can be designed. The fabricator will provide a detail design of the connections based on the sizes of beams and columns of the frame.

To select a suitable M-ϕ curve from the database, the method illustrated in section 10.7.1 can be followed. The EC 3 method is used to classify the moment rotation response (section 10.3.4). At this stage, the designer can change the connection design if the strength of connection does not fulfil the design criteria. Moreover, the classified behaviour of connection i.e. rigid or flexible can be used to provide a condition (secant stiffness of C_{10} or C_5) for the beam serviceability check in the later procedure.

The beam design is based on two checks, ultimate limit state and serviceability limit state. For the ultimate limit state, the modified plastic hinge calculation with a known value of λ (ultimate capacity of connection is determined from the M-ϕ curve) is used to check the ultimate strength of the laterally restrained beams. For the serviceability checking the linear elastic method with a secant stiffness of C_5 or C_5'(for the rigid connection) and C_{10} or C_{10}' (for the other connections) illustrated in section 10.4 should be adopted.

Finally, the α_β approach is employed to provide a check on ultimate column capacity (section 10.6). The size of beams, columns can be reduced if necessary and re-checked again following procedure 2.

(3) Design Example for Semi-Rigid Design

An existing frame (frame 5) is selected to illustrate in detail the procedure to analyse and redesign of this frame adopting the proposed semi-rigid design methods. The benefits available with the semi-rigid design frame are demonstrated. The design procedure outlined in section 10.7.1. is used.

1. Using the same type of connections (flush end-plate and extended end-plate) in frame 5

   From section 10.5, trial lowest values of λ within the suggested range of 0.20 for the flush end-plate and 0.54 for the extended end-plate without stiffener are considered to design the trial beams. Those are the lowest values within the suggested range as recommended in section 10.5. However, as explained in section 10.5. It is important to note that designers do not need to select an accurate value of λ in this stage, refinement of the design can be achieved after the connection moment is determined from the M-ϕ response in procedure 6. Trial columns are found using the α_{pin} approach.

   (a) Trial Beam

      i. For beams 1 to 3

         Joint moment = 0.2 x plastic moment of beam

      Frame 5 with applied load at its quarter points, equation 10.19 can be rearranged,

$$M_j + M_p = \frac{WL_b}{8}$$

$$1.20\ M_p = (200)(4.95)/8$$

$$M_p = 103.1 \text{ kNm}$$

$$S_x = (103.1/275) \text{ x } 10^3$$

$$= 375 \text{ cm}^3$$

Try 254 x 146 UB 31, $S_x = 396 \text{ cm}^3 > 375 \text{ cm}^3$

$M_p = 109$ kNm

ii. For beams 4 to 6

Joint moment = 0.54 x plastic moment of beam

$$M_j + M_p = \frac{WL_b}{8}$$

$$1.54\ M_p = (200)(4.95)/8$$

$$M_p = 80.4 \text{ kNm}$$

$$S_x = (80.4/275) \times 10^3$$

$$= 292 \text{ cm}^3$$

Try 254 x 102 UB 25, $S_x = 306 \text{ cm}^3 > 292 \text{ cm}^3$

$M_p = 84$ kNm

(b) Trial Column

i. For the Central Column

The column is designed as a minor axis restrained pin ended condition under axial load only (α_{pin} approach). As described in previously section, the axial load is determined as 600 kN in the lowest segment of column (column 6) which controls the design.

Try 152 x 152 UC 23 for column (bent about major axis):

Determine the ultimate capacity of column in accordance with BS 5950 simplified approach under axial load only (cl.4.8.3.3.1)

For $\frac{L_E}{L} = 1.00$: $\frac{L_E}{r_x} = \frac{3600}{65.1} = 55.3$

From table 27(b) $(p_y = 275\ N/mm^2)$ $p_c = 228\ N/mm^2$

$$F \not> (228)\ (2.98) = 679 \text{ kN}$$

Additional axial load required to give ultimate loading,

$$679 - 600 = 79 \text{ kN}$$

ii. For the Edge Columns

The external columns are only required to sustain an axial load of 300 kN in the lowest lifts (columns 3 and 9), this column section is thus also suitable.

Additional axial load required to give ultimate loading,

$$679 - 300 = 379 \text{ kN}$$

2. The M-ϕ curves are now collected from the database. However, it is discovered that the database does not contain the connections matching the design condi-

tion. Connections with a slightly lower plastic capacity of beam 254 x 102 UB 22 conducted by Davison is selected (test reference JT/12 for flush end-plate and JT/13 for extended end-plate). These connections have a lower ultimate capacity and lead to a more conservative design check. Figure 10.36 illustrates a plot of two selected M-ϕ curves.

3. The EC 3 classification system is again adopted to classify the behaviour of connections. Figure 10.37 illustrates a curve containing two connections plotted in the EC 3 classification system. Observation of this figure shows that the flush end-plate connection could be classified as semi-rigid. For the extended end-plate connection, it can be classified as partial strength based on the ultimate capacity. For the initial stiffness, this connection is observed to be rigid.

4. Using the semi-rigid design methods for hand calculation.

5. Beam Design

   A slightly lower connection moment is taken at the rotation of 0.005 rad, as discussed in section 10.5.2, for a more conservative design of the strength of beams.

   (a) For beams 1 to 3

      i. Ultimate check

         Joint moment = 18 kNm

         M_p =(200)(4.95)/8 - 18

         105.8 kNm

         S_x =(105.8/275) x 10^3

         = 385 cm^3

      For 254 x 146 UB 31, S_x = 396 cm^3 > 385 cm^3

      ii. Deflection Check

      Consider the serviceability checking, service loads may be taken as the unfactored imposed load. In this frame, the beam load was designed of 200 kN under its design load. The working load of 133 kN approximates to $\frac{2}{3}$ of its design beam load. Assuming the ratio of the dead load to the imposed load is 1 : 2, the imposed load is calculated as 88 kN. Table 10.30 records the results.

      At working load condition, using the linear elastic method with secant stiffness of C_{10}, deflections are calculated;

For Beam 1

Stiffness stiffness:

Joints A and B: C_{10} = 21.5 / 0.01 = 2150 kNm/rad

Rigid frame moment:

Joint A: M_R = 15.50 kNm

Joint B: M_R = 51.00 kNm

Semi-rigid frame moment:

Joint A: $M_{SR} = \frac{15.50}{1+(15.50)/(2150\times0.011)} = 9.31$ kNm

Joint B: $M_{SR} = \frac{51.00}{1+(51.00)/(2150\times0.011)} = 16.00$ kNm

The dimensionless factor:

Joint A: α = 9.31 / 15.50 = 0.60

Joint B: α = 16.00 / 51.00 = 0.31

Average $\overline{\alpha}$ = (0.60 + 0.31) / 2 = 0.46

Determine the mid-span deflection used equation 10.17:

δ_{SR} = 7.9 + (1 - 0.46) × (16.4 - 7.9) = 12.5 mm

Deflections in beams 2 and 3 are determined using the same procedures. All predicted beam deflections under its unfactored imposed load are recorded in Table 10.30 and the results are shown all under to the limited value of L/360 = 13.75 mm

The beam size satisfied the checking

(b) For Beams 4 to 6

i. Ultimate check

Joint moment = 42 kNm

M_p =(200)(4.95)/8 - 42

81.8 kNm

S_x =(81.8/275) x 10^3

= 297 cm^3

For 254 x 102 UB 25, S_x = 306 cm^3 > 297 cm^3

ii. Deflection Check

At the working load condition, using the linear elastic method with secant stiffness of C_{10}. As the methods used in beams 1 to 3, deflections are calculated and recorded in Table 10.30;

All predicted beam deflections under its unfactored imposed load are under to the limited value of L/360 = 13.75 mm

The beam size satisfied the checking

In conclusion, the beams satisfy all the checking. An economical design is expected to be obtained used this new proposed methods. In this instant, an average potential saving about 14 % based on the weight of beam are obtained using the proposed semi-rigid design methods.

6. Column Design for Ultimate Check using the α_β Approach

Finally, the α_β approach is used for checking the ultimate capacity of column. As explained before, only the most critical case, the lowest lift of the columns are checked.

(a) For the Central Column

The maximum axial load at the lowest lift of the column = 600 kN

Degree of rigidity:

Beam 3: $\gamma_{10} = (10 \times 10^{-3}) / (21.5 \times 10^{6}) = 4.65 \times 10^{-10}$ rad/Nmm

Beam 6: $\gamma_{10} = (10 \times 10^{-3}) / (51.0 \times 10^{6}) = 1.96 \times 10^{-10}$ rad/Nmm

Slip factor:

Beam 3: $\beta_{10} = [(2 \times 210 \times 10^3 \times 4440 \times 10^4) / (4953)] \times 4.65 \times 10^{-10}$
$= 1.75$

Beam 6: $\beta_{10} = [(2 \times 210 \times 10^3 \times 3410 \times 10^4) / (4953)] \times 1.96 \times 10^{-10}$
$= 0.57$

Beam stiffness:

Beam 3: $K_b = (4440 \times 10^4) / 4953 = 8964$ mm^3

Beam 6: $K_b = (3410 \times 10^4) / 4953 = 6885$ mm^3

Modified beam stiffness:

Beam 3: $K_b^1 = 8964 \times \frac{1+(3\times1.75)/2}{1+4\times1.75+3\times1.75^2} = 1891$ mm^3

Beam 6: $K_b^1 = 6885 \times \frac{1+(3\times0.57)/2}{1+4\times0.57+3\times0.57^2} = 3002$ mm^3

Column Stiffness:

$K_c = (1260 \times 10^4) / 3600 = 3500$ mm^3

Using the sway prevented alignment chart (Figure 23) in BS 5950 Appendix E:

$k_1' = (3500 \times 2) / (3500 \times 2 + 1891 + 3002) = 0.59$

$k_2' = (3500) / (3500 \times 2) = 0.5$ (for rigid base)

$\frac{L_E}{L} = 0.71$

This gives an effective length of:

$L_E = 0.71 \times 3600 = 2556$ mm

Determine the ultimate capacity of column in accordance with BS 5950 simplified approach under axial load only:

For $\frac{L_E}{L} = 0.71$: $\frac{L_E}{r_z} = 0.71 \times \frac{3600}{65.1} = 39.3$

From table 27(b) $(p_y = 275\ N/mm^2)$ $p_c = 251\ N/mm^2$

$$F \not> (251)\ (2.98) = 748\ \text{kN}$$

Additional axial load required to give ultimate loading,

748 - 600 = 148 kN

Thus the central column satisfied the capacity check

(b) For the Edge Columns

As the procedures used to design the central column, two edge columns are designed using same methods. The predicted ultimate capacity of two edge columns are recorded in Table 10.33.

10.7.3 Deflection and Capacity Assessment of Frame using Validated Computer Program

The new design frame is now checked for the computer program SERFA which had been validated in chapter 8. The model shown in Figure 8.1 is used in this study. All the columns included an initial sinusoidal geometric deformation with a maximum amplitude of L/1000 (3.6 mm). The assumed pattern of member residual stress is shown in Figure 8.27. The moment rotation curves shown in Figure 10.36 is adopted.

Several different runs of the program are conducted in order to provide enough analytical results for the serviceability and ultimate checking. For the ultimate capacity checking for the beam design, all the beams were loaded up to their design load of 200 kN in twenty equal increments, each beam was then loaded to cause failure individually. For the columns, the same increments of load were applied to the beams up to the design load, additional load was then applied to the head of each column individually up to failure. Thus the strength of each member is computed. For the beam serviceability checks, the mid-span deflection for each beam under its imposed load is taken from the output file and compared with the predicted results using the proposed methods.

Table 10.30 (b) show the predicted mid-span deflection of six beams computed from SERFA and the new proposed method together with two extreme conditions i.e. truly pin and fully rigid. As expected, the deflection computed from plane frame analysis program with rigid joint give the lowest values as recorded in column (1) whilst the simply support

beams give the highest in column (2). It is worth noting that the predictions in column (3) used the proposed method are all slightly higher than the values taken from the computer program as presented in column (4). This suggests that the proposed method gives conservative predictions of the mid-span deflection of beams at the serviceability limit state.

Table 10.31 show the λ values computed from SERFA at the load level of design load. It is noted that average values of 0.24 for beams 1 to 3 (flush end-plate) and 0.55 for beams 4 to 6 (extended end-plate) are determined. For the extended end-plate connections, the average value of λ given from the analysis is close to the lowest of the suggested range. This may be due to the adoption of a slightly lower strength of connection as described in section 10.7.2.

The failure load of the beams computed from SERFA are shown in the column (1) of Table 10.32. In column (2), the strength of beams are determined from the plastic hinge calculation (equation 10.20) using the connection moment from the M-ϕ curves (18 kNm in beams 1 to 3 and 42 kNm in beams 4 to 6) as described in section 10.5.2. Column 3 shows a ratio of the analytical results to the predictions using the new approach. It is noted that the ratios are all greater than unity. It suggests that the proposed method is conservative to predict the strength of beams.

Finally, the predicted ultimate capacity of columns are compared with the analytical results as recorded in Table 10.33. Column (1) are the results determined from the BS 5950 method with the moment applied at the column face plus 100 mm eccentricity as noted in cl.4.8.3.3.1. The results in column (2) are the ultimate capacity of a pin ended column under its axial load only. Column (3) is the results using the α_β approach but with the consideration of the applied moment due to beam reaction at an eccentricity of the column face plus 100 mm. The ultimate capacities shown in Column (4) are used the α_β approach under axial load only. The results determined from the computer program SERFA are illustrated in column (5). It is noted that the analytical results give a highest ultimate capacity for all columns which indicates that all the predictions using methods (1) to (4) are all conservative. It is noted in Table 10.33 that the α_{pin} approach predicts a higher ultimate capacity for the edge columns (columns 3 and 9) whilst a lower value for the central column than the BS 5950 method. The new approach with consideration of the moment effect, method (3), are observed better than the BS 5950 method. The most important feature which needs to be highlighted here is that the α_β approach with its axial load only predicts a highest ultimate capacity for all three columns than methods (1) to (3) and the results are all lower than the analytical results computed from SERFA. This suggests that the new

approach seems to be the best considering the fact that it provides an economical but still conservative enough for modern non-sway column design.

10.8 Concluding Remarks

In this chapter, the existing simplified analytical models to predict the M-ϕ characteristics proposed by EC 3 and by Liew and Chen have been investigated. The EC 3 method is found to be reasonable and conservative but is quite complex and difficult to follow. The Liew and Chen method is easier to use but the prediction is unreliable and moreover may produce non-conservative estimates of joint response. The database contains the actual test results and thus provides more reliable M-ϕ curves for semi-rigid design.

A complete set of semi-rigid design methods for beams and columns in non-sway frames with laterally restrained beams has been developed and a good agreement is obtained with experimental results. All the new approaches are found to be suitable for adoption in a design office and can be used directly to design a frame for desk calculation. Methods are proposed to predict the mid-span deflection of beams in the serviceability condition and also their ultimate capacity. All the predictions are shown to be conservative.

More importantly, a new method for the design of column in non-sway frames, the α_β approach, is proposed and validated using more than 50 test or analytical results. The new approach is found to be more economical than the existing approaches but is still essentially conservative. Moreover, it only needs slightly more calculation than the α_{pin} approach and is thus easy to use.

One of the most important features is that significant variation of the M-ϕ response has been shown to have a negligible effect on the predicted mid-span deflection of beams and ultimate capacity of columns using the new proposed method. This implies that the precise form of the M-ϕ responses are not important.

The final part of this chapter demonstrates how to link the proposed methods to form a complete semi-rigid design method for non-sway planar frame design. An example based on an existing frame (frame 5) is investigated and the frame is checked using the proposed semi-rigid method and a validated computer program. Examination of the results has shown that the new semi-rigid design methods provide more than 10 % saving depending on the weight of steel for the beams when compared with the existing design method. For

the non-sway column design, the new approach should be capable of saving on the weight of steel, as it can provide more than 10 % higher ultimate capacity than the BS 5950 method.

It is believed that semi-rigid design has considerable potential. However, these results are only based on a limited study. Further work is recommended to validate the proposed design methods. For the α_β approach, two extreme base conditions, i.e. fully rigid and truly pinned, have been considered when calculating the ultimate load of columns. However, as discussed in chapter 9, realistic column bases are semi-rigid and it is recommended that this is taken into account when using the new approach. For laterally restrained beam design, a further study could concentrate on investigating the range of λ values (defined as ratios of the capacity of connections to the plastic moment of beams) for the different sections of beams and columns and types of connections to provide a good initial estimation of these values in the early design stage. The secant stiffnesses, i.e. C_5 and C_{10}, have been adopted by the author to determine the beam deflection in the serviceability condition. The ultimate capacity of columns has been accomplished using C_{10}. It is thus suggested that further work should be undertaken concerning a simple method of obtaining these secant stiffnesses for different conditions which make the semi-rigid design method more attractive to engineers in the near future.

References

[10.1] British Standards Institution BS 5950: Part 1: Structural Use of Steelwork in Building. BSI, London, British Standards Institution 1985.

[10.2] British Standard BS 449, 'The Use of Structural Steel in Buildings', the British Standards Institution, London, 1932.

[10.3] PD3343, 'Recommendations for Design', Supplement No.1 to BS 449, British Standards Institution, London, 1971.

[10.4] Eurocode 3 - ENV 1993-1-1 : Design of Steel Structures Part 1.1 : General Rules and Rules for Building (together with United Kingdom National Application Document', European Committee for Standardization, 1992.

[10.5] Barakat, M, and Chen, W. F., 'Practical Analysis of Semi-Rigid Frames', Engineering Journal, AISC, Second Quarter, 1990, pp. 55-68.

[10.6] Dol, C. and Steenhuis, C. M., 'Use of the Dutch Steel Codes in the Design Process of a Steel Structure (in Dutch), Bouwen Met Staal, November 1991, Staalbouwkundly Genootschap, Rotterdam.

[10.7] Lau, S. M., Davison, J. B. and Kirby, P. A., 'Joint Behaviour in Frame Tests: Comparison Actual Response with that predicted by EC 3', in press.

[10.8] Jaspart, J. P. and Maquoi, R., 'Survey of Existing Types of Joint Modelling', Proceedings of the First State of the Art Workshop, Cost C1, 1992, pp. 370-381.

[10.9] Ho, W. M. and Chan, S. L., 'An Accurate and Efficient Method for Large Deflection Inelastic Analysis of Frames with Semi-Rigid Connections', Journal of Constructional Steel Research, Vol. 26, Nos. 2 and 3, 1993, pp. 171-191.

[10.10] Kishi, N. and Chen, W. F., 'Moment-Rotation Relation of Semi-Rigid Connections with Angles', Journal of Structural Engineering, ASCE, Vol. 16, No. 7, July, 1990, pp. 1813-1834.

[10.11] Liew, J. Y. R. and Chen, W. F., 'Limit States Design of Semi-Rigid Frames using Advanced Analysis : Part 1 : Connection Modelling and Classification', Journal of Constructional Steel Research, Vol. 25, No.4, 1993, pp. 1-27.

[10.12] Nethercot, D. A. and Zandonini, R., 'Methods of Prediction of Joint Behaviour Beam-to-Column Connections, 'Chapter of a Volume in the 'Stability and Strength', Series published by Elsevier.

[10.13] Bursi, O., 'Behaviour and Modelling of Semi-Rigid Beam-to-Column Steel Joints', Sprint Contract RA351, University of Trento (I), University of Liege (6), CRIF(B), CTICM(I), ENSAIS Strasbourg (F), LABEIN (E).

[10.14] Moore, D., 'The Design of End-Plate Connection', R. H. Wood Memorial Conference, Garston, Watford, 1988, pp. 75-107.

[10.15] Weller, A. D., 'An Introduction to EC 3', Journal of the Institution of Structural Engineers, The Structural Engineer, Vol. 71, No. 18, September, 1993, pp. 326-331.

[10.16] Jaspart, J. P., 'Etude de la semi-rigidite des noeuds poutre-colonne et son influence sur la resistance et la stabilite des ossatures en acier', Doctoral Thesis, Liege, 1991.

[10.17] Steenhuis, C. M. and Bijlaard, F. S. K., 'Example Calculation of Mechanical Properties of Beam-Column Connection According to Eurocode 3, TNO-Report, B-91-0405, 1991.

[10.18] Lennon, T., 'Assessment of Annex J', Note N4/93, Building Research Establishment, January, 1993.

[10.19] Wald, F. and Steenhuis, M., 'The Beam-to-Column Bolted Joint Stiffness according Eurocode 3', Proceedings of the First State of the Art Workshop, Cost C1, 1992, pp. 505-516.

[10.20] Jaspart, J. P., 'Theoretical Prediction of the Joint Response for Different Connection Types', Internal Report, University of Liege.

[10.21] Kishi, N., Chen, W. F. and Nimachi, S. G., 'Moment-Rotation Relation of Top- and Seat-Angle Connections', Proceedings of the Workshop on Connections and the Behaviour, Strength and Design of Steel Structures, Cachan, France, May 25-27, Elsevier, London, 1988, pp. 121-134.

[10.22] Drucker, D. C., 'The Effect of Shear on the Plastic Bending of Beams', Journal of Appl. Mech., ASME, 23(4) (1956) pp. 509-514.

[10.23] Hechtman, R. A. and Johnson, B. G., 'Riveted Semi-Rigid Beam-to-Column Building Connections, Progress Report No. 1, AISC Research at Lehigh University, Bethlehem, PA, 1947.

[10.24] Altman, W. G., Azizinamini, A., Bradburn, J. H. and Radziminiski, J. B., 'Moment-Rotation Characteristics of Semi-Rigid Steel Beam-to-Column Connections', Department of Civil Engineering, University of South Carolina, Columbia, SC, 1982.

[10.25] Azizinamini, A, Bradburn, J. H. and Radziminiski, J. B., 'Static and Cyclic Behaviour of Semi-Rigid Steel Beam-Column Connections', Structural Research Studies, Department of South Carolina, Columbia, SC, 1985.

[10.26] Bjorhovde, R., Brozzetti, J. and Colson, A., A Classification System for Beam to Column Connection', Journal of Structural Engineering, ASCE, 116(11) (1990) pp. 3059-3076.

[10.27] Gibbons, C., ' The Strength of Biaxially Loaded Beam Columns in Flexibly Connected Steel Frames', Ph.D. Thesis, University of Sheffield, England, December, 1990.

[10.28] Nethercot, D. A., 'Joint Action and the Design of Steel Frames', Journal of the Institution of Structural Engineers', Vol. 32A, No.12, December, 1985, pp. 371-379.

[10.29] Gerstle, K. H., 'Effect of Connection on Frame', Journal of Constructional Steel Research, Vol.10, 1988, pp. 241-267.

[10.30] Lau, S. M., 'A Study of Results from a Full Scale Frame Test', M.Sc.(Eng.) Dissertation, University of Sheffield, September 1990.

[10.31] Bjorhovde, R., 'Effect of End Restraint on Column Strength Practical Application', ATSC, Engineering Journal, Vol.20, No.1, 1st Quarter, 1984, pp. 1-13.

[10.32] Lau, S. M., 'Full Scale Frame Tests with Semi-Rigid Connections', Progress Report no.3, Department of Civil and Structural Engineering, University of Sheffield.

[10.33] Ahmed, I., 'Semi-Rigid Action of Steel Frames', Ph.D. Thesis, University of Sheffield, England, September, 1992.

[10.34] Azizinamini, A., Bradburn, J. H. and Radziminski, J. B., 'Initial Stiffness of Semi-Rigid Beam-to-Column Connections', Journal of Research Steel Research,' No.8, 1987, pp. 71-90.

[10.35] Jones, S. W., Kirby, P. A. and Nethercot, D. A., 'Effect of Semi-Rigid Connections on Steel Column Strength', Journal of Constructional Steel Research, No.1, September, 1980, pp. 38-46

[10.36] Lothers, J. E., 'Elastic End Restraint Equations of Semi-Rigid Connections', Trans. Am. Soc. Civil Engineering, No.116, 1951, pp. 480-502

[10.37] Baraket, M. and Chen W. F.,' Practical Analysis of Semi-Rigid Frames', AISC, Engineering Journal, 2nd Quarter, 1990, pp. 54-68

[10.38] Moore, D. A. and Nethercot, D. A., 'Testing Steel Frames at Full Scale', Appraisal of Results and Implication for Design', Journal of Institution of Structural Engineers, Vol.71, Nos. 23 & 24, December, 1993, pp. 428-435.

[10.39] Prescott, A. T., 'The Performance of End-Plate Connections in Steel Structures and their Influence on Overall Structural Behaviour', Ph.D. Thesis, Hatfield Polytechnic, July, 1987.

[10.40] Joint Committee of Institution of Structural Engineers and Welding Institute, 'Fully-Rigid Multi-Storey Welded Steel Frames', First Report 1964, Second Report 1971.

[10.41] Davison, J. B., 'Strength of Beam-Columns in Flexibly Connected Steel Frames' Ph.D. Thesis, University of Sheffield, June, 1987.

[10.42] Chakrabarti, B., 'Tests of Unstiffened End-Plate Beam-Column Connection', Building Research Establishment, Report No. N123/87.

[10.43] Anderson, D., Colson, A. and Jaspart, J. P., 'Connections and Frame Design for Economy', New Steel Construction, October, 1993, pp. 30-33.

[10.44] Nethercot, D. A., 'Frame Analysis and the Link between Connection Behaviour and Frame Performance', R. H. Wood Memorial Conference, Garston, Watford, 1988, pp. 57-74.

[10.45] Liew, J. Y. R., White, D. W. and Chen, W. F., 'Beam-Column Design in Steel Frameworks-Insights on Current Methods and Trends', Journal of Constructional Steel Research, Vol.18, 1991, pp 269-308.

[10.46] Kirby, P. A., Bitar, S. S. and Gibbons, C., 'Design of Columns in Non-Sway Semi-Rigidly Connected Frames', Constructional Steel Design, World Developments, Elsevier Applied Science, 1992, pp. 54-63.

[10.47] Baker, J. F., 'A Note on the Effective Length of a Pillar forming part of a continuous Member in a Building Frame', Second part of the Report, Steel Structures Research Committee, DSIR; HMSO, 1934.

[10.48] Chen, W. F., 'End Restraint and Column Stability', Journal of Steel Structural Division, ASCE, Vol.106, No.ST11, Proc. Paper 15796, November, 1980, pp. 29-73.

[10.49] Wood, R. H., 'Effective Length of Columns in Multi-Storey Buildings, Part 1, Effective Lengths of Single Columns and Allowances for Continuity', Journal of the Institution of Structural Engineers, Vol. 52, July, 1974, pp. 235-240.

[10.50] Carr, J. F., 'A 'Simplified Approach' to the Design of Semi-Rigidly connected Columns in Multi-Storey Non-Sway Steel Framed Buildings', MPhil. Thesis, University of Sheffield, May, 1993.

[10.51] Celikag, M., 'Moment-Rotation Behaviour of Steel Beam-to-Column Connections', Ph.D. Thesis, 'Department of Civil and Structural Engineering, University of Sheffield, U.K., February, 1990.

[10.52] Kim, Y. W., 'The Behaviour of Beam to Column Web Connections with Flush End-Plates', M.Sc. Thesis, University of Warwick, 1988.

Type	Author	Year	Method
1	Sommer	1969	Polynomial
	Kennedy	1969	Polynomial
	Frye and Morris	1975	Polynomial
	Jones *et. al*	1981	Cubic B-Spline
	Jaspart	1985	Beziers.
	Richard *et. al*	1980	Richard Formula
	Ang and Morris	1984	Ramberg-Osgood
	Lui and Chen	1986	Exponential
	Krishnamurthy *et. al*	1979	Power
	Murray *et. al*	1987	Power
	Ho and Chan	1993	Power
2	Lothers	1951	Double Web Cleats
	Johnson and Law	1981	Flush End Plate
	Yee and Melchers	1986	End Plate
	Chen *et. al*	1987/88	Flange and/or Web Cleats
	Kishi and Chen	1990	Flange and/or Web Cleats
	Jaspart	1991	Welded End Plate and Flange Cleat
	Liew and Chen	1993	Flange and/or Web Cleats
	EC3 (Annex J)	1993	End Plate and Welded Joints
3	Wales and Rossow	1983	Double Web Cleats
	Kennedy and Hafez	1984	Header Plate
	Richard *et. al*	1987	Cleated Connections
	Tschemmernegg *et. al*	1988	Fully Welded and End-Plate
	Jaspart	1990	Composite Connection with End Plate and Cleated Connections - also applicable to similar steel connections
4	Bose *et. al*	1972	Welded Connections
	Lipson and Hague	1978	Single angle Bolted-Welded Connections
	Richard *et. al*	1980	Single Web Plate
	Krishnamurty	1980	End Plate Connection
	Richard *et. al*	1983	Double Web Cleats
	Patel and Chen	1984	Welded Connections
	Patel and Chen	1985	Fully Bolted Connections
	Murray *et. al*	1987	Flush End Plate
	Atamaz Sibai *et. al*	1988	Weld Connections

Remarks: Type 1 - Curve fitting

Type 2 - Simplified analytical models

Type 3 - Mechanical models

Type 4 - Finite element analysis

Table 10.1 : Current Practice for the Moment Rotation Models

Frame	Joint	Type	Side	t_p (mm)	Force Resistance (kN)				Ultimate Moment (kNm)	Rotation Capacity (mrad)
					(1)	(2)	(3)	(4)		
1 and 2	A	F	E	12	326	919	550	362	54.9	32.0
	E	F	E	15	406	919	550	362	65.2	Sufficient
	C	F	E	20	461	919	550	362	63.4	Sufficient
	B D F	F	I	20	461	919	550	362	76.5	22.0
	H	E	E	20	469	1016	550	362	89.8	Sufficient
	G	E	I	20	469	1016	550	362	110.0	10.6
	J L	E	E	25	481	1016	577	362	98.6	Sufficient
	I K	E	I	25	481	1016	577	362	121.0	10.6
5	A C E	F	E	12	208	511	277	210	32.4	Sufficient
	B D F	F	I	12	208	511	277	210	32.4	34.3
	H J L	E	E	15	221	615	248	210	51.1	Sufficient
	G I K	E	I	15	221	615	248	210	53.2	32.0

Remarks: Type : F = Flush End Plate, E = Extended End Plate
Side : E = External Joint, I = Internal Joint
t_p = thickness of end plate
(1) Resistance of all the bolt-rows in the tension zone
(2) Resistance of the column web in the tension zone
(3) Resistance of the column web in the compression zone
(4) Resistance of the column web in the shear zone

Table 10.2 : Ultimate Capacities predicted by EC3

Frame	Joint	Initial Stage			Ultimate Moment Stage		
		Stiffness C_i (kNm/rad)	Moment $M_{Rd/1.5}$ (kNm)	Rotation $\phi_{Rd/1.5}$ (mrad)	Stiffness C_{Rd} (kNm/rad)	Moment M_{Rd} (kNm)	Rotation ϕ_{Rd} (mrad)
1 and 2	A	5260	36.8	6.0	2720	54.9	20.0
	E	6420	43.7	6.8	3760	65.2	17.0
	C	9540	42.5	2.9	6420	63.4	9.9
	B D F	14600	51.3	3.5	7140	76.5	11.0
	H	26100	60.2	2.3	17200	89.8	5.2
	G	42200	73.7	1.7	20900	110.0	5.3
	J L	26200	66.1	4.6	18100	98.6	6.7
	I K	40900	81.1	3.0	19700	121.0	6.2
5	A C E	2880	21.7	7.5	1700	32.4	19.1
	B D F	3160	21.7	6.8	1930	32.4	16.8
	H J L	9880	34.2	3.5	5370	51.1	9.5
	G I K	11600	35.6	3.0	6570	53.3	8.1

Table 10.3 : Moment, Rotation and Stiffness predicted by EC 3 for Frames 1, 2 and 5

Frame	Joint	Ultimate Moment (kNm)			Initial Stiffness (kNm/rad)		
		Frame	Joint	EC3	Frame	Joint	EC3
1	A	-	76.0	54.9	-	77500	5260
	B	74.0	105.0	76.5	24100	62500	14600
	C	42.0	105.0	63.4	6000	62500	9540
	D	51.0	105.0	76.5	9900	62500	14600
	E	37.5	85.0	65.2	9500	125000	6420
	F	62.0	105.0	76.5	9600	62500	14600
	G	125.0	172.0	110.0	25100	48000	42200
	H	-	172.0	89.8	-	48000	26100
	I	143.0	160.0	121.0	41700	65000	40900
	J	143.0	160.0	98.6	76500	65000	26200
	K	143.0	160.0	121.0	42600	65000	40900
	L	143.0	160.0	98.6	33000	65000	26200
2	A	16.0	76.0	54.9	10900	19500	5260
	B	-	95.0	76.5	-	90000	14600
	C	34.0	95.0	63.4	12000	90000	9540
	D	56.0	95.0	76.5	9330	90000	14600
	E	46.0	85.0	65.2	75000	117000	6420
	F	68.0	95.0	76.5	15100	90000	14600
	G	-	160.0	110.0	-	57100	42200
	H	90.0	160.0	89.8	-	57100	26100
	I	143.0	160.0	121.0	32600	39100	40900
	J	143.0	160.0	98.6	45000	39100	26200
	K	143.0	160.0	121.0	53200	39100	40900
	L	143.0	160.0	98.6	26500	39100	26200
5	A	22.0	55.0	32.4	3600	6700	2880
	B	31.0	55.0	32.4	4420	6700	3160
	C	21.0	55.0	32.4	2220	6700	2880
	D	31.0	55.0	32.4	4190	6700	3160
	E	31.0	55.0	32.4	3170	6700	2880
	F	28.0	55.0	32.4	3870	6700	3160
	G	64.0	90.0	53.2	26700	11600	11600
	H	57.0	90.0	51.5	6670	11600	9880
	I	58.0	90.0	53.2	9520	11600	11600
	J	-	90.0	51.5	-	11600	9880
	K	61.0	90.0	53.2	9090	11600	11600
	L	65.0	90.0	51.5	6060	11600	9880

Table 10.4 : Comparisons of EC 3 Predictions to the Frame and Joint Test Results in Frames 1, 2 and 5

Frame	Type	Initial Stiffness (kNm/rad)			Ultimate Moment (kNm)		
		Test (1)	Prediction (2)	(2)/(1)	Test (3)	Prediction (4)	(4)/(3)
3	Frame	4160	47700	11.5	16	34	2.1
	Joint	5710	47700	8.3	18	34	1.9

Table 10.5 : Compared the predicted Initial Stiffness and Ultimate Moment to the Joint and Frame Test Results used Liew & Chen Model for Frame 3

	Stiffness (kNm/rad)							
	Frame Test					Joint Test		
	C_i	C_m	C_5/ C'_5	C_{10}/ C'_{10}	C_c	C_i	C_5	C_{10}
A	-	-	3760	1880	-	77500	9700	5800
B	24100	24100	9200	4600	16000	62500	12400	8300
C	4100	6000	5900	3300	-	62500	12400	8300
D	9900	9900	9800	5100	10600	62500	12400	8300
E	9500	9500	5200	2600	8770	125000	10300	6900
F	5200	9600	6600	5300	6670	62500	12400	8300
G	8200	25100	17800	9400	17000	48000	18000	13800
H	-	-	-	8300	-	48000	18000	13800
I	35300	41700	33800	16900	36800	65000	23000	16000
J	28900	76500	32800	16400	48510	65000	23000	16000
K	42600	42600	32000	16000	42600	65000	23000	16000
L	33000	33000	25200	12600	30000	65000	23000	16000

Table 10.6 : Stiffness from the Frame and Joint Tests in Frame 1

	Stiffness (kNm/rad)							
	Frame Test					Joint Test		
	C_i	C_m	C_5/ C_5'	C_{10}/ C_{10}'	C_c	C_i	C_5	C_{10}
A	10900	10900	3200	1600	10800	19500	10000	6200
B	-	-	-	-	-	90000	14400	8300
C	7000	12000	6800	3400	10300	90000	14400	8300
D	9300	9300	9000	5600	9300	90000	14400	8300
E	57500	57500	9200	4600	32000	117000	12700	7500
F	15100	15100	13400	6800	15100	90000	14400	8300
G	-	-	-	-	-	57100	25100	14600
H	71700	71700	18000	9000	62100	57100	25100	14600
I	25400	32600	27400	14400	26500	39100	25000	15600
J	45000	45000	28600	14300	35500	39100	25000	15600
K	53200	53200	28600	14300	45400	39100	25000	15600
L	26500	26500	25600	14300	23800	39100	25000	15600

Table 10.7: Stiffness from the Frame and Joint Tests in Frame 2

	Stiffness (kNm/rad)							
	Frame Test					Joint Test		
	C_i	C_m	C_5	C_{10}	C_c	C_i	C_5	C_{10}
C	6670	6670	2800	1720	3800	5710	1900	1200
D	-	-	-	-	-	5710	1900	1200
E	5030	5030	2000	1300	2970	5710	1900	1200
F	4210	4210	1320	960	4240	5710	1900	1200
G	1070	1070	1070	920	720	5710	1900	1200
H	6670	6670	2320	1520	5000	5710	1900	1200
I	3810	3810	1600	1000	2470	5710	1900	1200
J	-	-	-	-	-	5710	1900	1200
K	5000	5000	2000	1080	2560	5710	1900	1200
L	5330	5330	1920	1220	2600	5710	1900	1200

Table 10.8: Stiffness from the Frame and Joint Tests in Frame 3

	Stiffness (kNm/rad)							
	Frame Test					Joint Test		
	C_i	C_m	C_5	C_{10}	C_c	C_i	C_5	C_{10}
A	2330	2350	1900	1300	1870	10700	2480	1360
B	8700	8700	2600	1750	3900	10700	2480	1360
C	2670	2670	1760	1200	1630	10700	2480	1360
D	6060	6060	2360	1450	3860	10700	2480	1360
E	2410	2410	1900	1400	1740	10700	2480	1360
F	11100	11100	2100	1370	4250	10700	2480	1360
G	5710	5710	2000	1400	2380	10700	2480	1360
H	3510	3510	2200	1250	2650	10700	2480	1360
I	8330	8330	2300	1350	6670	10700	2480	1360
J	1280	1280	1200	1070	-	10700	2480	1360
K	9090	9090	2900	1850	4330	10700	2480	1360
L	2990	2990	1800	1050	1800	10700	2480	1360

Table 10.9 : Stiffness from the Frame and Joint Tests in Frame 4

	Stiffness (kNm/rad)							
	Frame Test					Joint Test		
	C_i	C_m	C_5	C_{10}	C_c	C_i	C_5	C_{10}
A	3330	3600	3200	2150	2830	6700	5000	3500
B	2990	4420	3600	2300	3180	6700	5000	3500
C	2230	2220	2220	1800	1900	6700	5000	3500
D	2000	4190	3000	2700	2840	6700	5000	3500
E	630	3170	-	-	-	6700	5000	3500
F	2270	3870	3000	2500	2670	6700	5000	3500
G	26700	26700	8200	5900	10500	11600	8000	5800
H	6670	6670	5600	4250	4700	11600	8000	5800
I	9520	9520	7600	4900	6150	11600	8000	5800
J	-	-	-	-	-	11600	8000	5800
K	9090	9090	8200	5150	6770	11600	8000	5800
L	6060	6060	-	-	-	11600	8000	5800

Table 10.10: Stiffness from the Frame and Joint Tests in Frame 5

Frame	Beam	Dimensionless Factor α							
		Methods							
		Frame Test					Joint Test		
		(1)	(2)	(3)	(4)	(5)	(1)	(2)	(3)
1	1	0.68	0.47	0.31	0.58	0.67	0.90	0.62	0.51
	2	0.52	0.52	0.37	0.54	0.53	0.90	0.64	0.49
	3	0.58	0.46	0.35	0.53	0.51	0.91	0.62	0.53
	4	0.85	0.80	0.69	0.79	0.80	0.93	0.82	0.78
	5	0.92	0.88	0.80	0.91	0.80	0.94	0.85	0.79
	6	0.90	0.88	0.78	0.90	0.88	0.94	0.85	0.80
2	1	0.75	0.47	0.31	0.75	0.63	0.86	0.64	0.52
	2	0.59	0.52	0.38	0.57	0.58	0.93	0.66	0.53
	3	0.75	0.61	0.45	0.73	0.78	0.93	0.66	0.53
	4	0.95	0.84	0.72	0.95	0.98	0.94	0.87	0.79
	5	0.90	0.87	0.77	0.88	0.88	0.90	0.86	0.79
	6	0.90	0.87	0.78	0.89	0.90	0.91	0.86	0.79
3	2	0.84	0.69	0.58	0.75	0.73	0.76	0.52	0.41
	3	0.68	0.44	0.35	0.63	0.33	0.73	0.47	0.37
	4	0.65	0.55	0.48	0.58	0.51	0.82	0.59	0.48
	5	0.53	0.32	0.23	0.42	0.47	0.70	0.44	0.33
	6	0.72	0.50	0.37	0.56	0.32	0.74	0.49	0.38
4	1	0.77	0.61	0.53	0.66	0.48	0.87	0.63	0.50
	2	0.71	0.55	0.44	0.60	0.42	0.86	0.59	0.45
	3	0.76	0.55	0.47	0.63	0.40	0.85	0.59	0.47
	4	0.76	0.60	0.51	0.63	0.37	0.86	0.64	0.51
	5	0.63	0.46	0.39	0.43	0.41	0.83	0.56	0.43
	6	0.77	0.59	0.48	0.64	0.41	0.85	0.60	0.47
5	1	0.54	0.50	0.40	0.47	0.29	0.66	0.59	0.51
	2	0.43	0.39	0.35	0.36	0.22	0.62	0.55	0.46
	3	0.48	0.36	0.32	0.33	0.17	0.63	0.56	0.47
	4	0.83	0.71	0.65	0.72	0.54	0.80	0.74	0.68
	5	0.72	0.67	0.57	0.62	0.51	0.79	0.72	0.65
	6	0.71	0.67	0.56	0.63	0.54	0.79	0.73	0.65

where $\alpha = \frac{M_{SR}}{M_R}$

method (1) : used secant stiffness of C_i or C_m

method (2) : used secant stiffness of C_5 or C_5'

method (3) : used secant stiffness of C_{10} or C_{10}'

method (4) : used secant stiffness of C_c

method (5) : used rigidity factor of R

Table 10.11: Dimensionless Factors determined from Five Frame Tests

Frame	Beam	Connection	Mid-Span Deflection (mm)							
			Test Result	Rigid Frame	Pinned Beam	Methods				
						(1)	(2)	(3)	(4)	(5)
1	1	FEP	1.68	1.80	5.30	2.92	3.66	4.22	3.27	2.96
	2	"	2.71	2.10	7.00	4.45	4.45	5.19	4.35	4.40
	3	"	2.94	1.50	6.80	3.73	4.36	4.95	3.99	4.10
	4	EEP	13.40	11.10	35.30	14.80	15.90	18.60	16.20	15.90
	5	"	14.00	11.30	45.80	14.00	15.40	18.20	14.40	18.20
	6	"	14.80	12.00	45.90.	15.40	16.10	19.50	15.40	16.07
2	1	FEP	1.50	1.90	5.40	2.78	3.76	4.32	2.78	3.20
	2	"	2.50	1.40	6.90	3.66	4.04	4.81	3.77	3.71
	3	"	2.10	1.30	6.80	2.68	3.45	4.33	2.79	2.51
	4	EEP	16.20	14.90	43.80	16.40	19.50	23.00	16.40	15.50
	5	"	18.50	16.30	58.80	20.60	21.80	26.10	21.40	21.40
	6	"	19.20	16.30	55.70	20.20	21.40	25.00	20.60	20.20
3	2	FC	14.30	9.80	22.90	11.90	13.90	15.30	13.10	13.30
	3	"	15.50	6.30	22.70	11.60	15.50	17.00	12.40	17.30
	4	"	15.30	14.60	23.10	17.60	18.40	19.00	18.20	18.70
	5	"	8.30	3.30	15.80	9.19	11.80	13.00	10.60	10.00
	6	"	14.90	7.70	23.60	12.20	15.70	17.70	14.70	18.50
4	1	FC	15.00	10.70	23.90	13.70	15.80	16.90	15.20	17.60
	2	"	15.50	10.40	22.90	14.00	16.00	17.40	15.40	17.70
	3	"	16.40	8.30	22.90	11.80	14.90	16.10	13.70	17.10
	4	"	17.50	10.20	23.00	13.30	15.30	16.50	14.90	18.30
	5	"	10.00	5.30	15.90	9.20	11.00	11.80	11.30	11.50
	6	"	15.60	8.90	23.40	12.20	14.80	16.40	14.10	17.50
5	1	FEP	9.20	5.30	16.70	10.00	11.30	12.20	11.40	13.40
	2	"	9.60	5.70	15.90	11.50	11.90	12.30	12.20	13.70
	3	"	9.30	5.40	15.90	10.80	12.10	12.50	12.40	14.10
	4	EEP	10.30	7.70	21.10	10.00	11.60	12.40	11.50	13.90
	5	"	8.70	6.30	20.30	10.10	10.80	12.30	11.50	13.10
	6	"	11.00	6.00	20.50	10.20	10.80	12.40	11.40	12.70

Remarks: method (1) - used secant stiffness of C_i or C_m

method (2) - used secant stiffness of C_5 or C_5'

method (3) - used secant stiffness of C_{10} or C_{10}'

method (4) - used secant stiffness of C_c

method (5) - used rigid factor of R

FEP - Flush End-Plate, EEP - Extended End-Plate, FC - Flange Cleats

Table 10.12 : Comparison with Mid-Span Deflection to predict Results from different Methods using Frame M-ϕ Curves

Frame	Beam	Connection	Mid-Span Deflection (mm)					
			Test	Rigid	Pinned	Methods		
			Result	Frame	Beam	(1)	(2)	(3)
1	1	FEP	1.68	1.80	5.30	2.15	3.13	3.52
	2	"	2.71	2.10	7.00	2.59	3.86	4.60
	3	"	2.94	1.50	6.80	1.98	3.51	3.99
	4	EEP	13.40	11.10	35.30	12.80	15.50	16.40
	5	"	14.00	11.30	45.80	13.40	16.50	18.60
	6	"	14.80	12.00	45.90	14.00	17.10	18.80
2	1	FEP	1.50	1.90	5.40	2.39	3.16	3.58
	2	"	2.50	1.40	6.90	1.79	3.27	3.99
	3	"	2.10	1.30	6.80	1.69	3.17	3.89
	4	EEP	16.20	14.90	43.80	16.60	18.70	21.00
	5	"	18.50	16.30	58.80	20.60	22.30	25.20
	6	"	19.20	16.30	55.70	19.90	21.80	24.60
3	2	FC	14.30	9.80	22.90	12.90	15.90	17.50
	3	"	15.50	6.30	22.70	10.70	15.00	16.60
	4	"	15.30	14.60	23.10	16.10	18.10	19.00
	5	"	8.30	3.30	15.80	7.06	10.30	11.70
	6	"	14.90	7.70	23.60	11.80	15.80	17.60
4	1	FC	15.00	10.70	23.90	12.40	15.60	17.30
	2	"	15.50	10.40	22.90	12.20	15.50	17.30
	3	"	16.40	8.30	22.90	10.50	14.30	16.10
	4	"	17.50	10.20	23.00	12.00	14.80	16.50
	5	"	10.00	5.30	15.90	7.10	9.96	11.30
	6	"	15.60	8.90	23.40	11.10	14.70	16.60
5	1	FEP	9.20	5.30	16.70	9.19	9.99	10.90
	2	"	9.60	5.70	15.90	9.58	10.30	11.20
	3	"	9.30	5.40	15.90	9.27	10.00	11.00
	4	EEP	10.30	7.70	21.10	10.40	11.20	12.00
	5	"	8.70	6.30	20.26	9.15	10.10	11.10
	6	"	11.00	6.00	20.50	9.05	9.92	11.10

Remarks: method (1) - used secant stiffness of C_i

method (2) - used secant stiffness of C_5

method (3) - used secant stiffness of C_{10}

FEP - Flush End-Plate, EEP - Extended End-Plate, FC - Flange Cleats

Table 10.13 : Comparison with Mid-Span Deflection to predict Results from different Methods using Joint M-ϕ Curves

Frame	Beam	Connection	Average Test Moment (kNm)	λ
1	1-3	Flush End Plate	35	0.22
	4-6	Extended End Plate	121	0.78
2	1-3	Flush End Plate	44	0.28
	4-6	Extended End Plate	130	0.83
3	1-6	Flange Cleat	16	0.22
4	1-6	Flange Cleat	18	0.25
5	1-3	Flush End Plate	26	0.20
	4-6	Extended End Plate	57	0.59

Table 10.14 : Values of λ determined from the Frame Tests

Frame	Beam	Failure Load (kN)		
		Test	Prediction	Simple Plastic Design
2	5	350	312	184
	6	335	309	181
3	3	145	140	114
	4	147	140	115
	5	138	140	114

Table 10.15 : Comparison of the predicted Ultimate Capacity of Beams used the Modified Plastic Hinge Calculation to the Frame Tests

Frame	Beam	Joint	Degree of Rigidity (rad/Nmm x 10^{-10})		Slip Factor		Average Value of Slip Factor	
			γ_w	γ_{10}	β_w	β_{10}	$\beta_{w_{ave.}}$	$\beta_{10_{ave.}}$
3	2	C	2.07	6.94	0.49	1.65	0.49	1.65
		D	-	-	-	-		
	3	E	7.28	7.69	1.73	1.83	2.08	2.13
		F	10.20	10.20	2.42	2.42		
	4	G	11.20	10.90	2.65	2.58	1.54	2.13
		H	1.8	7.04	0.43	1.67		
	5	I	7.77	10.20	1.85	2.42	1.85	2.42
		J	-	-	-	-		
	6	K	9.07	9.17	2.15	2.18	1.99	2.08
		L	7.71	8.33	1.83	1.98		
4	1	A	-	-	-	-	1.26	1.34
		B	5.30	5.65	1.26	1.34		
	2	C	6.30	8.33	1.50	1.98	1.52	1.80
		D	6.43	6.76	1.53	1.61		
	3	E	5.70	7.35	1.36	1.75	1.61	1.75
		F	7.80	7.35	1.86	1.75		
	4	G	7.80	7.14	1.86	1.70	1.40	1.81
		H	3.90	8.06	0.93	1.92		
	5	I	2.80	7.35	0.67	1.75	0.67	1.75
		J	-	-	-	-		
	6	K	4.41	5.56	1.05	1.32	1.72	1.85
		L	10.00	10.00	2.38	2.38		
5	1	A	2.86	4.76	1.32	2.19	1.29	1.89
		B	2.72	3.45	1.25	1.59		
	2	C	5.00	5.56	2.30	2.56	1.87	2.12
		D	3.10	3.64	1.43	1.67		
	3	E	3.23	4.17	1.49	1.92	1.58	1.88
		F	3.64	4.00	1.67	1.84		
	4	G	0.83	1.67	0.29	0.55	0.42	0.66
		H	1.67	2.33	0.55	0.77		
	5	I	1.18	2.04	0.39	0.68	0.39	0.68
		J	-	-	-	-		
	6	K	1.18	1.89	0.39	0.63	0.39	0.63
		L	-	-	-	-		

Remarks: γ_w - Degree of Rigidity in Working Load Condition

γ_{10} - Degree of Rigidity in Secant Stiffness of 0.01 rad

β_w - Slip Factor in Working Load Condition

β_{10} - Slip Factor in Secant Stiffness of 0.01 rad

$\beta_{w_{ave.}}$, $\beta_{10_{ave.}}$ - Average values of β_w , β_{10}

Table 10.16 : Slip Factors β for the Connections in Frames 3, 4 and 5

Method	Description
1	effective length determined from BS 5950 App. E assuming rigid joints
2	new approach base on γ at working load secant stiffness
3	new approach base on γ at secant stiffness of C_{10}
4	nominal assumed effective length of 0.85 L for lowest lift and 1.00 L for other lifts

Case	Description
1	no moment, nominal E and p_y
2	calculated moment from BS 5950, nominal E and p_y
3	measured beam moment, nominal E and p_y
4	measured column head moment, nominal E and p_y, m = 1
5	measured column head moment, nominal E and p_y, m determined from table 18 of BS 5950
6	no moment, test values of E and p_y
7	calculated moment from BS 5950, test values of E and p_y
8	measured beam moment, test values of E and p_y
9	measured column head moment, test values of E and p_y, m determined from Table 18 of BS 5950
10	test result from strain gauges
11	test result from load cells

Remark	Description
( )	α_{pin} factor determined from the out of plane action prevented column

Table 10.17 : Description of Methods and Cases used in Study

Column	Method	$\frac{L_E}{L}$	Type	Predicted Failure Load for Different Cases (kN)										
				1	2	3	4	5	6	7	8	9	10	11
4	1	0.630	Ax	763	609	595	239	518	733	597	585	498	542	529
			Ap	704	550	536	180	459	674	538	526	439	483	464
	2	0.780	Ax	733	585	572	229	498	706	575	564	478		
			Ap	674	526	513	170	439	647	516	505	419		
	3	0.830	Ax	721	575	563	226	490	694	565	554	471		
			Ap	662	516	504	167	431	635	506	495	412		
	4	1.000	Ax	679	542	530	213	461	656	534	523	445		
			Ap	620	483	471	154	402	597	475	464	386		
5	1	0.630	Ax	763	722	748	571	682	733	697	718	655	644	609
			Ap	618	577	603	426	537	588	552	573	510	499	464
	2	0.790	Ax	733	693	718	548	655	703	669	689	629		
			Ap	588	548	573	403	510	558	524	544	484		
	3	0.830	Ax	721	682	707	539	645	694	660	680	621		
			Ap	576	537	562	394	500	549	521	535	476		
	4	1.000	Ax	679	643	666	508	607	656	623	642	586		
			Ap	534	498	521	363	462	511	478	497	441		
6	1	0.660	Ax	757	755	744	733	748	727	725	715	718	789	783
			Ap	494	492	481	470	485	464	462	452	455	526	464
	2	0.760	Ax	739	737	726	715	730	712	710	701	704	(1.16)	(1.15)
			Ap	476	474	463	452	467	449	447	438	441		
	3	0.760	Ax	739	737	726	715	730	712	710	701	704		
			Ap	476	474	463	452	467	449	447	438	441		
	4	0.850	Ax	715	713	703	692	707	691	689	680	683		
			Ap	452	450	440	429	444	428	426	417	420		

Remarks: Ax = Axial Load in Column Segment
Ap = Applied Load at Column Head to cause failure
cases 1 to 11 explained in Table 10.17

Table 10.18 : Comparison with Different Effective Lengths to predict the Failure Load at Columns 4, 5 and 6 in Frame 3

Column	Method	$\frac{L_E}{L}$	Type	Predicted Failure Load for Different Cases (kN)										
				1	2	3	4	5	6	7	8	9	10	11
7	1	0.670	Ax	754	601	724	495	650	727	590	700	627	732	679
			Ap	695	542	665	436	591	668	531	641	568	673	620
	2	0.850	Ax	715	570	687	469	617	691	561	666	596		
			Ap	656	511	628	410	558	632	502	607	537		
	3	0.870	Ax	712	568	684	467	614	685	556	660	590		
			Ap	653	509	625	408	555	626	497	601	531		
	4	1.000	Ax	679	542	652	446	586	653	529	628	563		
			Ap	620	483	593	387	527	594	470	569	504		
8	1	0.710	Ax	748	713	672	676	716	718	687	650	687	782	706
			Ap	662	627	586	590	630	632	601	564	601	696	620
	2	0.900	Ax	706	673	634	638	676	679	650	615	650		
			Ap	620	587	548	552	590	593	564	529	564		
	3	0.910	Ax	703	670	632	636	673	676	647	612	647		
			Ap	617	584	546	550	587	590	561	526	561		
	4	1.000	Ax	679	648	610	614	650	653	624	591	625		
			Ap	593	562	524	528	564	567	538	505	539		
9	1	0.700	Ax	748	670	693	225	533	721	651	671	514	891	766
			Ap	602	524	547	79	387	575	505	525	368	745	620
	2	0.780	Ax	733	657	679	221	523	709	640	660	506	(1.31)	(1.13)
			Ap	587	511	533	75	377	563	494	514	360		
	3	0.780	Ax	733	657	679	221	523	709	640	660	506		
			Ap	587	511	533	75	377	563	494	514	360		
	4	0.850	Ax	715	641	662	215	510	685	619	638	489		
			Ap	569	495	516	69	364	539	473	492	343		

Remarks: Ax = Axial Load in Column Segment
Ap = Applied Load at Column Head to cause failure
cases 1 to 11 explained in Table 10.17

Table 10.19 : Comparison with Different Effective Lengths to predict the Failure Load at Columns 7, 8 and 9 in Frame 3

Column	Method	$\frac{L_E}{L}$	Type	Predicted Failure Load for Different Cases (kN)										
				1	2	3	4	5	6	7	8	9	10	11
1	1	0.570	Ax	623	407	486	69	384	668	436	521	412	520	529
			Ap	562	346	425	8	323	607	375	460	351	459	468
	2	0.700	Ax	548	358	428	60	338	584	381	456	360		
			Ap	487	297	367	-	277	523	320	395	299		
	3	0.710	Ax	542	354	424	60	335	575	376	449	355		
			Ap	481	293	363	-	274	514	315	388	294		
	4	1.000	Ax	385	251	300	42	237	399	261	312	246		
			Ap	324	190	239	-	176	338	200	251	185		
2	1	0.590	Ax	614	511	355	451	544	653	544	377	578	547	587
			Ap	495	392	236	332	425	534	425	258	459	428	468
	2	0.750	Ax	519	432	300	381	459	545	454	315	483		
			Ap	400	313	181	262	340	426	335	196	364		
	3	0.765	Ax	510	424	295	374	451	542	452	313	480		
			Ap	391	305	176	255	332	423	333	194	361		
	4	1.000	Ax	385	320	222	282	341	399	333	231	354		
			Ap	265	201	103	163	222	280	214	112	235		
3	1	0.640	Ax	584	486	418	212	424	632	526	452	459	632	646
			Ap	406	308	240	34	246	454	348	274	281	454	468
	2	0.720	Ax	536	446	384	195	389	572	476	409	415	(1.64)	(1.68)
			Ap	358	268	206	17	211	394	298	231	237		
	3	0.725	Ax	533	444	381	194	389	569	474	407	413		
			Ap	355	266	203	16	211	391	296	229	235		
	4	0.850	Ax	462	384	330	168	335	489	407	349	355		
			Ap	284	206	152	-	157	311	229	111	177		

Remarks: Ax = Axial Load in Column Segment
Ap = Applied Load at Column Head to cause failure
cases 1 to 11 explained in Table 10.17

Table 10.20 : Comparison with Different Effective Lengths to predict the Failure Load at Columns 1, 2 and 3 in Frame 4

Column	Method	$\frac{L_E}{L}$	Type	Predicted Failure Load for Different Cases (kN)										
				1	2	3	4	5	6	7	8	9	10	11
4	1	0.535	Ax	638	631	608	611	617	673	666	642	652	530	524
			Ap	519	512	489	492	498	554	547	523	533	411	404
	2	0.610	Ax	602	595	574	577	583	635	628	606	614		
			Ap	483	476	455	458	464	516	509	487	495		
	3	0.635	Ax	587	581	560	562	568	620	613	591	600		
			Ap	468	462	441	443	449	501	494	472	481		
	4	1.000	Ax	385	380	367	368	372	396	392	378	384		
			Ap	266	261	248	249	253	277	173	259	265		
5	1	0.540	Ax	641	584	626	629	636	679	619	664	674	628	610
			Ap	436	379	421	424	431	474	414	459	469	423	404
	2	0.650	Ax	578	527	565	568	573	611	557	597	606		
			Ap	373	322	360	363	368	406	352	392	401		
	3	0.675	Ax	563	513	550	553	559	593	540	579	588		
			Ap	358	308	345	348	354	388	335	374	383		
	4	1.000	Ax	385	350	376	378	381	396	361	387	393		
			Ap	180	145	171	173	176	191	156	182	188		
6	1	0.620	Ax	596	593	543	469	510	635	632	578	543	804	728
			Ap	273	270	220	146	187	307	309	255	200	481	404
	2	0.675	Ax	563	560	513	443	482	593	590	540	507	(2.09)	(1.89)
			Ap	240	237	190	120	159	265	267	217	184		
	3	0.680	Ax	560	557	510	441	479	590	587	538	504		
			Ap	237	234	187	118	156	262	264	215	181		
	4	0.850	Ax	462	460	421	364	395	483	480	440	413		
			Ap	139	137	98	41	72	155	157	117	90		

Remarks: Ax = Axial Load in Column Segment
Ap = Applied Load at Column Head to cause failure
cases 1 to 11 explained in Table 10.17

Table 10.21 : Comparison with Different Effective Lengths to predict the Failure Load at Columns 4, 5 and 6 in Frame 4

Column	Method	$\frac{L_E}{L}$	Type	Predicted Failure Load for Different Cases (kN)										
				1	2	3	4	5	6	7	8	9	10	11
4	1	0.605	Ax	1232	1208	986	998	1134	1204	1180	963	1108	725	705
			Ap	1022	998	776	788	924	994	970	753	898	510	490
	2	0.710	Ax	1199	1092	959	971	1103	1171	1147	937	1077		
			Ap	989	882	749	761	893	961	937	727	867		
	3	0.740	Ax	1190	1166	952	964	1095	1161	1138	929	1068		
			Ap	980	956	742	754	885	951	928	719	858		
	4	1.000	Ax	1104	1082	884	895	1016	1085	1064	868	999		
			Ap	894	872	674	685	806	875	854	658	789		
5	1	0.635	Ax	1223	1212	1137	1101	1174	1194	1184	1111	1147	944	893
			Ap	820	809	734	698	771	791	781	708	744	541	490
	2	0.760	Ax	1185	1174	1102	1067	1138	1157	1146	1076	1110		
			Ap	782	771	699	664	735	754	743	673	707		
	3	0.790	Ax	1176	1165	1093	1058	1128	1147	1137	1067	1101		
			Ap	773	762	690	655	725	744	734	664	698		
	4	1.000	Ax	1104	1094	1027	994	1060	1085	1076	1009	1042		
			Ap	701	691	624	591	657	682	673	606	639		
6	1	0.660	Ax	1213	1204	1104	1080	1153	1185	1176	1078	1126	1093	1100
			Ap	603	594	494	470	543	575	566	468	516	483	490
	2	0.725	Ax	1194	1185	1087	1063	1135	1166	1157	1061	1108	(1.00)	(1.00)
			Ap	584	575	477	453	525	556	547	451	498		
	3	0.740	Ax	1190	1180	1083	1059	1130	1161	1152	1057	1103		
			Ap	580	570	473	449	520	551	542	447	493		
	4	0.850	Ax	1157	1147	1052	1029	1099	1128	1119	1027	1072		
			Ap	547	537	442	419	489	518	509	417	462		

Remarks: Ax = Axial Load in Column Segment
Ap = Applied Load at Column Head to cause failure
cases 1 to 11 explained in Table 10.17

Table 10.22 : Comparison with Different Effective Lengths to predict the Failure Load at Columns 4, 5 and 6 in Frame 5

Frame	Type	Column	Orientation	Section	Connection	λ using L_0	$\frac{L_E}{L}$
3	I	C6	Major	152 x 152 UC 23	FC	55.30	0.760
	E	C9	Major	152 x 152 UC 23	FC	55.30	0.780
4	E	C3	Minor	152 x 152 UC 23	FC	97.80	0.725
	I	C6	Minor	152 x 152 UC 23	FC	97.80	0.680
5	I	C6	Major	152 x 152 UC 37	FEP & EEP	52.63	0.740

Remarks: FC - Flange Cleats, FEP - Flush End Plate, EEP - Extended End Plate
I - Internal Column, E - External Column
Base Condition - assumed fully fixed

(a) : Effective Length Ratio predicted by α_β approach

Frame	Column	Ultimate Capacity (kN)					
		Prediction			Test Result (4)	Analysis	
		BS 5950 (1)	α_{pin} (2)	α_β (3)		SERFA (5)	SERVAR (6)
3	C6	689	656	712	783	781	762
	C9	619	653	709	766	760	719
4	C3	407	399	569	646	706	-
	C6	480	396	590	728	823	-
5	C6	1119	1085	1161	1100	1252	1240

Remarks: (1) The BS 5950 method is the ultimate compressive load capacity taking into account the effect of applied moment, computed assuming reaction applied column face plus 100 mm eccentricity in accordance with BS 5950 simplified approach in cl.4.8.3.3.1

(2) The α_{pin} value is the ultimate compressive load capacity of a pin ended section with no applied moments, determined in accordance with BS 5950 simplified approach in cl 4.8.3.3.1.

(3) The α_β value is the ultimate compressive load capacity with no applied moment with the effective length ratio predicted using the degree of rigidity γ_{10} and slip factor β_{10}, and calculated accordance with BS 5950 simplified approach in cl 4.8.3.3.1.

(b) : Ultimate Capacity of Columns using Different Methods

Table 10.23 : Comparison of the Ultimate Capacity of Columns for New Design Approach to other Different Methods in Frames 3, 4 and 5

Frame	Type	Column	Section	Connection	λ using L_0	$\frac{L_E}{L}$	Base
F1	E	C5/1-2	152 x 152 UC 23	FEP	97.8	0.635	Second Lift
		C5/0-1	152 x 152 UC 23	FEP	97.8	0.665	Rigid
	C	C6/0-1	152 x 152 UC 23	FEP	97.8	0.705	Rigid
F2	C	C7/0-1	152 x 152 UC 23	FEP	97.8	0.710	Rigid
	E	C8/0-1	152 x 152 UC 23	FEP	97.8	0.710	Rigid

Remarks: FEP - Flush End Plate
E - Edge Column, C - Corner Column

(a) : Effective Length Ratio predicted by α_β approach

Frame	Column	Ultimate Capacity (kN)			
		Prediction			Test Result (4)
		BS 5950 (1)	α_{pin} (2)	α_β (3)	
F1	C5/1-2	294	384	587	662
	C5/0-1	406	384	569	781
	C6/0-1	353	384	545	719
F2	C7/0-1	371	384	542	698
	C8/0-1	380	384	542	776

Remark: methods (1) to (3) are explained in Table 10.23

(b) : Ultimate Capacity of Columns using Different Methods

Table 10.24 : Comparison of the Ultimate Capacity of Columns for New Design Approach to other Different Methods for 3-D Frames F1 and F2

Column Section	Connection	λ using L_0	$\frac{L_E}{L}$	Base
152 x 152 UC 23	FEP	103	0.610	Rigid
152 x 152 UC 23	WAS	103	0.635	Rigid
152 x 152 UC 23	WC	103	0.675	Rigid
152 x 152 UC 23	FEP	103	0.710	Pinned
152 x 152 UC 23	WAS	103	0.740	Pinned
152 x 152 UC 23	WC	103	0.780	Pinned

Remark: FEP - Flush End Plate, WAS - Web and Seat Cleats, WC - Web Cleats

(a) : Effective Length Ratio predicted by α_β approach

Loading Case	Base	Method	Predicted Ultimate Capacity (kN)		
			Connections		
			FEP	WAS	WC
0	Rigid	α_{pin}	358	358	358
		α_β	581	566	539
		Analysis	703	702	686
1	Rigid	α_{pin}	358	358	358
		α_β	581	566	539
		Analysis	702	701	686
2	Rigid	α_{pin}	358	358	358
		α_β	581	566	539
		Analysis	674	678	674
0	Pinned	α_{pin}	358	358	358
		α_β	519	501	477
		Analysis	583	577	537
1	Pinned	α_{pin}	358	358	358
		α_β	519	501	477
		Analysis	583	579	538
2	Pinned	α_{pin}	358	358	358
		α_β	519	501	477
		Analysis	550	555	527

Remarks: Loading Cases (0) - no applied beam load
Loading Cases (1) - Same load applied to both sides of primary beams
Loading Cases (2) - Load applied to one side of primary beam
Methods of α_{pin} and α_β are explained in Table 10.23

(b) : Ultimate Capacity of Columns using Different Methods

Table 10.25 : Comparison of the Ultimate Capacity of Columns for New Design Approach to other Different Methods for the Parametric Study

Frame	Type	Column	Section	Connection	Model	λ using L_0	$\frac{L_E}{L}$	Base
T.C.	I	C5/0-1	356 x 368 UC 153	HP	i	39.6	0.930	Pinned
	E	D6/2-3	305 x 305 UC 118	FEP	i	48.4	0.940	Pinned
					ii		0.960	
	C	DE6/0-1	305 x 305 UC 198	HP	i	46.8	0.940	Pinned
	I	C5/6-7	254 x 254 UC 89	FEP & HP	i	57.5	0.900	Pinned
					ii		0.870	
	E	D6/6-7	254 x 254 UC 89	FEP	i	57.5	0.920	Pinned
					ii		0.910	
	C	DE/6-7	254 x 254 UC 89	HP	i	57.5	0.930	Pinned
					ii		0.940	

Remarks: FEP - Flush End Plate, HP - Header Plate
I - Internal Column, E - Edge Column, C - Corner Column
Models (i) and (ii) are shown in Figure B3

(a) : Effective Length Ratio predicted by α_β approach

Frame	Column	Model	Ultimate Capacity (kN)			
			Prediction			Analytical Result (4)
			BS 5950 (1)	α_{pin} (2)	α_β (3)	
T.C.	C5/0-1	i	5531	5636	5772	5914
	D6/2-3	i	3914	4035	4140	4265
		ii	3914	4035	4110	4362
	DE6/0-1	i	6675	6854	7056	7345
	D5/6-7	i	2702	2782	2975	3134
		ii	2702	2782	3021	3200
	D6/6-7	i	2544	2782	2930	3018
		ii	2544	2782	2953	3155
	DE6/6-7	i	2534	2782	2918	2949
		ii	2534	2782	2907	3127

Remark: Methods (1) to (3) are explained in Table 10.23

(b) : Ultimate Capacity of Columns using Different Methods

Table 10.26 : Comparison of the Ultimate Capacity of Columns for New Design Approach to other Different Methods for Trinity Court in Manchester

Frame	Type	Column	Section	Connection	λ using L_0	$\frac{L_E}{L}$	Base
M.R.I.	I	B3	203 x 203 UC 86	HP	61.5	0.910	Pinned
		C2	203 x 203 UC 86	HP	61.5	0.910	Pinned
		C3	203 x 203 UC 86	HP	61.5	0.920	Pinned
	E	A2/A3	203 x 203 UC 71	HP	61.9	0.910	Pinned
		B2	203 x 203 UC 86	HP	61.5	0.900	Pinned
		B4	203 x 203 UC 71	FEP & HP	61.9	0.880	Pinned
		C1	203 x 203 UC 71	FEP	61.9	0.840	Pinned
		C4	203 x 203 UC 71	HP	61.9	0.910	Pinned
		D1	203 x 203 UC 71	FEP	61.9	0.850	Pinned
		D2	203 x 203 UC 86	HP	61.5	0.920	Pinned
		D3	203 x 203 UC 86	HP	61.5	0.920	Pinned
		D4	203 x 203 UC 71	FEP	61.9	0.900	Pinned
	C	A1/A4	203 x 203 UC 71	FEP	61.9	0.900	Pinned
		E1	203 x 203 UC 71	FEP	61.9	0.900	Pinned
		E4	203 x 203 UC 71	HP	61.9	0.910	Pinned

Remarks: FEP - Flush End Plate, HP - Header Plate
I - Internal Column, E - Edge Column, C - Corner Column
All Analysis are used model (i) and shown in Figure A.2.2

(a) : Effective Length Ratio predicted by α_β approach

Frame	Column	Ultimate Capacity (kN)			
		Prediction			Analytical Result (4)
		BS 5950 (1)	α_{pin} (2)	α_β (3)	
M.R.I.	B3	2365	2574	2750	2904
	C2	2373	2574	2750	2936
	C3	2574	2574	2728	2905
	A2/A3	1867	2122	2259	2301
	B2	2115	2574	2772	2855
	B4	1914	2122	2325	2264
	C1	1802	2122	2369	2449
	C4	1781	2122	2259	2269
	D1	2029	2122	2350	2561
	D2	2538	2574	2728	2857
	D3	2574	2574	2728	2852
	D4	1823	2122	2278	2421
	A1/A4	2012	2122	2278	2260
	E1	2012	2122	2278	2513
	E4	2012	2122	2259	2513

Remark: Methods (1) to (3) are explained in Table 10.23

(b) : Ultimate Capacity of Columns using Different Methods

Table 10.27: Comparison of the Ultimate Capacity of Columns for New Design Approach to other Different Methods for M.R.I. Building in Nottingham

Frame	Column	Section	$\lambda_{L=L_0}$	Variation of C_{10}	Predictions			Results or Analysis (kN)
					β_{10}	$\frac{L_E}{L}$	P_y (kN)	
F1	C5/0-1	152 x 152 UC 23 (FEP)	97.8	+ 20 %	0.90	0.655	575	719
				± 0 %	1.08	0.665	569	
				- 20 %	1.35	0.670	566	
M.R.I.	D2	203 x 203 UC 86 (HP)	61.5	+ 20 %	9.18	0.915	2740	2860
				± 0 %	11.00	0.920	2730	
				- 20 %	13.80	0.925	2720	
T.C.	C5/0-1	356 x 368 UC 153 (HP)	39.6	+ 20 %	5.00	0.920	5790	5910
				± 0 %	6.00	0.930	5770	
				- 20 %	7.50	0.940	5750	

Remark: FEP - Flush End Plate, HP - Header Plate

Table 10.28 : Comparison of the Ultimate Capacity of Columns used the New Design Approach due to the Variation of the C_{10}

Members	Original design	Simple design	New design	Saving	
	(1)	(2)	(3)	(3)/(1)	(3)/(2)
Beams 1 to 3	254 x 146 UB 37	254 x 146 UB 37	254 x 146 UB 31	16 %	16 %
Beams 4 to 6	254 x 102 UB 28	254 x 102 UB 28	254 x 102 UB 25	11%	11 %
Columns 1 to 9	152 x 152 UC 37	152 x 152 UC 23	152 x 152 UC 23	(38) %	-

Remarks: Saving based on the weight of steel
( ) indicates the reduction compared with the original design
In column (2), beams 1 to 3 are designed to a simply supported beam
beams 4 to 6 are designed to a fully rigid beam
columns 1 to 9 are designed to BS 5950 simplified approach

Table 10.29 : Comparison of the Member Sizes of Frame 5 to the Simple Design Frame and the New Semi-Rigid Design Frame

Joint	At the Load Level of Imposed Load			
	M_R (kN)	C_{10} (kNm/rad)	M_{SR} (kN)	α
A	15.50	2150	9.31	0.60
B	51.00	2150	16.00	0.31
C	25.40	2150	12.20	0.48
D	46.40	2150	15.50	0.33
E	21.20	2150	11.10	0.52
F	49.20	2150	15.80	0.32
G	50.70	5100	29.80	0.59
H	17.70	5100	14.20	0.80
I	46.00	5100	28.10	0.61
J	27.90	5100	20.10	0.72
K	48.90	5100	29.10	0.60
L	23.50	5100	17.70	0.75

(a) : Results determined from Linear Elastic Method

Beam	Mid-Span Deflection (mm)			
	(1)	(2)	(3)	(4)
1	7.9	16.4	12.5	10.6
2	6.6	16.4	12.4	9.5
3	6.0	16.4	12.0	9.0
4	9.1	21.4	12.8	11.4
5	7.6	21.4	12.2	9.1
6	7.1	21.4	11.7	9.3

Remarks: (1) Deflection using plane frame analysis program with rigid joints
(2) Deflection determined from simply supported beam
(3) Deflection determined from Linear Elastic Method using equation (10.16)
(4) Deflection computed from computer program SERFA

(b) : Comparison of Deflections using Different Methods

Table 10.30 : Predicted Deflections for New Design Frame used Different Methods

Beam	Joint	Type	Moment of Joint at Design Load (kN)	$\lambda = \frac{M_J}{M_P}$	$\bar{\lambda}$
1	A	FEP	15.5	0.14	0.23
	B	"	35.4	0.32	
2	C	FEP	24.1	0.22	0.25
	D	"	31.4	0.29	
3	E	FEP	22.2	0.20	0.25
	F	"	33.2	0.30	
4	G	EEP	50.4	0.60	0.51
	H	"	35.6	0.42	
5	I	EEP	50.6	0.60	0.59
	J	"	48.3	0.58	
6	K	EEP	51.3	0.61	0.56
	L	"	42.8	0.51	

Remarks: FEP - Flush End-Plate
EEP - Extended End-Plate

Table 10.31 : Comparison of the λ value computed from SERFA to the Values used in New Design Frame under Design Load

Beam	Ultimate Capacity (kN)		Capacity Comparison
	(1)	(2)	(3) = (1)/(2)
1	222	205	1.08
2	232	205	1.13
3	232	205	1.13
4	208	204	1.02
5	240	204	1.18
6	232	204	1.14

Remarks: (1) Failure load computed from computer program SERFA
(2) Ultimate capacity determined from the plastic hinge calculation using the connection moment from M-ϕ curves

Table 10.32 : Comparison of the Ultimate Capacity of Beams used Different Methods

Column	Ultimate Capacity (kN)				
	(1)	(2)	(3)	(4)	(5)
3	586	679	610	739	912
6	715	679	736	748	870
9	586	679	613	742	880

Remarks: (1) Failure load calculated from BS5950 simplified approach with applied moment with eccentricity at column face plus 100 mm
(2) Failure load calculated from α_{pin} approach with no applied moment
(3) Failure load calculated from the new proposed method but with applied moment with eccentricity at column face plus 100 mm
(4) Failure load calculated from the new proposed method with no applied moment (α_{β} approach)
(5) Results computed from the computer program SERFA

Table 10.33 : Comparison of the Ultimate Capacity of Columns used Different Methods

Rigid End–Plate and Column Flange

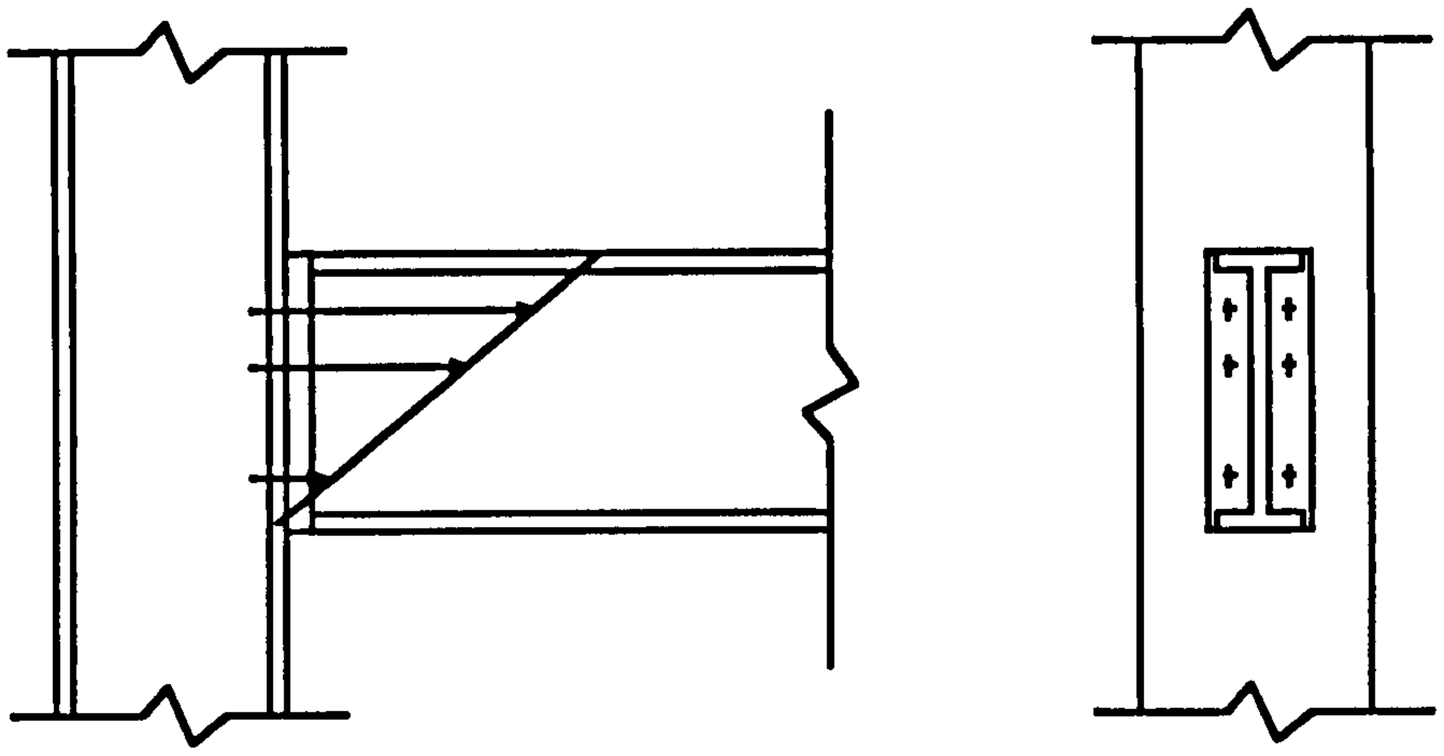

(a) Linear Bolt Force Distribution

Flexible End–Plate and Column Flange

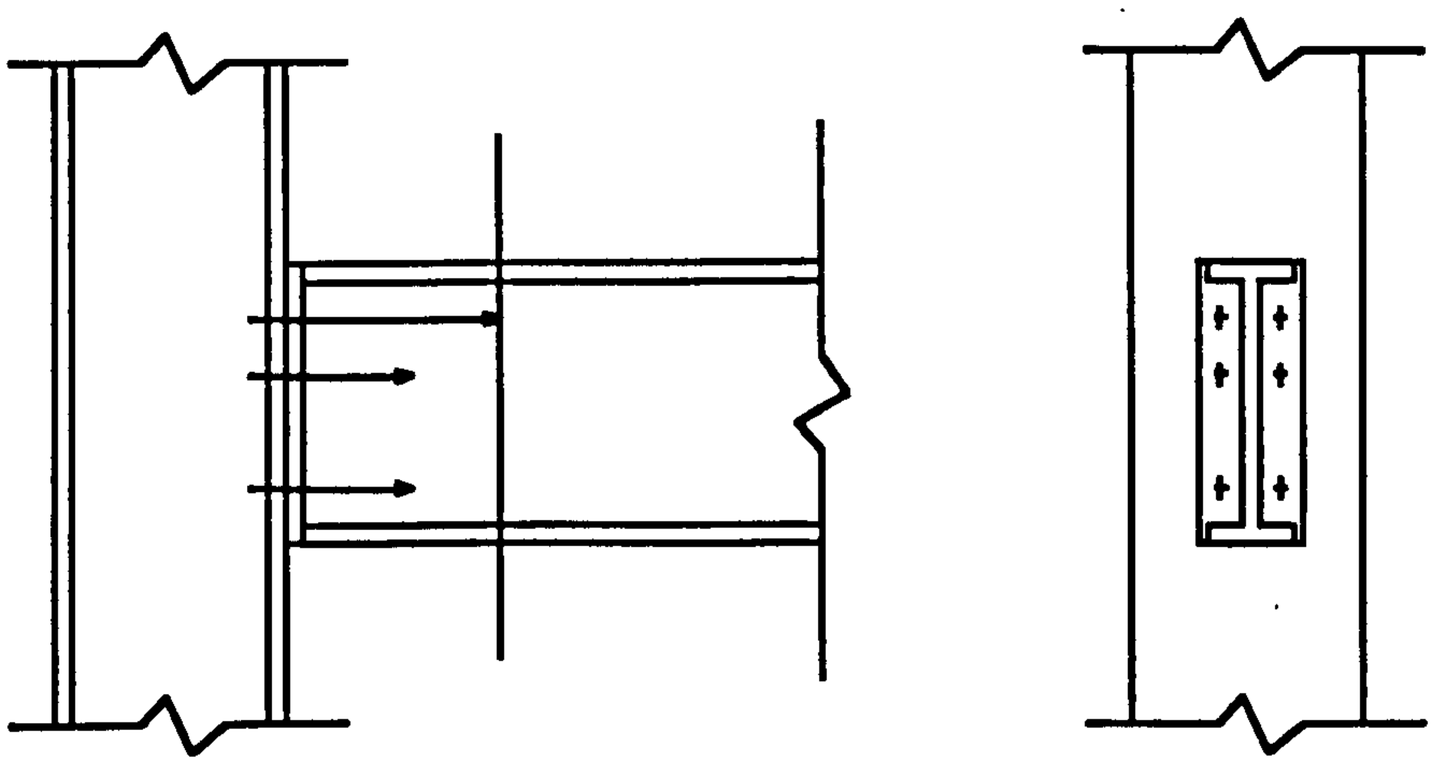

(b) Non–Linear Bolt Force Distribution

Figure 10.1 : Two Approaches for design of Flush End-Plate Connections

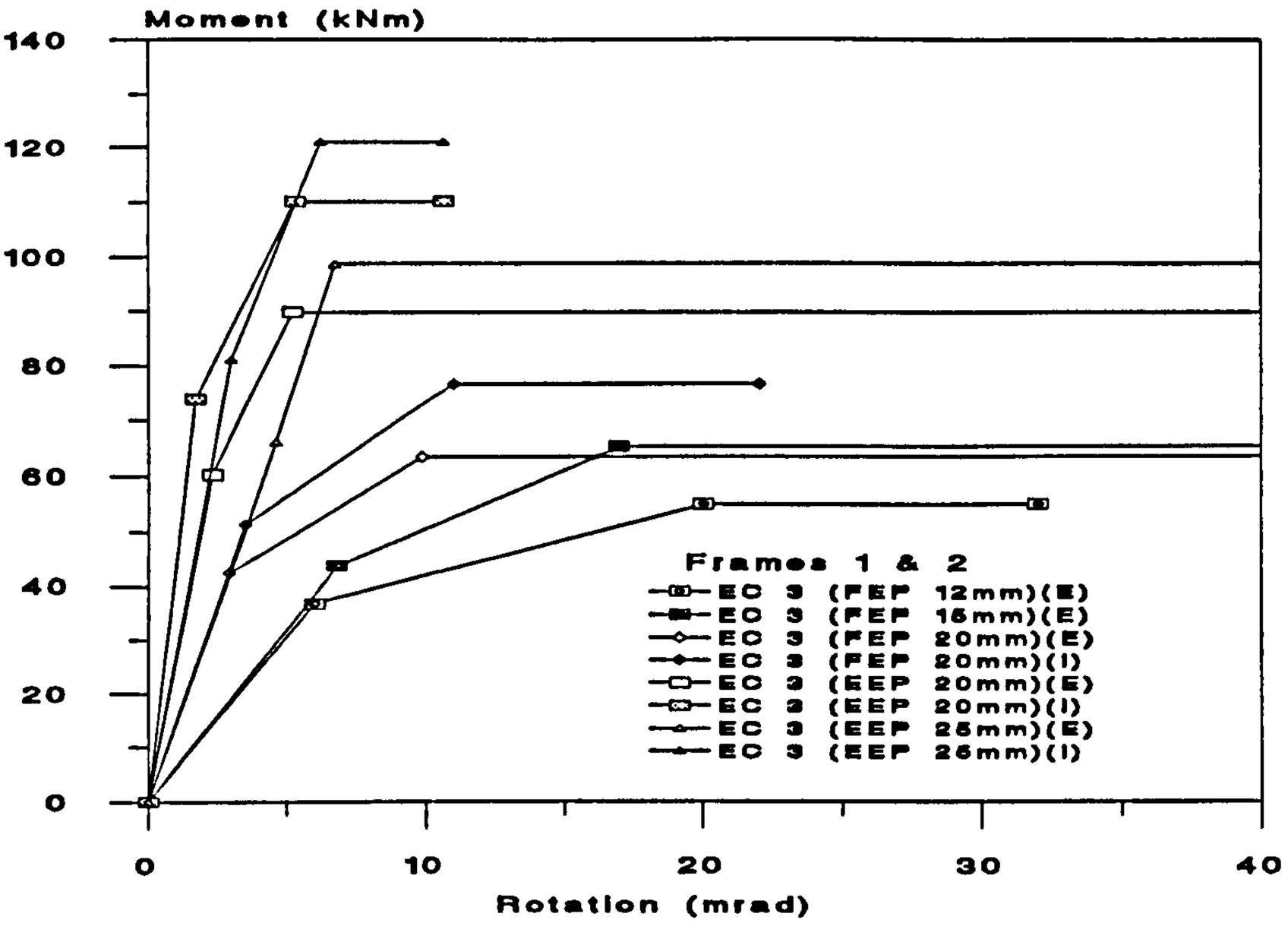

Figure 10.2 : Moment Rotation Curves predicted by EC 3 for Frames 1 & 2

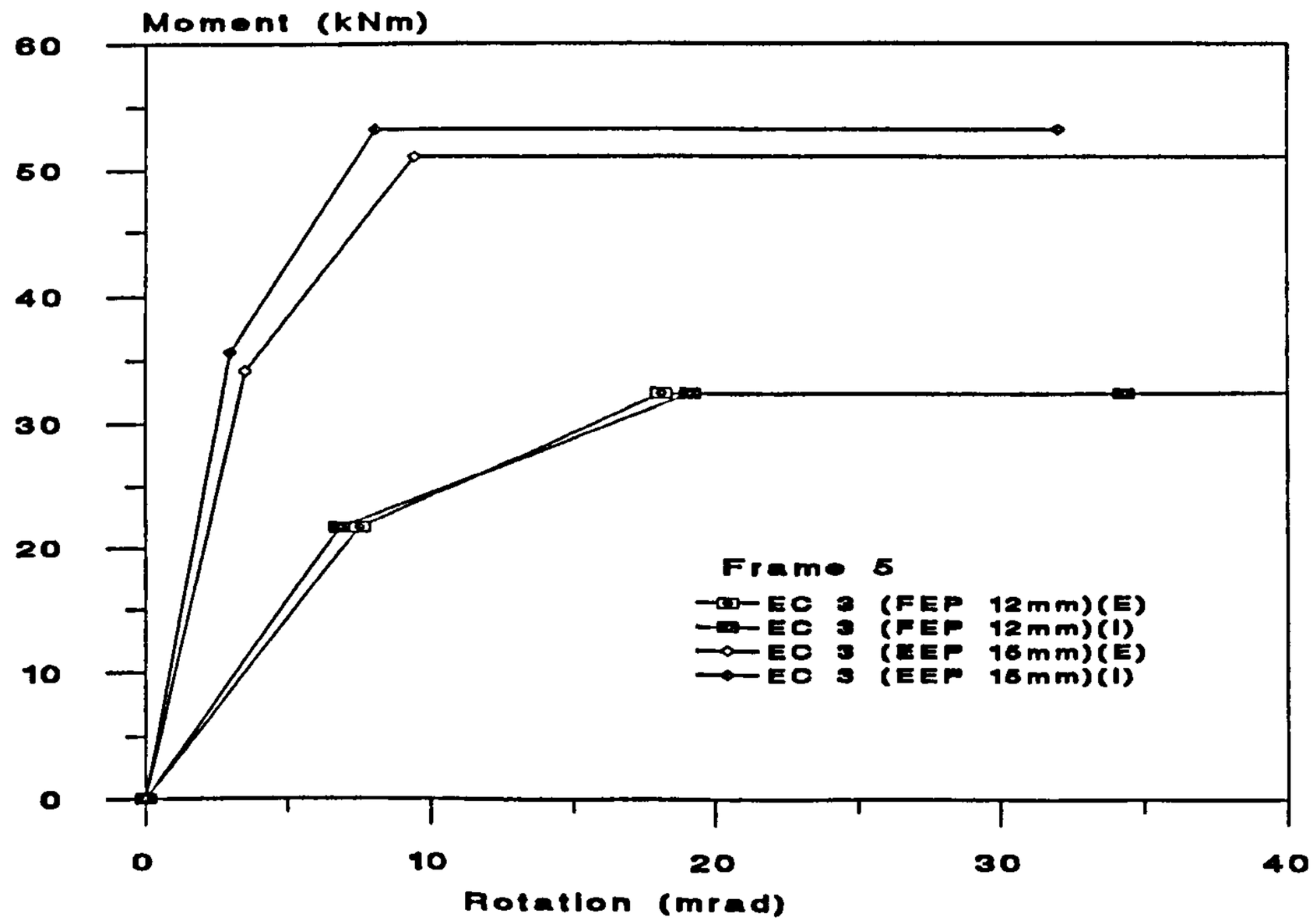

Figure 10.3 : Moment Rotation Curves predicted by EC 3 for Frames 5

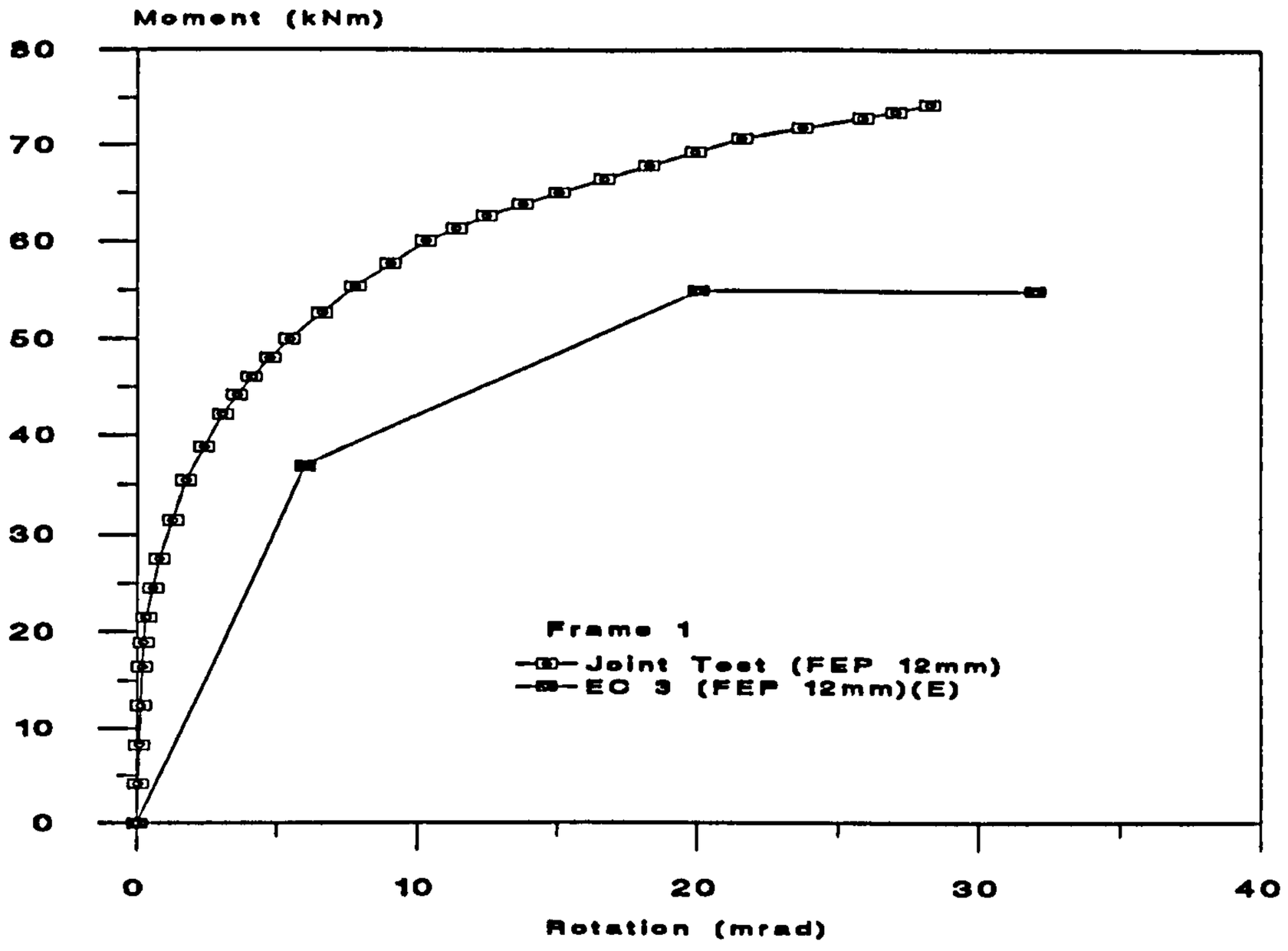

Figure 10.4 : Comparison of EC 3 prediction to Experimential Results (FEP 12mm) of Frame 1

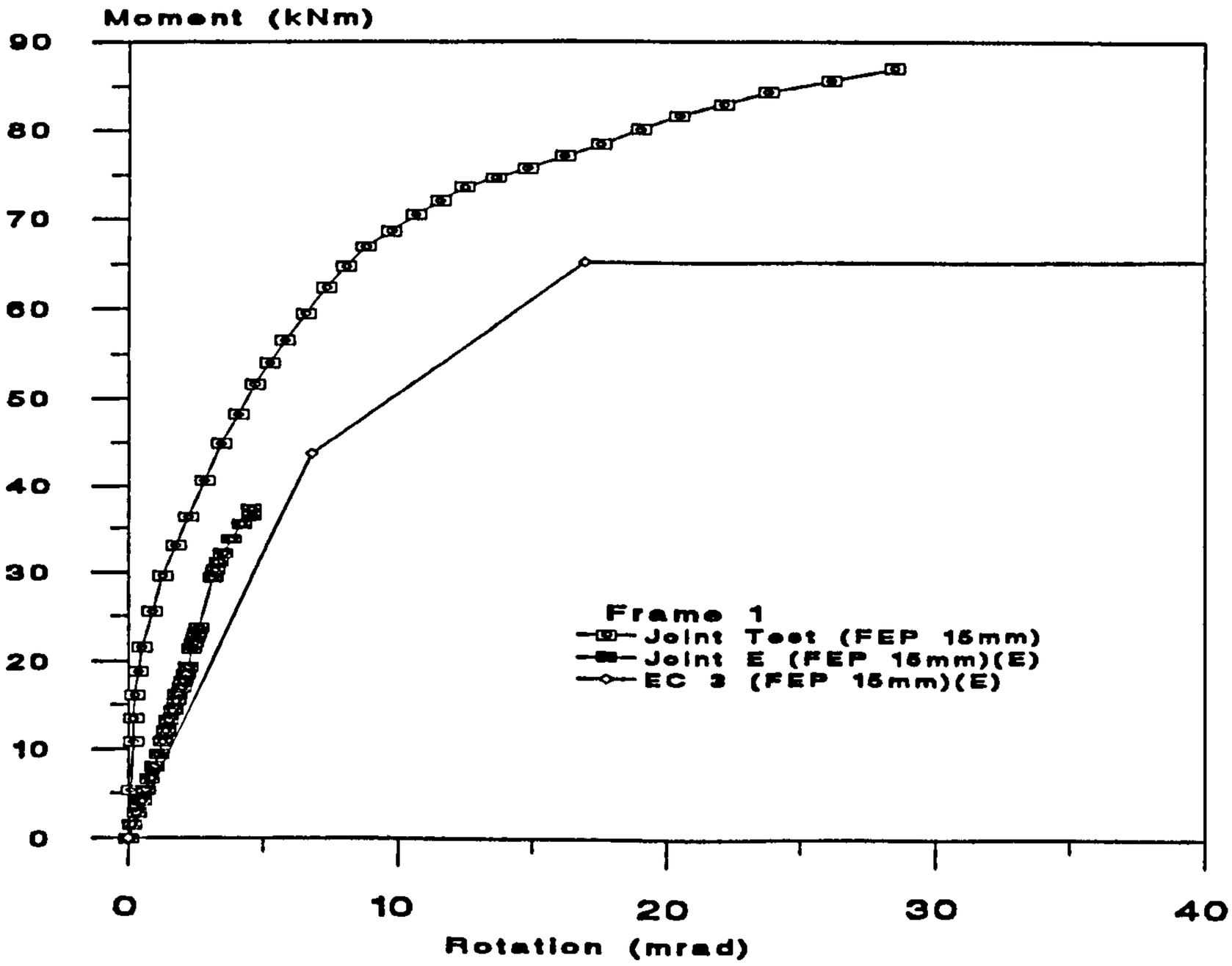

Figure 10.5 : Comparison of EC 3 prediction to Experimential Results (FEP 15mm) of Frame 1

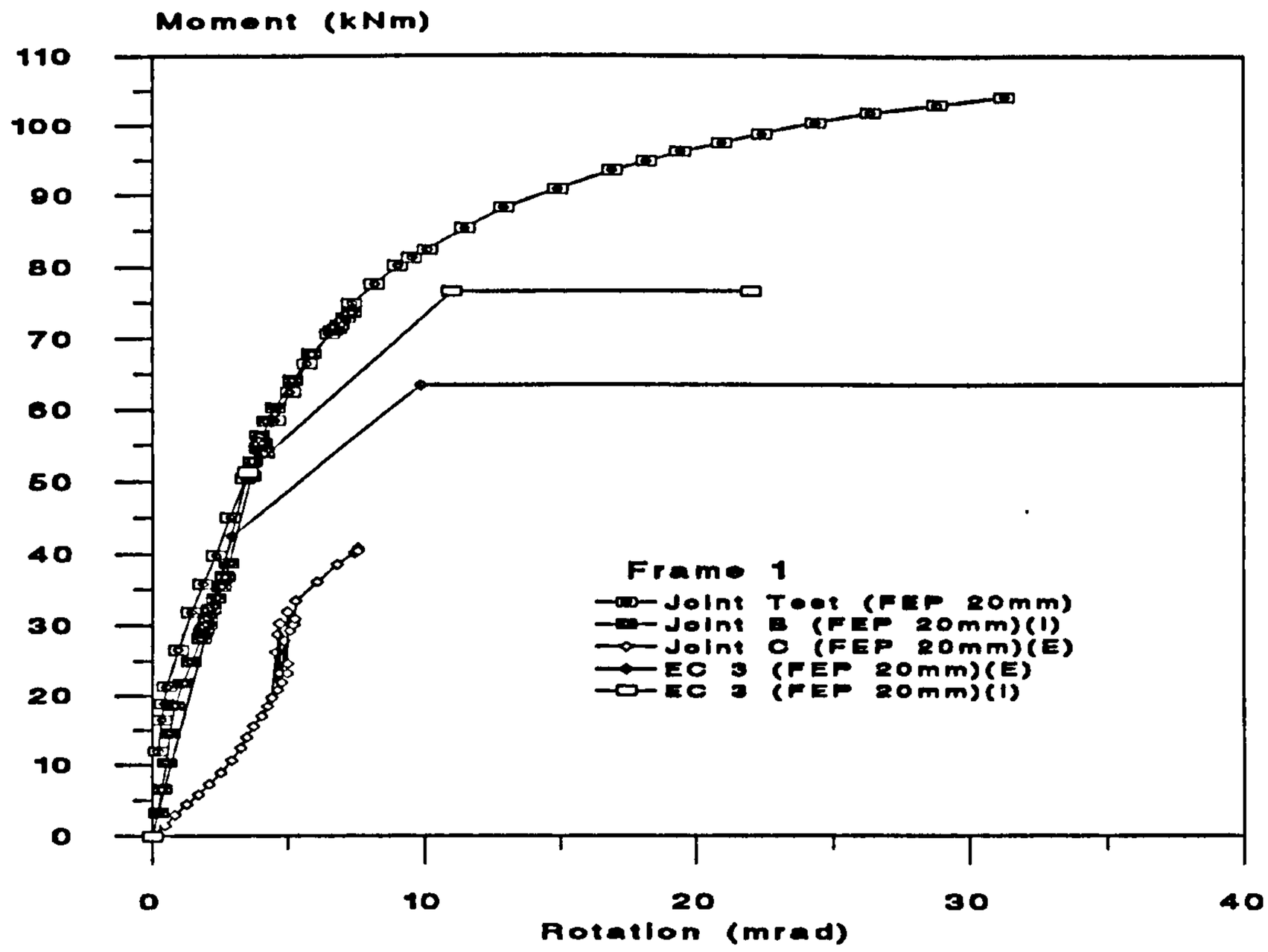

Figure 10.6 : Comparison of EC 3 prediction to Experimential Results (FEP 20mm) of Frame 1

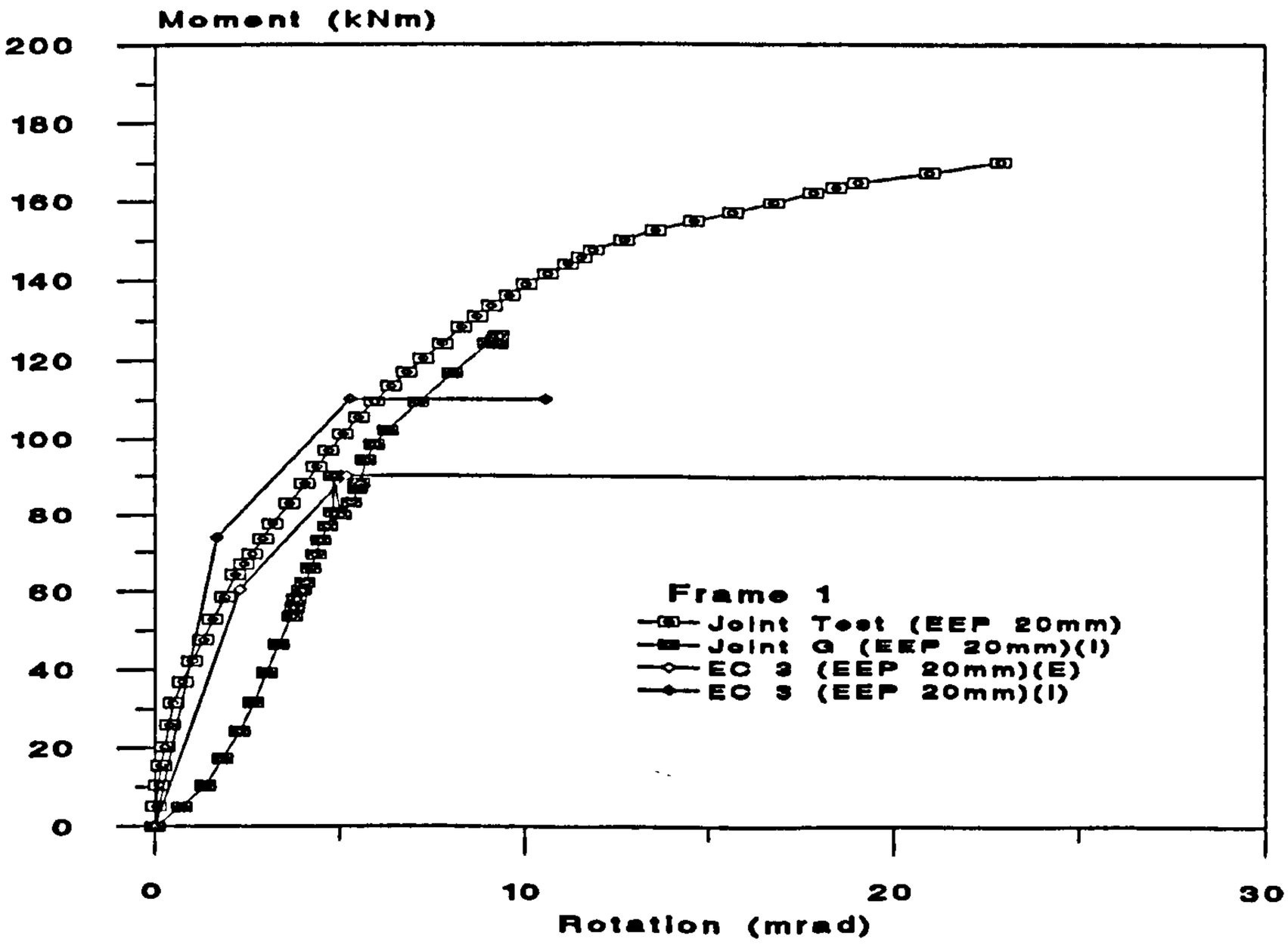

Figure 10.7 : Comparison of EC 3 prediction to Experimential Results (EEP 20mm) of Frame 1

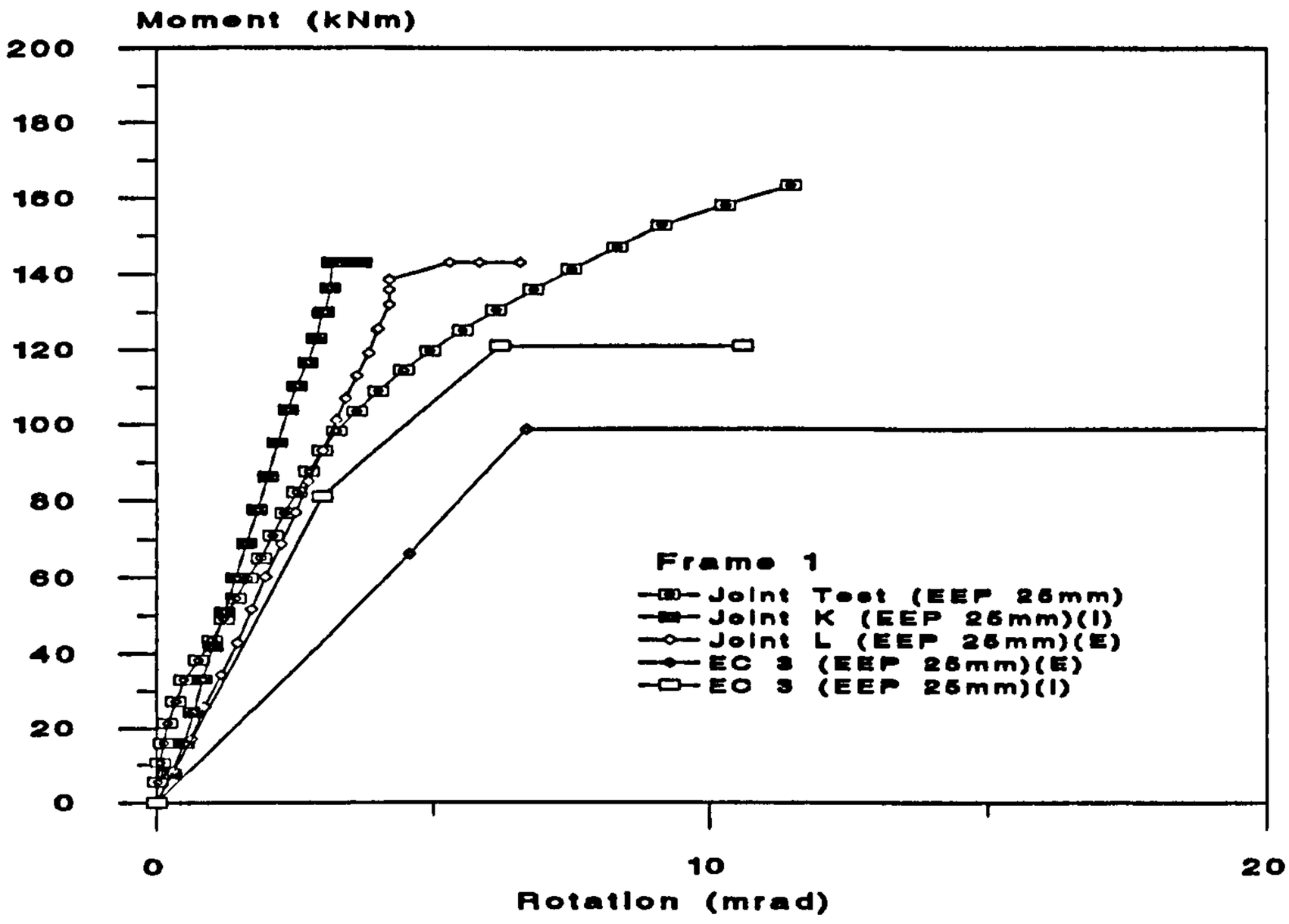

Figure 10.8 : Comparison of EC 3 prediction to Experimential Results (EEP 25mm) of Frame 1

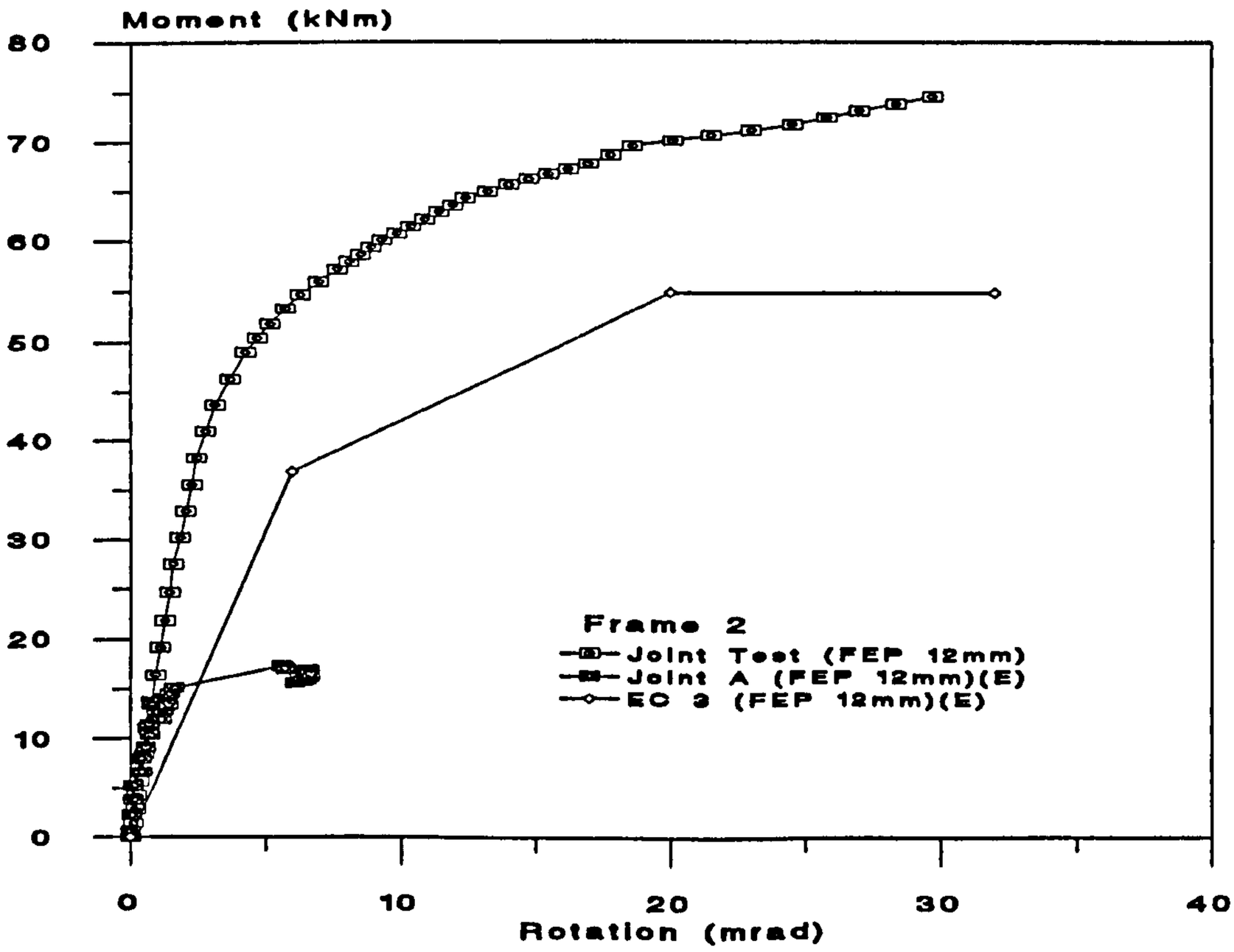

Figure 10.9 : Comparison of EC 3 prediction to Experimential Results (FEP 12mm) of Frame 2

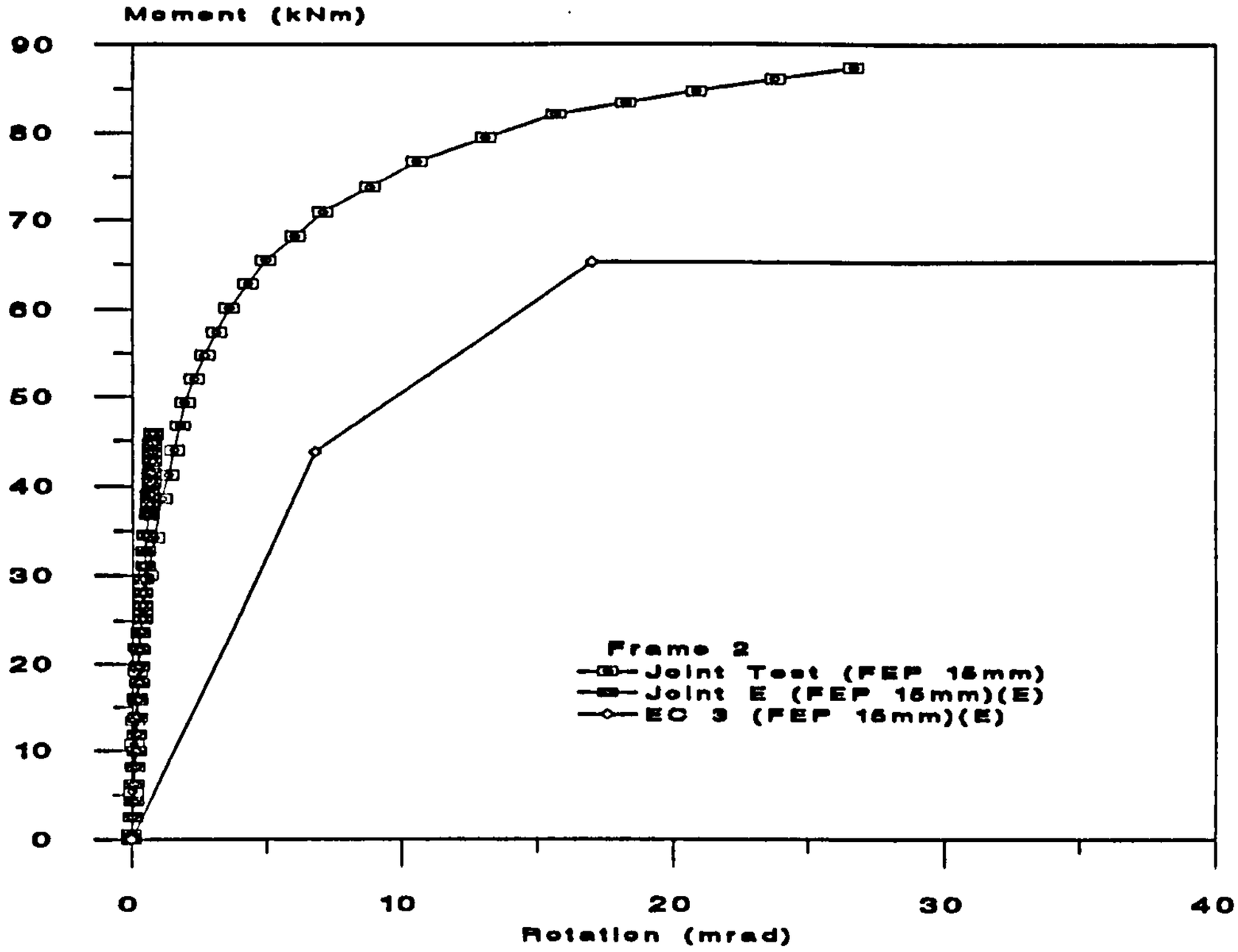

Figure 10.10 : Comparison of EC 3 prediction to Experimential Results (FEP 15mm) of Frame 2

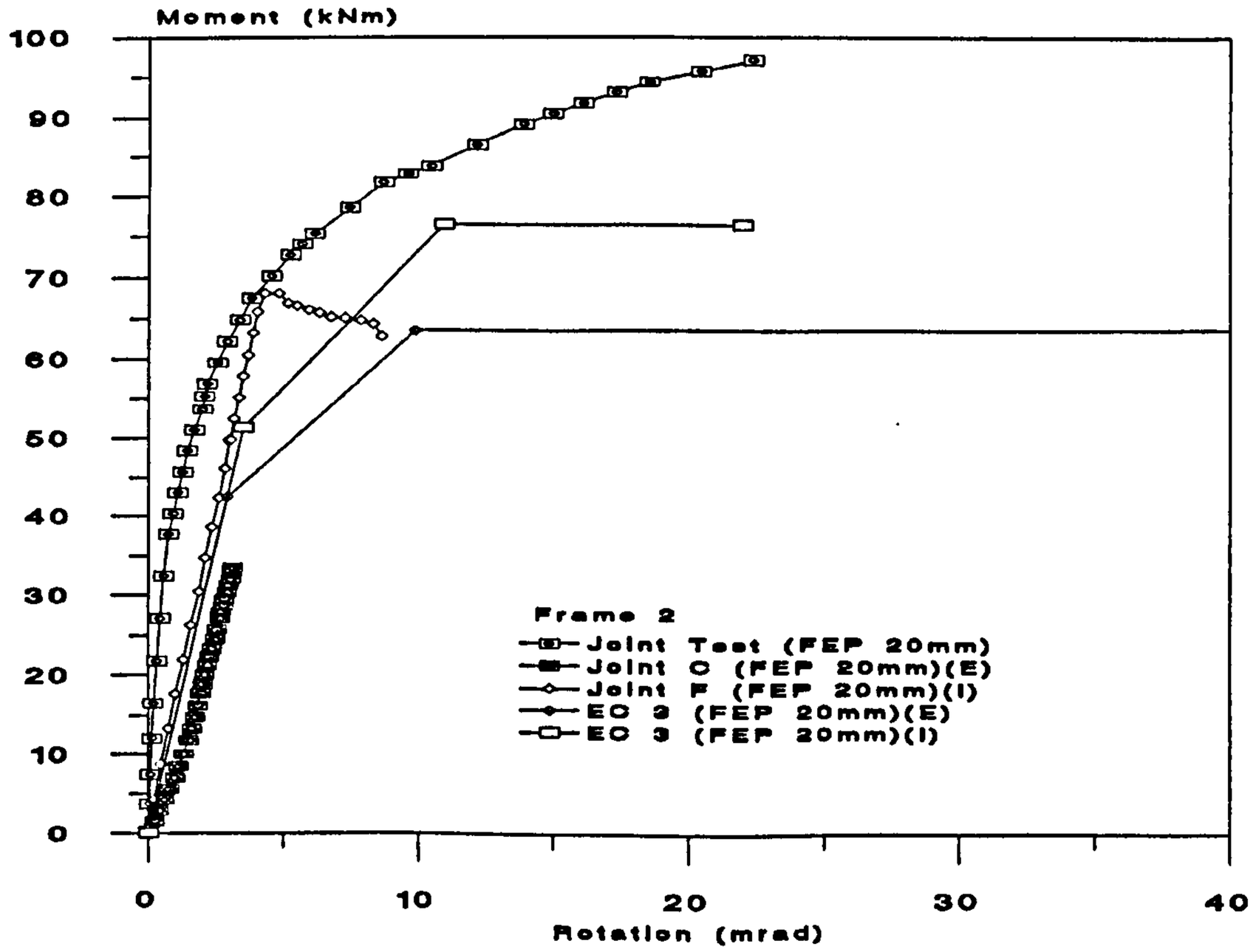

Figure 10.11 : Comparison of EC 3 prediction to Experimential Results (FEP 20mm) of Frame 2

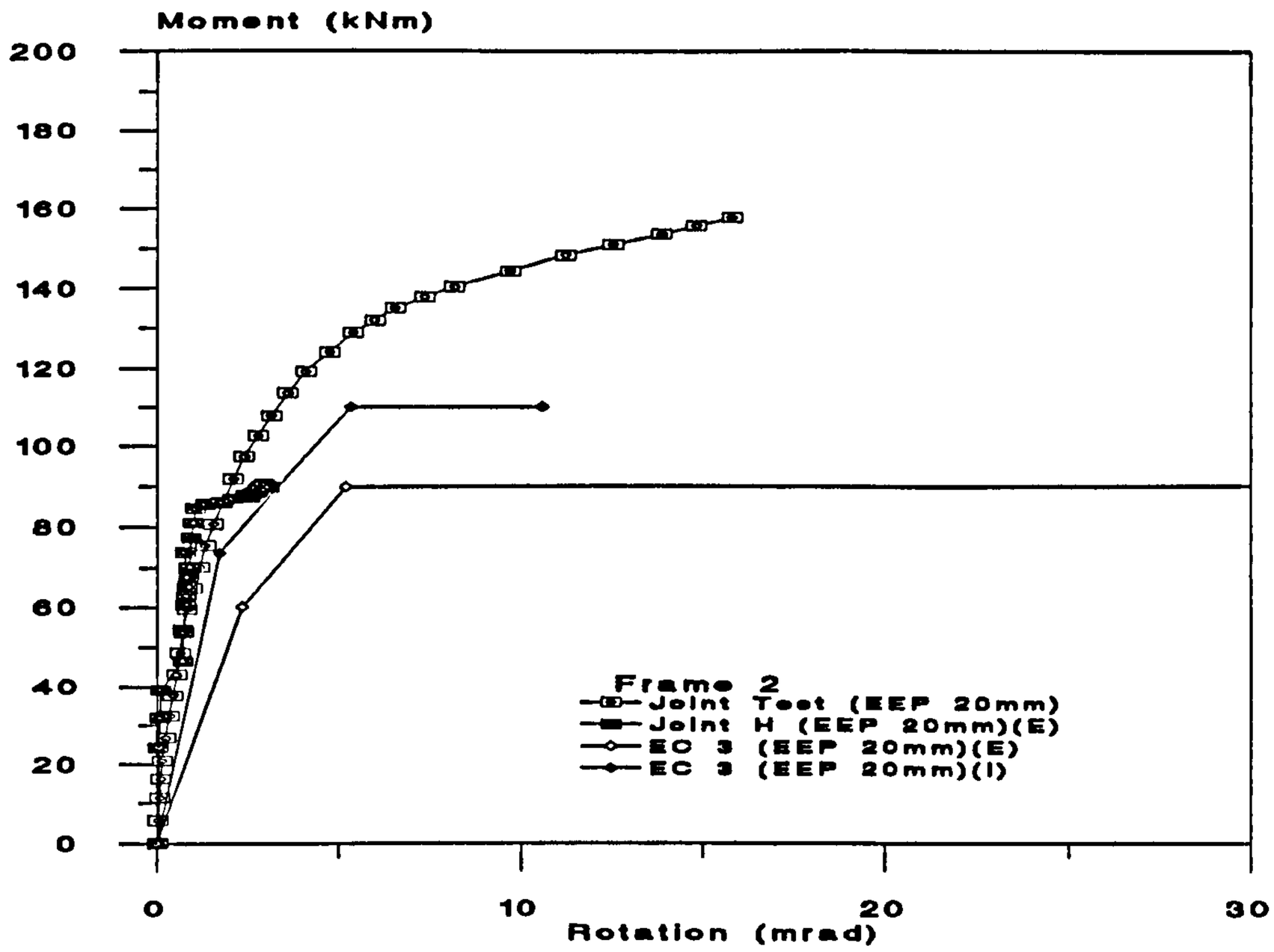

Figure 10.12 : Comparison of EC 3 prediction to Experimential Results (EEP 20mm) of Frame 2

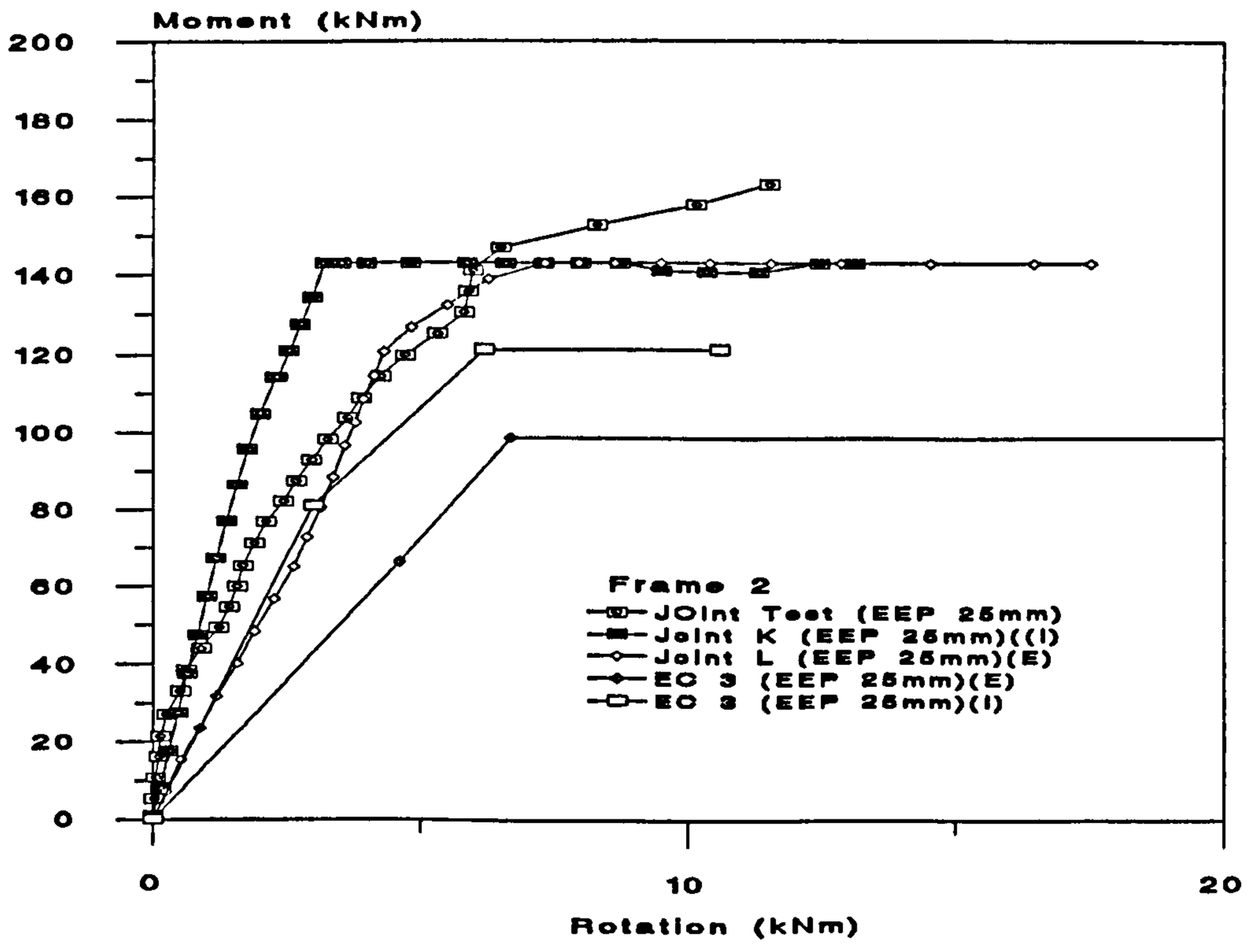

Figure 10.13 : Comparison of EC 3 prediction to Experimential Results (EEP 25mm) of Frame 2

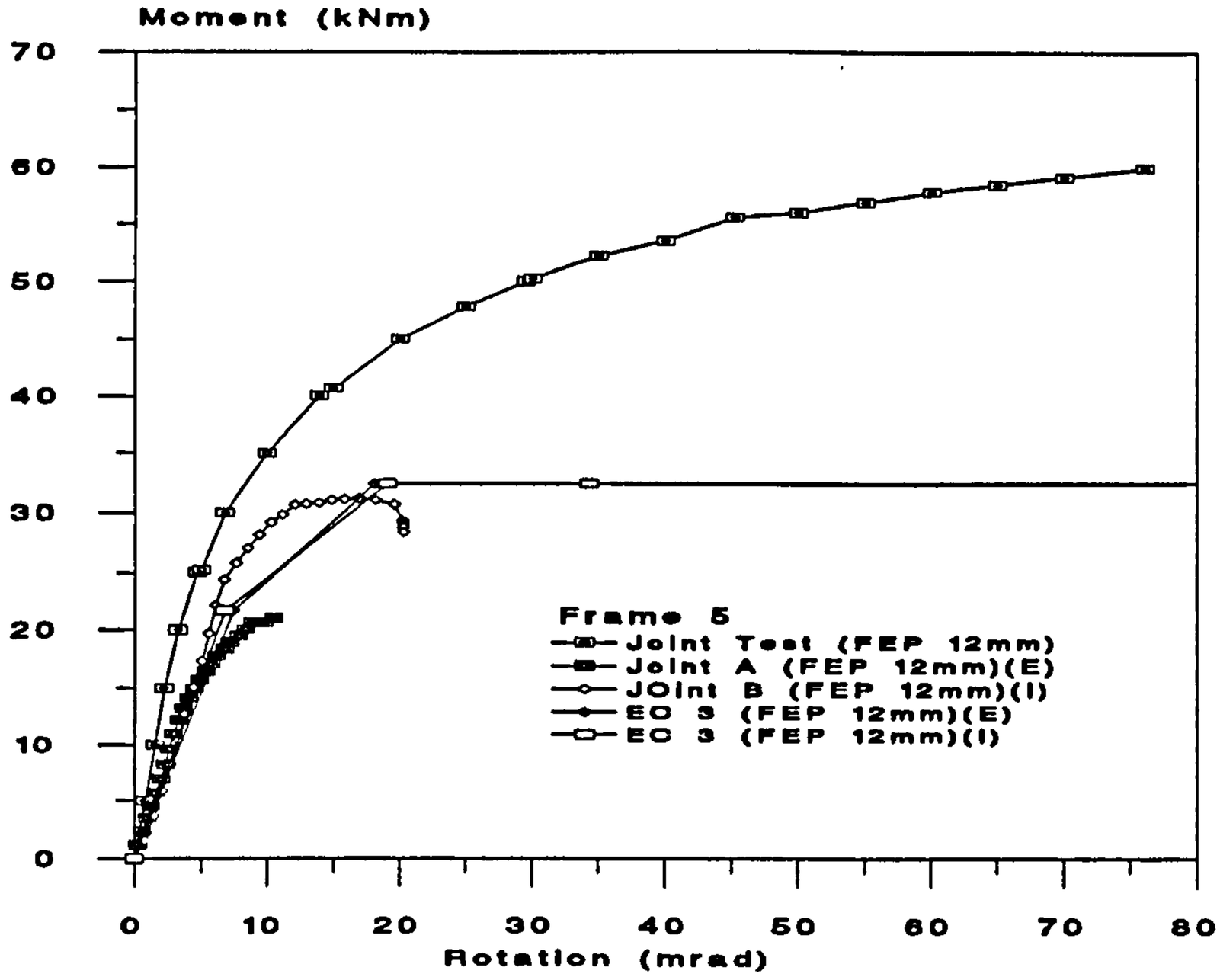

Figure 10.14 : Comparison of EC 3 prediction to Experimential Results (FEP 12mm) of Frame 5

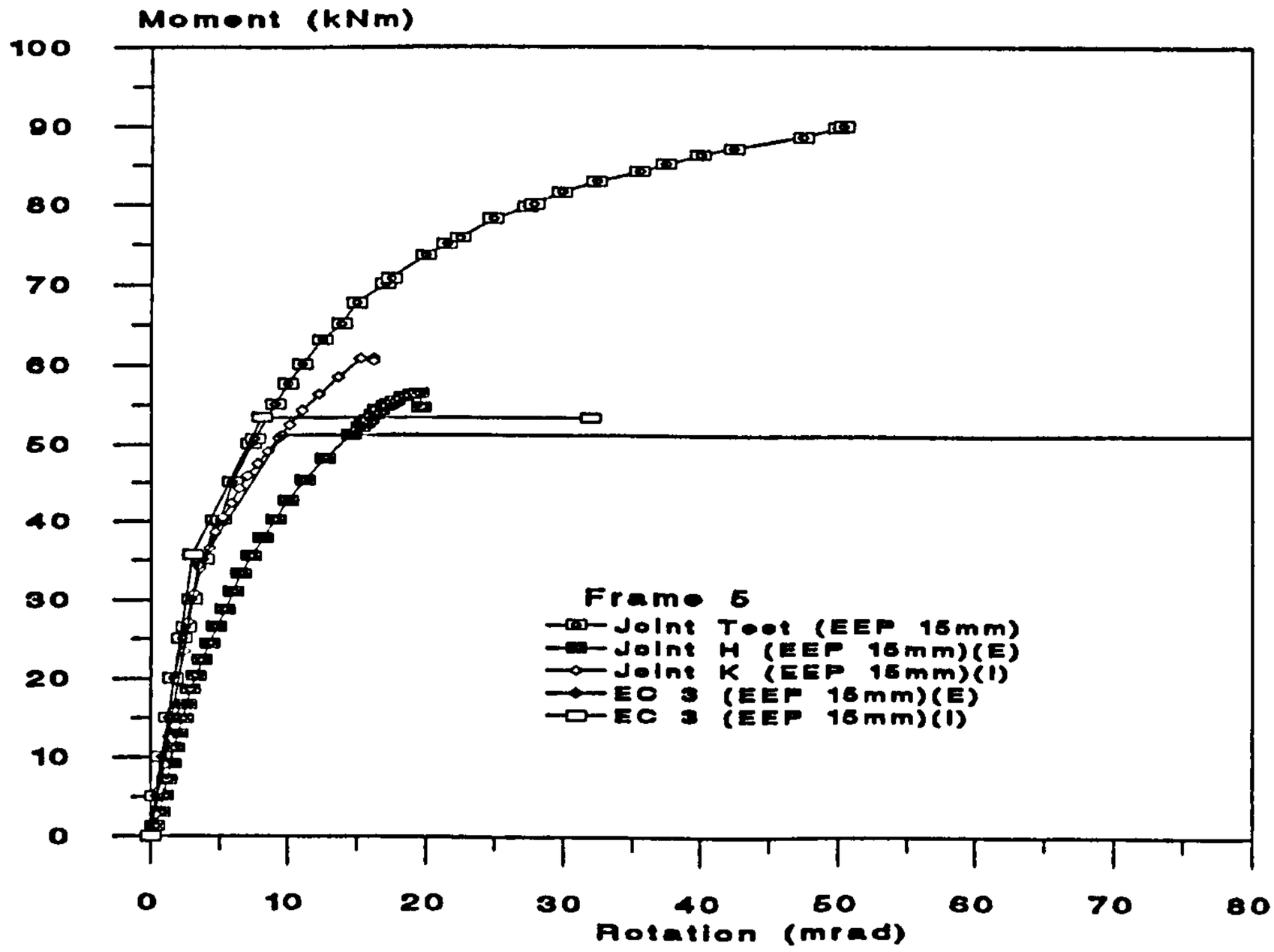

Figure 10.15 : Comparison of EC 3 prediction to Experimential Results (EEP 15mm) of Frame 5

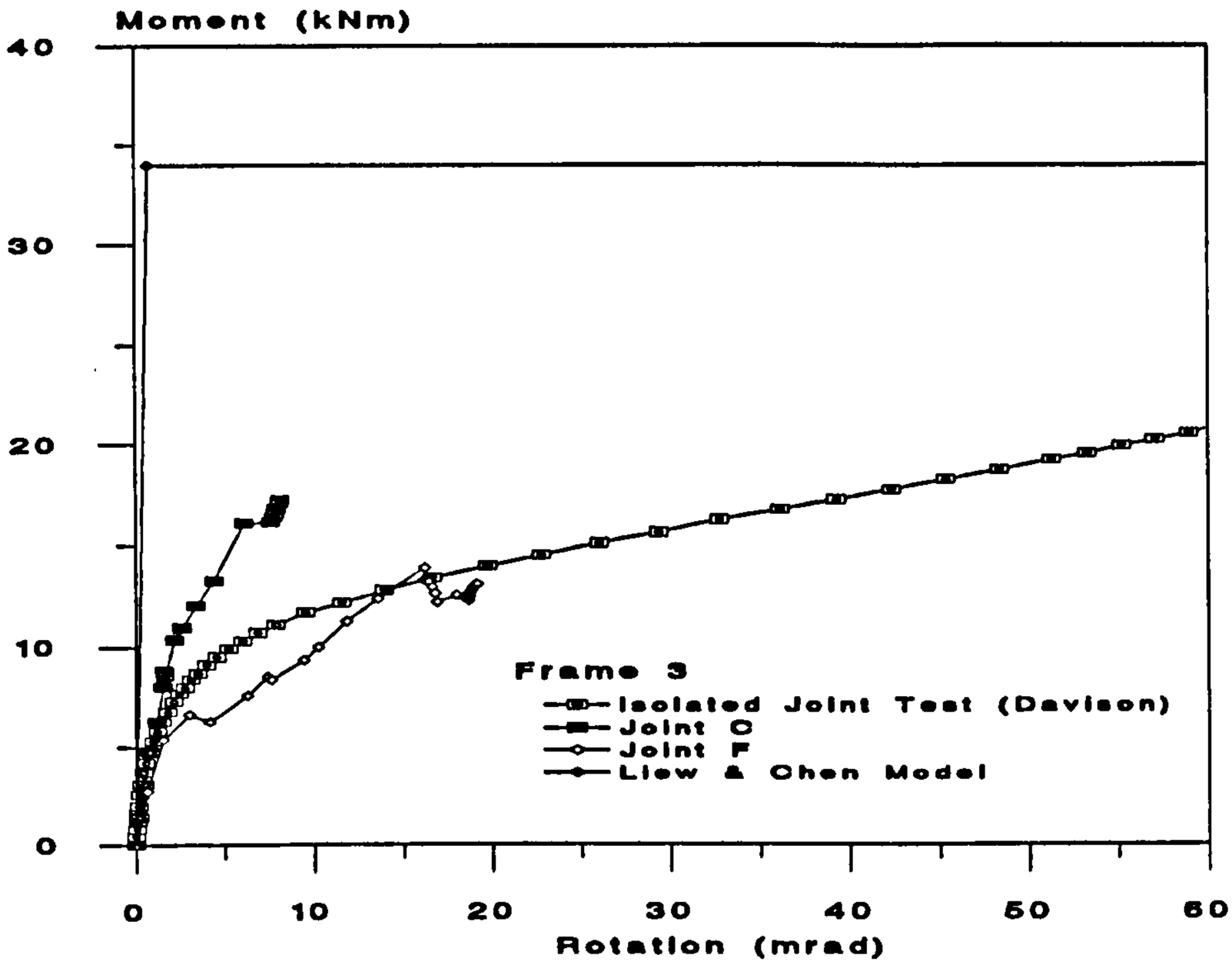

Figure 10.16 : Comparison of prediction from Liew & Chen Model to the Experimential Results (Flange Cleat Connection) of Frame 3

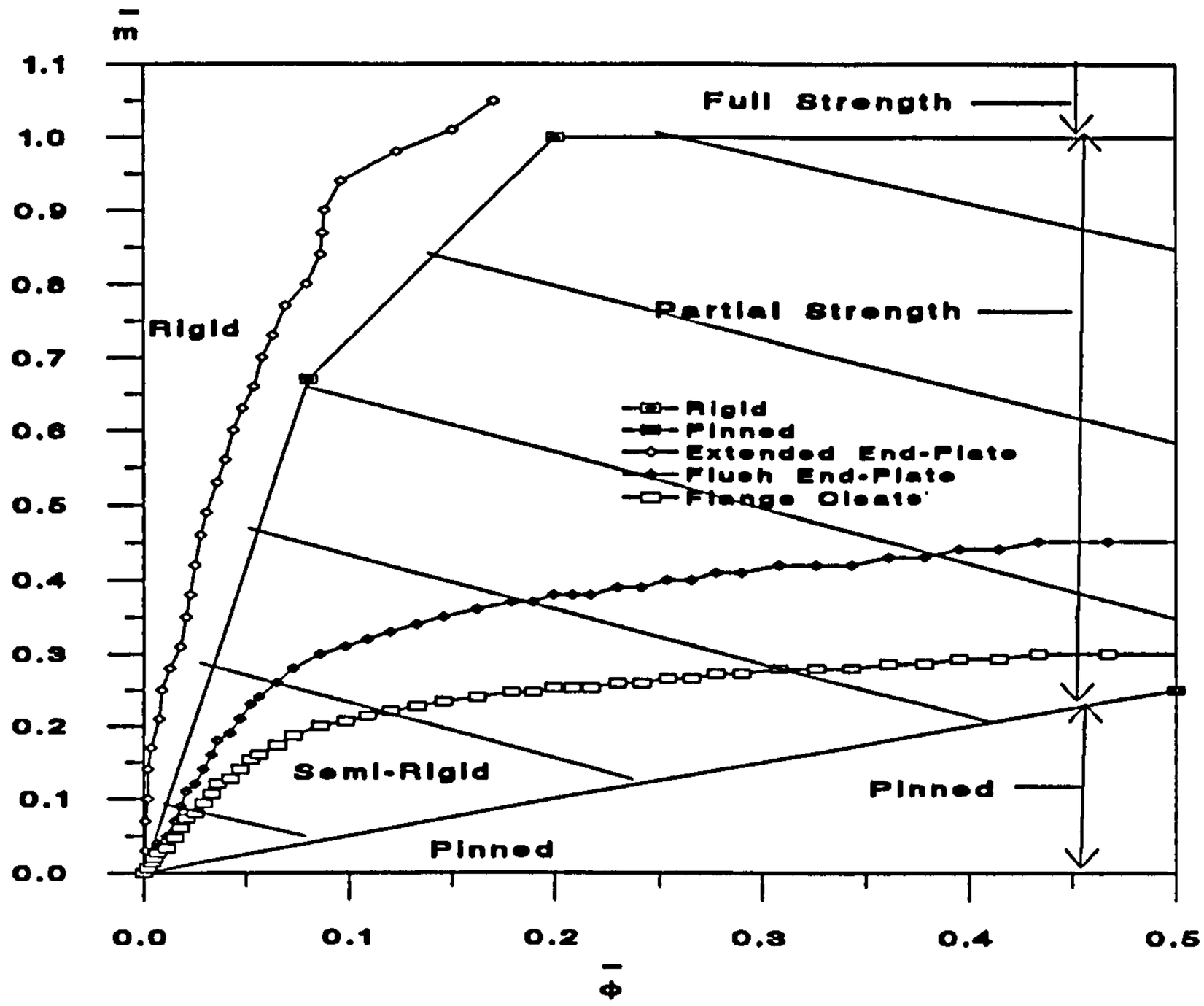

Figure 10.17 : Classification of Connection according to EC 3

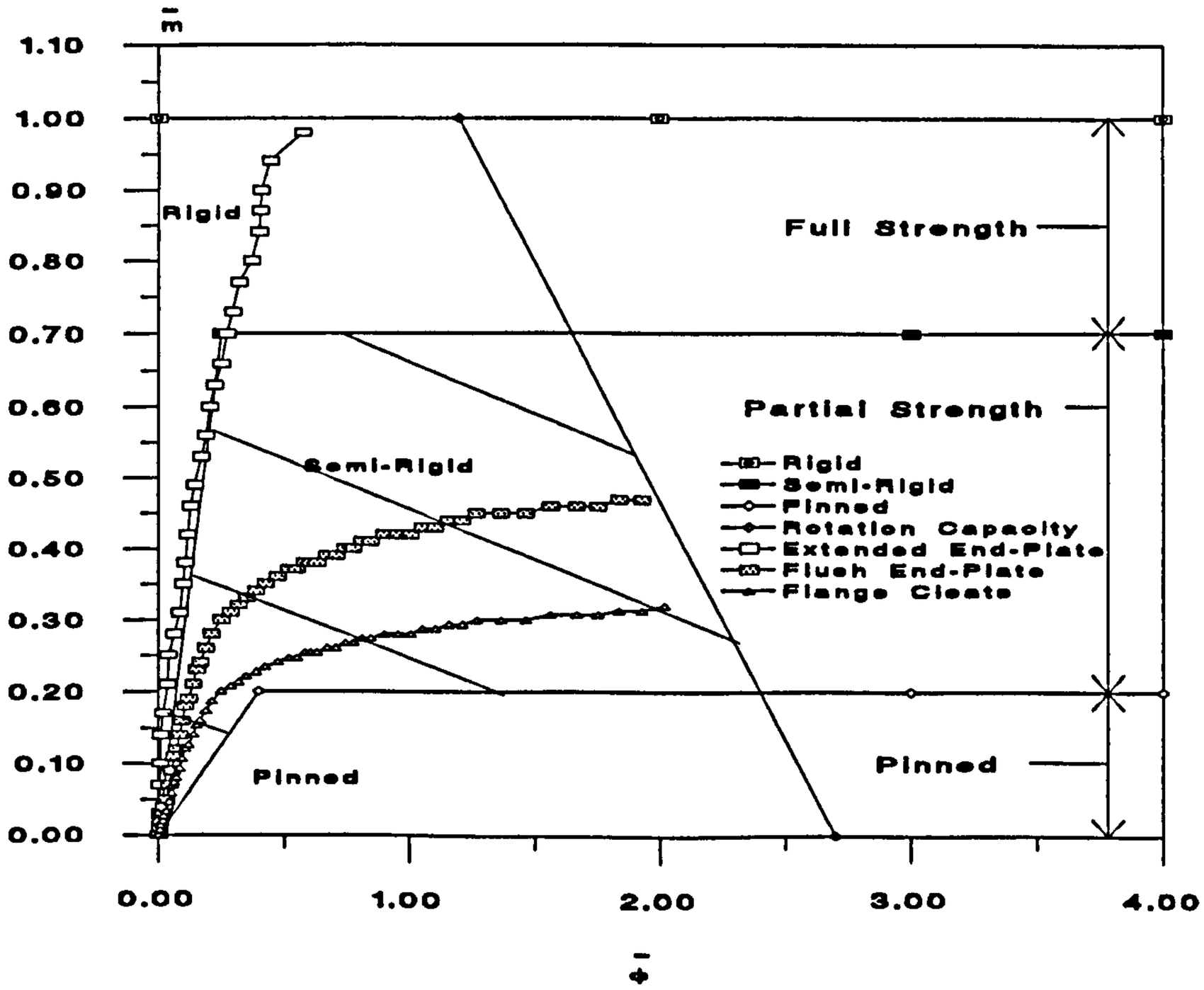

Figure 10.18 : Classification of Connections according to Bjorhovde

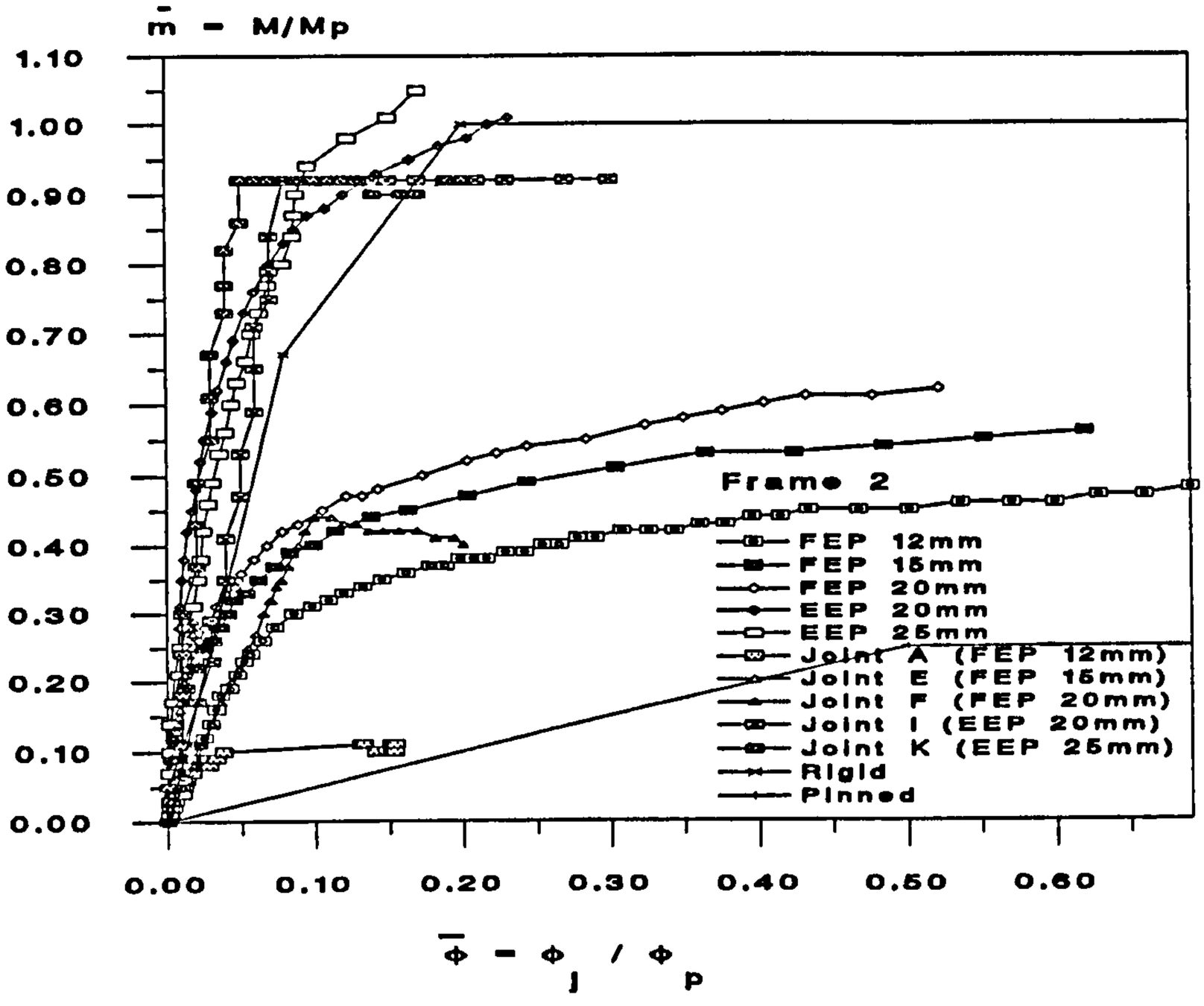

Figure 10.19 : Classification of Connections in Frame 2 using EC 3

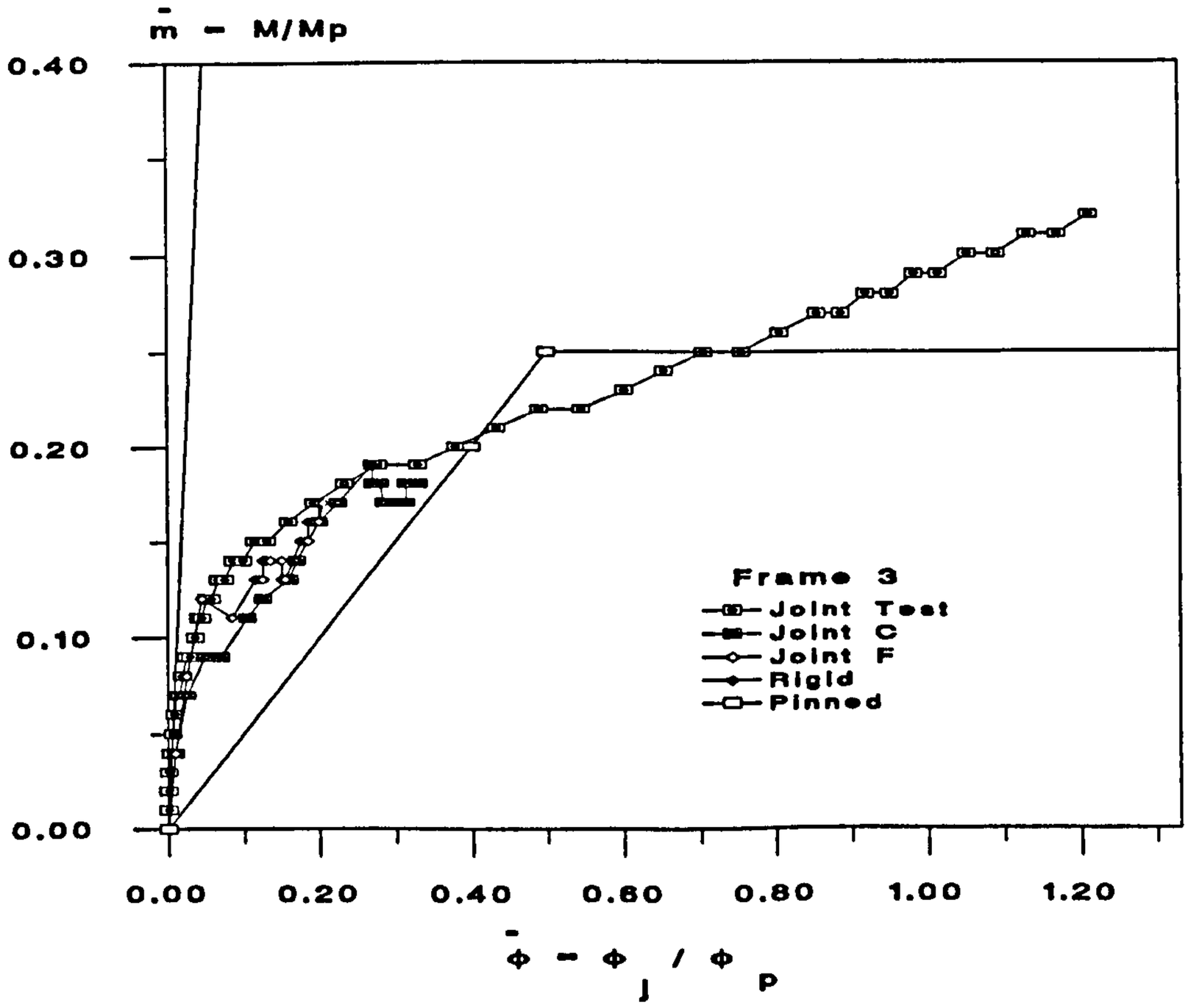

Figure 10.20 : Classification of Connections in Frame 3 using EC 3

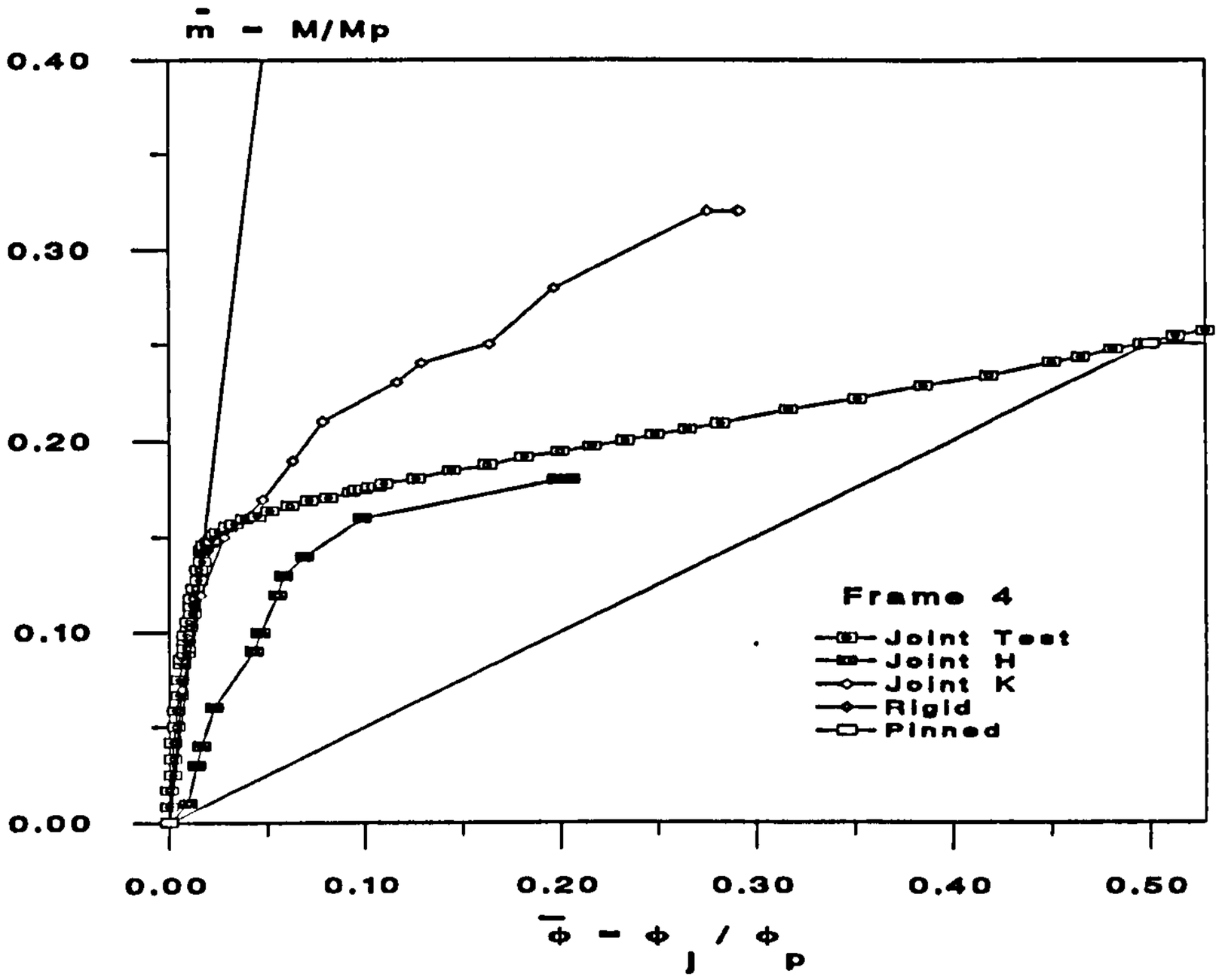

Figure 10.21 : Classification of Connections in Frame 4 using EC 3

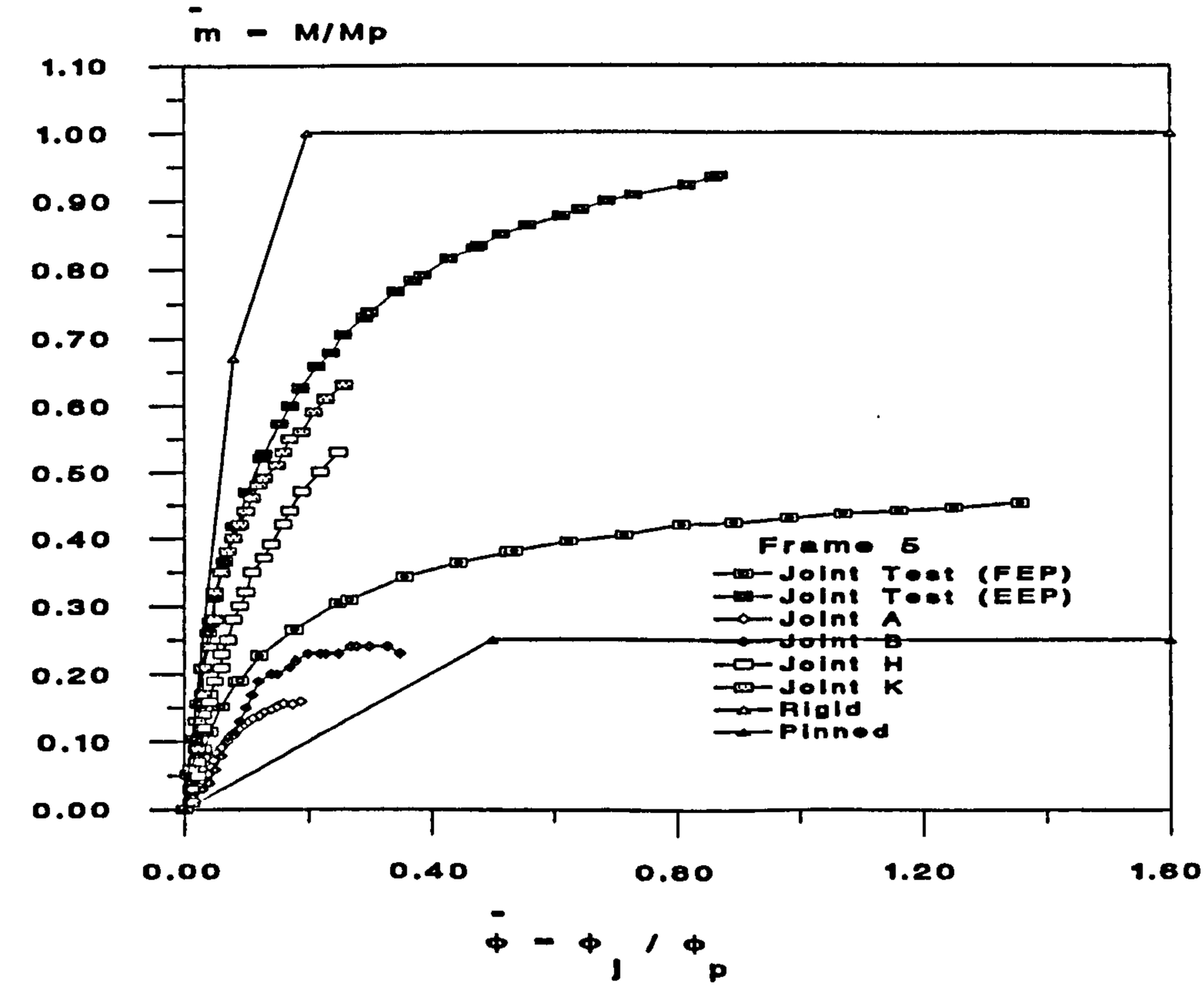

Figure 10.22 : Classification of Connections in Frame 5 using EC 3

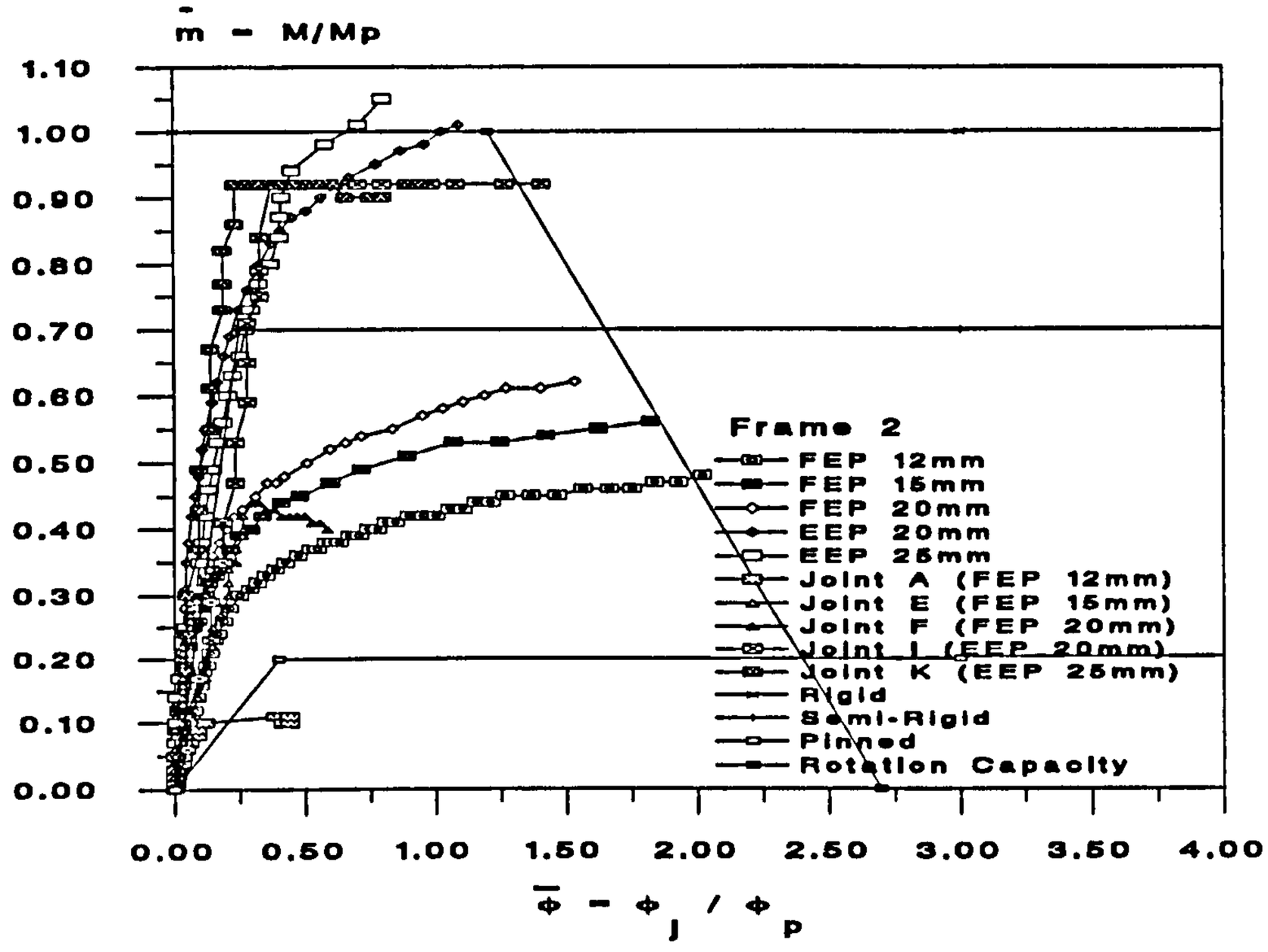

Figure 10.23 : Classification of Connections in Frame 2 using Bjorhovde

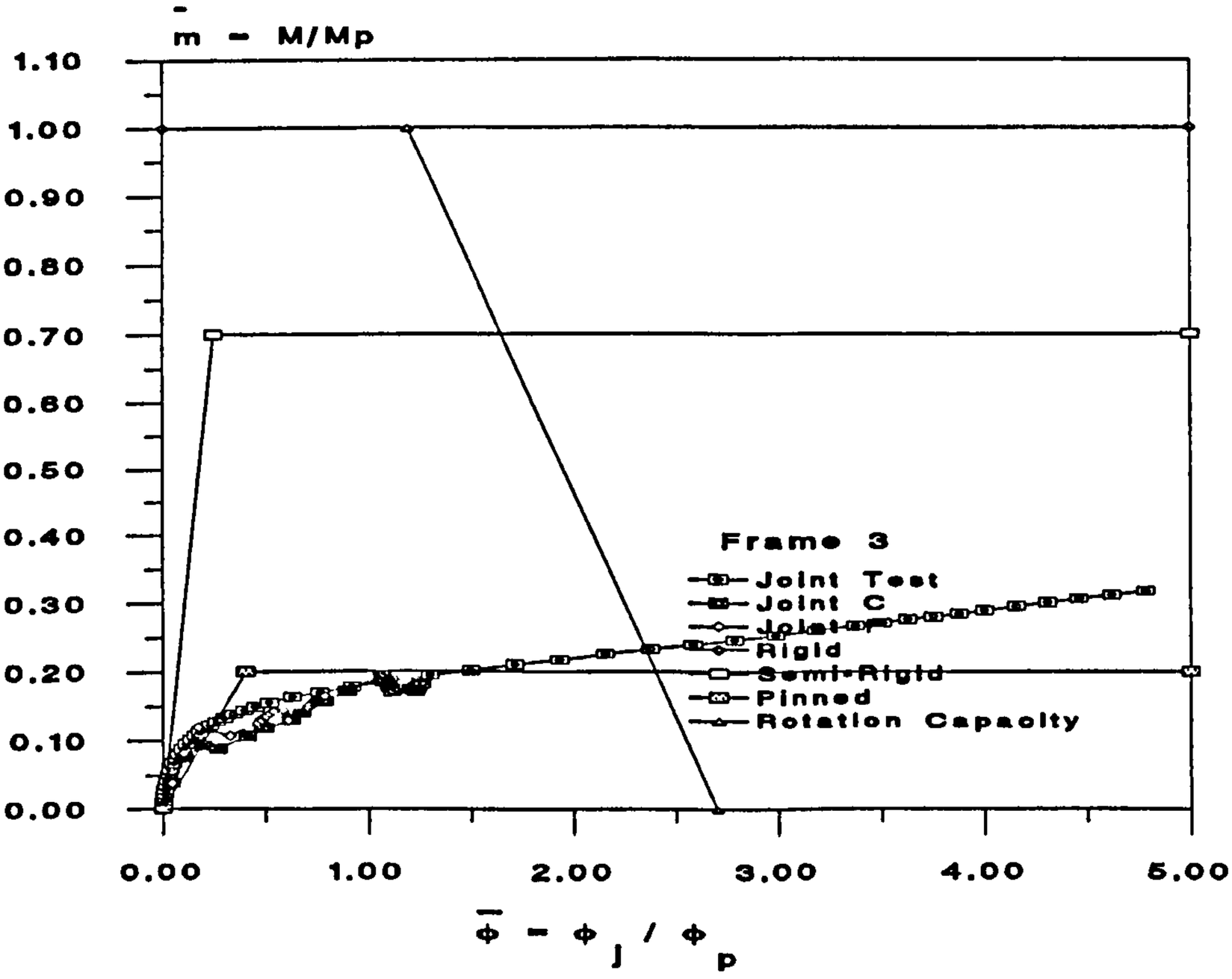

Figure 10.24 : Classification of Connections in Frame 3 using Bjorhovde

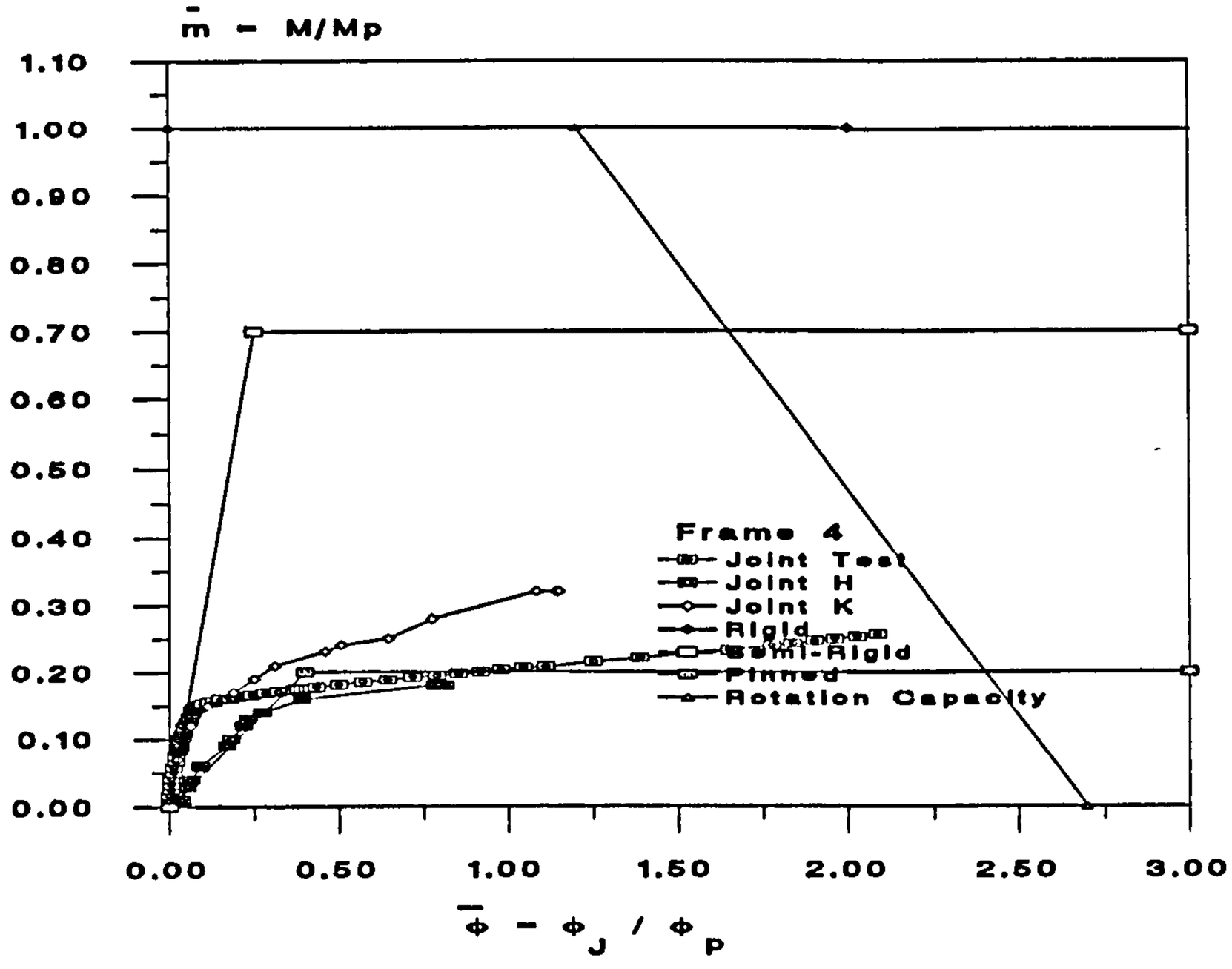

Figure 10.25 : Classification of Connections in Frame 4 using Bjorhovde

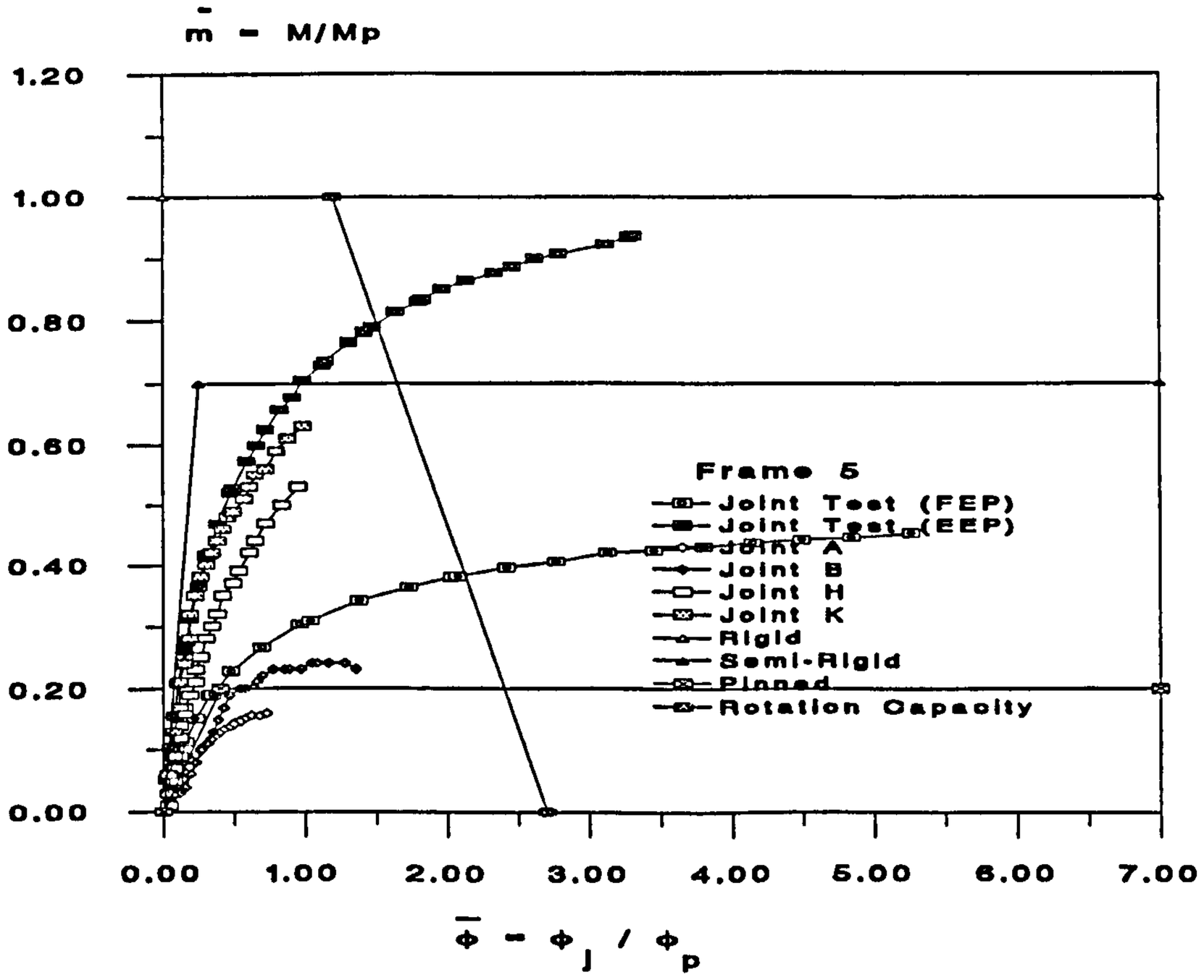

Figure 10.26 : Classification of Connections in Frame 5 using Bjorhovde

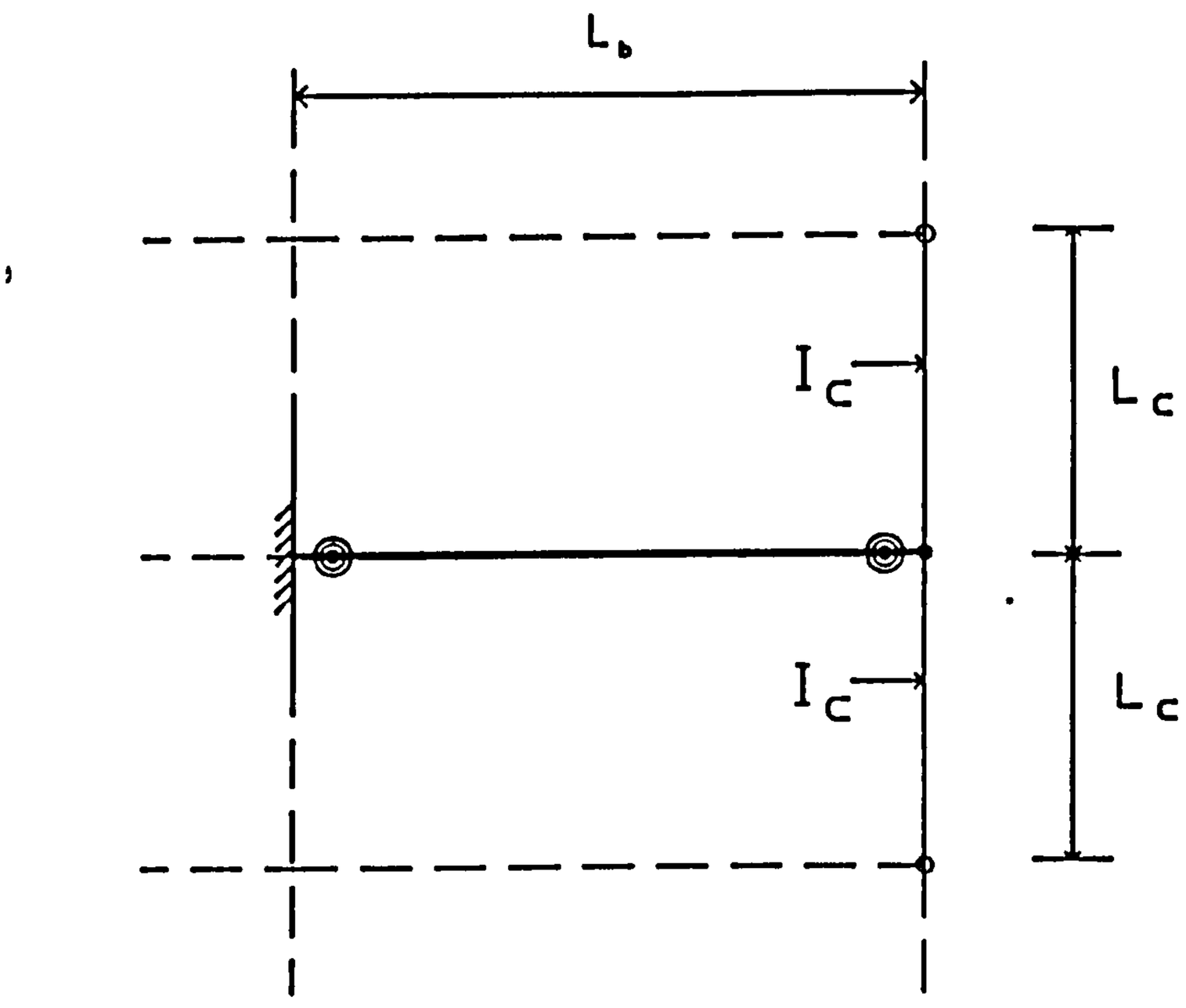

Figure 10.27 : Beam-to-Column Sub-Frame

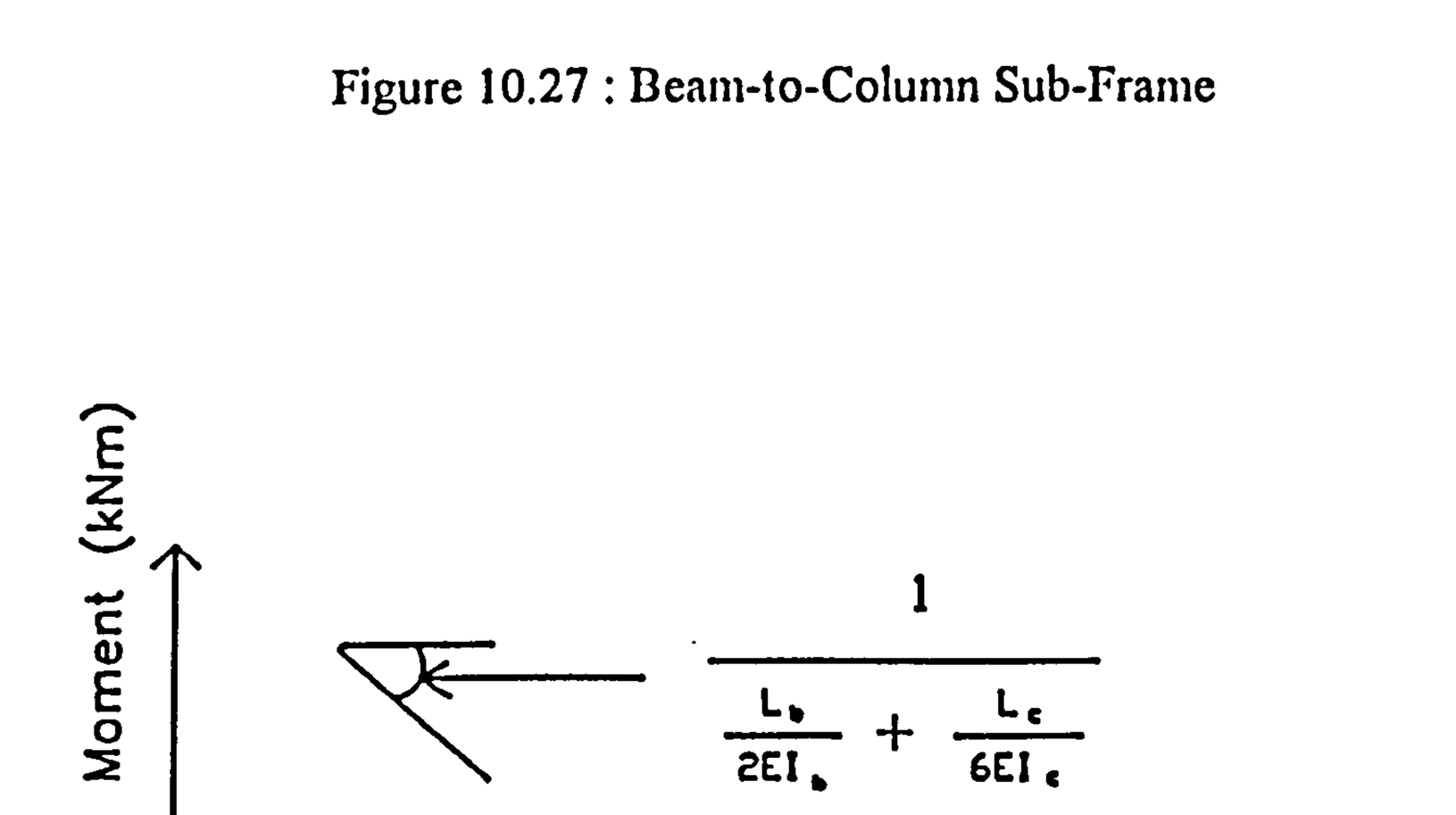

Figure 10.28 : Beam Line Method to estimate the Semi-Rigid Moment

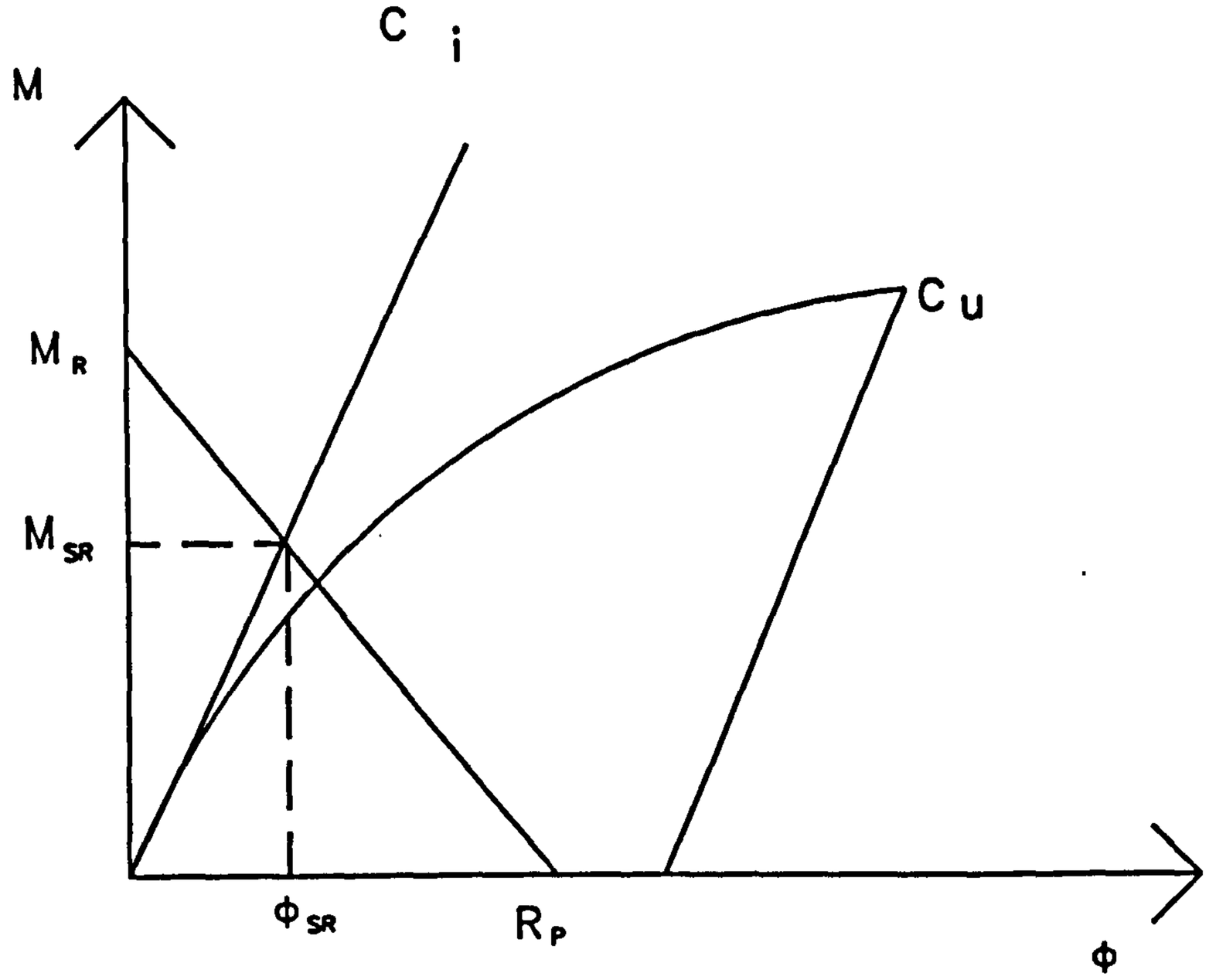

(a) The Initial Stiffness of Connection without effect due to Lack-of-fit

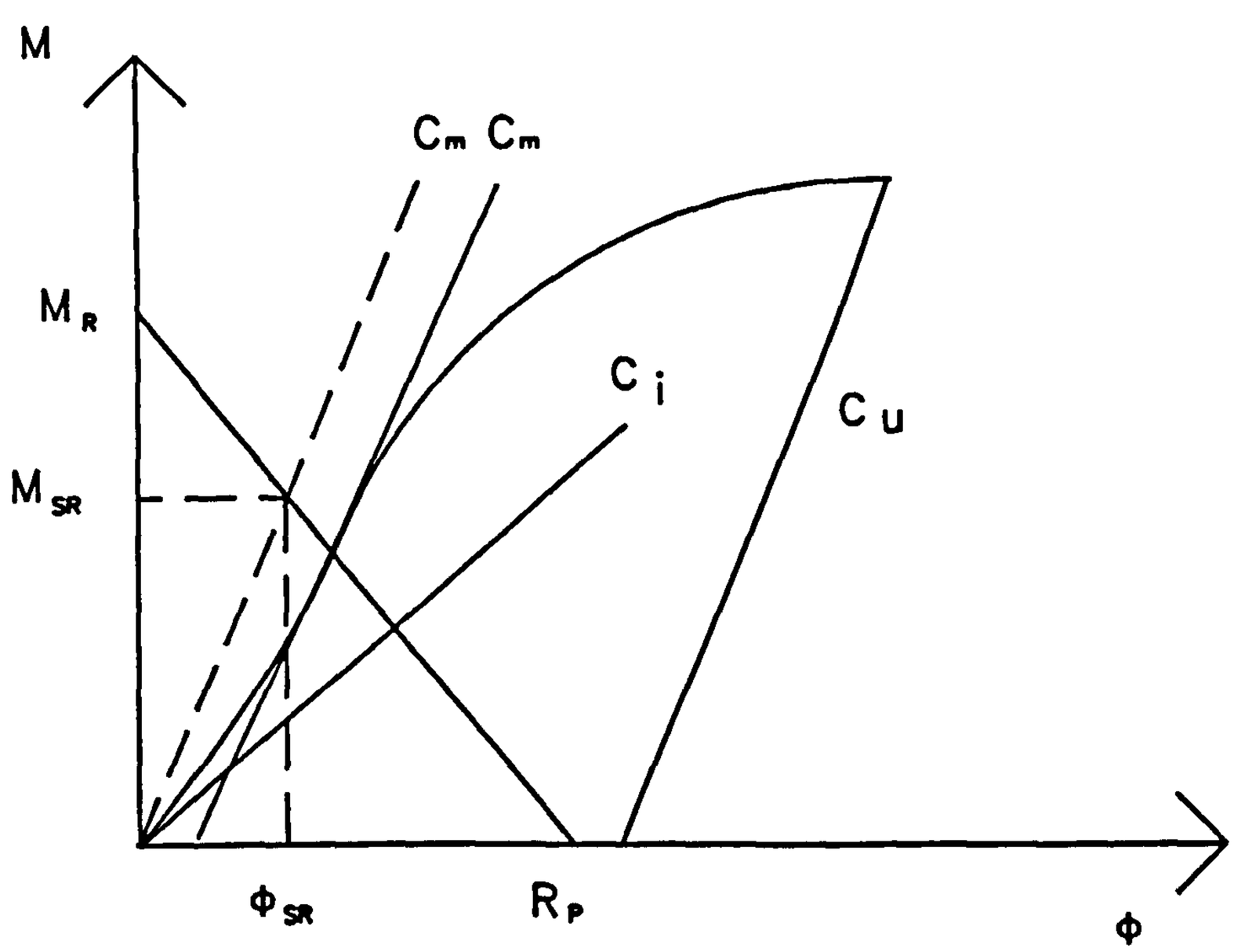

(b) Reduction of the Initial Stiffness of Connection due to Lack-of-fit

Figure 10.29 : Method used the Initial Stiffness of Ci

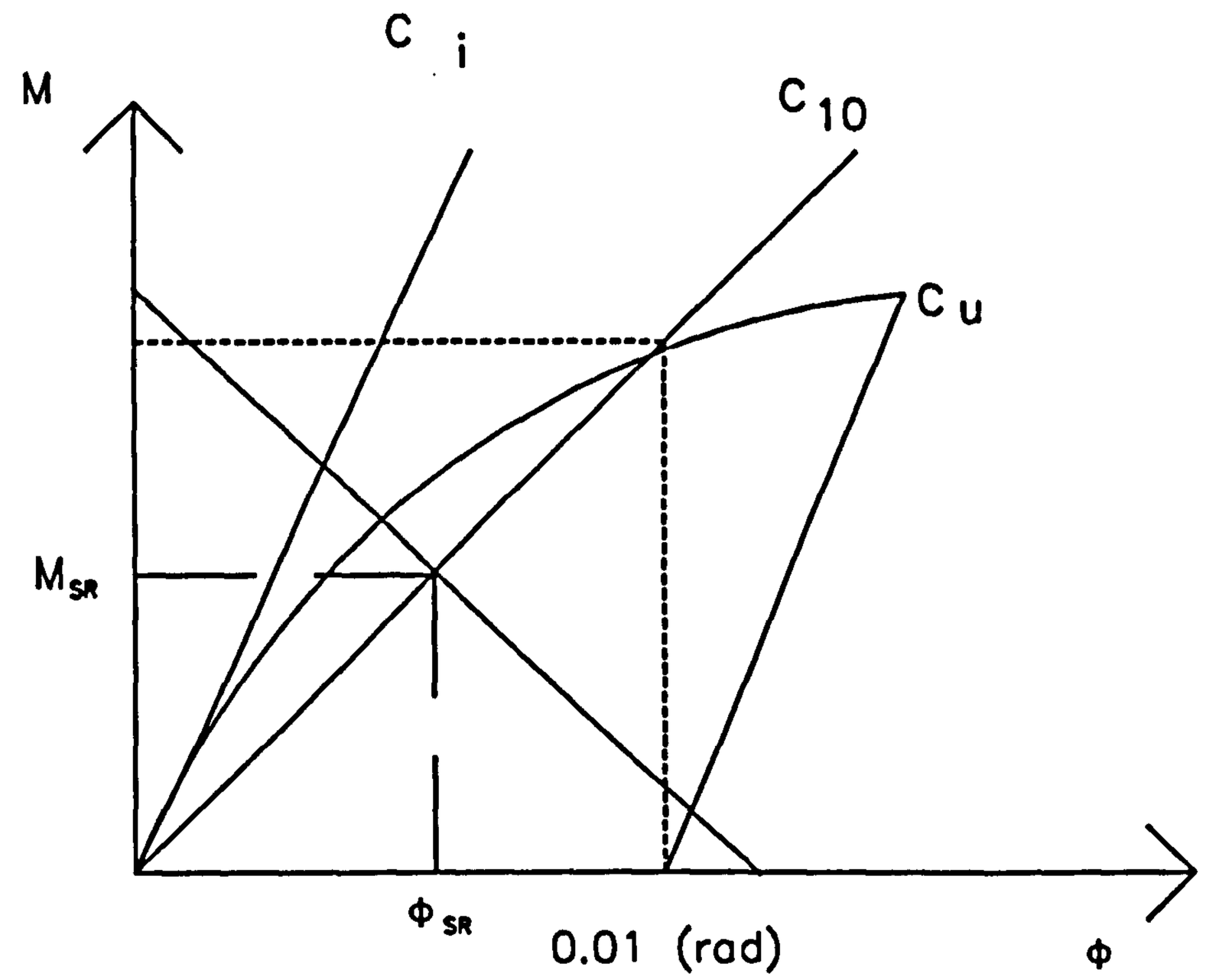

(a) The Secant Stiffness C_{10} at rotation of 0.01 (rad)

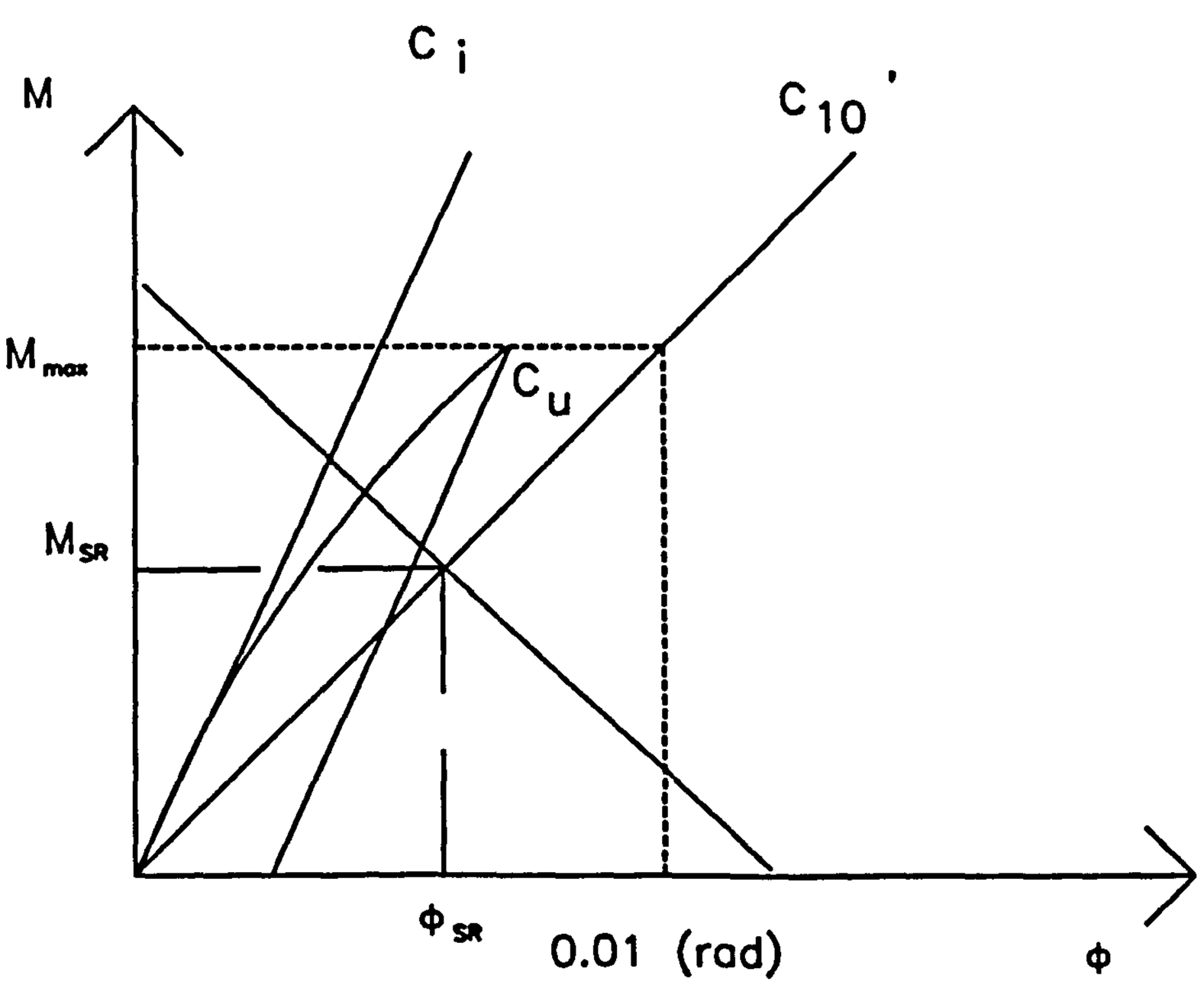

(b) Modified Method for Secant Stiffness C_{10}' for Stiff Connection which does not rotate to 10 mrads

Figure 10.30 : Method used the Secant Stiffness of C_{10}

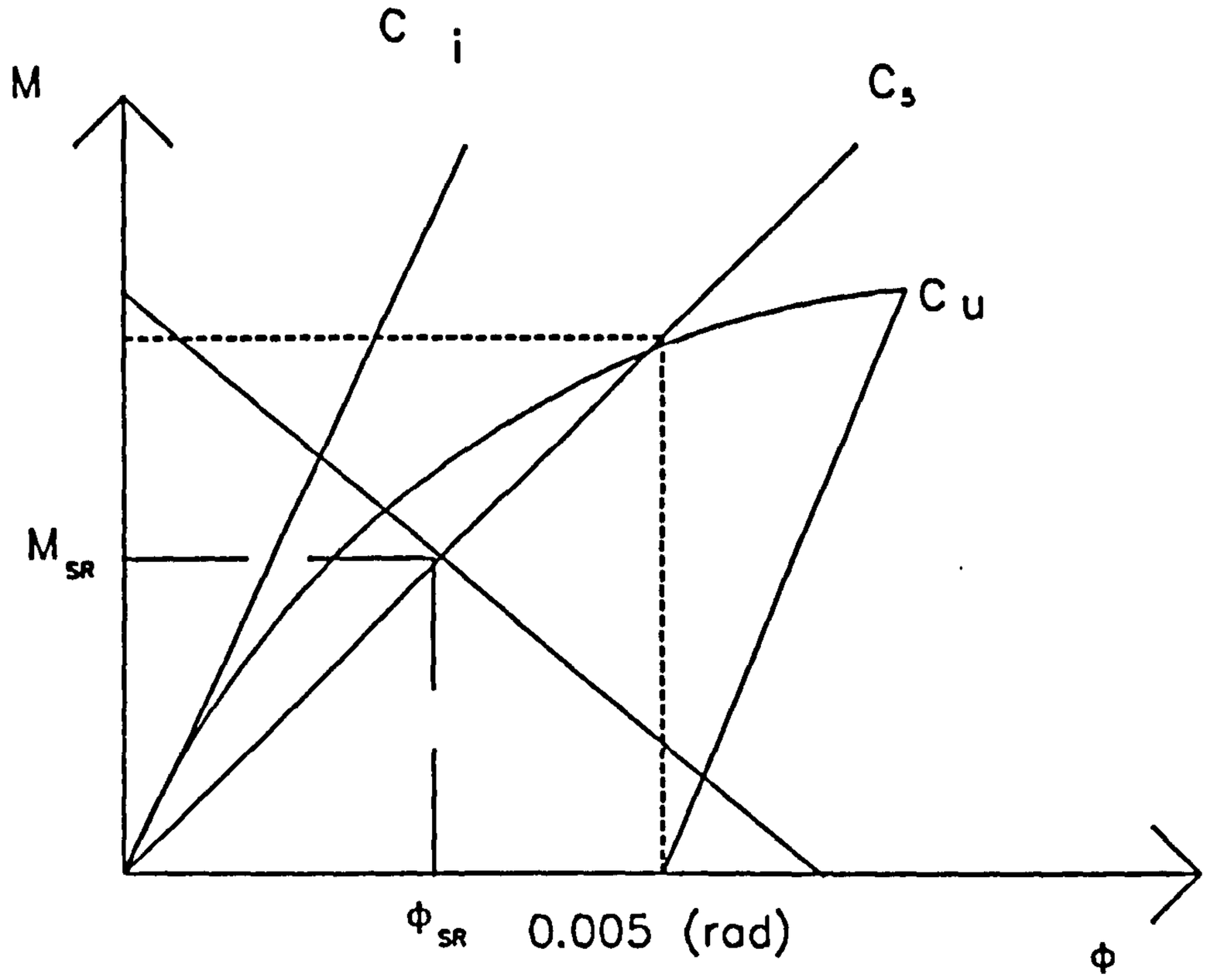

(a) The Secant Stiffness C_s at rotation of 0.005 (rad)

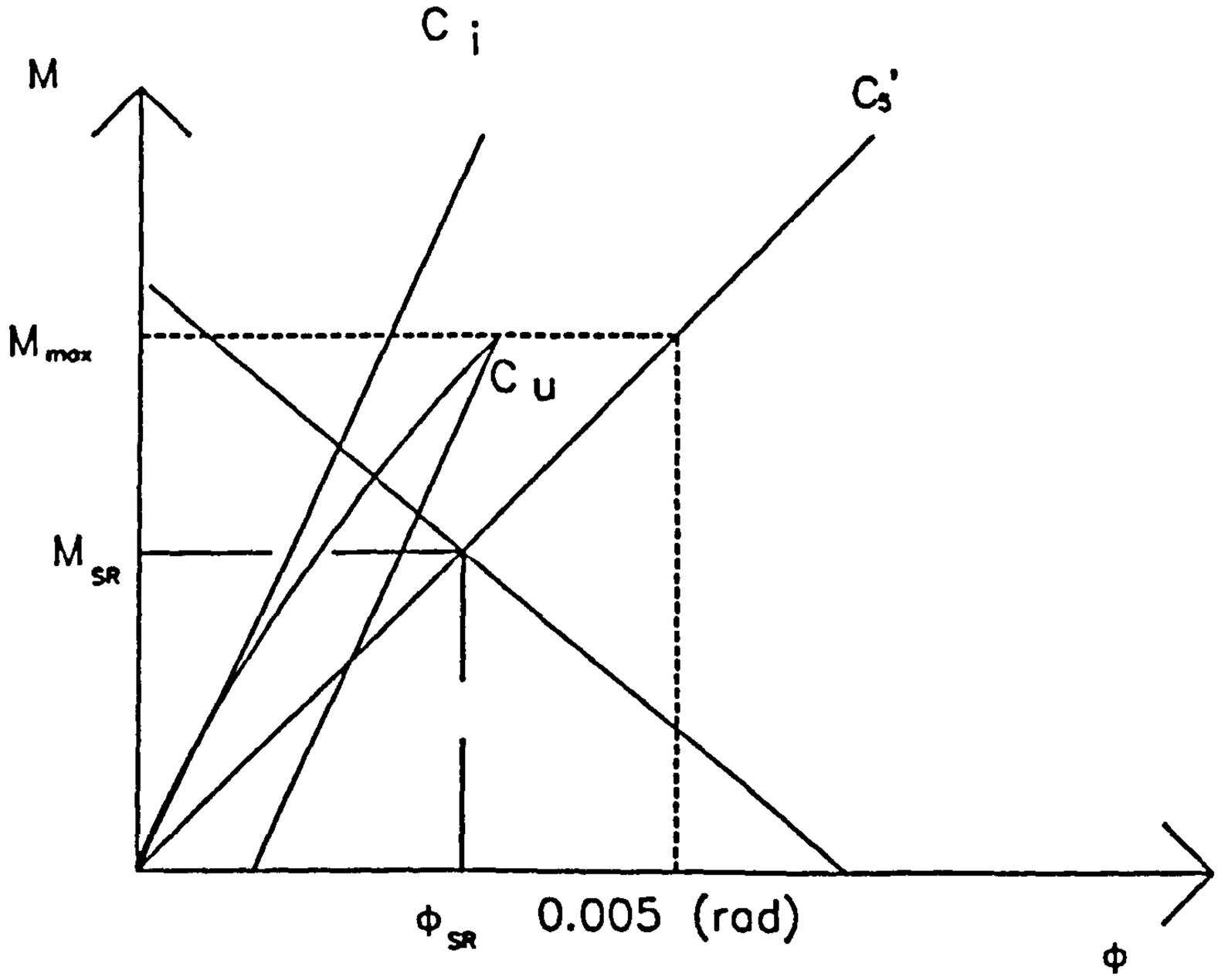

(b) Modified Method for Secant Stiffness C_s' for Stiff Connection which does not rotate to 5 mrads

Figure 10.31 : Method used the Secant Stiffness of C_s

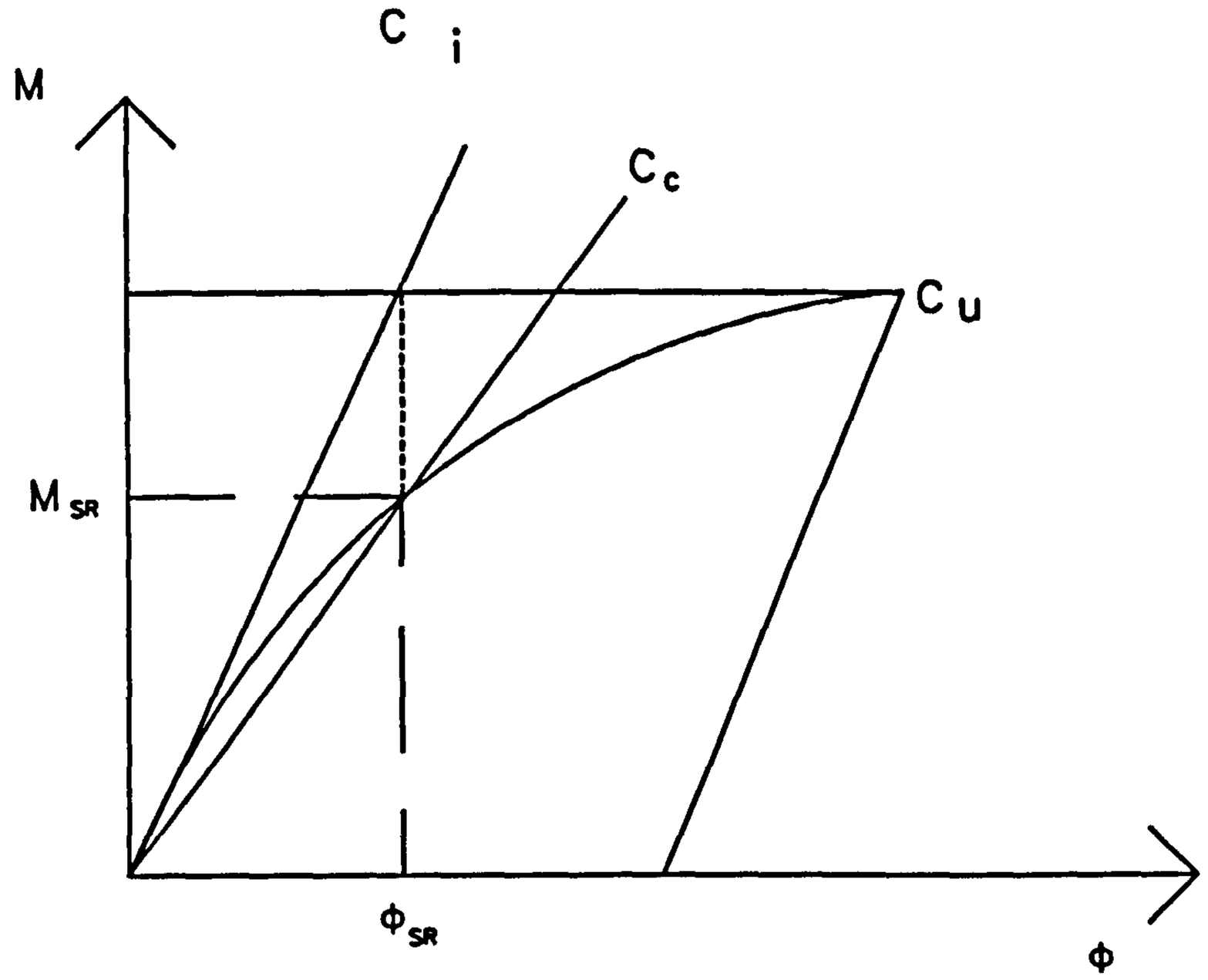

(a) Method used C_c without the effect due to lack-of-fit

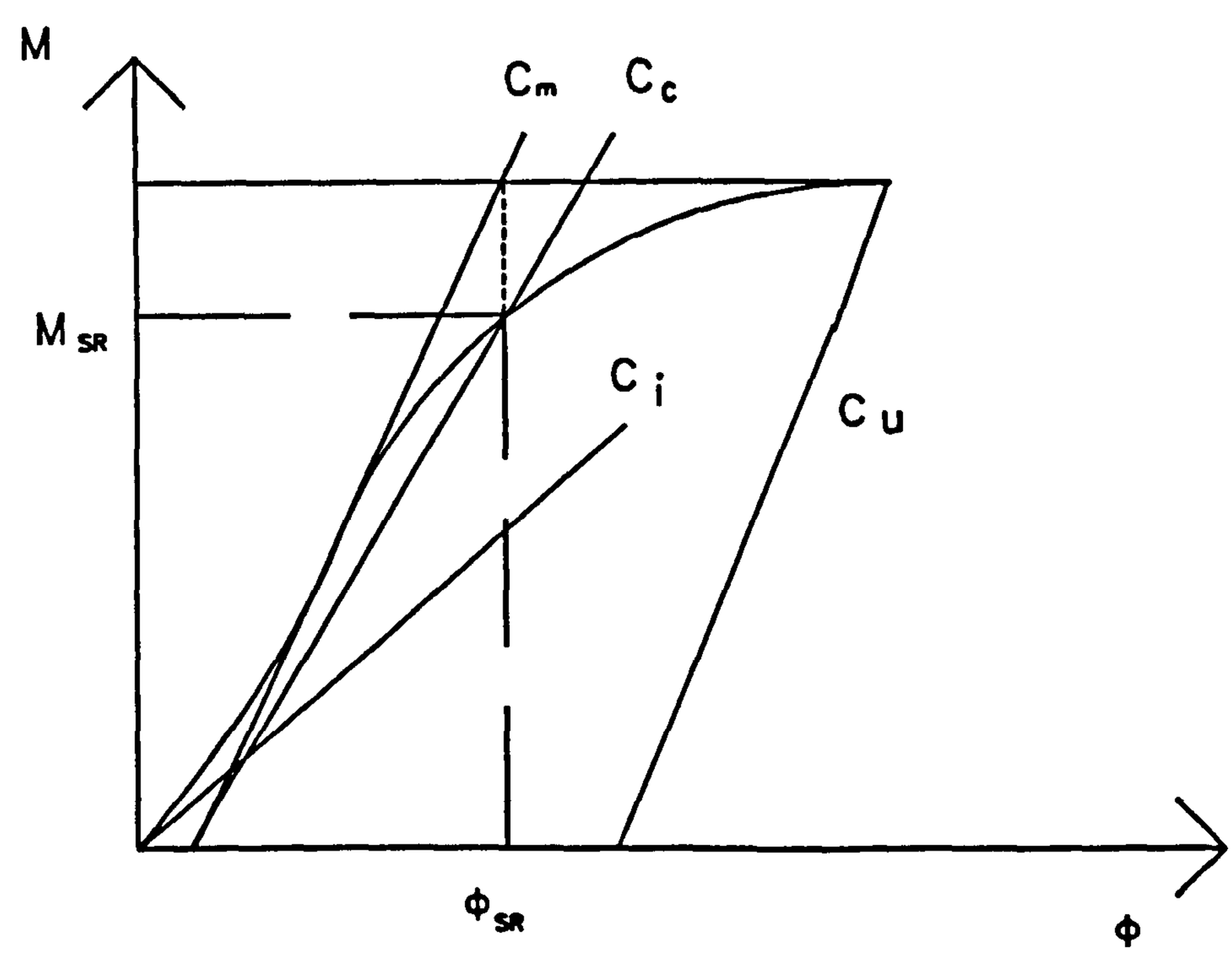

(b) Modified Method used C_c with the effect due to lack-of-fit

Figure 10.32 : Method used the Stiffness of Cc

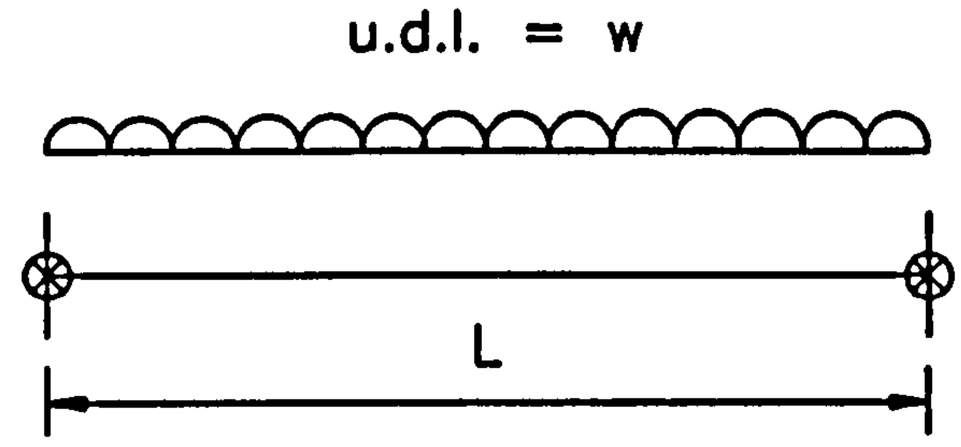

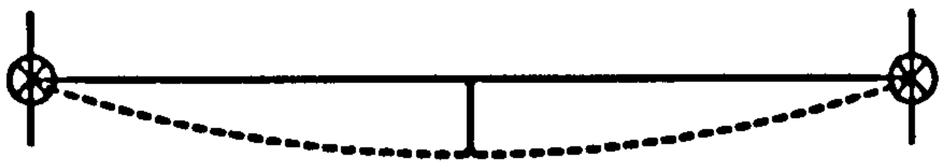

pin ended beam

$M_J = 0$ $\qquad M_B = \frac{wL^2}{8}$

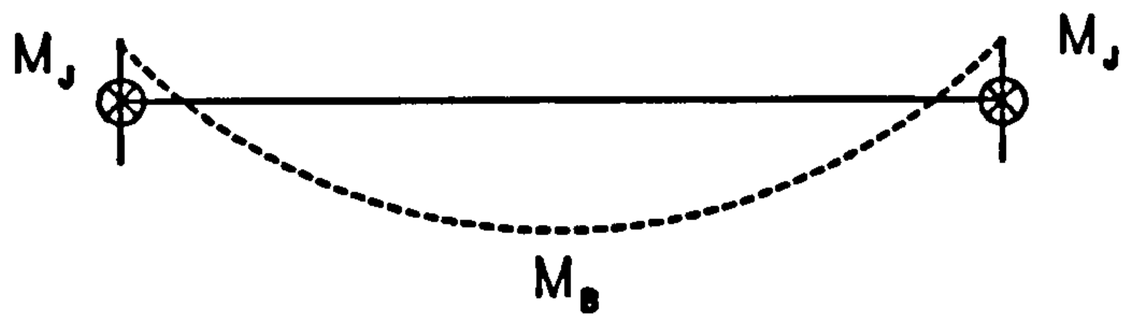

actual beam

$M_J < \frac{wL^2}{12}$ $\qquad M_B < \frac{wL^2}{8}$

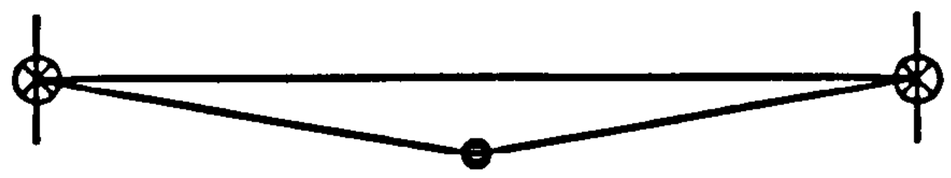

$$\frac{8M_p}{L^2} \leqslant w_c \leqslant \frac{16M_p}{L^2}$$

For $\lambda = \frac{M_J}{M_p}$

$$w_c = \frac{8(\lambda+1)M_p}{L^2}$$

Figure 10.33 : Behaviour of Beam with Semi-Rigid Connections

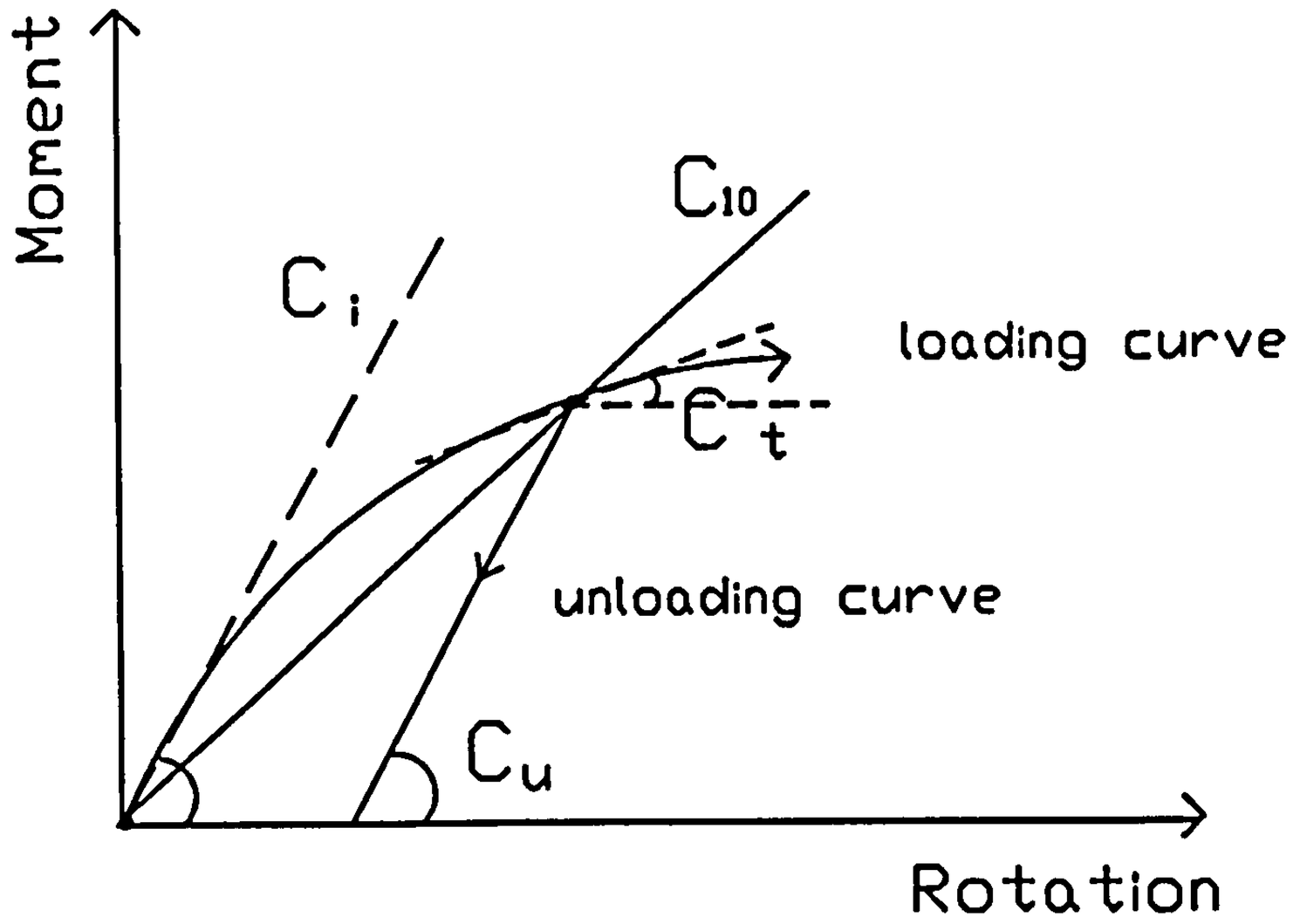

Where $C_i = C_u$

$$C_{10} \doteq \frac{C_i + C_u}{2}$$

Figure 10.34 : The Relationship between the Secant Stiffness of C_{10} to the Loading C_t and Unloading C_u Stiffnesses of Connections

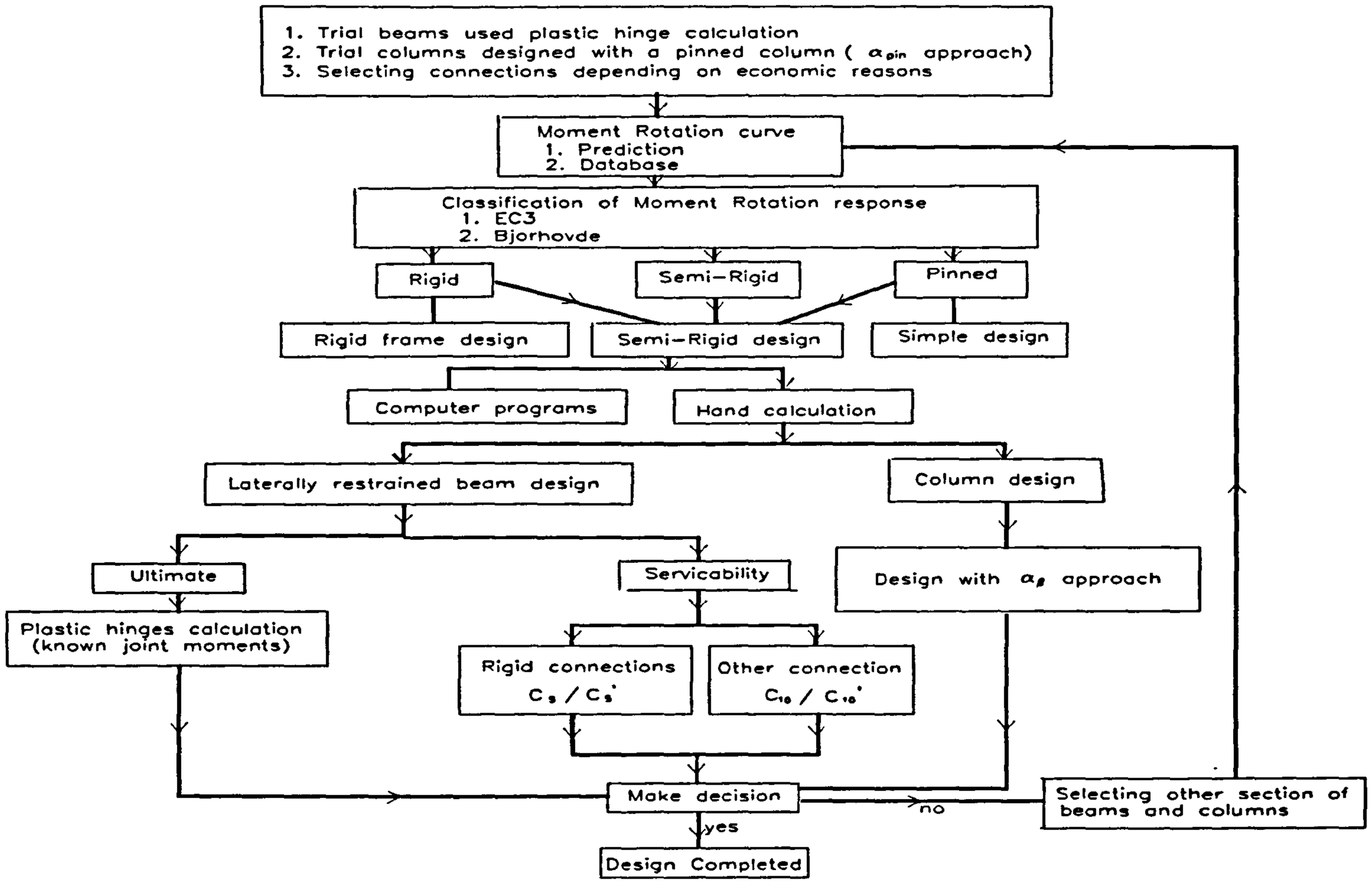

Figure 10.35 : Development of Semi-Rigid Design Methods

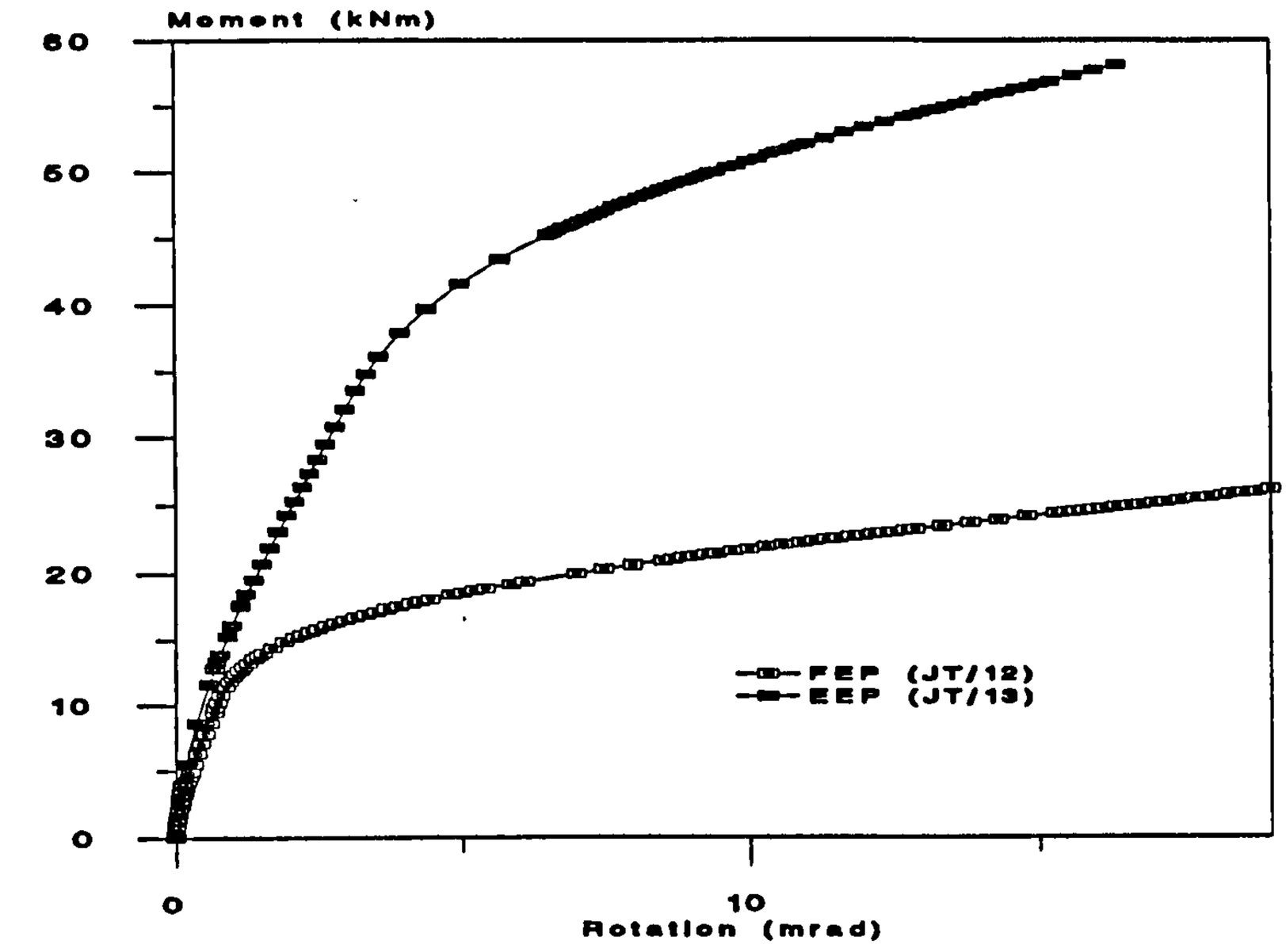

Figure 10.36 : Moment Rotation Curves for Flush End-Plate and Extended End-Plate Connections for Example

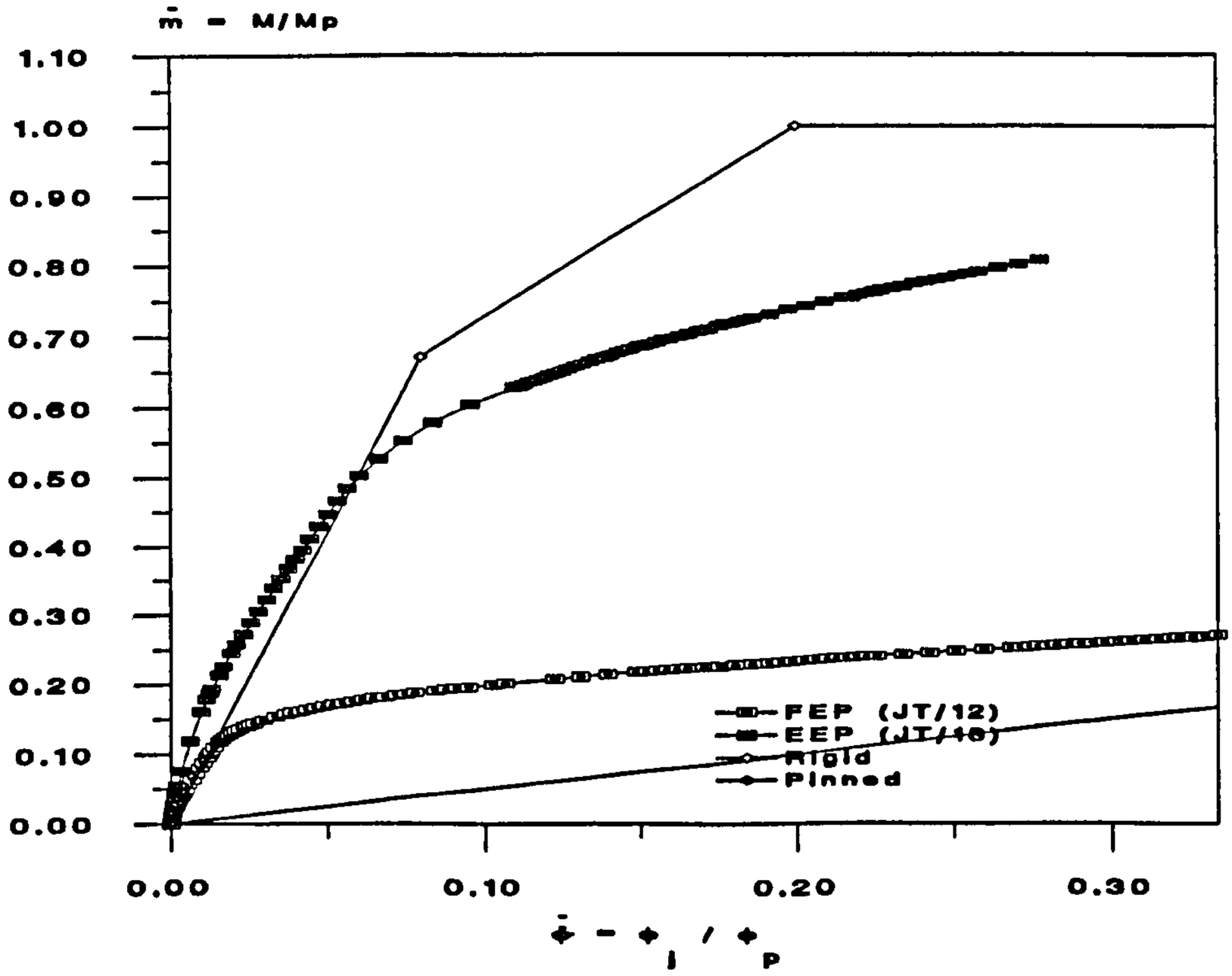

Figure 10.37 : Classification of Connections using EC 3 for Example

Chapter 11

Conclusions and Recommendations for Further Research

Five two dimensional full scale frames have been tested at the Building Research Establishment, Garston, Watford, using a facility developed there. In this thesis, an in-depth appraisal of the most significant of the test results from the five frames is reported. The main objective was to study the performance of the connections and their influence on the behaviour of planar frame elements, under practical loading conditions. The test results are also used to verify two sophisticated computer analysis programs.

Frame test data was collected in order to provide access to moment-rotation characteristics and corresponding parameters of semi-rigid beam-to-column connections in a convenient computerised form and is the motivation behind the current steel beam-to-column connection database at the University of Sheffield. This existing databank of the moment-rotation test result computer program has been modified in order to provide a more efficient and user friendly tool for research workers. Finally a set of new semi-rigid frame design methods are proposed. The predictions are compared with the experimental result.

Conclusions are drawn and reported in this chapter and further research topics are recommended.

11.1 Conclusions

11.1.1 Connection Behaviour and Frame Response

1. The experimental M-ϕ responses showed that use of pre-loaded bolts in connections increased the initial stiffness and thus reduced the deflection of the beams at low levels of load when compared to frame using hand-tightened bolts. The use of the pre-loaded bolt would lead to a large stiffness but there was no significant change of the ultimate capacity of the connections between pre-loaded or hand-tightened bolts.

2. For the flange cleat connections, slip was observed in some joints at some stage of loading when the bolts were not fully tightened due to the use of oversize holes. This increases the connection flexibility but has no significant effect on the moment capacity. The methods to improve this problem could be used fully torqued bolts or High Strength Friction Grip (HSFG) bolts.
   A lower stiffness occur of moment relation may be observed in the initial stage of loading of end-plate connections due to the lack-of-fit. The maximum connection stiffness was then observed after some lack of fit was taken up and this value is suitable to use in the analysis. This assumption is supported and noted in EC 3. Examination of the result suggests that increasing the bolt pre-load in connections can overcome some of the lack-of-fit flexibility in the end-plate connections.

3. Observation on frames 3 and 4 demonstrated that flange cleat connections provide restraint to the beam and hence reduce mid-span deflection and moment. It indicates that even the weak connections can enhance the load capacity of the columns.
   Although flush end-plates are usually considered to operate in shear only, they can be classified as semi-rigid. The stiffness observed indicates that significant reductions in beam span moment and deflections occur due to the inherent strength and stiffness of these connections.
   Larger stiffness of the extended end-plate is observed in tests when compared with the flush end-plate. The assumption that extended end plate connections may be regarded as 'Rigid' appears highly questionable since this type of connection could also perform as semi-rigid. Moreover, use of the EC 3 classification system shows that they are not always classified as rigid. The behaviour of extended end-plate connections are highly dependent on the connection design (thickness

of plate), section size of the connected beams and columns and whether or not stiffeners are incorporated. If extended end-plate joints have to be rigid, i.e. using EC 3 classification system, the additional fabrication may be required. This together with the inconvenience of using a joint that extended beyond the beam depth, would seem to point to change to a flush end-plate arrangement with the use of semi-rigid design.

4. Examination of the results of the five frame tests suggests that all the different stiffness and strength of joints exhibited some degree of moment and rotation stiffness, leading to frame responses involving significant interaction between beams and columns. This affected beam and column deformation, the pattern of frame moment, ultimate capacity of members and type of collapse modes. The results from the five frame tests show that the exploitation of semi-rigid joint action in frames has the potential to lead to more economic design.

11.1.2 Frame Analysis

1. A good agreement has been obtained between the measured response of five frame tests and the prediction of two computer programs SERFA and SERVAR. The degree of correlation which has been attained has validated two programs and demonstrated their usefulness as an analytical research tool. One of the most significant findings in this study is that the behaviour of the frame and the ultimate capacity of members are not significantly affected by the modest differences in the moment rotation characteristics obtained in the frame tests and joint tests.

2. The parametric study reported in chapter 9 used a 3-D subassemblage finite element computer program to investigate the behaviour of the subassemblage employing a range of connection types and stiffness.
The predicted ultimate capacities are expresed in the form of α_{pin} factors which are defined as the ratio of the ultimate capacity of a semi-rigidly restrained column to that of an equivalent axially loaded pinned end column. Examination of the results showed that the influence of the restraint to the column from the semi-rigid beam-to-column connections exceeded the detrimental effect of the moment transferred. The M-ϕ characteristics obtained from different test arrangements and conditions predicted a similar behaviour and ultimate capacity for the column in a subassemblage structure.

The variation of the M-ϕ response did not significantly affect the load carrying of the column and it is concluded that the precise forms of the M-ϕ responses are not important.

11.1.3 Semi-Rigid Frame Design Methods

1. In order to account for the semi-rigid behaviour of the frame, it is necessary to incorporate actual joint flexibility in routine design practice. The current existing mathematical models are reported and the latest simplified analytical models proposed by EC 3 and Liew and Chen are examined. All the predictions have been compared with the experimental results for the frame tests.
   Examination of the results suggest that EC 3 underestimates the ultimate capacity and predicts either a lower or similar initial stiffness of connection. Thus it is safe for use in design. However, the design procedure is found to be too complex and some procedures are not explained in detail. The Liew and Chen model is easier to use but the prediction is unreliable and moreover may produce non-conservative estimates of joint response.
   M-ϕ characteristics could be obtained from a database. The data are collected from actual tests and thus provides more reliable M-ϕ curves than the existing design models for the parameters study or analysis. The database has already been modified and the test data updated. A set of programs was developed which enable a user to load and unload the test information to and from the SQL system. A study to extend the facility to include composite steel and concrete joint has been conducted and accepted by European partners and has been made available to a team in Aachen who are working on a PC version of the Sheffield facility.

2. A method proposed by the author in section 10.4 for predicting the deflection of semi-rigid frames under serviceability loading conditions gave a good correlation with the experimental results in five frame tests.

3. For collapse governed by the formation of a beam plastic mechanism, a modified plastic hinge calculation has been shown to closely predict ultimate capacity.

4. The author has proposed an ultimate limit state design method for non-sway column design, the α_β approach, in which the inherent benefits of semi-rigid frame action are taken into account. For collapse due to column buckling, for

which the use of the effective length based on the consideration of the relative stiffness of beams, connections and columns incorporated in established interaction equation is proposed and developed. A good agreement is obtained with the actual experimental results and the predictions are superior to those obtained using some existing approaches including BS 5950.

5. A complete set of semi-rigid design methods for the non-sway laterally restrained frames is developed by linking all new approaches together. The design procedures are outlined in section 10.7.1. The advantage of the new design methods is clearly demonstrated from the redesign of an existing frame. The methods are found to be easy to follow and simple to use. The most important result for the beam design is that over 10 % saving is determined based on the weight of steel using the new semi-rigid design methods than the existing design methods. For the non-sway columns design, the new approach sometimes cannot provide any saving depending on the weight of steel, but it can provide more than 10 % higher ultimate capacity than the BS 5950 method.

11.2 Recommendations for Further Research

11.2.1 Database

The database has been modified and updated by the author as reported in chapter 3. It contains over 550 M-ϕ characteristics and makes the results available to researchers. The current database contains only the M-ϕ characteristics of bare steel beam to column connections. Nowadays, composite structures have become a common feature in typical European buildings. To increase the usefulness of the Database, the test data for joints with composite members should also be incorporated in order that the additional information is more readily available for researchers. Thus, insertion of test data for joints with composite members is suggested.

Due to the difficulty of describing information in a tabular form, the author strongly recommends the use of drawings to describe the connection, the composite Beam and Column for each individual test inside the database.

Collaboration with the University of Aachen to develop the PC version of database was undertaken, the Sheffield data was transferred and the technique and structure of the

Sheffield database were discussed and made available to the group. A user friendly, more efficient and more powerful PC version is highly recommended for development.

11.2.2 Frame Tests

An in depth examination of the results from five full scale frames is reported in chapters 4 to 7. However, it is only limited to a few frames and connection types. For a more complete understanding of the actual behaviour of frames, more tests are suggested to include a range of frame geometry, loading, section sizes of beams & columns and type of connections. Furthermore, all five frames were tested under in-plane action. Further experiments including the three dimensional response of end-restrained columns is of a high priority.

11.2.3 Frame Analysis and Parametric Study

Chapter 8 reported a detailed comparison which had been performed between the observed experimental frame behaviour and that predictions from two in house finite element computer programs. A good agreement is obtained.

More parametric studies should be conducted including the study of the influence of the practical range of connections on steel frame of realistic geometry and section size, the sensitivity of the behaviour of frame due to variation of M-ϕ response.

The programs only handle the bare steel beam and column sections, their appliability is in many cases restricted as nowadays composite structures have becomes a common feature in typical buildings. To increase the useful of programs, the composite sections should be included. Currently, the column bases can be input as either truly pin or fully rigid but in reality they are semi-rigid joints which provide some rotational restraint to columns. The semi-rigid response for the column bases should be also included.

Due to the difficult and inconvenience to use the output data in a tabular form for the researchers, the author strongly recommends these programs to be involved some graphics facilities to direct output some important figures i.e. load deflection curve, load moment curve and moment distribution around the frame. At this time, these programs are limited to in plane actions, an improvement to include spatial action of steel frames is suggested.

11.2.4 Frame Design

The existing simplified analytical beam-to-column connection models are only suitable for predicting the moment rotation characteristics for some specific joints. Thus it is suggested to extend their study to involve different types of connections and other parameters. All the models are found to be either unreliable or complex to use. Development of some computer programs for EC 3 are suggested in order to make this design method more efficient and user friendliness.

For the α_β approach, two extreme base conditions, i.e. fully rigid and truly pinned, have been considered when calculating the ultimate load of columns. However, realistic column bases are semi-rigid and it is recommended that this is taken into account when using the new approach. For laterally restrained beam design, a further study could concentrate on investigating the range of λ values (defined as ratios of the capacity of connections to the plastic moment of beams) for the different conditions to provide a good initial estimates of these values in the early design stage. The secant stiffnesses, i.e. C_5 and C_{10}, have been adopted to determine the beam deflection in the serviceability condition. The ultimate capacity of columns has been accomplished using C_{10}. It is thus suggested that further work should be undertaken concerning a simple method of obtaining these secant stiffnesses for different conditions which make the semi-rigid design method more attractive to engineers in the near future. Although the new semi-rigid design methods are developed and validated, it is compared with a limited experimental results. Detailed and extensive comparisons using more test results are suggested to fully verify the proposed design methods.

These methods are thought suitable to use for the U.K. designer, part of the methods can also be applied to the relevant parts of other design codes. However, different construction practices and methods are adopted in U.K. and different countries. For example, a guaranteed minimum yield stress of 235 N/mm^2 is adopted for the grade 43 steel in most of the European countries whilst 275 N/mm^2 is used in the U.K. Furthermore, different factors of safety or load factors are adopted for different countries. It suggests the new design methods need to be further developed and improved to consider all factors in order to be accepted by the European design code.

Appendix A

Liew and Chen Connection Modelling

Flange Cleat Connections

1. Standardized Parameters for Angle Connections

   For convenience, the following non-dimensional parameters are used to described the geometry of angle connection (see Figure A1):

   $\beta = \frac{g_c}{l}, \gamma = \frac{l}{t}, \delta = \frac{d}{t}$

   $k' = \frac{k}{t}, w = \frac{W}{t}, \rho = \frac{t_w}{t_t}$

   where

   g_c = distance from the edge of the angle to the centre of the bolt line

   t = thickness of the angle; subscripts w and t may be used to refer to web = angle and top angle respectively.

   k = distance from the angle hell to the toe of the fillet

   l = length of the angle

   d = beam depth

   W = nut diameter

   The subscripts t, s and w, which refer to the top, seat and web angle respectively, may be applied to the parameters in equations outlined above to describe the geometry and stiffness of the connection subassemblage.

2. Initial Connection Stiffness

   The normalized initial connection stiffness is given as:

$$D_{ts} = \frac{C_i}{EI_{ot}} \frac{1}{(1+\delta_t)^2} = \frac{3}{\beta_t'(\gamma_t^2 \beta_t'^2 + 0.78)} \tag{A.1}$$

where

$$\beta_t' = \beta_t - \frac{1}{2\gamma_t}(1 + w_t) \tag{A.2}$$

3. Ultimate Connection Moment Capacity

$$\varepsilon_t^4 + \beta_t^* \varepsilon_t - 1 = 0 \tag{A.3}$$

in which

$$\beta_t^* = \beta_t' \gamma_t - k_t \tag{A.4}$$

and β_t' is defined in equation (A.2).

The ultimate moment capacity is obtained by summing the moments about the centre of rotation of the connection. It may be written in a dimensionless form as:

$$\frac{M_{uts}}{M_{otl}} = \gamma\{1 + \varepsilon_t[1 + \beta_t^* + 2(k_t' + \delta_t)]\} \tag{A.5}$$

The ε_t term in equation (A.5) can be obtained from equation (A.3) for the pre-determined value of β_t^*.

4. Shape Parameter

The shape parameter is defined as:

$$n = 2.003 \log_{10} \theta_p' + 6.070 \leq 0.30 \tag{A.6}$$

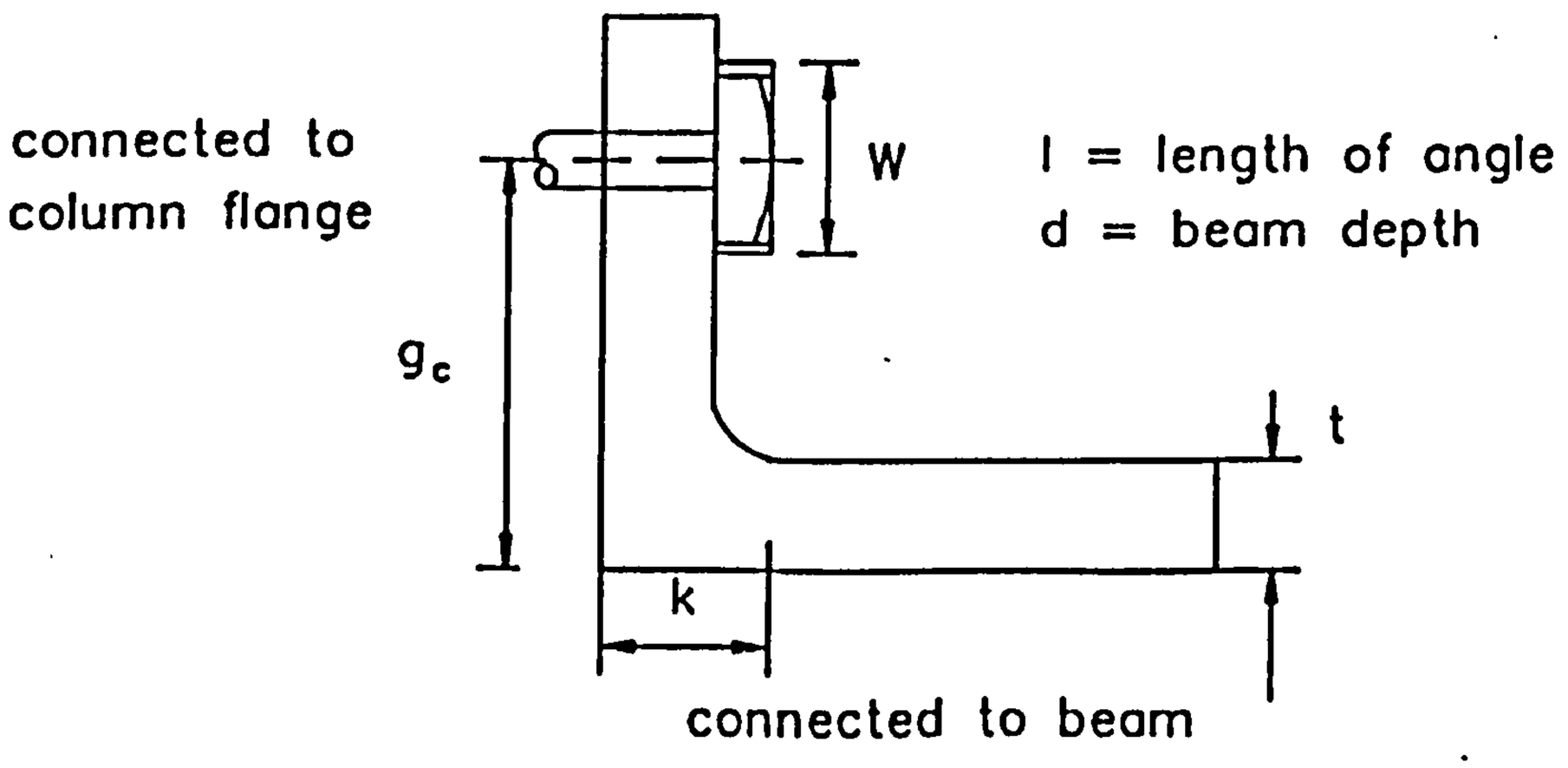

Figure A1 : Standard Dimensions of an Angle Connection for Liew and Chen Model

Appendix B

Figures

Figure B1 : Genernal Arrangement of 3-D Frame F1 conducted by Gibbons (F2 similar)

Figure B2 : Typical Floor Layout of Trinity Court in Manchester

Figure B3 : Typical Subassemblages and Models used in Carr's Study

Figure B4 : Typical Floor Layout of M.R.I. Building in Nottingnam

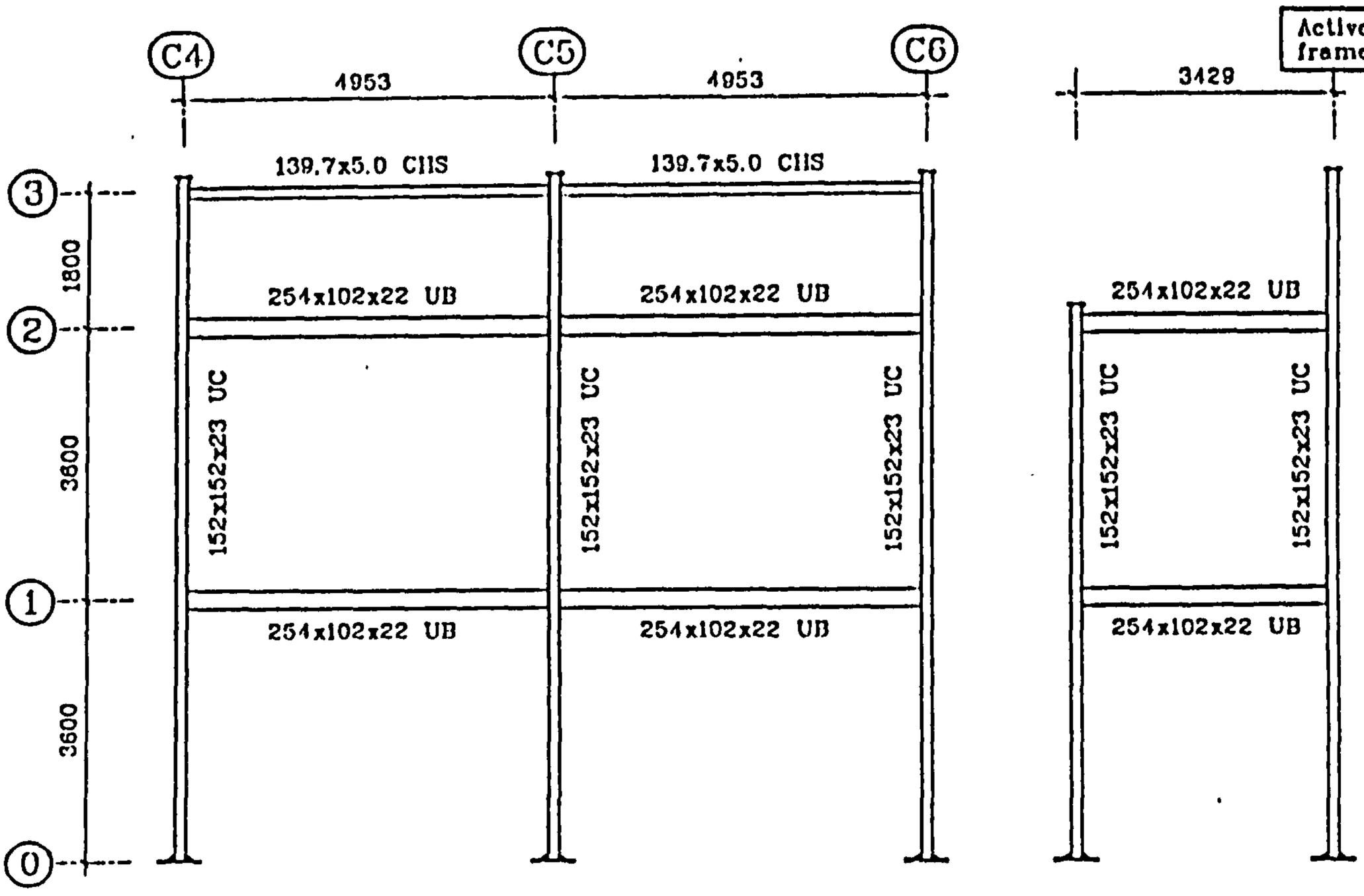

Elevation

Section

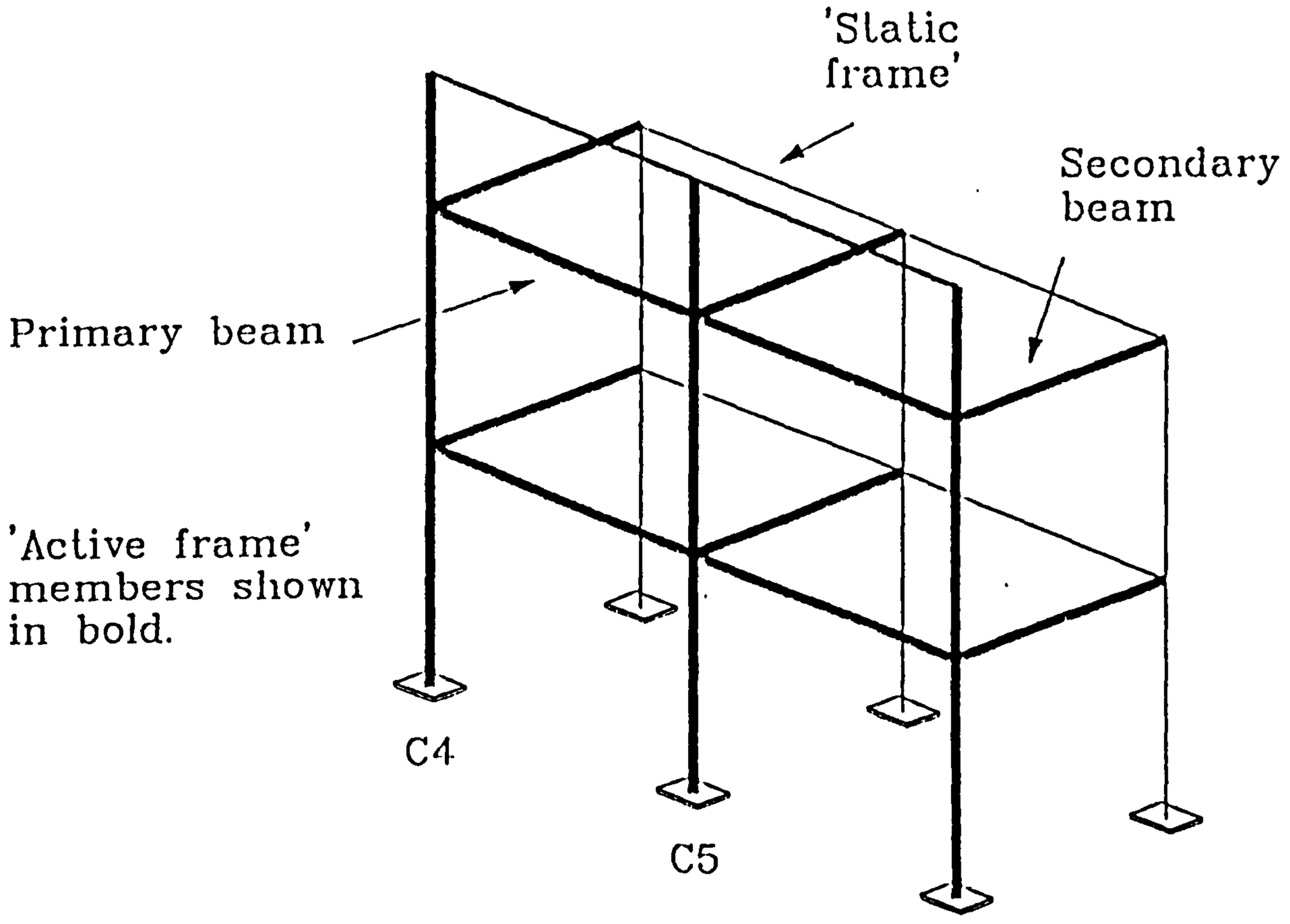

Figure B1 : Genernal Arrangement of 3-D Frame F1 conducted by Gibbons

(F2 similar)

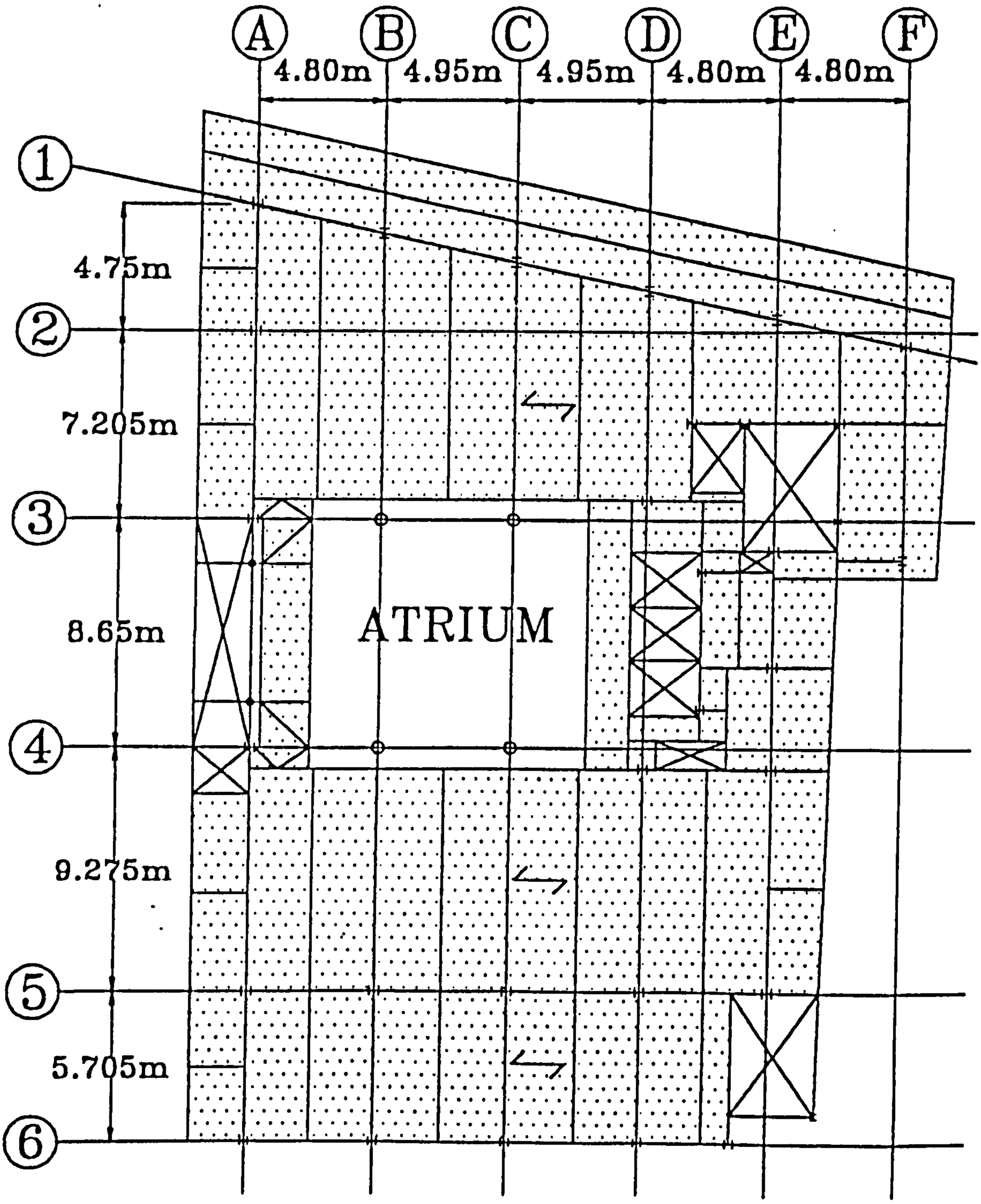

Figure B2 : Typical Floor Layout of Trinity Court in Manchester

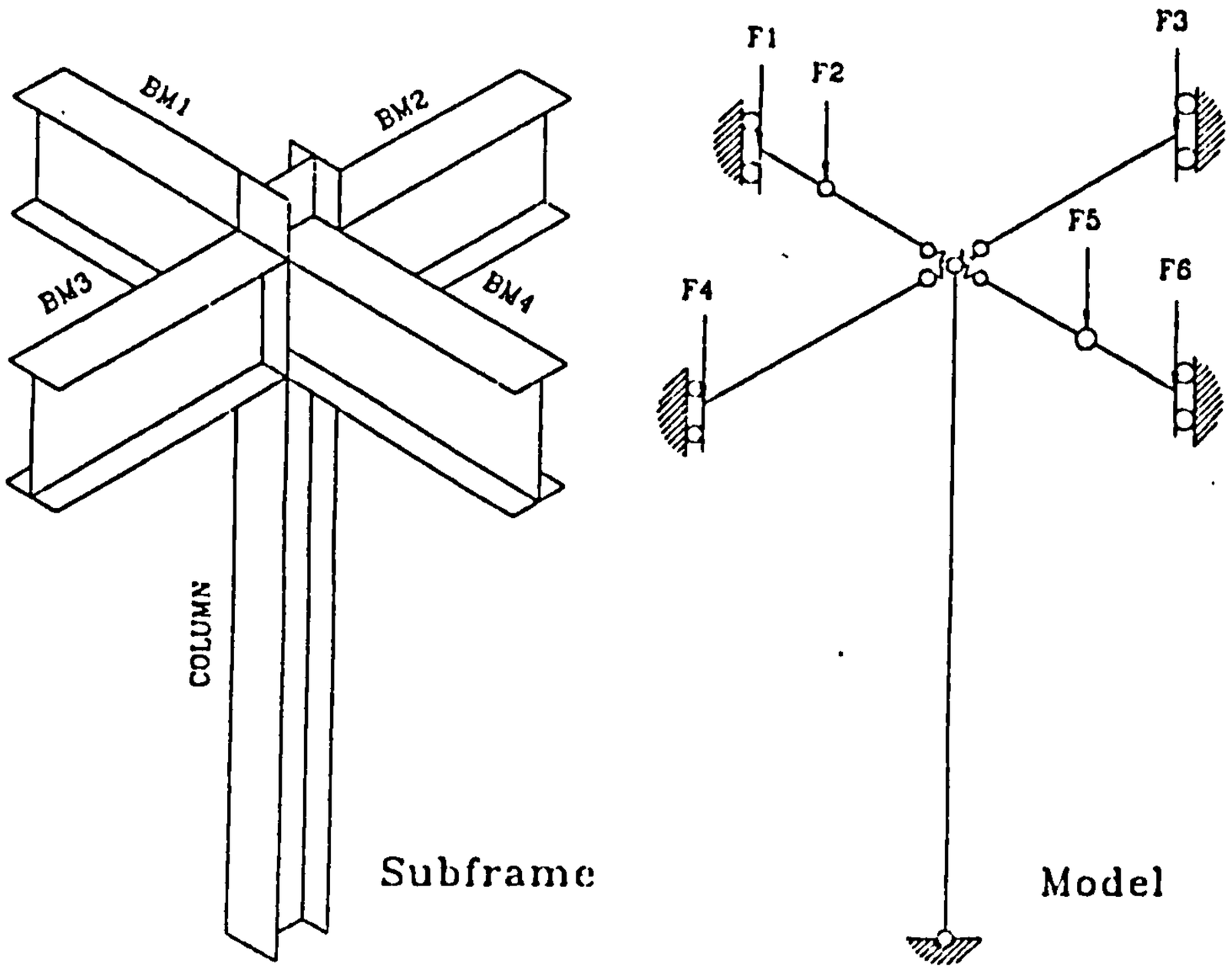

Subframe

Model

Model (i)

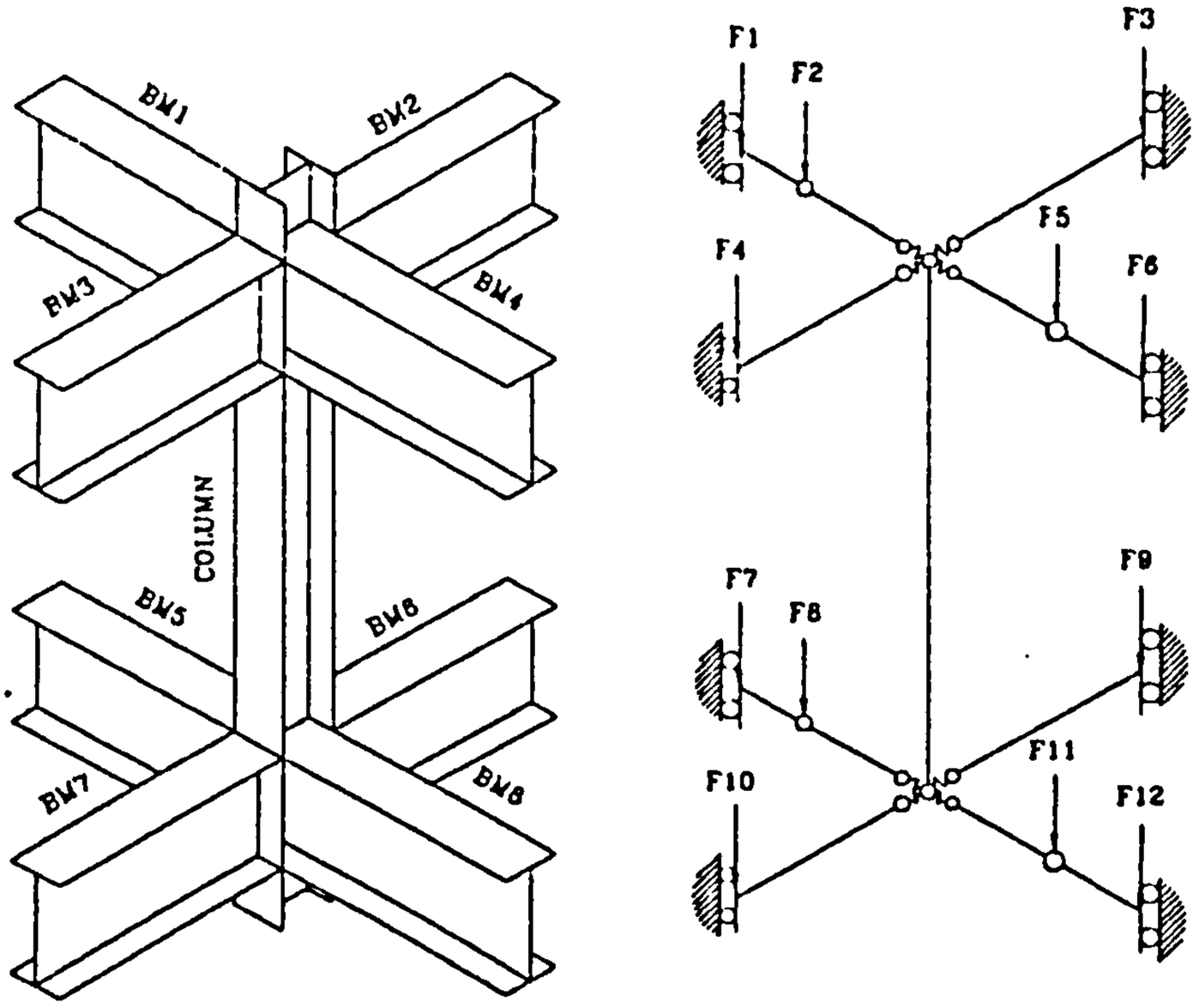

Subframe

Model

Model (ii)

(a) Internal Column with Four connected Beams

Figure B3 : Typical Subassembages and Model used in Carr's Study

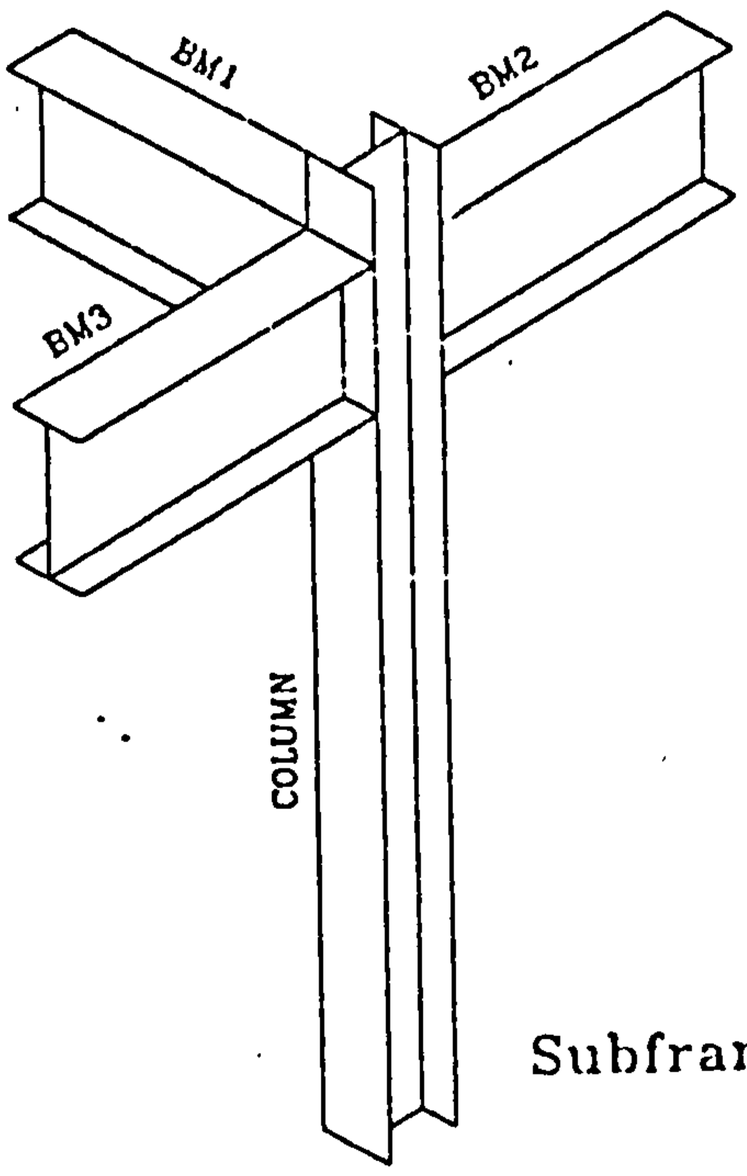

Subframe

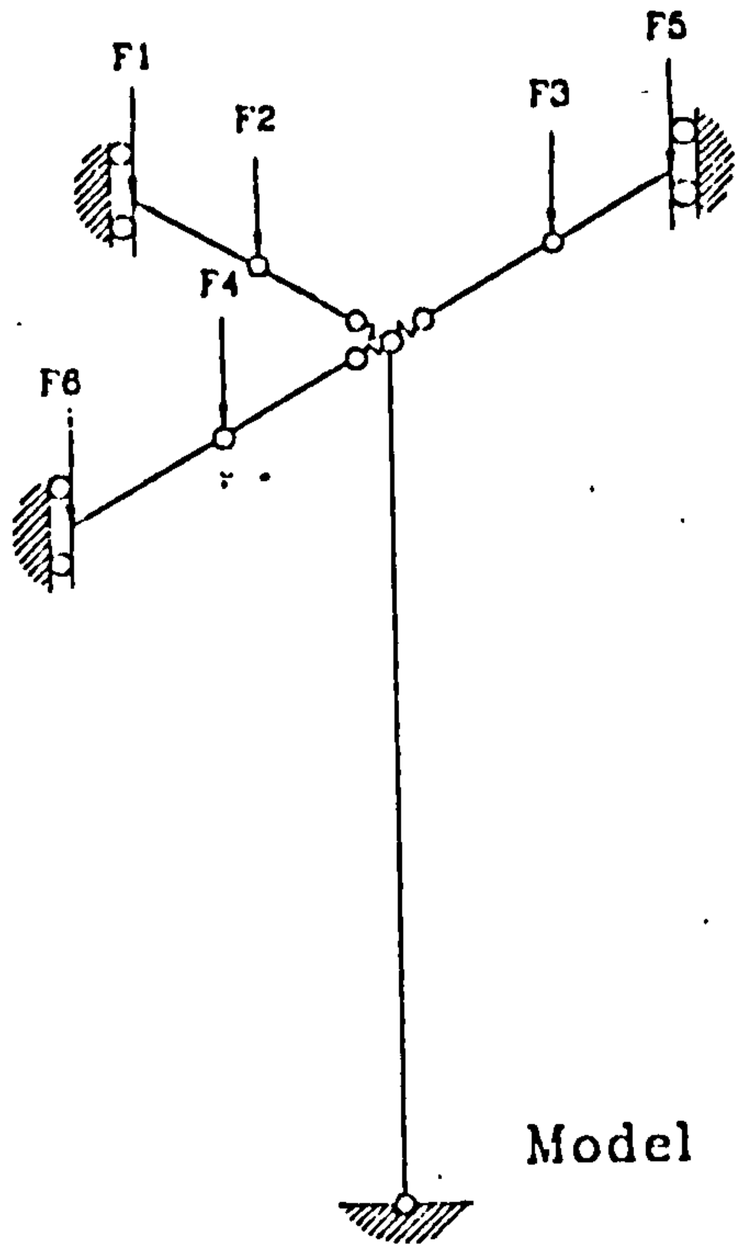

Model

Model (i)

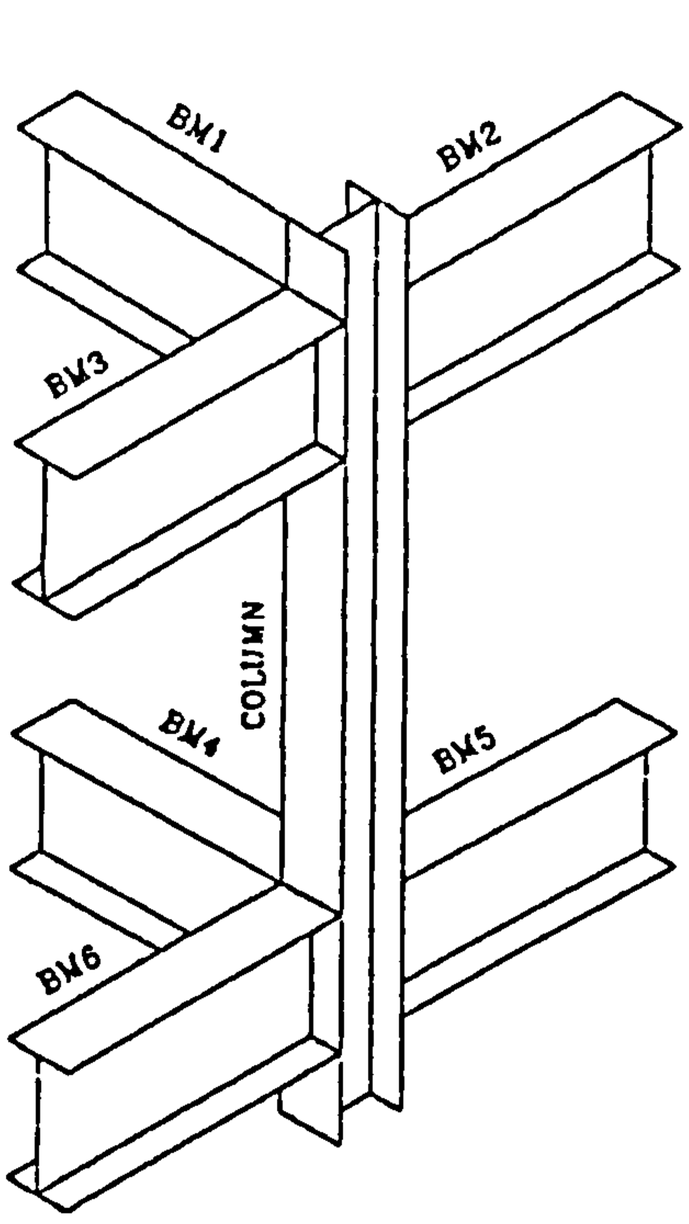

Subframe

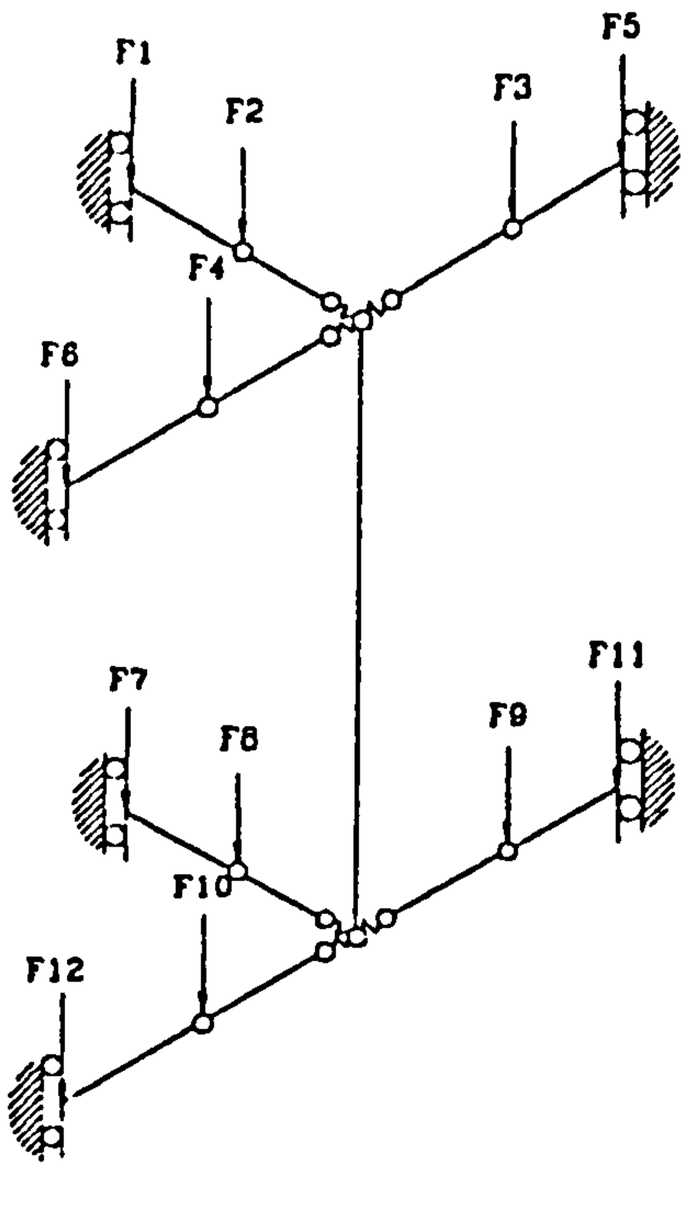

Model

Model (ii)

(b) Edge Column with Three connected Beams

Figure B3 : Typical Subassembages and Model used in Carr's Study

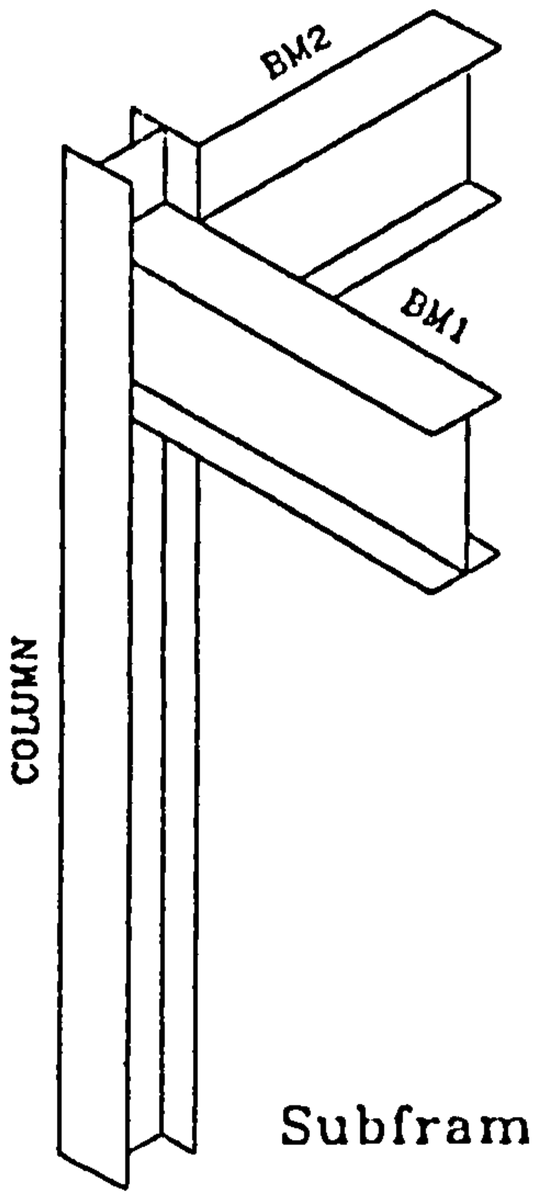

Subframe

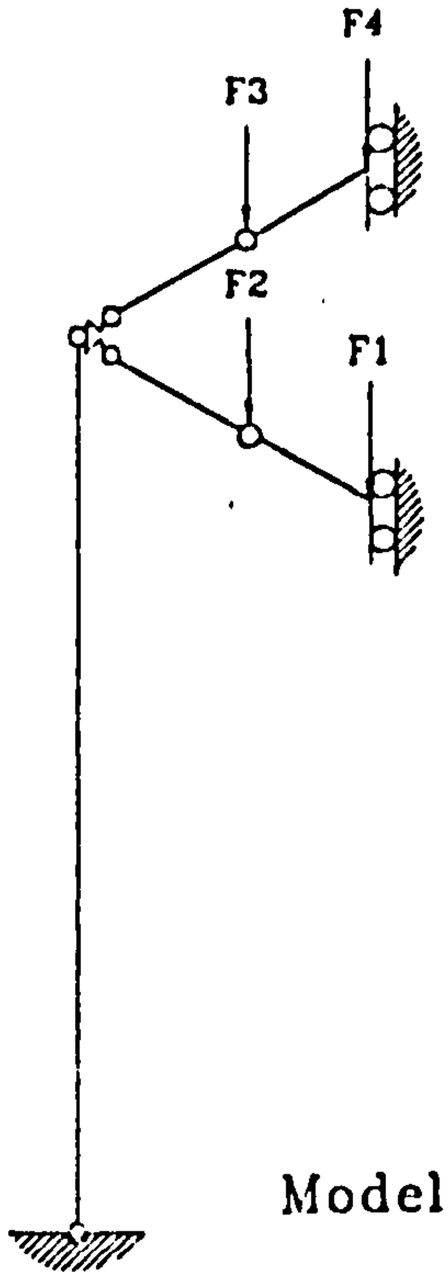

Model

Model (i)

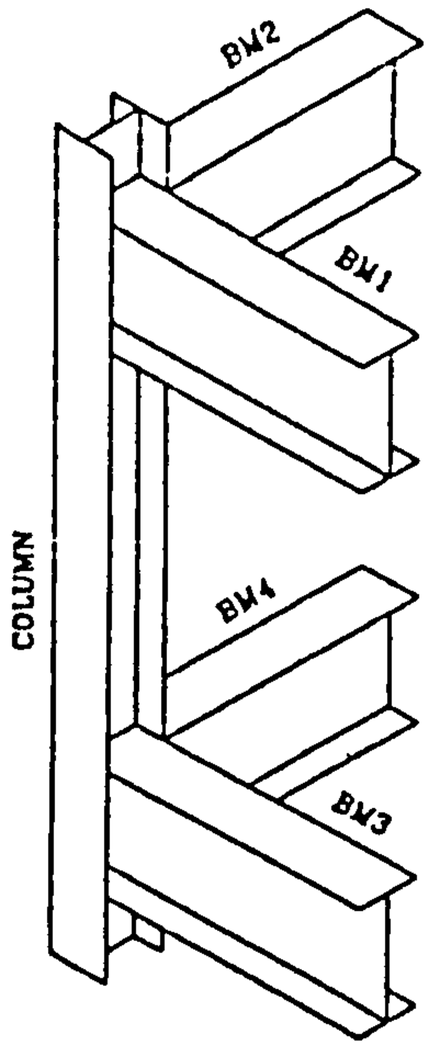

Subframe

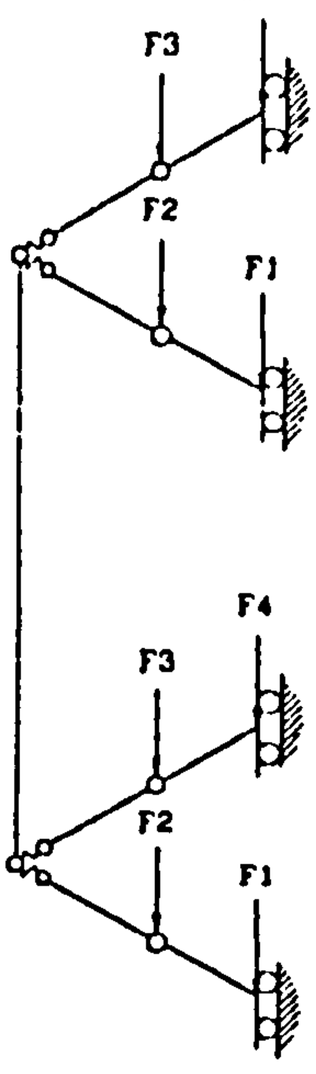

Model

Model (ii)

(c) Corner Column with Two connected Beams

Figure B3 : Typical Subassembages and Model used in Carr's Study

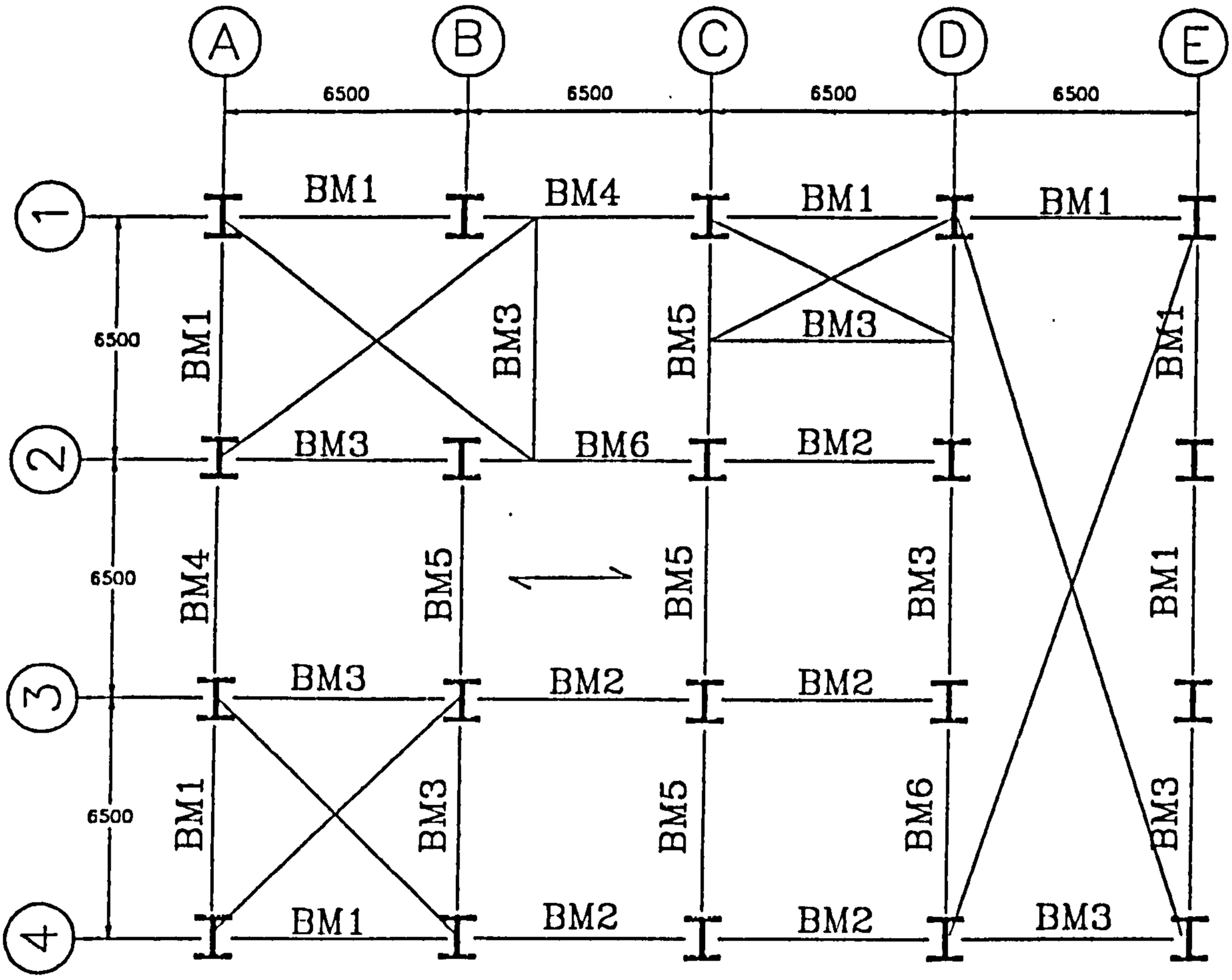

Figure B4 : Typical Floor Layout of M.R.I. Building in Nottingham